

Sulfur Nutrition of Tomato
(*Solanum lycopersicum*) in Relation to
its Resistance against Pathogens

Von der Naturwissenschaftlichen Fakultät
der Gottfried Wilhelm Leibniz Universität Hannover

zur Erlangung des Grades

DOKTORIN DER NATURWISSENSCHAFTEN

Dr. rer. nat.

genehmigte Dissertation

von

M. Sc. Katharina Klug

geboren am 13 Oktober 1982, in Rheinbach

2013

Referent: Prof. Dr. agr. Walter J. Horst

Korreferent: Prof. Dr. rer. nat. Helge Küster

Tag der Promotion: 08.02.2013

Zusammenfassung

Die *Verticillium*-Welke wird durch den bodenbürtigen Pilz *Verticillium dahliae* (*V. dahliae*) ausgelöst, welcher weltweit eine große Anzahl von Wirtspflanzen infiziert. Die ausschließlich im vaskulären Gewebe lokalisierte Krankheit verursacht jährlich dramatische Ertrags- und Qualitätseinbußen in vielen wirtschaftlich bedeutenden Früchten einschließlich der *Solanaceae*n. Die äußerliche Krankheitsbekämpfung gestaltet sich schwierig, da Eindämmungsstrategien oftmals eine zu geringe Wirkung aufweisen oder eine Gefährdung für die Konsumenten und die Umwelt darstellen. Daher ist die Anwendung einer wirkungsvollen und sicheren Krankheitskontrolle sehr wichtig. In diesem Zusammenhang ist der Prozess der Schwefel (S)-basierten Abwehr eine vielversprechende Strategie. Die Synthese S-haltiger Verteidigungsstoffe einschließlich des elementaren S (S^0) nach einer Pilzinfektion ist für einige Pflanzenarten sowie für die den *Solanaceae*n zugehörige Tomate beschrieben worden. Daher setzt diese Arbeit mit Hilfe von physiologischen und transkriptomischen Ansätzen einen Fokus auf (I) den Einfluss der S Ernährung auf das Verteidigungspotenzial der gegen *V. dahliae* Resistenz-vermittelnden S-basierten Abwehr, (II) die Gewebe spezifische Genexpression von S Metabolismus assoziierten Genen im Zusammenhang mit der Aktivierung der S-basierten Abwehr und der Synthese von S^0 , (III) die genotypischen Unterschiede zwischen S-basierter Abwehr und Resistenzgen-basierter Verteidigung. Eine hohe externe S-Applikation konnte das für den Pilz toxische Potential der Gewebe internen S-basierten Abwehr verstärken und damit die *in planta* pilzliche Besiedelung besonders im vaskulären Gewebe von *V. dahliae*-sensitiven Tomaten einschränken. Zudem bewirkte ein hohes S-Angebot einen deutlichen vaskulären S-Anstieg, welcher S^0 oder eine Ansammlung von S^0 Vorläufermolekülen repräsentieren könnte. Einzelne Schritte der S Assimilation zeigten ein besonderes räumliches Genexpressionsmuster im Zusammenhang mit hoher S-Ernährung und Pilzinfektion. Die Anregung von Glutathion (GSH)-synthetisierenden Stoffwechselschritten im gesamten Gewebe spiegelt die globale antioxidative Funktion von GSH bei der Bekämpfung radikaler Sauerstoffspezies wieder. Dahingegen zeigt die Anregung von Cystein (Cys)-synthetisierenden Stoffwechselschritten in vaskulären Zellen eine Rolle von Cys als lokaler Vorläufer für die Synthese von S^0 in Tomaten auf. Die Identifizierung *V. dahliae*-sensitiver und resistenter Ingressionslinien ermöglichte neue Einblicke in die Verbindung von S-basierter Abwehr und Resistenzgen-basierter Verteidigung. Genotypisch gesteuert wird die S-basierte Abwehr entweder durch eine Resistenzgen-basierte Verteidigung ergänzt oder komplett ersetzt. Für eine zukünftige Aufklärung der S^0 Synthese im vaskulären

Pflanzengewebe wurden molekulare Grundlagen zur homologen Überexpression spezieller S-Metabolismus assoziierter Gene etabliert. Die gegenwärtige Arbeit konnte einen positiven Einfluss hoher S-Ernährung auf die S-basierte Verteidigung feststellen, hat zudem Indizien für die Identität lokaler S⁰ Vorläufermoleküle geliefert, und konnte eine Vernetzung von S-basierter Abwehr und Resistenzgen-basierter Verteidigung aufzeigen.

Schlagwörter: *Verticillium dahliae*, Tomate, Schwefel-basierte Verteidigung

Abstract

Verticillium-wilt is caused by the soil-borne fungus *Verticillium dahliae* (*V. dahliae*), which infects a broad range of host plants on a worldwide level. This exclusively vascular-located disease annually causes dramatic yield and quality reductions in many economically important crops including the *Solanaceae*. External disease management is difficult since containment strategies showed limited effectiveness or put consumers and the environment at risk. Hence, the application of effective and safe disease-control is of major importance and a promising strategy therefore is the process of sulfur (S)-enhanced defence. The synthesis of S-containing defence compounds including elemental S (S^0) in response to a fungal infection has been described for several plant taxa including the solanaceous species tomato. Therefore, by means of physiological and transcriptomic approaches this study focused on (I) the effect of S nutrition on the protective potential of *V. dahliae* resistance-mediating SED, (II) the tissue-specific S metabolism-related gene expression in relation to SED activation and S^0 synthesis, (III) a genotype-specific emphasis between SED and resistance (R)-gene defence. Enhanced external S application was observed to activate the fungitoxic potential of tissue inherent SED mechanisms limiting the *in planta* fungal colonization particularly in *V. dahliae*-sensitive tomato vasculature. In addition, high S caused distinct vascular S peaks, representing S^0 or an accumulation of S^0 precursor substances. S assimilation-associated steps exhibited distinct spatial gene expression patterns in relation to high S nutrition and fungal infection. The induction of glutathione (GSH) biosynthesis-related steps in the entire tissue depicted a global antioxidative function of GSH in reactive oxygen species detoxification whereas the induction of cysteine (Cys)-biosynthesis linked steps in vascular cells stated Cys to be a local key precursor for the synthesis or accumulation of S^0 in tomato plants. The identification of *V. dahliae*-sensitive and resistant tomato introgression lines gave new insights into the connection of SED mechanisms and R gene defence. Depending on the genetic make-up of genotypes, SED processes were either supplemented or displaced by an R gene defence. Finally, for a future elucidation of the S^0 synthesis in plant vascular tissue, molecular tools for a homologue overexpression of selected S metabolism-related candidate genes were established. In summary, the current work confirmed a beneficial role of enhanced S nutrition on SED mechanisms, provided circumstantial evidence for the identity of local S^0 precursors, and indicated an interconnection of SED and R gene defence.

Keywords: *Verticillium dahliae*, tomato, sulfur-enhanced defence

Contents

Zusammenfassung	III
Abstract	V
Contents.....	VII
Abbreviations	IX
General Introduction	11
Tomato (<i>Solanum lycopersicum</i>).....	11
Physiological and molecular aspects of <i>Verticillium dahliae</i> and the <i>Verticillium</i> -wilt disease.....	13
Mechanisms of sulfur-enhanced defence and synthesis of sulfur-containing defence compounds.....	16
Chapter I - Sulfur supply impairs spread of <i>Verticillium dahliae</i> in tomato.....	19
Abstract.....	20
Introduction.....	21
Material & Methods.....	23
Results.....	28
Discussion.....	38
Chapter II - Spatial expression analysis of sulfur metabolism-related genes in hypocotyl tissues of tomato genotypes differing in <i>Verticillium dahliae</i> resistance.....	45
Abstract.....	46
Introduction.....	47
Material & Methods.....	49
Results.....	55
Discussion.....	64
Chapter III - Physiological and transcriptomic characterization of the response of <i>Solanum habrochaites</i> / <i>Solanum lycopersicum</i> introgression lines to <i>Verticillium dahliae</i> infection...	71
Abstract.....	72
Introduction.....	73
Material & Methods.....	76

Results.....	81
Discussion.....	89
Chapter IV - Construction of binary T-DNA vector systems for the molecular characterization of sulfur-enhanced <i>Verticillium dahliae</i> plant defence mechanisms	97
Abstract.....	98
Introduction.....	99
Material & Methods.....	101
Results.....	112
Discussion.....	130
General Discussion.....	137
Outlook.....	143
Supplementary Materials.....	147
Supplementary Material for Chapter I.....	147
Supplementary Material for Chapter II.....	150
Supplementary Material for Chapter IV	152
References	159
Erklärung zur Dissertation	175
Publikationsliste	176
Curriculum Vitae.....	178
Danksagung.....	179

Abbreviations

ANOVA	analysis of variance
<i>A. tumefaciens</i>	<i>Agrobacterium tumefaciens</i>
bp	base pair
°C	degree Celsius
CaMV	Cauliflower mosaic virus
cDNA	copy DNA
CDS	coding sequence
cm	centimeter
cv.	cultivar
Cys	cysteine
dH ₂ O	demineralized water
DNA	deoxyribonucleic acid
dNTP	deoxyribonucleoside triphosphate
dpi	days past inoculation
<i>E. coli</i>	<i>Escherichia coli</i>
EST	expressed sequence tag
g	gram
µg	microgram
gDNA	genomic DNA
Gen	genotype
GSH	reduced glutathione
h	hour(s)
hpi	hours past inoculation
HPLC	high performance liquid chromatography
IL	introgression line
L	liter
LA-ICP-MS	laser ablation inductively coupled plasma mass spectroscopy
LMPC	laser microdissection pressure catapulting
M	molar concentration
Mb	megabases
mg	milligram

Abbreviations

min	minute
mL	milliliter
mm	millimeter
μm	micrometer
mM	millimolar
μM	micromolar
n	number of observations
nm	nanometer
nM	nanomolar
n.s.	not significant
PCR	polymerase chain reaction
RNA	ribonucleic acid
ROS	reactive oxygen species
RP	recurrent parent
rpm	rounds per minute
S	sulfur
S ⁰	elemental sulfur
SD	standard deviation
SDC	sulfur-containing defence compound
SED	sulfur-enhanced defence
qRT-PCR	quantitative real-time polymerase chain reaction
v	volume
<i>V. dahliae</i>	<i>Verticillium dahliae</i>
<i>Ve1</i>	<i>Verticillium</i> race 1 resistance gene
w	weight
WT	wild type

General Introduction

Tomato (*Solanum lycopersicum*)

Tomato (*Solanum lycopersicum*) is a fleshy fruit-producing vegetable crop belonging into the genus *Solanum* of the family *Solanaceae*, which is commonly also called the ‘nightshades’. The genus *Solanum* is said to have evolved about 12 million years ago starting a rapid evolution and environmental adaption in multiple habitats (Wikström et al., 2001). Wild relatives of today’s cultivated tomato genotypes were native to the ‘new world’ mostly originating from the Southern American countries Ecuador, Peru, Chile and the Galápagos islands (Peralta and Spooner, 2007). The first domestication of tomato is thought to have taken place in Mexico or Peru. The Spanish conquerors started a larger distribution of tomato including the dispersal in Europe, and in the 18th century early colonist brought tomato to North America. After its introduction to Europe in the 16th century the close connection of tomato to the genus *Solanum* was already recognized mostly based on morphological characteristics, and in the middle of the 18th century two major phylogenetic systems were established within the family *Solanaceae* (Labate et al., 2007). The classification of tomato either into the rarely mentioned genus *Solanum* (Linnaeus, 1753) or the traditionally employed genus *Lycopersicon* (Tournefort, 1694; Miller, 1768) competed for more than 300 years. Only recently molecular genetics tools besides morphological and geographical characteristics lead to a re-evaluation, and with increasing acceptance tomato is today assigned into the phylogenetic genus *Solanum* (Spooner et al., 2005).

As a major contributor of vitamins, fiber, carbohydrates, nutrient metabolites, *Solanaceae* crops have a high nutritional importance and their fruits, tubers or seeds represent an essential part of the modern human diet (Labate et al., 2007). Particularly tomato is one of the world’s most popular vegetable crops with high economic value for the fresh vegetable market or for the production of processed food products (Labate et al., 2007). With an average production quantity of 151.699.405 t on 4.412.757 ha tomato was the second most important solanaceous vegetable crop in 2010 on a worldwide level following potato (FAOSTAT, 2012). In 2010, China was the top tomato producing country (47.116.084 t, 924.735 ha), followed by the European Union (16.881.321 t, 304.509 ha) and the United States of America (12.858.700 t, 15.859 ha) (FAOSTAT, 2012).

Over the last 40 years the considerable upward trend of the global tomato production was accompanied by an increase in the average harvested area (Table 1).

Table 1 Increase of tomato world production quantity and harvested area from 1970 – 2000 (FAOSTAT, 2012).

Year	Production quantity [t]	Area harvested [ha]
2000	110.026.417	4.029.366
1990	76.309.669	2.901.534
1980	52.650.437	2.443.422
1970	35.884.494	1.856.709

With a 950 Mb containing small diploid genome distributed on 12 chromosomes, a short regeneration time, routine transformation technology and a rich genetic and genomic resource, tomato is an excellent crop model organism (Matsukura et al., 2008). To get a deeper understanding on how the genomic evolution of the *Solanaceae* family accounts for phenotypic diversification and environmental adaption and effects genetic improvement, in 2004 a systems biology approach was initiated by the International *Solanaceae* Genome Project (SOL). A major goal of this multinational consortium was the identification of a tomato genome sequence as a reference for solanaceous plants and related taxa (Müller et al., 2005 b), and a high quality reference genome sequence of domesticated tomato was finally published and annotated in 2012 (The Tomato Genome Consortium, 2012). As a single entry point to a network of integrated resources, the major platform SOL Genomics Network (SGN) (<http://sgn.cornell.edu/>) offers detailed genomic information on tomato and related *Solanaceae* species (Müller et al., 2005 a). SGN provides the genome sequences, catalogues high-density physical and genetic linkage maps, quantitative trait loci (QTL) maps, introgression line (IL) maps, Contig maps, fluorescence *in situ* hybridization (FISH) maps, offers comprehensive molecular and physiological database resources and the appropriate bioinformatics analysis tools. Additionally, numerous tomato-specific expressed sequence tags (ESTs), full length cDNA sequences, unigene sequences, gene expression and metabolite data have been produced and are available worldwide in different databases including NCBI, SGN, MiBASE, SolEST, KafTom, TFGD (Matsukura et al., 2008; Aoki et al., 2010; Fei et al., 2011). Moreover, the central source providing collections of various tomato germplasm stocks, distributing seeds and maintaining a collection-related database is the Tomato Genetic

Resource Centre (TGRC) (<http://tgrc.ucdavis.edu/>). Altogether, these molecular resources promote forward genetics approaches to analyze the genetic basis of a certain phenotypic outcome but they also enable reverse genetic approaches to study changed phenotypic performances after gene modification.

Physiological and molecular aspects of *Verticillium dahliae* and the *Verticillium*-wilt disease

The agricultural value and the profitable production of the vegetable crop tomato are worldwide constrained due to multiple disease infestation. Therefore, a key topic in current tomato biotic stress research is the elucidation of plant diseases resistance mechanisms (Matsukura et al., 2008). Today, tomato is a well established model organism for the investigation of plant–pathogen relationships exhibiting susceptibility but also resistance against a broad range of pathogens (Arie et al., 2007). A prominent tomato-infecting pathogen is the soil-borne fungus *Verticillium dahliae* (*V. dahliae*), which causes the *Verticillium*-wilt disease on a worldwide level in temperate and subtropical regions (Bhat and Subbarao, 1999; Agrios, 2005). Together with the today generally recognized subspecies *V. nubilum*, *V. tricorpus*, *V. longisporium*, *V. albo-atrum*, *V. dahliae* belongs to the heterogeneous genus *Verticillium*, which is part of the large fungal phylum of ascomycota, also known as the ‘sac fungi’ (Inderbitzin et al., 2011). The *V. dahliae* genome consists of seven chromosomes and has an average total size of 28 Mb (Pantou and Typas, 2005). A classical criterion for the taxonomic order of subspecies in the genus *Verticillium* is the individual type of durable resting structures. *V. dahliae* produces dark pigmented microsclerotia which are clusters of dark melanized thick-walled hyphae cells separated from the parental mycelium (Inderbitzin et al., 2011). In addition, phylogenetic analysis focusing on species-specific ribosomal RNA gene-sequence differentiation is the most frequently employed way for a taxonomic classification of fungi (Pramateftaki et al., 2000; Fahleson et al., 2004).

The sexual reproduction of ascomycota is based on a multistep production of meiotic self-distributing ascospores within tube-shaped asci positioned on the ascocarp (Trail, 2007). However, a stage for a sexual recombination has not yet been described for the genus *Verticillium*, and *V. dahliae* is only known to propagate by asexual reproduction (Usami et al., 2009). In this process, vegetative mitotic spores, the conidia, are produced at the end of conidophores, a kind of specialized hyphae. During conidogenesis, the ovoid to elongated conidia arise at the open end of the conidophores and are ejected from specialized

conidiogenic cells called phialides. The typical 'verticillate' appearance of branched conidophores carrying whorls capped with flask-shaped and pointed phialides is name giving for the genus *Verticillium* (Klosterman et al., 2009; Pegg and Brady, 2002).

As the predominant causal agent of the *Verticillium*-wilt disease, the plant-pathogenic fungus *V. dahliae* covers a very broad spectrum of over 200 economically important mainly dicotyledonous host plant species including vegetables, fruits, ornamentals, high-value annual or perennial crops or woody perennials (Fradin and Thomma, 2006). *V. dahliae* infection-based reductions in yield or nearly complete yield losses annually cause huge financial problems for farmers worldwide (Subbarao et al., 1997). Moreover, due to the huge variance in symptom development and the similar appearance of several other fungal wilting diseases, no unique disease symptoms can be assigned to an infection by *V. dahliae*, and a specific visual diagnose is difficult. In tomato a typical symptom is the wilting of single leaflets or leaves after 4 - 5 dpi, followed by a 2 - 3 day recovery period with symptoms alleviation, and finally in sensitive plants the disease progresses with pronounced symptoms (Heinz et al., 1998; Chen et al., 2004). With ongoing infection leaves become chlorotic, necrotic and finally abscise. Additionally, a brown discoloration of vascular tissue may be visible in stem cross-sections and may be accompanied by whole-plant wilting and stunted grows. Following a dormant mycostatic phase, the monocyclic *Verticillium*-wilt disease-course begins with an activation of the soil-inherent vegetative primary inoculum. The durable microsclerotia start to germinate upon recognition of host and non-host plant root exudates in the rhizosphere (Krikun and Bernier, 1990). Hyphae structures are produced and extend towards the host roots (Fitzell et al., 1980). A parasitic phase begins with an initial colonization at different preferential host-root surface-sites, e.g. the root tip, the root elongation zone, the root hairs or the developing and lateral roots (Zhou et al., 2006; Vallad and Subbarao, 2008). After successful penetration of the root epidermis and cortical cells, at 4 dpi fungal hyphae start to grow in a spatial and temporal dynamic cyclic manner acropetally through the vascular tissue. In tomato stems the fungus is present at 2 - 4 dpi, rapidly becomes eliminated in vascular tissue from 6 - 8 dpi but in a compatible interaction with tomato host plants further spreads systemically from 9 - 10 dpi (Chen et al., 2004; Robb et al., 2007). Subsequent, conidia are produced and move with the transpiration stream through the xylem vessels until they are trapped in cavities between vessels. From there they start germinating and penetrate adjacent xylem vessels to continue the colonization of neighboring vascular cells and initiate new sporulation events. The successful vascular infection induces the host senescence and tissue

chlorosis and necrosis thereby starting into the final saprophytic phase of the wilt disease (Fradin and Thomma, 2006). The fungus now systemically colonizes its host plant and the increased production of *V. dahliae* microsclerotia assures its later survival after decomposition of infected plant material up to 15 years.

The production of cell wall-degrading enzymes is known for *Verticillium* species, but the exact molecular mechanisms and components contributing to fungal pathogenicity are not yet characterized (Dobinson et al., 1997; 2004). In contrast, the physiology of the host-plant defence is well studied. Many infections stay in a pre-vascular phase where the suberized endodermis and also the deposition of lignin on epidermal and cortical cell walls or around penetrating fungal hyphae represent physical barriers (Fradin and Thomma, 2006). The main physical barrier in the vascular phase is a suberization of vascular xylem vessel walls to limit the spread of the fungal pathogen (Robb et al., 1989; Robb et al., 1991). This suberin-based coating response starts already 4 hpi and only in a compatible interaction the fungal hyphae can escape and suppress these trapping sites leading to systemic plant colonization (Chen et al., 2004).

Despite these physical defence mechanisms recent analysis provided deeper insights into the genetics of plant-pathogen interaction. Tomato host plants were shown to possess a monogenic source of resistance against race 1 strains of *V. dahliae* and *V. albo-atrum* in their genome (Schaible et al., 1951). The dominant *Ve* locus exists on the short arm of chromosome 9 and has been cloned and sequenced from tomato (Kawchuk et al., 2001). The locus comprises two inversely orientated open reading frames (ORF) of the closely linked genes *Ve1* (*Verticillium* race 1) and *Ve2* which encode cell-surface receptors belonging into the family of extracellular leucine-rich repeat (eLRR) receptor-like proteins (RLP) (Diwan et al., 1999; Wang et al., 2008). Detailed single nucleotide polymorphism analysis revealed a single point mutation resulting in a premature stop codon within the *Ve1* gene in susceptible tomato genotypes (Fradin et al., 2009). This mutation causes an incomplete translation resulting in a truncated *Ve1* protein. Subsequent investigation of both genes by virus-induced gene silencing (VIGS) experiments as well as overexpression studies further proved that only the intact *Ve1* gene product provides race 1-specific resistance against *V. dahliae* (Fradin et al., 2009). The identification of downstream signalling components remains difficult since the *Ve1* resistance signalling only partially overlapped with the comparable well-studied tomato-*Cladosporium fulvum* (*Cf*) interaction (Thomma et al., 2005; Fradin et al., 2009). The

functional integration of tomato-derived *Ve1* into *Arabidopsis* is expected to clarify the molecular basis of signal transduction following *Ve1*-mediated pathogen recognition (Fradin et al., 2010).

Mechanisms of sulfur-enhanced defence and synthesis of sulfur-containing defence compounds

The protective management of the *Verticillium*-wilt disease remains to be difficult, since the presence of a molecular source for resistance against *Verticillium* in commercially used tomato plants is still not sufficient to completely prevent an initial infestation with the pathogen. Furthermore, in related plant species *Ve1* homologues have been identified, but an active functioning was not confirmed and most plant species completely lack a genomic source for resistance (Chai et al., 2003; Fei et al., 2004; Simko et al., 2004). Therefore, a huge number of different management strategies were developed over the past decades. Due to the exclusively vascular tissue localization of the fungus, the majority of approaches focused on a plant external reduction or elimination of sources for the primary inoculum. The protective impact of all strategies remained inconsistent and was, in partial, even associated with environmental and human risk. All together, these circumstances call for a more effective and safe protection mechanism against *V. dahliae*.

A promising strategy, therefore, seems to be the plant innate process of S-enhanced defence (SED). The special connection between plant S supply and resulting plant S nutritional status in establishment of biotic stress resistance is known for a long time. In a number of experiments supplementary fertilization with S was shown to have a negative effect on the colonization of plants by different fungal pathogens (Klickoka et al., 2005; Bloem et al., 2005; Dubuis et al., 2005; Salac et al., 2006). These observations can be assigned to the antimicrobial mechanisms of SED, which utilize S-containing defence compounds (SDCs) for the plants protection against fungal pathogens. The biosynthesis of the antifungal SDCs is closely connected to the primary plant S metabolism (Rausch and Wachter, 2005; Kruse et al., 2007). In general, the primary S metabolism exhibits a demand-driven gene regulation pattern, with S deficiency activating the uptake of sulfate by root-located sulfate transporters and subsequently enhancing the assimilation of sulfate at the step of adenosine 5-phosphosulfate reduction (Takahashi et al., 2011; Kopriva et al., 2012). Under conditions of optimal or supra-optimal S supply, all steps of the primary plant S metabolism are saturated but the pool of secondary S metabolites is increasingly filled with reduced S for the synthesis

of a wide variety of SDCs (Rausch and Wachter, 2005). Additionally, in the presence of a fungal pathogen S metabolite pools are further increased and particularly in resistant plants high concentrations of cysteine (Cys) and different SDCs were measured (Williams et al., 2002; Falk et al., 2007; Kruse et al., 2012; Chapter I). The group of constitutive and pathogene-inducible SDCs includes plant secondary S-rich metabolites with a great diversity in chemical structures and modes of action. The most important and best-studied secondary S metabolites are glutathione, glucosinolates, alliins, S-rich thionines and defensins, phytoalexins, H₂O₂, and H₂S (Rausch and Wachter, 2005; Burow et al., 2008). A relatively new member in the group of active S-defence compounds is the inorganic phytoalexin elemental sulfur (S⁰), which was found in different plant taxa (*Malvaceae*, *Solanaceae*, *Fabaceae*) in relation to an infection with fungal and bacterial vascular pathogens (Resende et al., 1996; William et al., 2002; Williams and Cooper, 2003; Novo et al., 2007). As an example for the family of *Solanaceae* high levels of S⁰ were detected in the plant vascular tissue of resistant tomato and pepper plants after colonization with *V. dahliae* (Williams et al., 2002; Novo et al., 2007). S⁰ is one of the oldest non-systemic fungicides and today still applied in integrated pest management programs or organic farming mostly against powdery mildew infestations on fruit and vegetable crops (Williams and Cooper, 2004). *In vitro* bioassay experiments were conducted to assess the toxicity of plant S⁰ towards plant vascular fungal pathogens and clearly demonstrated an inhibition of spore germination, germ tube germination and mycelium growth (Williams and Cooper, 2004). However, neither the exact *in planta* mode of fungitoxic S⁰ action nor the *in planta* S⁰ biosynthesis pathway with its participating genes are yet characterized.

Therefore, this study will focus on tomato as a plant model organism to characterize the processes involved in vascular located SED and to identify key players participating in the biosynthesis of S^0 . The following study was divided into four consecutive fields of research:

- (1) Establishment and physiological characterization of the Tomato-*Verticillium* pathosystem in relation to the plant S nutritional status.
- (2) Transcriptional identification of tissue-specific S metabolism-related gene expression profiles in the tomato-*Verticillium* pathosystem.
- (3) *Verticillium*-related physiological and transcriptional characterization of SED mechanisms in a tomato introgression line population.
- (4) Development of forward genetics molecular tools for an overexpression of selected S metabolism-related candidate genes in the tomato-*Verticillium* pathosystem.

Chapter I - Sulfur supply impairs spread of *Verticillium dahliae* in tomato

Katharina Bollig¹, André Specht¹, San Shwe Myint², Marc Zahn¹ and Walter J. Horst¹

(1) Institute for Plant Nutrition, Leibniz University Hannover, Herrenhäuserstraße 2, 30419 Hannover, Germany

(2) Department of Horticulture, Yezin Agricultural University, Ministry of Agriculture and Irrigation, Myanmar

Published in: European Journal of Plant Pathology (2013), 135 (1), 81 – 96.
doi: 10.1007/s10658-012-0067-5

Abstract

Vascular wilt caused by the soil-borne fungus *Verticillium dahliae* is a major yield and quality-limiting disease in a broad spectrum of crop plants worldwide. Sulphur-enhanced plant defence mechanisms provide an opportunity to effectively and environmentally safely constrain the wilt disease levels *in planta*. To evaluate the influence of sulphur nutrition on the protective potential of these mechanisms, two near-isogenic tomato genotypes differing in fungal susceptibility, were treated with low or supra-optimal sulphur supply. Microscopic analysis revealed a significant sulphur-induced decrease in the amount of infected vascular cells in both genotypes. However, plant shoot and severely pathogen-affected root growth did not display this distinct alleviating influence of sulphur nutrition. Rates of leaf photosynthesis were impeded by *Verticillium dahliae* infection in both genotypes especially under low sulphur nutrition. However, assimilate transport rates in the phloem sap were enhanced by fungal infection more in the resistant genotype and under high sulphur nutrition suggesting a stronger sink for assimilates in infected plant tissues possibly involved in sugar-induced defence. A SYBR Green-based absolute quantitative Real-Time assay using a species-specific primer was developed which sensitively reflected sulphur nutrition-dependent changes in fungal colonization patterns. High sulphur nutrition significantly reduced fungal spread in the stem in both tomato genotypes. Concentrations of selected sulphur-containing metabolites revealed an increase of the major anti-oxidative redox buffer glutathione under high sulphur nutrition in response to fungal colonization. Our study demonstrates the existence of sulphur nutrition-enhanced resistance of tomato against *Verticillium dahliae* mediated by sulphur-containing defence compounds.

Keywords: Absolute Real-Time; Sulphur-enhanced defence; Sulphur-containing defence compound; Tomato; *Verticillium dahliae*

Introduction

Verticillium dahliae (*V. dahliae*), a soil-borne phyto-pathogenic ascomycete, is a prominent generator of monocyclic vascular wilt disease in plants worldwide. A wide spectrum of more than 200 economically important dicotyledonous plant species, legumes, vegetables, ornamentals, trees, and weeds serve as host plants (Fradin and Thomma, 2006; Klosterman et al., 2009). An easy-to-use chemical containment of this serious agronomic disease proves to be difficult, since the affected vascular plant tissue cannot be directly reached from outside. For a number of susceptible crops the main protection methods include crop rotation, grafting, addition of soil amendments, and fumigation (Larkin et al., 2010; Bletsos et al., 2003; Goicoechea, 2009). Until today the methods for non-chemical disease suppression have limited long-term effectiveness. In combination with yield and quality losses which set high economic pressure on the farmers, these unsatisfying circumstances call for a simple, effective and environmentally acceptable defence strategy. A genetic source for resistance against *V. dahliae* race 1 strains in *Solanaceae* is the dominant *Ve* resistance locus, which has been sequenced and cloned from tomato (Diwan et al., 1999; Kawchuk et al., 2001; Fradin et al., 2009). Other than this no effective fungicide preventing pathogen infestation is available and once infected there are currently no possibilities to overcome disease in most susceptible plants. Therefore, current research focuses on the elucidation of further resistance-promoting mechanisms. Sulphur (S)-deficient growth conditions were shown to promote plants disease susceptibility against selected fungal pathogens (Dubuis et al., 2005). In turn a soil-applied S fertilization leads to a reduction in symptom development and fungal pathogen content (Klikocka et al., 2005). Therefore, a promising strategy seems to be the plant-innate process of S-enhanced defence (SED) which is closely linked to reductive S assimilation (Kruse et al., 2007). SED is an effective protection against the colonization of plants by diverse fungal pathogens. A variety of S-containing defence compounds (SDCs) derived from primary S metabolism are known to serve as constitutive and induced antimicrobial metabolites under biotic stress conditions (Rausch and Wachter, 2005). Belonging into the group of active S-defence compounds, the inorganic phytoalexin elemental S (S^0) was found to be synthesized in several plant families in response to fungal contact (Williams and Cooper, 2003). Within members of the *Solanaceae* family resistant tomato and pepper genotypes accumulated high levels of S^0 in vascular plant tissue upon *V. dahliae* inoculation (Williams et al., 2002; Novo et al., 2007). It was proposed that S^0 may enter fungal cell walls where it is reduced to fungicidal H_2S , disturbs fungal redox homeostasis or competes as an electron acceptor in the fungal respiratory chain (Beffa, 1993; Tweedy, 1981). But so far, the real mode of action and

the elucidation of the exact mechanisms and participating genes of S^0 synthesis in the plant vasculature remain a topic of basic plant research.

The aim of this study was to investigate the potential of supra-optimal S nutrition to activate SED mechanisms limiting fungal growth in tomato plants colonized by *V. dahliae*. Therefore, we developed a SYBR Green-based quantitative Real-Time polymerase chain reaction (qRT-PCR) assay, including a *V. dahliae* specific primer pair localized within the variable internal transcribed spacer 2 (ITS2) region of the fungal ribosomal operon. The sensitive measurement of fungal genomic DNA (gDNA) in tomato plants with contrasting S nutritional status, and the combined analysis of selected physiological parameter including quantification of suberized xylem vessels, root development and architecture, photosynthesis rates, phloem exudates, cysteine (Cys) and glutathione (GSH) measurement enabled deeper insights into the role of SED and associated SDCs in the tomato-*Verticillium* pathosystem.

Material & Methods

Cultivation of plant material

The near-isogenic tomato cultivars (cvs) Craigella GCR 26 (GCR 26) (LA3247) and GCR 218 (LA3428) (*V. dahliae*-sensitive and resistant, respectively; Chen et al., 2004) were cultivated in a climate chamber, with a 16 / 8 h light / dark regime, 25 / 20 °C day / night temperatures, 70 % relative air humidity and a photon flux density of 200 mmol m⁻² s⁻¹ (photosynthetic active radiation). After germination, plants were transferred to peat moss (Klasmann-Deilmann GmbH, Geeste, Germany) limed with CaCO₃ to pH 5.0 in 1-l pots. Plants were pre-cultured for 3 weeks until fungal inoculation and harvested 7 dpi. During this 4 week cultivation period a full nutrient solution was applied every second day. The composition of the solution was: 7.00 mM KNO₃, 0.90 mM MgCl₂, 1.00 mM KH₂PO₄, 1.70 mM Mg(NO₃)₂, 0.10 mM NaCl, 5.00 mM Ca(NO₃)₂, 2.00 mM CaCl₂, 50 µM FeNaEDTA, 1.3 µM ZnSO₄, 24.5 µM H₃BO₃, 6.0 µM CuSO₄, 0.8 µM (NH₄)₂ MoO₄, 9.3 µM MnSO₄. Plants treated with low S supply did not receive additional S. To obtain a supra-optimal S supply plants were additionally supplied with 25.0 mM K₂SO₄.

Cultivation of fungal pathogens and inoculation method

All fungal isolates used in this study are described in Table 1. Long term culturing occurred on potato dextrose agar (Duchefa, Haarlem, Netherlands) in the dark at 24°C. For the production of inoculum, fungi were transferred into sucrose sodium nitrogen medium and cultivated at 100 rpm and 26 °C for 3 weeks. The spore concentration was diluted to 1·10⁻⁷ spores ml⁻¹ with water (dH₂O) in a haemocytometer. Plants were carefully uprooted and roots were gently washed free of substrate in dH₂O. Then 1 / 3 of the total root mass was cut off and roots were inoculated in 80 ml spore suspension for 1 h at 110 rpm. Control plants were mock inoculated in 80 ml dH₂O following the same procedure. Afterwards all plants were transferred into new CaCO₃-limed peat moss.

Table 1 Selected fungal isolates used in a cross-reaction absolute qRT-PCR assay to identify the LeVD isolate-specific binding sensitivity.

Species	Host	Isolate Code ^a	Origin ^b
<i>Alternaria alternata</i> (<i>A. alternata</i>)	<i>Beta vulgaris</i>	DSM 62006	1
<i>Alternaria solani</i> (<i>A. solani</i>)	Tomato	DSM 2947	1
<i>Aspergillus niger</i> (<i>A. niger</i>)	Soil	DSM 2182	1
<i>Botrytis cinerea</i> (<i>B. cinerea</i>)	Tomato	DSM 877	1
<i>Pseudocercospora fuligena</i> (<i>P. fuligena</i>)	Tomato	n. a.	2
<i>Verticillium dahliae</i> (<i>V. dahliae</i>)	Tomato	n. a.	3

^a n. a., isolate code not available.

^b 1, isolate from German Resource Centre for Biological Material, Braunschweig, Germany; 2, isolate from Prof. Hau, Institute of Plant Diseases and Plant Protection, Hannover, Germany, isolated at the Asian Institute of Technology, Pathumthani, Thailand; 3, isolate from Institut für Gemüse- und Zierpflanzenbau, Grossbeeren, Germany.

DNA extraction

The epidermis and outer cortical cell layers were removed mechanically and the remaining surgically dissected hypocotyl tissue including plant vascular tissue was homogenized under liquid nitrogen. The isolation of genomic DNA (gDNA) followed a modified cetyltrimethylammonium bromide (CTAB) method including 200 mg (fresh weight) dissected hypocotyl tissue or 50 mg (fresh weight) homogenized fungal mycelia as described in Zahn et al. (2011).

Identification and cloning of fungal ITS region

For the identification of the *V. dahliae* ITS regions a 50 µl conventional PCR reaction was set up (iProof HF buffer (5 x), dNTPs (200 nM each), iProof HF Polymerase (5 U) (BioRad Laboratories, Hercules, USA)), including 50 ng of fungal gDNA and 400 nM Primer ITS 4 and ITS 5 (White et al., 1990). The PCR parameters comprised an initial denaturation of 30 s at 98°C, followed by 33 cycles at 98 °C for 10 s, 60 °C for 30 s and 72 °C for 30 s, and a final elongation step at 72 °C for 7 min. For sequencing the purified fragment was cloned into the

pGEM-T-Easy vector system (Promega Corporation, Madison, USA). The sequence from isolate *V. dahliae* TomIGZ was submitted to GenBank (GU060637).

Primer design for absolute qRT-PCR

The sequence of the isolate *V. dahliae* TomIGZ and a selection of related ITS regions from tomato-infecting fungal pathogens were aligned using Vector NTI Advanced 10 (Invitrogen, San Diego, USA). The ITS sequences of *A. alternata* (AF347031), *A. solani* (AY154715), *P. fuligena* (GU060636), *B. cinerea* (AJ716294), *A. niger* (FJ668837), *Verticillium albo-atrum* (AY555955), *Fusarium oxysporium* (AB369259), and *Solanum lycopersicum* (AY552528) were obtained from the ncbi public database. Primer pairs were designed using the primer 3 plus software (Untergasser et al., 2007) and annealed to non-conserved regions within the fungal ribosomal operon.

Absolute qRT-PCR conditions

The 25 μ l SYBR Green-based mix included Hot-Start PCR buffer (1 x), MgCl₂ (3.6 mM), 1,000 x SYBR Green-I (0.1 x) (Invitrogen GmbH, Darmstadt, Germany), dNTPs (200 nM each), forward and reverse primer (252 nM each), 0.75 U DCS Hot-Start DNA polymerase (DNA Cloning Service, Hamburg, Germany), 100 ng gDNA template. Thermal qRT-PCR cycling stages were performed in a CFX96™ Real-Time detection system (BioRad Laboratories, Hercules, USA) and consisted of an initial denaturation at 95 °C (10 min), followed by 30 cycles at 95 °C (15 s), 60 °C (30 s), 72 °C (30 s) and a final melting curve analysis from 60 °C to 95 °C with a 0.5 °C · 5 s⁻¹ increasing temperature gradient.

Primer Evaluation

All primer pairs were initially tested for the amplification of predicted fragment sizes, primer dimerization, or multiple unspecific amplification in 25 μ l a conventional PCR assay including Hot-Start PCR buffer (1 x), MgCl₂ (3.6 mM), dNTPs (200 nM each), forward and reverse primer (252 nM each), 0.75 U DCS Hot-Start DNA polymerase (DNA Cloning Service, Hamburg, Germany), 100 ng gDNA template. The amplification efficiency was tested in an absolute qRT-PCR for each primer pair including a *V. dahliae* gDNA serial dilution of 20, 4, 0.8, 0.16, 0.032, 0.0064 ng. To determine the potential interference of tomato gDNA, each *V. dahliae* gDNA dilution point was mixed with 20 ng of gDNA from uninfected tomato plants. An isolate-specific binding of the *V. dahliae* ITS2 primer pair LeVD was tested in an absolute qRT-PCR assay with selected tomato-infecting fungal

isolates. For the determination of cross-reaction levels, 20 ng gDNA of each selected fungal isolate were checked against the five-fold *V. dahliae* gDNA serial dilution.

Cytological staining procedures

For histochemical analysis of suberization in tomato vascular tissue, free-hand sections were obtained using a razor blade and stained with a sudan III / IV based method according to Robb et al. (1991). Staining of *V. dahliae*-specific mycelium within infected hypocotyl tissue was performed using the fluorescent lectin Alexa Fluor[®] 488 (Invitrogen GmbH, Darmstadt, Germany). Free-hand sections were incubated according to the manufacturer's protocol and observed under UV illumination with an Axioscope microscope (Zeiss, Jena, Germany).

Analysis of photosynthesis rate and phloem exudates

The photosynthesis rate was measured with a portable gas-exchange system (LI-6400, LICOR, Lincoln, NE, USA) at a photosynthetic photon flux density of 1,000 $\mu\text{mol m}^{-2} \text{s}^{-1}$ and an incoming CO_2 concentration of 360 $\mu\text{mol mol}^{-1}$. Measurements included 6 cm^2 of the terminal leaflet from the youngest fully expanded leaf on each plant. Phloem exudates were collected according to Cakmak et al. (1994) using intact tomato shoots. Plants were cut off below the hypocotyl 4 h after the onset of the light period. Immediately after recutting under dH_2O , plants were placed in 5 ml 20 mM Na-EDTA solution (pH 6.0). About 1 cm of the shoot was immersed in solution while plants were kept in the dark at high humidity. Phloem sap was sampled after 2 h and sugars were quantified with the anthrone method (Dreywood, 1946) in a μQuant Scanning Microplate Spectrophotometer (BioTek, Bad Friedrichshall, Germany) at $\lambda = 620 \text{ nm}$. A standard curve included 0, 25, 50, 100, 150, 200 $\mu\text{g ml}^{-1}$ D-glucose.

Sulphur and potassium analysis

Following analysis of plant height and fresh weight, leaves and hypocotyls were dried at 65 °C for 72 h. The dry weight was measured and samples were grinded and homogenized for determination of total S using a Vario EL CNS analyzer (Dumas Elementar Analysensysteme GmbH, Hanau, Germany). For potassium (K) analysis, leaf material was wet digested with ultrapure concentrated HNO_3 at 135 °C for 35 min in a MLS-ETHOS plus microwave oven (Mikrowellen-Laborsystem, Leutkirch, Germany). Concentrations in the solutions were quantified by inductively coupled plasma optical emission spectrometry (Spektro Analytical Instruments, Kleve, Germany).

Determination of sulphur containing metabolites

High pressure liquid chromatography (HPLC) measurements were made with an Agilent reversed phase column (Eclipse XDB C18, 5 μm , 4.6 150 mm) in an Agilent 1200 infinity series HPLC system (Agilent Technologies Deutschland GmbH, Böblingen, Germany). For the analysis of thiols 50 mg fresh plant material were extracted and derivatized as described by Riemenschneider et al. (2005). Elution was performed with a gradient of solvent B (100 % methanol) in solvent A (0.1 M potassium acetate buffer, pH 5.5) at a flow rate of 0.5 ml min⁻¹: 18.5 % for 9 min, 18.5 % - 100 % for 2 min, 100 % solvent B for 13 min, and fluorescence of the column eluent was detected at λ_{ex} 380 / λ_{em} 480. For the analysis of S⁰ 300 mg fresh plant material were mixed with 1 ml dichloromethane (DCM), incubated for 15 min in an ultrasonic bath and centrifuged at 10,000 g for 10 min. The supernatant was kept and the remaining pellet was dissolved in 0.5 ml DCM and transferred to a 0.2 μm GHP Membrane Nanosep[®] MF Centrifugal Devices (Pall GmbH, Dreieich, Germany). Samples were centrifuged two times at 5,000 g for 5 min and rinsed with 0.5 ml DCM. All extracts were pooled. For the standard curve and the calibration of HPLC measurements S⁰ was dissolved in DCM. A recovery rate of 77 % was detected after addition of S⁰ to fresh plant material. Elution was performed with 100 % methanol at a flow rate of 1.0 ml min⁻¹ for 10 min, and the signal was detected at $\lambda = 264$ nm with a DAAD. S⁰ elemental spectrum was recorded at $\lambda = 230 - 600$ nm.

Statistical analysis

A completely randomized design including three biological replicates each composed of three individual plants was used for the experiments. Analysis of variance was performed using the general linear model procedure of the statistical program SAS 9.1 (SAS Institute, Cary, NC, USA) testing for genotype, fertilization, infection and their interaction effects.

Results

Symptoms of *V. dahliae*-induced wilting disease were visible within 7 dpi in both tomato genotypes. Growth reduction particularly of the sensitive tomato genotype was accompanied by severe wilting symptoms including flagging of single leaflets within whole leaves (Figure 1 a). With ongoing disease development wilted tissue turned chlorotic and later necrotic showing a typically V-shaped lesion pattern especially on leaf tips. *V. dahliae*-induced plant protective mechanisms included suberinization of vascular tissue in tomato hypocotyls. Cross sections below cotyledons revealed dark brown discoloration of vascular bundles (Figure 1 b) representing the cell-wall coating response aiming at limiting pathogen spread by penetration of lateral xylem vessels.

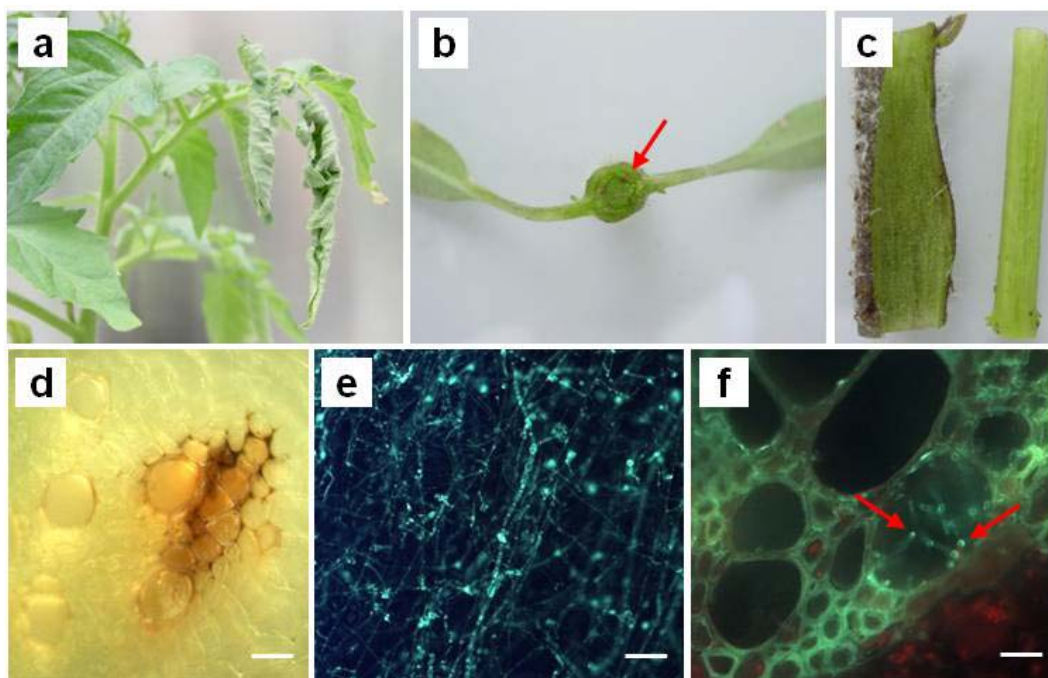


Figure 1 Typical symptoms of *Verticillium* wilt disease 7 dpi in sensitive tomato GCR 26 plants. **a** Severe *V. dahliae* derived tracheomyces of vascular tissue resulted in the wilting of single leaflets. **b** Infection-induced browning of tomato vascular tissue. Red arrow indicates dark brown occlusions of vascular vessels. **c** Mechanical removal of the epidermis and outer cortical cell layers from harvested hypocotyls. **d** Sudan III / IV stained pathogen-induced suberin deposition in infected vascular bundle. The *white bar* represents a scale of 10 μm at a magnification of 100 fold. Sections were examined under bright-light. **e** Alexa Fluor[®] 488 staining of *V. dahliae* structures on PDA plates and **f** in free-hand hypocotyl cross-sections. Sections were examined under UV-light. *Red arrows* indicate green fluorescent fungal mycelium structures emerging from colonized xylem vessels. The *white bars* represent a scale of 10 μm at a magnification of 200 fold.

From harvested hypocotyls the outer epidermal and cortical cell layers were removed from the inner vascular tissue parts mechanically (Figure 1 c). Hypocotyl cross sections revealed suberin depositions on cell walls of infected xylem vessels and in intercellular spaces. The plants protective vascular coating reaction of xylem vessels could be visualized with a Sudan III / IV staining procedure (Figure 1 d). Specific binding of fluorescent wheat germ agglutinin conjugates to carbohydrate residues in fungal cell walls (Figure 1 e) enabled monitoring of fungal spread at the single cell level. The colonization of xylem vessels and xylemparenchyma cells could be detected by lectin-based immunolabeling 7 dpi in both tomato genotypes and showed a close spatial relation to the coating response and cell occlusion within vascular tissue (Figure 1 f).

As could be expected, the differing S supply led to plants with widely differing S concentrations in the plant tissues. The S concentrations of the leaves (Figure 2 a) of about 2 and 9 mg g⁻¹ dry wt. indicated weak S deficiency (in agreement with slight chlorosis of leaves, not shown) and luxury consumption at the low and high S supplies, respectively. The infection increased the S concentrations in the plant tissue at the low S supply, but decreased them at the high supply (significant S x VD interaction).

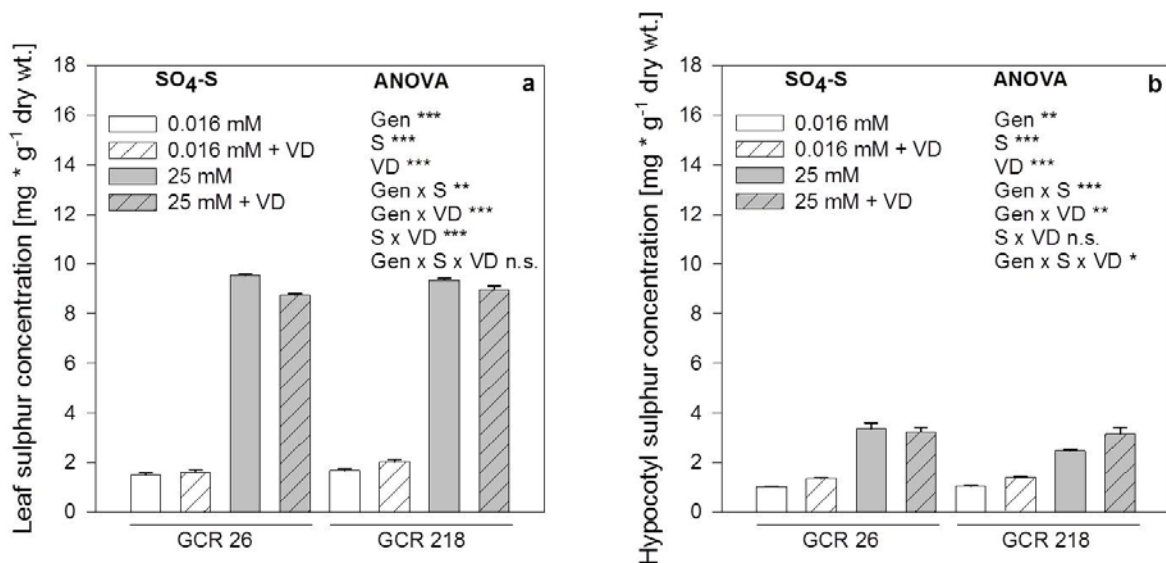


Figure 2 Effect of S supply on S concentrations in **a** leaves and **b** hypocotyls of *V. dahliae* (VD) - infected tomato genotypes differing in fungal resistance. (After 3 weeks of pre-culture at 25 mM or 0.016 mM SO₄-S plants were root inoculated and harvested 7 dpi. Data represent means ± SD *n* = 3. Results of the analysis of variance are given according to their level of significance as *, **, ***, for P ≤ 0.05, 0.01, 0.001, respectively, n.s. non-significant.)

The tomato genotypes differed slightly in S concentrations which were lower in the sensitive and higher in the resistant genotype (significant S x Gen interaction). The S concentrations in the hypocotyl tissue (Figure 2 b) were much lower particularly at the supra-optimal S supply ranging from about 1 to 4 mg g⁻¹ dry wt. The treatment effects were similar in the hypocotyl and leaf tissues.

Plants fertilized with full nutrient solution received potassium (K) in the form of KNO₃ and KH₂PO₄. Supra-optimal S-supplied plants additionally received K in the form of K₂SO₄. High K uptake might influence the applied parameters throughout the whole experiment, thus the leaf K concentration was analyzed 7 dpi (Table 2). After four weeks of cultivation leaf K concentrations revealed differences depending on fertilization level, infection status and genotype. Whereas K concentrations only slightly differed between infected and control plants at high S supply, infection reduced K concentrations greatly at low S supply. However, all values were in the nutritional sufficiency range of 30 – 60 mg g⁻¹ dry wt. (Zorn et al., 2006).

Table 2 Leaf potassium concentrations [mg g⁻¹ dry wt.] of tomato genotypes harvested 7 dpi.

Genotype	25 mM SO ₄ - S		0.016 mM SO ₄ - S	
	Infection	Control	Infection	Control
GCR 26	45.55 ± 0.03	47.51 ± 2.42	33.89 ± 1.80	44.03 ± 1.48
GCR 218	43.34 ± 0.26	47.40 ± 3.61	32.75 ± 1.71	41.03 ± 0.79

The light microscopic visualization of suberin-coated xylem vessels in the sudan III / IV stained hypocotyl cross sections allowed the counting of *V. dahliae* infected vascular cells (Figure 3 a), which represents the level of fungal penetration into above-ground plant parts as affected by genotype and S nutrition. Comparison of both tomato genotypes under low S nutrition revealed the highest number of suberin-coated vessels in the sensitive genotype GCR 26. Supra-optimal S supply significantly reduced the number of infected cells in both genotypes. These differences in response to *V. dahliae* infection between the genotypes developed into significant differences in plant growth measured as shoot height (Figure 3 b). The infection by *V. dahliae* but not the S nutrition resulted in slightly, but highly significantly (VD***) reduced shoot growth. The uninfected resistant genotype showed an overall higher

shoot length (Gen***). Genotypic differences in response of shoot length to pathogen infection (Gen x VD) were not significant (n.s.) at 7 dpi, but became significant only at longer treatment periods (data not shown).

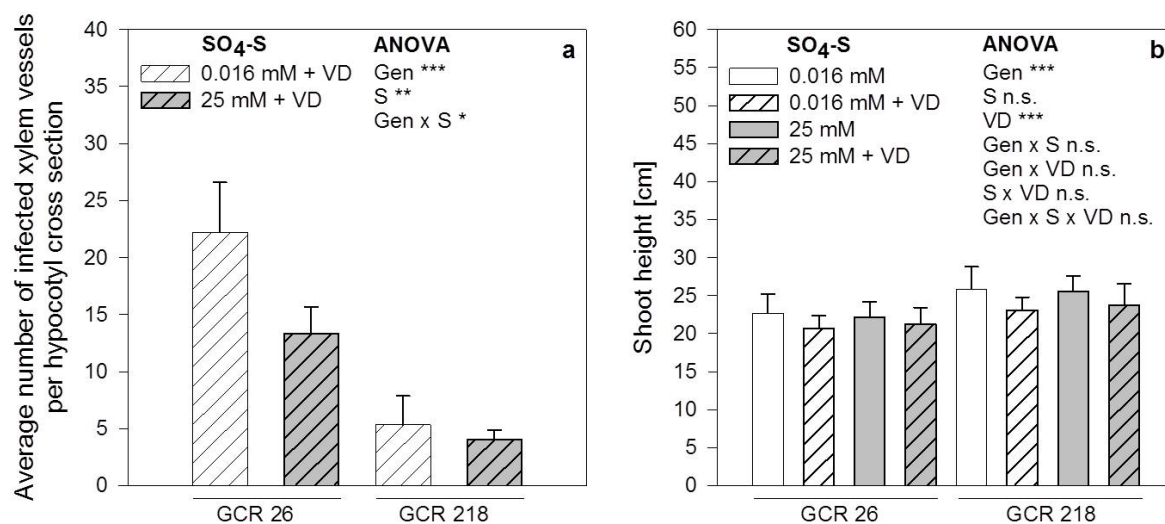


Figure 3 The average number of suberized xylem cells and the average shoot height as affected by the plant S status and *V. dahliae* (VD) infection. **a** The distribution of the fungal pathogen was analyzed on the single-cell level. The colonization level of xylem tissue is represented by the number of suberin-coated xylem vessels which were light microscopically detected in sudan III / IV stained hypocotyl cross sections. Non-infected plants did not show any suberization (not shown). **b** The effect of S nutrition and fungal inoculation on tomato shoot height. (After 3 weeks of pre-culture at 25 mM or 0.016 mM SO₄-S plants were root inoculated and harvested 7 dpi. Data represent means \pm SD $n = 3$. Results of the analysis of variance are given according to their level of significance as *, **, ***, for $P \leq 0.05$, 0.01, 0.001, respectively, n.s. non-significant.)

In contrast to the shoots both tomato genotypes showed a distinct response of the root system to fungal infection and S supply (Figure 4 a, b). The colonization by *V. dahliae* had a major impact on tomato roots already 7 dpi. In comparison to newly initiated growth after root-cutting of control plants, the root-length reduction was clearly visible due to an infection in high and low S-supplied plants. The stunted root architecture was characterized by a low branching rate of the fine root system, shorter roots and thus lower root biomass. The distinct visual changes could be confirmed by root-length measurements (Figure 4 c). *V. dahliae* infection inhibited root growth (highly significant VD effect) with the exception of the

resistant genotype GCR 218 at low S supply. High S supply enhanced root growth in both genotypes in control but not in infected plants (significant S x VD interaction)

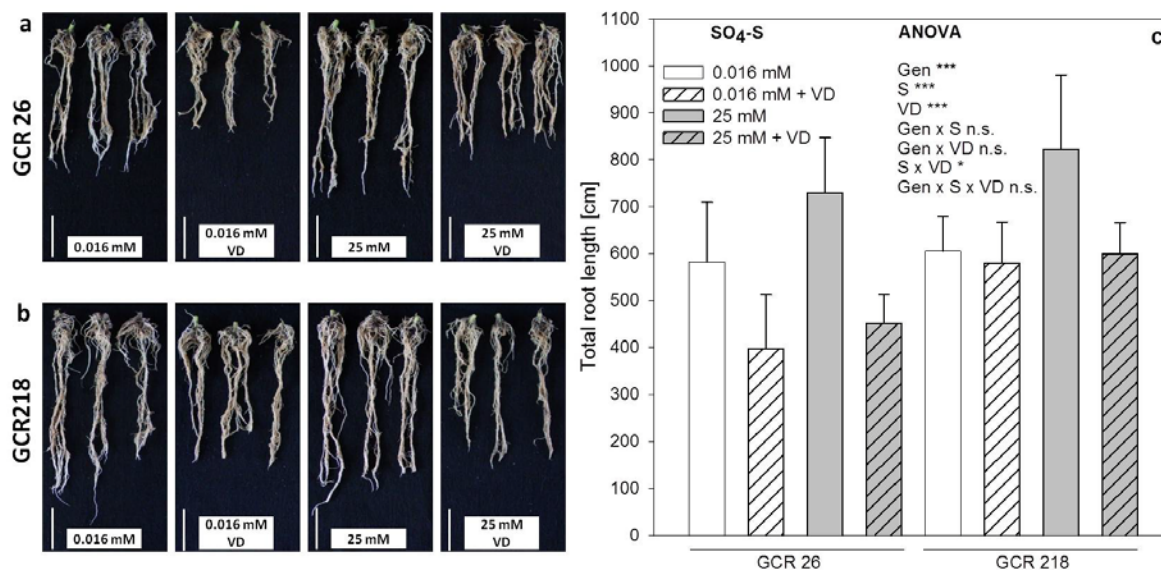


Figure 4 Root systems of **a** the *V. dahliae* (VD) resistant genotype GCR 218, **b** the sensitive genotype GCR 26 and **c** total root-length measurement of both tomato genotypes 7 dpi. Bar represents 5 cm. (After 3 weeks of pre-culture at 25 mM or 0.016 mM SO₄-S plants were root inoculated and harvested 7 dpi. Data represent means \pm SD, $n = 3$. Results of the analysis of variance are given according to their level of significance as *, **, ***, for $P \leq 0.05$, 0.01, 0.001, respectively, n.s. non-significant.)

Low S supply decreased photosynthesis of the youngest fully developed leaf in both tomato genotypes and, additionally, a *V. dahliae* infection reduced photosynthesis in the sensitive and resistant genotypes by 89 and 79 %, respectively (Figure 5 a). However, the pathogen infection-induced reduction of photosynthesis was equal but less at high compared to low S supply in the resistant and sensitive genotype (60, 61 %). Phloem-sap samples collected after 2 h of exudation did not reveal significant differences in sugar transport rates in relation to S supply in all control plants (Figure 5 b). In contrast, the fungal colonization of the tomato tissue initiated an increase in the rate of assimilate transport with the exception of the sensitive genotype GCR 26 at low S supply (significant Gen x VD interaction). Sugar transport rate was intensified by supra-optimal S nutrition leading to a sugar transport rate of 177 and 382 $\mu\text{g h}^{-1}$ in the phloem of the plants of the sensitive and resistant genotype, respectively.

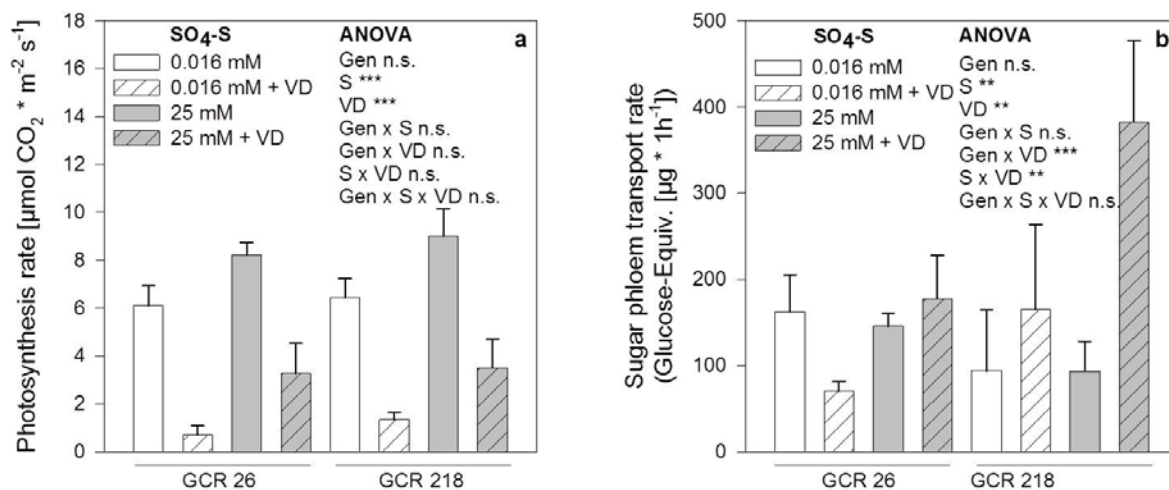


Figure 5 Photosynthesis rate in tomato single leaflets of the youngest fully developed leaf **a** and sugar transport rate in phloem exudates **b** collected after dissection of shoots from plants of two tomato genotypes differing in *V. dahliae* (VD) resistance. (After 3 weeks of pre-culture at 25 mM or 0.016 mM SO₄-S plants were root inoculated and harvested 7 dpi. Data represent means \pm SD, $n = 5$. Results of the analysis of variance are given according to their level of significance as *, **, ***, for $P \leq 0.05$, 0.01, 0.001, respectively, n.s. non-significant.)

Adoption of the primers ITS1 and ITS4 from White et al. (1990) which span the highly variable ITS1 and ITS2 area surrounding the 5.8S-coding sequence in the fungal ribosomal operon, enabled the identification of this ribosomal DNA (rDNA) region in the hyphae of the *V. dahliae* isolate TomIGZ. The amplification product was cloned into the pGEM-T-Easy vector system prior to sequencing. Subsequently, a sequence alignment of fungal rDNA regions including *V. dahliae* in comparison to a selection of typically tomato-infecting fungi revealed heterogeneous DNA sections suitable for the design of *V. dahliae*-specific forward and reverse primers within the ITS2 area. LeVD amplified a predicted 126 bp fragment, which did not show significant homology to other fungal DNA sequences (Figure 6 a) and was, therefore, chosen for absolute qRT-PCR analysis. Dimerization products or multiple non-specific amplification products were not detectable in a conventional PCR (Figure 6 b). The species-specific primer pair LeVD (GTG TTG GGG ATC TAC GTC TGT A / TCT AAA CCC CCT ACA AGC CC) was located within non-conserved parts of the ITS2 region of the *V. dahliae* isolate TomIGZ (Figure 6 c).

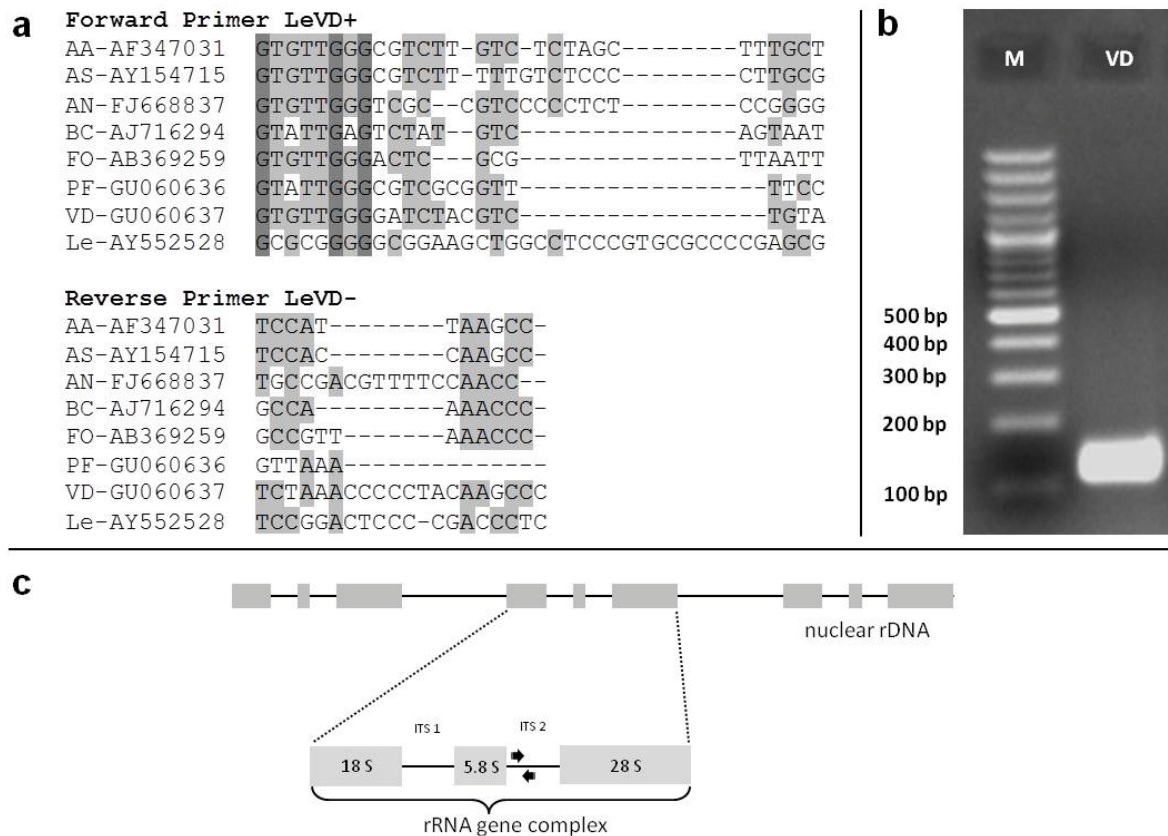


Figure 6 Specificity analysis of *V. dahliae* isolate TomIGZ specific primer pair LeVD. **a** Sequence alignment including *V. dahliae* isolate TomIGZ, a selection of fungal pathogens and a tomato reference for the identification of variable sequences within the ITS2 region (dark grey: identical, light grey: conservative, white: non-similar) (*A. alternaria* (AA), *A. solani* (AS), *A. niger* (AN), *B. cinerea*, (BC), *F. oxysporium* (FO), *P. fuligena* (PF), *S. lycopersicum* (Le), 100 bp molecular marker (M), *V. dahliae* isolate TomIGZ (VD)). **b** Detection of the specific LeVD amplification product in a conventional PCR. **c** Strategy for an absolute qRT-PCR based quantification of *V. dahliae* *in planta*. Within the nuclear ribosomal DNA (rDNA) the three highly conserved ribosomal RNA (rRNA) encoding genes (18S, 5.8S, 28S) are localized in consecutive complexes and therein separated by internal transcribed spacers (ITS1, ITS2). The highly variable sequences of this ITS regions represent ideal primer targets for species-specific fungal quantification. The *V. dahliae*-specific primer LeVD (black arrows) selectively binds to the ITS2 region, thereby amplifying a 126 bp product.

The potential interference of host gDNA on the qRT-PCR performance was analyzed in the presence of 20 ng gDNA from disease-free tomato plants and the amplification efficiency of

the primer pair LeVD reached 98.1 % in the presence of plant DNA ($R^2 = 0.99$) (data not shown). An isolate-specific amplification of the variable ITS2 sequence with the primer pair LeVD was evaluated in a cross-reaction with 20 ng gDNA from each of the selected tomato-infecting fungi in comparison to the *V. dahliae* TomIGZ isolate by an absolute qRT-PCR assay (Figure 7). The *V. dahliae* fungal rDNA was clearly distinguishable from other fungi up to a concentration of > 0.0064 ng. The first cross-reaction of LeVD was measurable at a content of 8.18 pg for *P. fuligena* and 7.12 pg for *A. alternata*. For the other fungal pathogens a *V. dahliae*-specific differentiation was possible even below 3.2 pg. Within 20 ng starting template 2.88 pg in *A. niger*, 2.02 pg in *A. solani* and only 1.04 pg in *B. cinerea* isolates could be detected with the LeVD primer pair. A five-fold serial dilution of *V. dahliae* gDNA was used to determine an amplification efficiency of 98.5 % for the primer pair LeVD ($R^2 = 0.99$) (Figure S1).

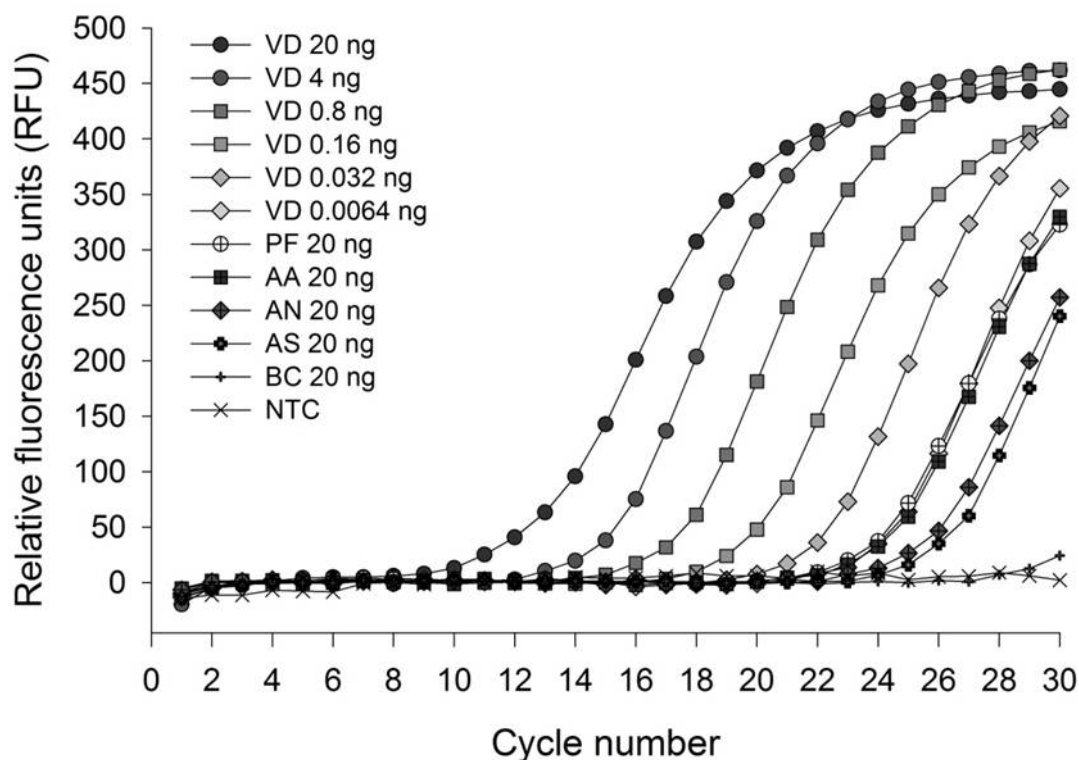


Figure 7 Fungal cross-reaction sensitivity-analysis of *V. dahliae* isolate TomIGZ-specific primer pair LeVD. A SYBR-Green I based absolute qRT-PCR assay was developed to determine the cross-binding level of primer pair LeVD with rDNA sequences of selected fungal pathogens. A serial-dilution of *V. dahliae* gDNA ranging from 20 ng to 6.4 pg was tested against 20 ng of gDNA from *P. fuligena*, *A. alternata*, *A. niger*, *A. solani*, *B. cinerea*, fungal isolates. In a negative control (NTC) DNA was replaced by dH₂O.

The developed quantification method for *V. dahliae* gDNA was used to study the spread of the fungus from the roots to the shoots as affected by genotype and S nutrition. The vascular tissue of the hypocotyl proved to be the most sensitive indicator of fungal spread 7 dpi. *V. dahliae*-sensitive genotype GCR 26 showed the highest fungal rDNA levels under low S nutrition compared to the resistant genotype (Figure 8). The amount of *V. dahliae* gDNA was highly significantly reduced under supra-optimal S supply in the sensitive genotype more than in the resistant genotype (highly significant Gen x S interaction) suggesting a major role of the S nutrition on *V. dahliae* resistance particularly in sensitive tomato genotypes.

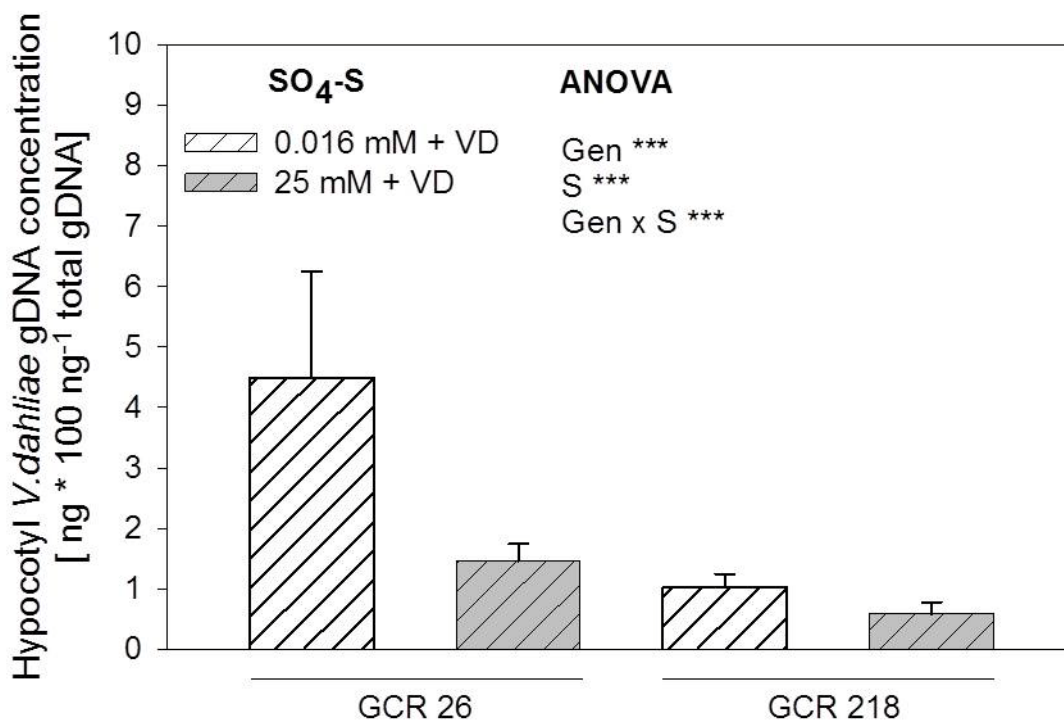


Figure 8 Effect of S supply on the amount of fungal gDNA in hypocotyls of *V. dahliae* (VD) infected tomato genotypes differing in *V. dahliae* resistance. (After 3 weeks of pre-culture at 25 mM or 0.016 mM SO₄-S plants were root inoculated and harvested 7 dpi. Data represent means \pm SD $n = 3$. Results of the analysis of variance are given according to their level of significance as *, **, ***, for $P \leq 0.05$, 0.01, 0.001, respectively, n.s. non-significant.)

Since the S nutrition had a major influence on the resistance against *V. dahliae* particularly in the sensitive tomato genotype we studied the concentrations of the S metabolites which have been implicated in SED. The S⁰ analysis of infected four weeks-old surgically dissected tomato hypocotyl vascular bundles did not show a significant difference in S⁰ concentrations between the sensitive and the resistant tomato genotypes 7 dpi in relation to variable S fertilization. At supra-optimal S sensitive plants contained $7.73 \pm 1.12 \mu\text{g g}^{-1}$ fresh wt. and

resistant plants $10.10 \pm 1.43 \mu\text{g g}^{-1}$ fresh wt. and low S supply resulted in concentrations of $8.91 \pm 1.52 \mu\text{g g}^{-1}$ fresh wt. in the sensitive genotype and $9.81 \pm 1.44 \mu\text{g g}^{-1}$ fresh wt. in resistant plants. No S^0 was detectable in control plants. S supply greatly increased the concentrations of both Cys (Figure 9 a) and GSH in the vascular tissue of the hypocotyl. GSH was more abundant than Cys by a factor of 20 - 40 (Figure 9 b). The S effect was more pronounced in the *V. dahliae*-sensitive genotype GCR 26 than in the resistant genotype GCR 218 (significant Gen x S interaction). The genotypes did not differ in Cys concentration. However, the GSH concentration was higher in the *V. dahliae*-resistant genotype. An infection increased the Cys and GSH concentrations in the sensitive but decreased them in the resistant genotype (significant Gen x VD interaction). The S supply effect on both metabolites was greater in non-infected than in infected plants (significant S x VD interaction).

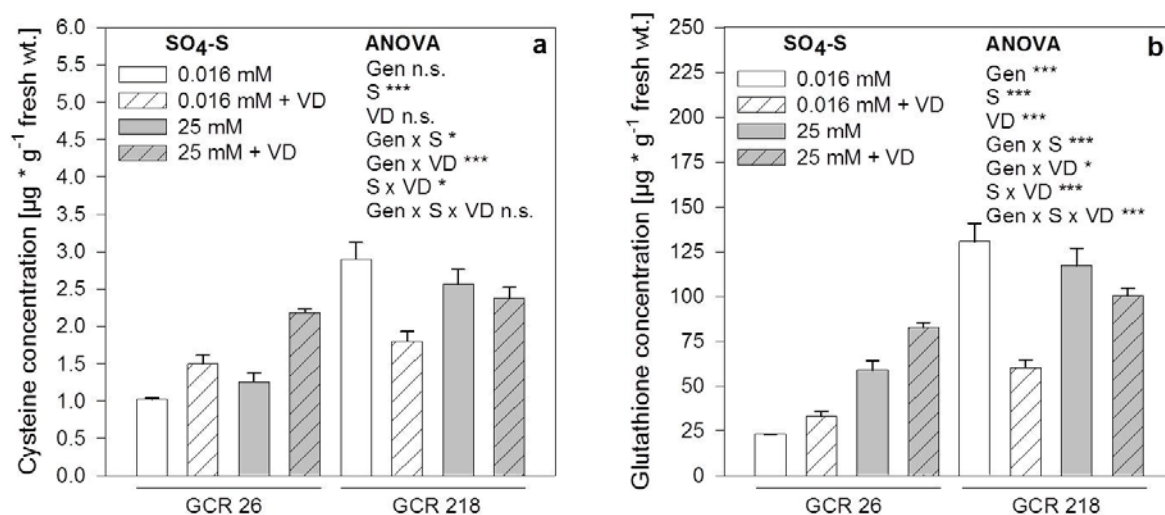


Figure 9 The impact of S supply on the concentrations of **a** Cys and **b** GSH in hypocotyl vascular tissue of the *V. dahliae* (VD) sensitive (GCR 26) and resistant tomato genotype (GCR 218). (After 3 weeks of pre-culture at 25 mM or 0.016 mM $\text{SO}_4\text{-S}$ plants were root inoculated and harvested 7 dpi. Data represent means \pm SD $n = 3$. Results of the analysis of variance are given according to their level of significance as *, **, ***, for $P \leq 0.05$, 0.01, 0.001, respectively, n.s. non-significant.)

Discussion

In order to analyze the influence of enhanced S nutrition on disease development and thus to get deeper insights into the role of SED in tomato protection against the vascular wilt pathogen *V. dahliae*, plants were grown either with luxury or low S nutrition. Preliminary experiments comparing 1 and 5 mM S supply did not lead to differences in total S concentration (Figure S2) and number of suberized xylem vessels in response to *V. dahliae* infection. Therefore, it was decided to compare the application of supra-optimal and low S as a more discriminative fertilization strategy. Total S concentrations were determined in single leaflets and surgically dissected hypocotyl tissue of the resistant and sensitive tomato genotype (Figure 2 a, b). Since a major part of the hypocotyl tissue is composed of non-living xylem vessels and vacuolar storage and reductive assimilation of S require living cells, higher S concentrations were obtained under supra-optimal S supply in leaves than in hypocotyls. Although tissue S concentrations differed significantly according to S supply and genotype, the absolute differences were too small to explain the major differences in colonization of the vascular tissue owing to S supply and genotype (Figure 8). Therefore, differences in S uptake and translocation seem not to play a decisive role for the differences in pathogen resistance.

As described by Chen et al. (2004) the initial colonization of tomato roots by *V. dahliae* is rapidly followed by sporulation and invasion of vascular tissue and subsequent penetration of neighboring cells up to 6 dpi. Therefore, we evaluated the host's cell-wall coating response seven days after fungal infection of the tomato root systems first by microscopic counting of suberized xylem vessels. The deposition of suberin in the xylem vessel cell walls is regarded as a sensitive response of the xylem tissue to fungal colonization aiming at impeding pathogen hyphae to further spread in the shoot (Fradin and Thomma, 2006). Clear differences in the suberization as influenced by genotype and plant S status were observed (Figure 3 a). Under S-deficient conditions the resistant genotype showed on average four times less coating initiation sites 7 dpi, whereas the sensitive genotype responded to fungal infection by a much higher number of suberized xylem vessels. Higher S nutrition considerably improved the protection capacity especially of the sensitive tomato plants, setting both genotypes to a similar cell suberization level. This visual rating procedure proved to be a sensitive parameter for the *in planta* detection of the fungal colonization status and the S response of both tomato genotypes 7 dpi. However, a principal shortcoming of this phenotyping is the exact identification of suberized vascular cells. The reproducibility of counting results is

closely connected to the experimenter; thus the selection of cells being included into the assay always depicts a subjective statement.

Despite an early genotypic discrimination of infected vascular tissue (Figure 3 a), considerable genotypic differences in shoot and root growth appeared in response to fungal infection only after longer treatment periods (> 7 dpi). This can be assigned to the longer cyclic colonization pattern of alternating *V. dahliae* proliferation and elimination, which results in pronounced consistent disease symptoms not before 8 dpi (Chen et al., 2004; Robb et al., 2007). Stunted shoot growth is known as a vascular-wilting disease symptom in *V. dahliae*-infected older tomato plants (Williams and Cooper, 2003). Thus, shoot length was measured (Figure 3 b). Besides the detection of growth differences in control plants, with slightly longer shoots of the resistant genotype, the growth retardation in relation to a *V. dahliae* colonization was small but significant for both tomato genotypes. A curative effect of supra-optimal S nutrition for tomato plants was not reflected. Therefore, this parameter proved to be unsuitable for the combined detection of a fungal and S nutritional impact in tomato plants.

The tomato root growth clearly demonstrated a positive influence of a high S nutritional status on control plants but at the same time a general negative impact of *V. dahliae* infection on resumed growth and root biomass production after trimming of the root system for infection was observable particularly in plants of the sensitive genotype (Figure 4 a, b; Figure S3 a, b). Roots of both tomato genotypes formed during preculture were vital, but the sensitive genotype failed to induce the synthesis of a new fine root system and roots were severely stunted 7 dpi (Figure 4 c). Although, several reports mention enhanced root growth or lateral root formation under S deficiency (Juszczuk and Ostaszewska, 2011; Nikiforova et al., 2004), root growth was less than at supra-optimal S supply. This could be explained by lower photosynthesis of the leaves (Figure 5 a) and thus less assimilate allocation to the roots which, however, is not reflected by a lower phloem sugar-transport rate (Figure 5 b). The constant low S supply with the micronutrients seemed to prevent severe S deficiency reflected by the leaf S concentrations in low S plants of 2 mg g⁻¹ dry wt. (Figure 2 a). Shoot-growth reduction could not be detected, providing further evidence for an only week S deficiency. Additionally, recovery of previously pruned root systems from the substrate strongly impaired lateral root integrity, thus impeding total root length analysis. However, the root analysis allowed the identification of a clear fungal impact whereas the S nutritional status of the plants did not

affect the negative impact of *V. dahliae* infection on root growth in none of the genotypes. This indicates that the beneficial effect of S nutrition on resistance against *V. dahliae* is expressed in the shoot rather than the root.

Impeded root growth and colonization of vascular tissue leads to xylem vessels blockage and reduces water movement within conductive elements inducing a water deficit that initiates stomata closure thus reducing leaf photosynthesis rate of infected plants (Bowden et al., 1990; Saeed et al., 1999). Especially after fungal infection, a water deficit through the blockage of xylem vessels and tissue dehydration was shown to decrease photosynthesis-related parameters in a way comparable to artificially applied soil-water deficit conditions (Pascual et al., 2010; Nogués et al., 2002 Pshibytko et al., 2006). In the present study analysis of photosynthesis rates underlined the role of *V. dahliae* as a biotic stressor causing wilting disease in several plant species. Our measurements indicated a reduction of tomato photosynthesis directly linked to systemic *in planta* fungal proliferation and xylem vessel occlusion. The occurrence of more severe true wilting symptoms especially on leaflets and a more drastic reduction of photosynthesis confirmed the genotypic differences in diseases resistance (Figure 5 a). An S-enhanced *V. dahliae* resistance is supported by less inhibition of photosynthesis at high S supply in infected plants of both genotypes. The sugar phloem-transport rates (Figure 5 b) did not reflect leaf photosynthesis.

In contrast, sugar transport was enhanced by *V. dahliae* infection in the resistant tomato genotype. The manipulation of carbohydrate metabolism in combination with a decrease of photosynthesis in source tissues seems to be a frequent plant response towards the biotic stress of fungal infection (Berger et al., 2007). Fungal elicitor molecules can induce specific sugar-metabolizing enzymes which contribute to replenishment of metabolic energy demand in sink organs by sugar cleavage (Sinha et al., 2002; Roitsch et al., 2003). Subsequently, key pathogenesis-related genes, which are inducible via the local sugar status (Roitsch, 1999), can facilitate in-plant defence mechanisms. An infection-based induction of sugar levels is known for members of the *Solanaceae* family (Scharte et al., 2005). It appears that also in tomato the presence of *Verticillium* represents a major sink for photoassimilates and induces sugar-channeling to infected roots especially in the resistant genotype. However, since root growth was inhibited in infected plants of the sensitive genotype at both S supplies and in resistant genotype only at high S supply despite enhanced allocation of assimilates, insufficient availability of assimilate appears not to be the limiting factor. Thus a possible consumption of

the photoassimilates by the fungus or the production of rhizotoxic compounds, which is known for some fungal species to occur in host-specific interactions (Walton, 2006), might limit root growth. In non-infected plants the S nutritional status had little impact on sugar transport-rates in both genotypes. However, in infected plants high S nutrition clearly enhanced phloem sugar-transport particularly in the resistant genotype. On the basis of the available data it is difficult to decide, whether the enhanced transport in the phloem of sugars is the reflection of less shoot and vascular bundle injury owing to S nutrition and constitutive resistance mechanisms in the resistant genotype or the consequence of an improved control over the pathogen by sugar-signaling facilitated build-up of defence mechanisms.

Results obtained by classical disease-rating approaches indicated genotypic differences in disease severity comparable to a sensitive and resistant plant-pathogen interaction. However, for the reliable quantitative specification of fungal proliferation and effects within the host tissue, we backed up these methods by a highly sensitive and specific quantification using absolute qRT-PCR which allows the exact discrimination and graduation of resistant, tolerant or susceptible plant pathogen interactions. The absolute qRT-PCR is a common method for the detection of fungal pathogens in diverse plant species (Duressa et al., 2010; Moradi et al., 2010). The development of SYBR Green-based assays allows high throughput screening at low costs including high reproducibility and accuracy (Zahn et al., 2011). This technique requires the design of fungal species-specific primers, frequently focusing on the highly variable ITS 1 and ITS 2 areas surrounding the conserved 5.8 S rRNA encoding sequence located in the ribosomal operon (White et al., 1990). We developed a SYBR Green-based assay including the self-designed species-specific primer pair LeVD specifically binding to a variable part within the ITS2 region of the fungal isolate *V. dahliae* TomIGZ (Figure 6 a). A subsequent cross-sensitivity test confirmed the LeVD-based sensitive discrimination of typically tomato-infecting fungi (Figure 7). By the application of LeVD a significant influence of elevated S supply on the fungal colonization levels within the tomato hypocotyls (Figure 8) was identified. A luxury S supply reduced fungal growth as shown by a decline of *V. dahliae* gDNA particularly in hypocotyls of infected sensitive tomato genotypes. Therefore, application of this technique supported the concept of SED (Kruse et al., 2007). In comparison to classical procedures or conventional semi-quantitative PCR analysis our study demonstrates the simple, specific and sensitive measurement of fungal gDNA by absolute SYBR Green-based qRT-PCR thus highlighting its suitability.

The *in-planta* antimicrobial impact of externally applied S against *V. dahliae* in the current experiment is in line with reports on beneficial sulfate-S fertilization effects on different fungal or viral diseases (Klikocka et al., 2005; Höller et al., 2010). The resistance-promoting S-induced changes of the colonization pattern which we observed in tomato might be tightly correlated to mechanisms of SED. For tomato a special role of the SDC S^0 has been implicated in genotypically enhanced *V. dahliae* resistance using the same tomato genotypes as used in our study. Fungicidal effects of S^0 have been supported by in-vitro spore germination tests and high S^0 contents in infected vascular tissue of a resistant tomato genotype (Williams et al., 2002; Williams and Cooper, 2003). Our study confirmed a significant effect of supra-optimal S on pathogen infestation particularly in the sensitive genotype, but could not attribute this to differences in S^0 contents of the vascular tissue. Unlike Williams et al. (2002) we used a HPLC method for the quantification of plant tissue S^0 contents. Intensive studies in cooperation with the group of Analytical Chemistry of LUH proved this method to be more reliable (reproducibility and recovery rate) and sensitive. Possibly more important, Williams et al. (2002) found genotypic differences in S^0 in 11 week-old plants 21 dpi but not 7 dpi. In the presented studies four week-old plants were analyzed 7 dpi and the differences in S^0 contents might have been still too small to show significant differences between the genotypes. Whether the process of S^0 generation reflects an enzymatic reaction or a non-enzymatic xylem-localized oxidation of reduced S species still needs explanation.

Cys is an essential S donor for the non-protein thiol GSH (Droux, 2004) and the degradation of high GSH concentrations might lead to a local accumulation of S^0 (Rausch and Wachter, 2005). Therefore, we focused on the analysis of these SDCs which are described as possible precursor molecules in S^0 synthesis. The S-containing amino acid Cys and the tripeptide GSH showed distinct concentration patterns influenced by S supply and genotype in tomato hypocotyl tissue (Figure 9 a, b). A high S supply generally increased the concentration of both metabolites. This reflects the general trend in different plant species that S supply results in higher concentrations of total S, Cys and GSH indicating a strong dependency of these S-containing metabolites on the plant S nutritional status (Schnug et al., 1995; Bloem et al., 2010). In addition, an enhanced formation of Cys and even more of its follow-up product GSH (as predicted by Rausch and Wachter, 2005) due to *Verticillium* infection has been observed in the sensitive genotype, whereas in the resistant genotype infection reduced the concentrations of both thiols particularly at low S supply. The consumption of Cys and GSH

after *V. dahliae* infection in resistant plants suggests that these thiols might be implicated in the resistance mechanism. An initial reduction was also detected in the early phase of other plant diseases (Höller et al., 2010; Vanacker et al., 2000). Especially GSH, the predominant form of soluble organic S in plants, serves in its reduced form as major buffering pool for scavenging reactive oxygen species, which are increasingly formed in response to abiotic and biotic stressors (Foyer and Noctor, 2011). A pathogen-effected antioxidative role of GSH might be important also for *Verticillium* defence in the resistant tomato genotype. However, under low S supply the resistance cannot be fully maintained because of depletion in thiols, whereas supra-optimal S supply allows maintenance of thiol levels further limiting the fungal colonization. Additionally, the sensitive and resistant genotypes constitutively differed in their Cys and GSH concentrations possibly indicating constitutive differences in their level of pathogen resistance. Whether in tomato-*Verticillium* interactions GSH directly acts as a reducing agent in antioxidative protection mechanisms or serves as substrate for further SDC assembly still needs to be clarified.

In conclusion, the analysis of selected physiological parameters in combination with an absolute quantification of the *in planta* fungal spread revealed a reduced fungal colonization particularly of the disease-sensitive tomato genotype. The results provide circumstantial evidence that the SDC GSH may directly or indirectly as precursor of S^0 be implicated in SED. The exact mechanism of S^0 formation awaits further clarification.

Chapter II - Spatial expression analysis of sulfur metabolism-related genes in hypocotyl tissues of tomato genotypes differing in *Verticillium dahliae* resistance

Katharina, Bollig¹, André Specht¹, Claudia Hogeckamp², Helge Küster² and Walter J. Horst¹

(1) Institute for Plant Nutrition, Faculty of Natural Science, Leibniz University Hannover, Herrenhäuserstraße 2, 30419 Hannover, Germany

(2) Institute for Plant Genetics, Unit IV Plant Genomics, Faculty of Natural Science, Leibniz University Hannover, Herrenhäuserstraße 2, 30419 Hannover, Germany

To be submitted

Abstract

Verticillium dahliae (*V. dahliae*) is a prominent generator of plant vascular wilting disease. Sulfur (S)-enhanced defence (SED) mechanisms are contributing to *in planta* pathogen elimination. The synthesis of specific S-containing defence compounds (SDCs) including elemental S (S^0) in response to fungal infection has been described for tomato. To better understand the effect of S nutrition on *V. dahliae* resistance of tomato, two near-isogenic tomato lines differing in fungal susceptibility and capable of S^0 synthesis were treated with low or supra-optimal S supply. High frequency of peak accumulations of S in vascular bundles of the resistant tomato genotype were detected after fungal colonization by laser ablation - inductively coupled plasma - mass spectrometry (LA-ICP-MS). A quantitative Real-Time analysis suggested that early steps of the primary S metabolism and reactions mediated by sulfurtransferases did not contribute to the synthesis of plant-protective S^0 or other SDCs on the whole hypocotyls tissue level since gene expression was down-regulated by fungal colonization. Enhanced S fertilization mostly alleviated the repressive effect of *V. dahliae* but did not reverse it. Up-regulation of glutathione (GSH)-associated genes in bulk hypocotyls but not in vascular bundles indicate a global role of GSH for detoxification of reactive oxygen species in hypocotyls. In contrast, in vascular bundles of high S-supplied resistant tomato plants a fungal infection switched the transcription to genes directly connected with cysteine (Cys) synthesis. The up-regulation of *LeOastlp1* underlined the importance of Cys as a local key precursor for S^0 production. The current study reveals a tissue-specific contribution of Cys synthesis-associated genes to SED mechanisms against *V. dahliae* in tomato vascular bundles.

Keywords: relative quantitative Real-Time; laser ablation ICP-MS, laser microdissection, sulfur-enhanced defence; sulfur-containing defence compound; tomato; *Verticillium dahliae*

Introduction

Wilting disease caused by the soil-borne phyto-pathogenic fungus *Verticillium dahliae* (*V. dahliae*) is a serious agronomic threat particularly in temperate but also in subtropical regions (Fradin and Thomma, 2006). A major problem with newly infected plants is the exclusive vascular location of the fungus, which minimizes the impact of an external chemical treatment (Klosterman et al., 2009). Chemical containment including the application of fungicidal phytochemicals, but also non-chemical protection methods may bear health and environmental risks, can be cost intensive and often show limited effectiveness (Goicoechea, 2009; Lazarovits, 2010). Additionally, the inheritance of a genetic source of resistance is restricted to only a small number of plant species. Owing to this insufficient protective means, a major focus has to be on plant innate pathogen resistance mechanisms. In some members of the *Solanaceae* family the introduction of the single dominant resistance gene *Ve1* (*Verticillium* race 1), which encodes a cell-surface receptor for recognition of fungal elicitor molecules, confers resistance against *V. dahliae* race 1 strains (Diwan et al., 1999; Kawchuk et al., 2001; Fradin et al., 2009). Several plant species possess sulfur (S)-enhanced defence (SED) mechanisms which are based on the antimicrobial action of a number of S-containing defence compounds (SDCs) generated within plant tissues primarily in response to colonization by biotic stressors (Dixon, 2001; Rausch and Wachter, 2005; Kruse et al., 2007; Burow et al., 2008;). Patterns and concentrations of specific SDCs are clearly induced after pathogen or herbivore attack in plants (Clay et al. 2009; Schlaeppi et al., 2010). Additionally, the synthesis of a number of SDCs is S-responsive, which is reflected in a stimulation or repression of SDC pools depending on the external S availability (Nikiforova et al., 2005; Falk et al., 2007; Schonhof et al., 2007). In connection with the *V. dahliae*-induced vascular wilting disease, mechanisms of SED using elemental S (S^0) as an induced fungitoxic S-containing phytoalexin proved to be inherent in some higher plant species (Cooper et al., 1996; Williams et al., 2002; Novo et al., 2007). Following high S supply, S^0 was found in response to an infection by *V. dahliae* in the vascular tissue of members of the *Solanaceae* family. Resistant tomato and pepper genotypes accumulated high concentrations of S^0 in vascular cells (Williams et al., 2002; Novo et al., 2007). So far the mechanisms of S^0 formation in the plant tissue remains uncharacterized, and only few possible metabolic pathways of S^0 synthesis in higher plants have been discussed. An association with the reductive S assimilation in form of the degradation of cysteine (Cys) has been proposed to contribute to S^0 formation (Cooper and Williams, 2004). Also the transport, local accumulation and subsequent oxidation of glutathione (GSH) might be involved in the

accumulation of S^0 in specific plant tissues (Rausch and Wachter, 2005). An enzymatic oxidation of sulphide by sulphide oxidase but also a non-enzymatic oxidation might contribute to generation of S^0 as well (Joyard et al., 1988; Cooper and Williams, 2004).

In this study the influence of low and supra-optimal S nutrition on the localization and accumulation of S metabolites and the involvement of the transcription of S metabolism-related genes in SED were investigated. Two tomato genotypes, differing in their level of *V. dahliae* resistance, were colonized with the fungus. Laser ablation - inductively coupled plasma - mass spectrometry (LA-ICP-MS) was applied for the spatial identification of cell-specific vascular S accumulation in a previously established tomato-*Verticillium* pathosystem (Chapter I). To check for a possible contribution of plant S metabolism-related candidate genes to SED, gene expression was studied using quantitative Real-Time polymerase chain reaction (qRT-PCR). A general overview of the gene regulation in entire tomato hypocotyl tissue was followed by a laser microdissection-based spatial expression analysis of the S assimilation-related candidate genes in hypocotyl vascular bundles. Based on these experiments it was shown that the up-regulation of GSH synthesis-related genes constitutes a global antioxidant protection against *V. dahliae*. Additionally, a cell-specific contribution of Cys synthesis-associated genes is linked to S-enhanced protective mechanisms including the synthesis of S^0 against *V. dahliae* in tomato vascular bundles.

Material & Methods

Cultivation of plant material

For the relative quantification of candidate gene expression in hypocotyls and for the LA-ICP-MS-based analysis the near-isogenic tomato cultivars Craigella GCR 26 (GCR 26) (LA3247) and GCR 218 (LA3428) (*V. dahliae*-sensitive and resistant, respectively; Chen et al., 2004) were cultivated in a climate chamber, with a 16 / 8 h light / dark regime, 25 / 20 °C day / night temperatures, 70 % relative air humidity and a photon flux density of 200 mmol m⁻² s⁻¹ (photosynthetic active radiation). After germination, plants were transferred to peat moss (Klasmann-Deilmann GmbH, Geeste, Germany) limed with CaCO₃ to pH 5.0 in 1 l pots. Plants were pre-cultured for three weeks until fungal inoculation and harvested 7 dpi. During the three weeks pre-cultivation and one week treatment period, every second day a full nutrient solution of the following composition was applied: 7.00 mM KNO₃, 0.90 mM MgCl₂, 1.00 mM KH₂PO₄, 1.70 mM Mg(NO₃)₂, 0.10 mM NaCl, 5.00 mM Ca(NO₃)₂, 2.00 mM CaCl₂, 50 µM FeNaEDTA, 1.3 µM ZnSO₄, 24.5 µM H₃BO₃, 6.0 µM CuSO₄, 0.8 µM (NH₄)₂ MoO₄, 9.3 µM MnSO₄. Plants treated with low S supply did not receive additional S. For a supra-optimal S supply plants were additionally supplied with 25.0 mM K₂SO₄. For the LMPC-based spatial analysis of candidate gene expression patterns in hypocotyl tissue the *V. dahliae*-resistant tomato genotype GCR 218 was cultivated as described above with the full nutrient solution in combination with supra-optimal 25.0 mM K₂SO₄ supply (for justification of the S supplies see Chapter I).

Cultivation of the fungal pathogen and inoculation method

The *V. dahliae* isolate TomIGZ (GU060637) was grown for long-term cultivation of fungal mycelium on potato dextrose agar (PDA) (Duchefa, Haarlem, Netherlands) in the dark at 24°C. Fungal inoculum was produced from mycelium slices (ø 1 cm) in sucrose sodium nitrogen (SSN) liquid culture at 100 rpm and 26°C for three weeks. The spore concentration was adjusted to 1·10⁻⁷ spores mL⁻¹ with dH₂O in a haemocytometer. Three-week-old plants were carefully uprooted and roots were gently washed free of substrate in dH₂O. Then 1 / 3 of the total root mass was cut off and plant roots were inoculated by incubation in 80 ml spore suspension for 1 h at 110 rpm. Control plants were mock-inoculated in 80 mL dH₂O following the same procedure. All plants were transferred into new CaCO₃-limed peat moss.

Isolation of total RNA and cDNA synthesis

Harvested whole tomato hypocotyls were frozen immediately in liquid nitrogen. For RNA isolation, samples were ground under liquid nitrogen and total RNA was isolated from 100 mg (fresh weight) hypocotyl tissue with the TRIsure® Reagent (Bioline, Luckenwalde, Germany) following the manufacturer's instructions. For the synthesis of cDNA 1 µg of total RNA was combined with random hexamer primer in the RevertAid™ H Minus First Strand cDNA Synthesis Kit (Fermentas, St. Leon-Roth, Germany) according to the manufacturer's instructions.

Selection of genes of interest

To study the expression of genes related to S metabolism a list of candidate genes associated with the reductive S assimilation pathway was created. *Arabidopsis* full-length coding sequences (CDS) of nine selected genes was obtained from the TAIR gene database (www.arabidopsis.org) and searched against the nucleotide database of the Basic Local Alignment Search Tool (BLAST) Server (Altschul et al., 1990) available through the NCBI public database. Alignment parameters are given in Table S1. A taxonomy report-based analysis revealed the following tomato-derived CDS or expressed sequence tag (EST) results with highest sequence similarity scores: vacuolar sulfate transporter 4;1 (*LeSultr4;1*) AK320538, plastidic adenosine 5-phosphosulfate reductase (*LeAPR*) AK320536, plastidic sulfite reductase (*LeSiR*) DB698163, plastidic *O*-acetylserine-(thiol)-lyase isoform 1 (*LeOastlp1*), plastidic γ -glutamylcysteine synthetase (*LeGSH1*) AF017983, plastidic and cytosolic glutathione synthetase (*LeGSH2*) AF017984, plastidic glutathione reductase isoform 2 (*LeGR2*) EU285581, plastidic and mitochondrial sulfurtransferase 1 (*LeMSt1*) FJ711706, and cytosolic sulfurtransferase 2 (*LeMSt2*) FJ711707.

Primer design

A sequence alignment of *A. thaliana* CDS and tomato CDS and EST results was performed using Vector NTI Advanced 10 (Invitrogen, San Diego, CA). Primer pairs for the qRT-PCR assay were designed using the primer 3 plus software (Untergasser et al., 2007). Primer sequences and PCR parameters are given in Table S2. Internal primer quality parameters included an amplicon size of 90 – 150 bp, a melting temperature of 59 – 61 °C, a primer length of 20 – 24 nucleotides, a GC content of 45 – 65 %, and matching of the primer 3' end to target transcript sequences. Chosen primer pairs were initially tested for the amplification of predicted fragment sizes, primer dimerization, or multiple unspecific fragment

amplification in a conventional PCR assay including the following components in a final volume of 25 μ L: Hot-Start PCR buffer B1 (1 x), $MgCl_2$ (3.6 mM), dNTPs (200 nM each) (Fermentas, St. Leon-Roth, Germany), forward and reverse primer (252 nM each), DCSHot DNA polymerase (0.75 U) (DNA Cloning Service, Hamburg, Germany), 50 ng cDNA from tomato hypocotyl tissue. The PCR parameters comprised an initial denaturation at 95 °C (10 min), followed by 30 cycles at 95 °C (15 s), 60 °C (30 s), and 72 °C (30 s). PCR products were analyzed on a 2 % (w / v) agarose gel in 1 \times TAE buffer with the Roti[®]-Safe GelStain (Carl Roth GmbH, Karlsruhe, Germany). The amplification efficiency was tested based on a standard curve method including a five-fold cDNA serial dilution starting with 20 ng cDNA from tomato hypocotyl tissue. The qRT-PCR efficiency was calculated using the CFX Manager[™] software (BioRad Laboratories, Hercules, California, USA).

Real Time qRT-PCR

For the analysis of gene expression in whole hypocotyl tissue and cortical tissue cDNA was synthesized starting from 1 μ g of total RNA by using random hexamer primers with the Revert Aid[™] H Minus Kit (Fermentas, St Leon-Rot, Germany). For analysis of gene expression in laser microdissection and pressure catapulting (LMPC) samples, 500 ng of *in-vitro* T7-amplified RNA were used in combination with random hexamer primers in the Revert Aid[™] H Minus Kit (Fermentas, St Leon-Rot, Germany). Due to its consistent expression tested in nutrient and cold-stress experiments, tomato elongation factor 1 α (*LeElf1a*, X14449) was used as internal reference gene (Løvdaal and Lillo, 2009). A SYBR-Green I based master mix included 50 ng of cDNA in the following 25 μ L reaction mixture: Hot-Start PCR buffer B1 (1 x), $MgCl_2$ (3.6 mM), 1000 x SYBR Green-I (0.1 x) (Invitrogen GmbH, Darmstadt, Germany), dNTPs (200 nM each) (Fermentas, St. Leon-Roth, Germany), forward and reverse primer (252 nM each), DCSHot DNA polymerase (0.75 U) (DNA Cloning Service, Hamburg, Germany). Thermal qRT-PCR cycling stages were performed in a CFX96[™] Real-time detection system (BioRad Laboratories, Hercules, California, USA) and consisted of an initial denaturation at 95 °C (10 min), followed by 35 cycles of 95 °C (15 s), 60 °C (30 s), and 72 °C (30 s) and a final melting curve analysis of 95 °C (10 s), 60 °C to 95 °C with a 0.5 °C 5 s⁻¹ increasing temperature gradient. For each target three technical and three biological replicates were used. Relative linear transcript levels were calculated using the 2^{- $\Delta\Delta$ CT} method (Livak and Schmittgen, 2001) including a primer efficiency correction.

Total Sulfur and LA-ICP-MS analysis

Following analysis of plant height and fresh weight, leaves were dried at 65 °C for 72 h. The dry weight was measured and samples were grinded and homogenized for determination of total S using a Vario EL CNS analyzer (Dumas Elementar Analysensysteme GmbH, Hanau, Germany). From each hypocotyl section of the sensitive and resistant tomato genotype a uniform cross-section in the middle position was selected for LA-ICP-MS analysis. For the analysis of the hypocotyl S spatial distribution, the $^{34}\text{S}:$ ^{13}C ratio of the ablated hypocotyl tissue was used. A ^{34}S -free calibration matrix reflecting the C content and fresh weight content of the tomato hypocotyl samples was not available. Therefore, the calibration of the signal with defined concentrations of S-containing metabolites or selected S species was not practicable. Tissues were ablated with a solid-state NYAG-laser (UP193 SS, New Wave Research Co. Ltd., Cambridge, UK). Three free-hand cross-sections from three hypocotyls of each treatment were analyzed each by four individual laser ablation scans. A quadrupole ICP-MS (7500 CX, Agilent technologies, CA, USA) coupled to the laser ablation system was used to determine the ^{34}S signal giving the spatial distribution in tomato hypocotyls. Samples were arranged in a laser ablation chamber (Supercell; New Wave Research Co. Ltd., Cambridge, UK). The ablated material was transported by argon as a carrier gas to the plasma. The ICP-MS instrument tuning was optimized with respect to the maximum ion intensity of low masses. The flow rate of the carrier gas and the make-up gas were adjusted to optimum output; the flow rate was 0.25 l min^{-1} for the carrier gas and 1.25 l min^{-1} for the make-up gas. Radiofrequency power was set to 1300 W and the reaction mode was off. The laser parameters were set to 2 J cm^{-2} of output energy, 10 Hz repetition rate, 50 μm diameter of the crater size, and $20 \mu\text{m s}^{-1}$ scan speed. Measured elements were ^{34}S and ^{13}C . ^{13}C was used as an internal standard to normalize for different quantities of hypocotyl tissue ablated. Each cross-sectioned hypocotyl was captured visually by microscopy, and the laser ablation system software (Version 11, New Wave Research Co. Ltd., Cambridge, UK) enabled the measurement of the individual diameter of each replicate.

Fixation, embedding and sectioning of plant material

Hypocotyl sections from the *V. dahliae*-resistant tomato genotype CGR218 were harvested 7 dpi. The epidermis and outer cortical cell layers were removed mechanically and homogenized under liquid nitrogen. The remaining surgically dissected hypocotyl tissue was prepared for LMPC using a modified Steedman's wax protocol according to Gomez et al. (2009) in combination with a modified vacuum-infiltration protocol according to Deeken et

al. (2008). The tissue was sectioned and immediately transferred into ethanol:acetic acid (5:1) fixation solution for 12 h at 4 °C. An adjacent dehydrating solvent-exchange procedure at 4 °C involved ethanol and Roticlear[®] (Carl Roth, Karlsruhe, Germany). A 1:1 Roticlear[®]: Steedman's wax (melting temperature 38°C, polyethyleneglycol and 1-hexadecanol (9:1)) mix incubated at 38 °C for 12 h. The plant tissue was vacuum-infiltrated with 100 % Steedman's wax and embedded into TurbOflow[®]II molds and cassettes (McCormick Scientific, Richmond, USA). Resulting blocks were stored at 4 °C (McCormick Scientific, Illinois, USA) until sections (20 µm) were prepared with a Hyrax M55 rotary microtome (Carl Zeiss GmbH, München, Germany).

Laser Microdissection and Pressure Catapulting (LMPC)

Sections were transferred onto 38 °C pre-warmed sterile glass slides, de-waxed with Roti[®]-Histol (Carl Roth, Karlsruhe, Germany), washed with 100 % ethanol and finally dried on the heating plate. Cell structures were selected with the P.A.L.M. Robo software and extracted by LMPC with the P.A.L.M. Microbeam system including a Capmover (Zeiss Microimaging GmbH, München, Germany). Each treatment comprised four biological replicates giving approximately 320 vascular areas including xylem and xylemparenchyma cells. Harvested cell areas were catapulted into 250 µl reaction tubes containing 5 µl buffer RLT (RNeasy Micro Kit, Qiagen, Hilden, Germany). Brief centrifugation (8,000 g) was used to collect excised cell structures, which were stored at -80 °C until further processing.

Isolation and amplification of LMPC-derived Poly (A) RNA

Total RNA was isolated from LMPC-derived cell structures with the RNeasy Micro Kit (Qiagen, Hilden, Germany). RNA integrity and concentration were monitored on a RNA 600 Pico chip (Agilent 2100 Bioanalyzer, Agilent, Böblingen, Germany). Using a synthetic oligo (dT) primer the TargetAmp[™] 2-Round aRNA Amplification Kit 2.0 (Epicentre Biotechnologies, Madison, USA) was applied for the *in vitro* transcription of the Poly(A) RNA compound within total RNA samples. The quality and quantity of RNA samples was monitored with the Agilent RNA 6000 Nano Kit (Agilent 2100 Bioanalyzer, Agilent, Böblingen, Germany).

Statistical analysis

For the identification of the hypocotyl-tissue gene expression and the spatial S metabolite localization by LA-ICP-MS a completely randomized design including three biological replicates each composed of three individual plants was used. The LMPC-based spatial analysis of candidate gene transcript levels included a completely randomized design with four biological replicates each composed of four individual plants. For all qRT-PCR experiments significant expression differences were indicated by non-overlapping of the 95 % confidence interval calculated including the Ct values (CFX Manager™ software, BioRad Laboratories, Hercules, California, USA). Analysis of variance was performed using the general linear model procedure of the statistical program SAS 9.1 (SAS Institute, Cary, NC, USA) testing for genotype, fertilization, infection and their interaction effects.

Results

Both tomato genotypes were cultured under low and high S supply which led to plants with widely varying S concentrations in the leaf tissue (Figure 1 a). Leaf S concentrations were about 3 mg g⁻¹ dry weight and 8 mg g⁻¹ dry weight at low compared to high S supply. The resistant genotype had lower S concentrations at low, but higher S concentrations at high S supply than the sensitive genotype (significant S x Gen interaction). The S leaf-tissue concentrations were reduced by fungal infection irrespective of the genotype more at high than at low S supply (significant S x VD interaction).

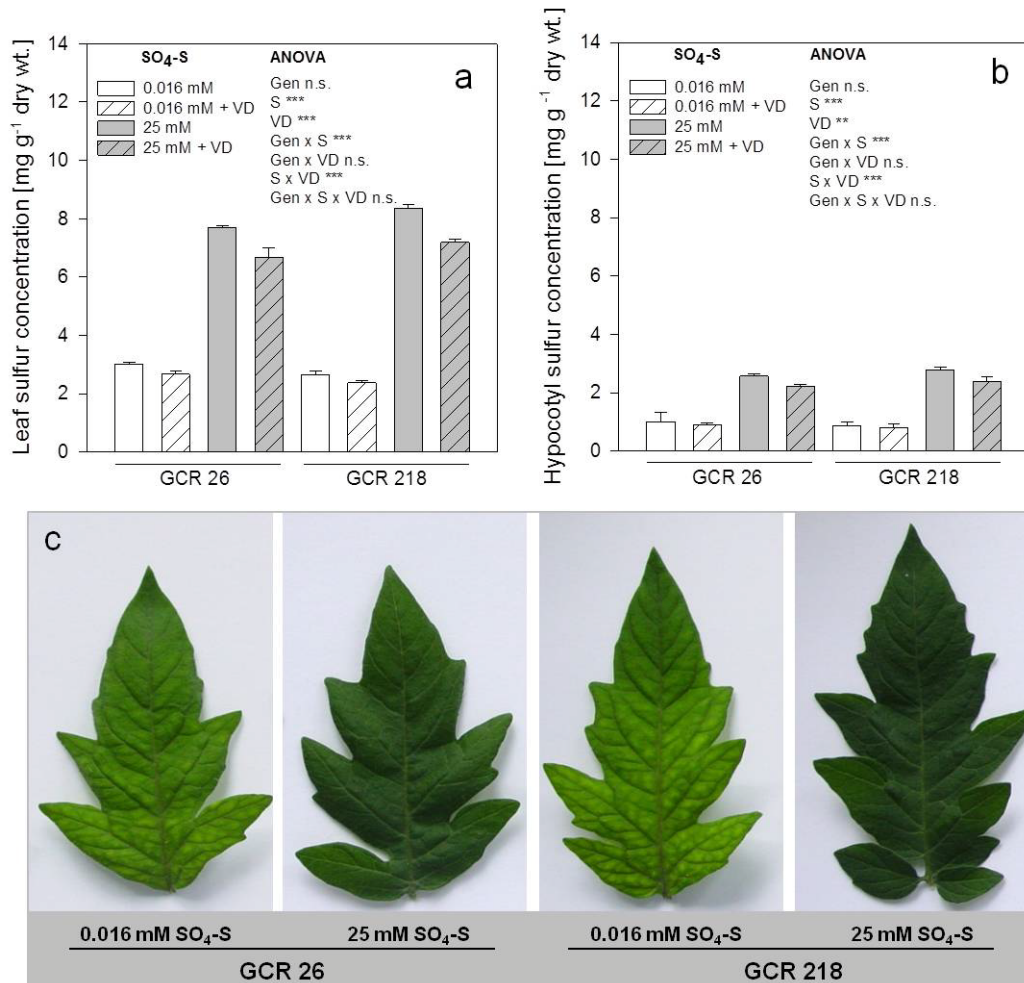


Figure 1 Effect of S supply on **a** leaf S concentrations, **b** hypocotyl S concentrations and **c** leaf blade coloration of *V. dahliae* (VD)-infected sensitive (GCR 26) and resistant (GCR 218) tomato genotypes. (After 3 weeks of pre-culture at 25 mM or 0.016 mM SO₄-S supply, plants were root-inoculated and harvested 7 dpi. Data represent means ± SD *n* = 3. Results of the analysis of variance are given according to their level of significance as *, **, ***, for P ≤ 0.05, 0.01, 0.001, respectively, n.s. non-significant.)

Hypocotyl tissue of both genotypes showed much lower S concentrations (Figure 1 b) at low and high S supply indicating S deficiency and supra-optimal S status, respectively. The effect of a fungal infection was similar in the hypocotyl and leaf tissues. The low plant S nutritional status resulted in a light green color of leaf blades against dark green leaf veins which was indicative for S deficiency in both genotypes at low S supply. In contrast, S concentrations at high S supply resulted in dark green leaves (Figure 1 c).

Seven days after fungal infection the tomato plants exhibited growth difference in relation to genotype, S treatment and *V. dahliae* infection (Figure 2). The sensitive genotype GCR 26 constitutively showed a lower overall shoot length (Figure 2 a).

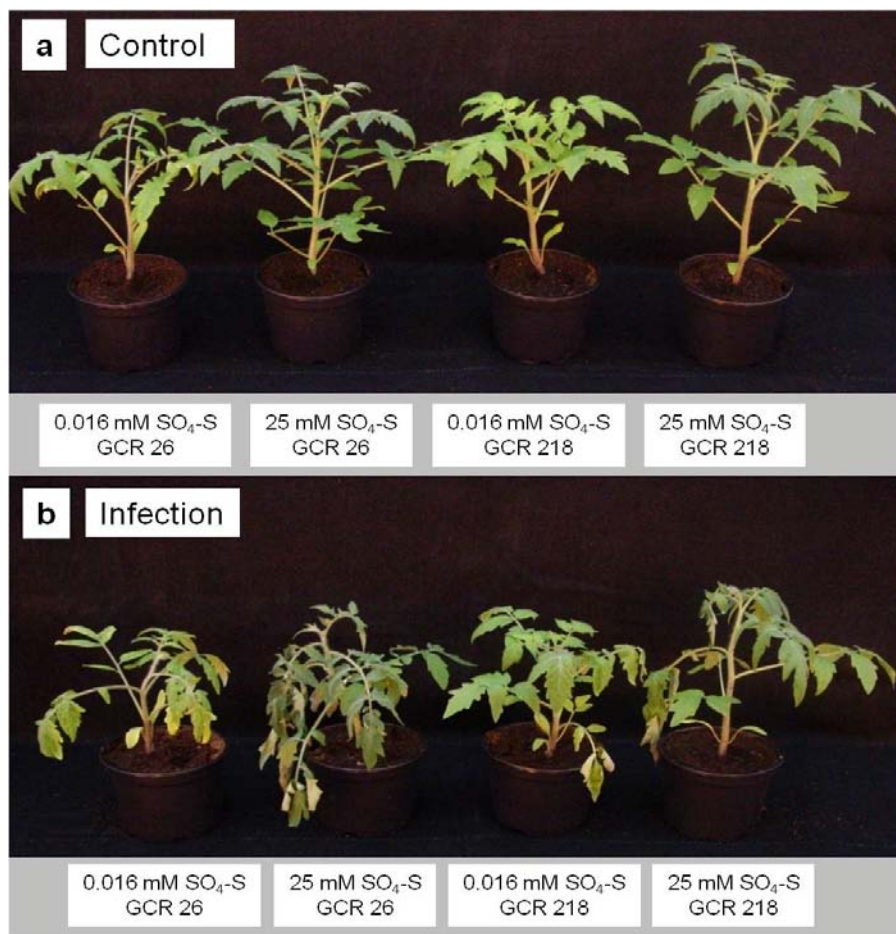


Figure 2 Growth and characteristic wilting symptoms of *V. dahliae* (VD)-infected plants of the sensitive (GCR 26) and resistant (GCR 218) tomato genotype. **a** Non-infected control plants were mock-inoculated. **b** Infected plants showed wilting of single leaflets or whole leaves and stunted shoots. (After 3 weeks of pre-culture at 25 mM or 0.016 mM $\text{SO}_4\text{-S}$ plants were root-inoculated and harvested 7 dpi.)

Low S-supplied plants of both genotypes were smaller in comparison to high S supply. *V. dahliae* infection induced symptoms including stunted shoot growth and wilting of younger leaflets which were already visible 7 dpi in all infected plants (Figure 2 b). The sensitive genotype showed more severe wilting.

Since leaf and hypocotyl-tissue analysis did not reveal differences in S concentrations between genotypes, LA-ICP-MS was applied for the localization and spatial distribution of S in tomato hypocotyl cross-sections. The laser ablation process started at the cross-section center, moved through the central cylinder tissue and crossed xylem and xylemparenchyma-cells to pass the cortical cell layers in the direction shown by the yellow arrows (Figure 3 a, b). The plant protective coating-response against *V. dahliae* was visible in form of a brown discoloration of suberized vascular bundles (Figure 3 b, d). The laser ablation images of scanned tissue areas shown are representative of three independent measurements of each treatment including four laser scans per hypocotyl cross-section (Figure 3 c, d). The ^{13}C signal was used as an internal calibrator for the normalization of the ^{34}S signal to account for the amount of laser beam-ablated cell material, which can be influenced by variable cell-layer density or tissue color along the ablation pathway. Results displayed in this study represent the comparison of $^{34}\text{S}:^{13}\text{C}$ signal intensities as affected by tomato genotype, plant S status and fungal infection (Figure 3 e, f). At low S supply in uninfected plants, S was uniformly distributed between the central cylinder, the vascular bundle and the cortex in both genotypes. High S supply increased the S concentration only slightly in the central cylinder (GRC 218 > GRC 26) and the cortex, but greatly in the vascular bundle. Within the vascular bundle S was non-uniformly distributed with locally very high S concentrations in both genotypes. *V. dahliae* infection markedly increased the S concentrations in the central cylinder with little differences between the genotypes at low S supply but great differences at high S supply (GRC 218 > GRC 26). The frequency of S peak concentrations (arrows in Figure 3 f) in the vascular bundle was particularly high in the *V. dahliae*-resistant genotype GCR 218.

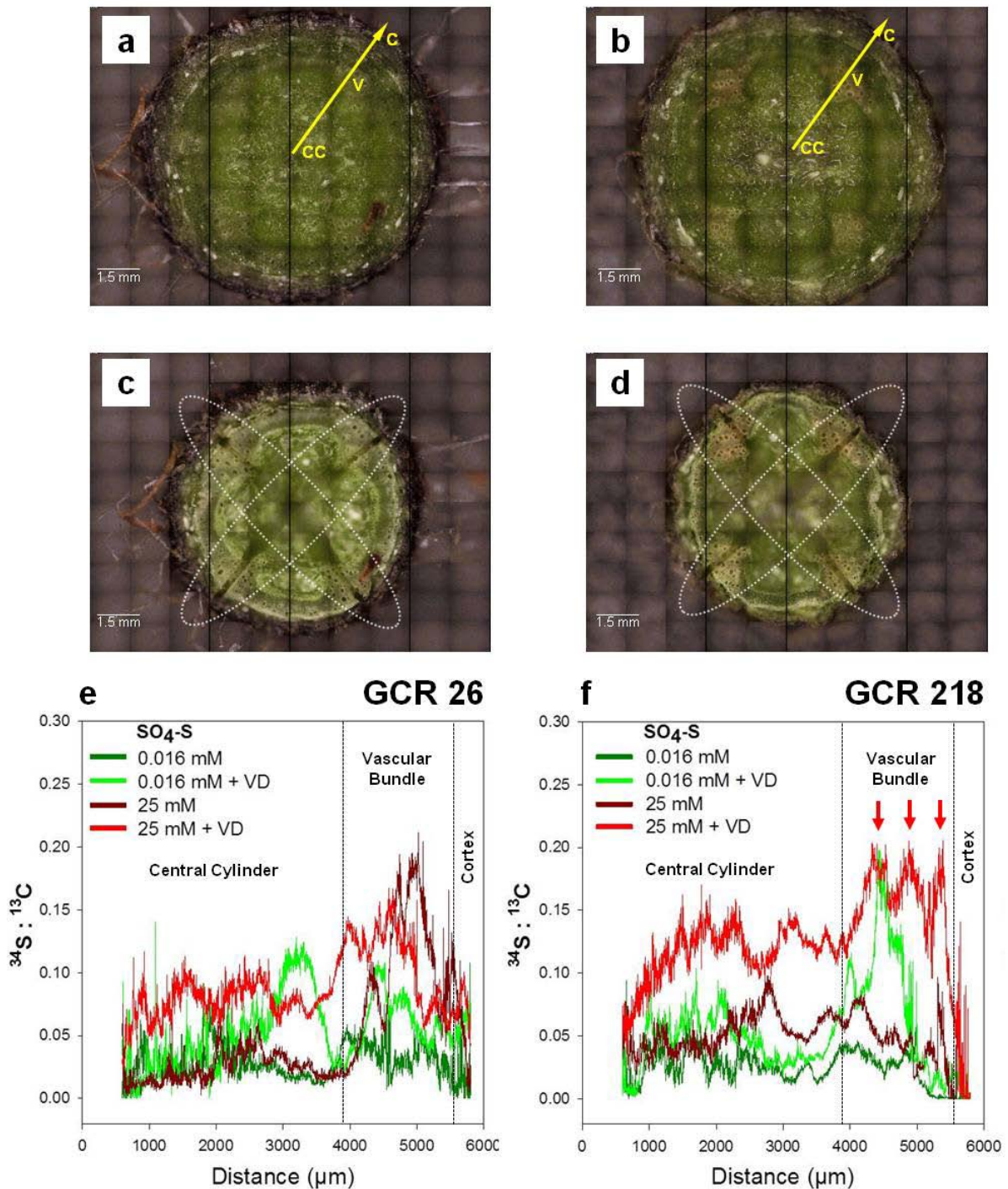


Figure 3 LA-ICP-MS analysis of the spatial S distribution in tomato hypocotyl cross-sections of plants of the sensitive (GCR 26) and resistant (GCR 218) tomato genotypes. Hypocotyl cross-section of **a** control and **b** *V. dahliae* (VD)-infected plants of the resistant tomato genotype GCR 218 before laser ablation. The yellow arrow indicates the direction of tissue ablation with increasing distance from the center of the central cylinder encompassing for each ablation run a distance of 6000 μm (CC: Central cylinder; V: Vascular bundle; C: Cortex). Hypocotyl cross-sections after laser ablation of **c** control and **d** *V. dahliae* (VD)-

infected plants of the resistant genotype. Tissue areas subjected to laser scanning are marked by white circles. The corresponding S contents along the ablation pathway are shown as the $^{34}\text{S}:$ ^{13}C signal intensities in **e** the sensitive and in **f** the resistant tomato genotype. Red arrows indicate local ^{34}S accumulation peaks in xylemparenchyma cells of the resistant genotype. (Hypocotyl tissues subjected to LA-ICP-MS were from plants pre-cultured at 25 mM or 0.016 mM $\text{SO}_4\text{-S}$ for three weeks before root inoculation and harvested 7 dpi.)

Based on a comparative sequence alignment with *A. thaliana* CDS and tomato CDS and EST sequences, specific primer pairs were designed for a relative quantification of the S metabolism-related gene expression. All candidate gene primer-pairs used in this study are described in Table S2. All selected primer pairs comprised the above-mentioned internal quality parameters with a tested PCR efficiency ranging from 90 – 110 %. Primer pairs for the quantification of the reference gene tomato elongation factor 1 α (*LeElf1a*) and for the quantification of nine selected S metabolism-related genes were initially tested for the amplification of the predicted amplicon sizes (Figure S1). After gel electrophoretic separation, distinct fluorescent bands were detectable and dimerization products as well as multiple unspecific fragment amplification could not be observed. In comparison to a molecular marker all detected PCR products showed the expected length.

To get a general overview of the transcriptional profile of primary S metabolism-related genes in tomato hypocotyls as influenced by variable plant S nutrition and fungal infestation, gene expression was analyzed by relative qRT-PCR in undissected tissue in a first step. Among the studied S pathway-related genes *LeAPR* and *LeSultr4;1* showed a strong and *LeSiR* and *LeOastlp1* a slight up-regulation at low compared to high S supply in the hypocotyls (Figure 4 b I - IV). *V. dahliae* infection strongly down-regulated the gene expressions at low S supply. At high S supply there was no or only a slight down-regulation in infected hypocotyls. The expression of these genes and the response to S supply and infection was similar in both genotypes. However, the expression at low S supply by *V. dahliae* infection was greater in the sensitive (GCR 26) than in the resistant genotype (GCR 218). The genes *LeMSt1* and *LeMSt2* appeared to be slightly up-regulated at low S supply in both genotypes (Figure 4 b V, VI). The two genes associated to GSH biosynthesis *LeGSH1*, *LeGSH2* and *LeGR2*, associated to reduction of oxidized GSH (GSSG), did not show a change in transcript levels in response to the S supply (Figure 4 b VII – IX). *V. dahliae* infection up-regulated these five genes particularly under low S supply, more in the resistant genotype GCR 218 than in the sensitive

genotype GCR 26. For *LeGSH1* this infection-induced up-regulation could also be observed at high S supply. The GSH biosynthesis-associated genes *LeGSH1*, *LeGSH2* and *LeGR2* were consistently and thus constitutively higher expressed in the resistant genotype.

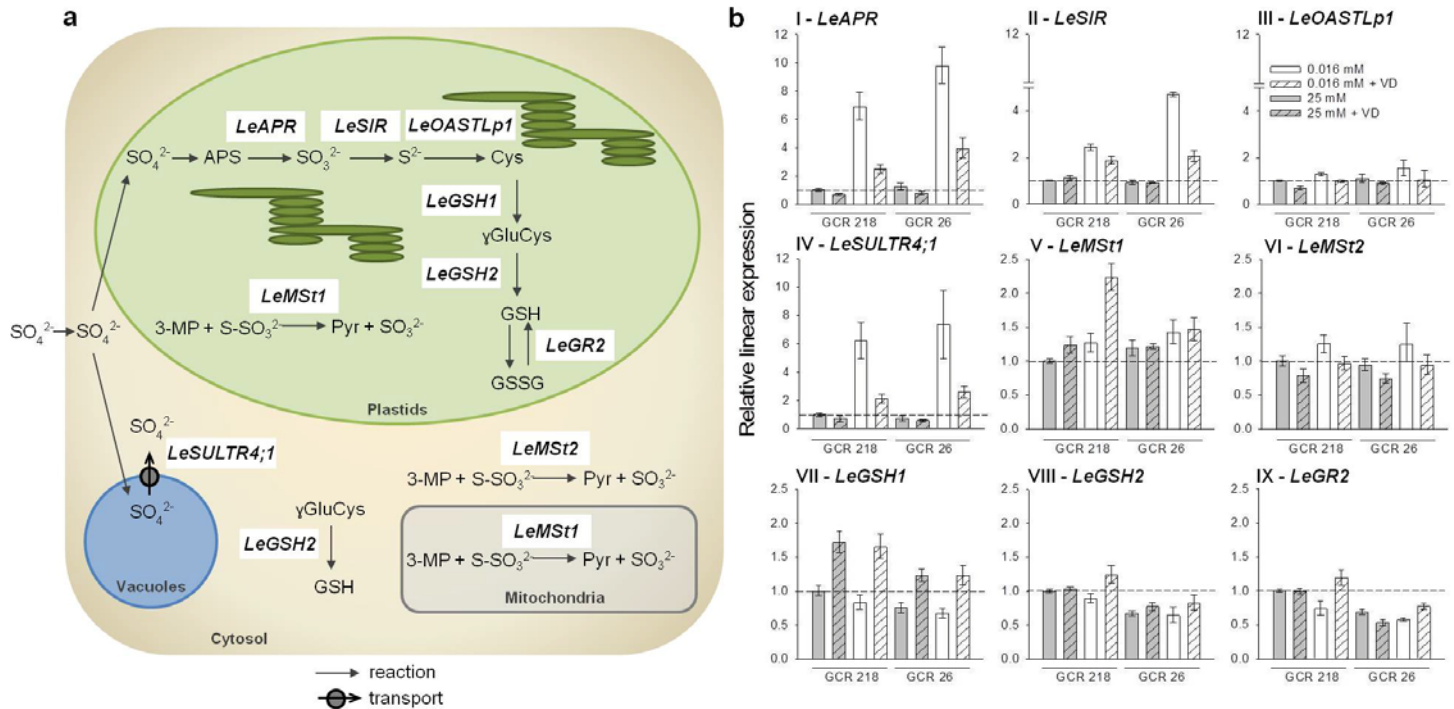


Figure 4 Cellular distribution, pathways of S assimilation and transport, and qRT-PCR expression analysis of nine selected S metabolism-related candidate genes in hypocotyls of the *V. dahliae* (VD)-resistant (GCR 218) and sensitive (GCR 26) tomato genotypes as affected by S nutrition and fungal infection. **a** Isoforms of the candidate genes selected for qRT-PCR analysis are present in vacuoles, plastids, mitochondria and the cytosol. Grey arrows indicate reactions for metabolite processing and white boxes indicate the candidate genes. **b** Relative linear gene expression analysis of the nine S assimilation-related genes. Plants were pre-cultured for three weeks at 25 mM or 0.016 mM SO_4 -S, root inoculated and harvested at 7 dpi. Total RNA was extracted from hypocotyl tissue and cDNA was synthesized from 1 μ g total RNA. Expression was calculated using the $2^{-\Delta\Delta CT}$ method (Livak and Schmittgen, 2001). Uninfected plants of the resistant genotype at high S supply as the calibrator were set to '1'. Expression data are means of three biological replicates. Error bars represent the 95 % confidence intervals.

For the identification of tissue-specific changes in the expression of the S metabolism-related genes only the resistant genotype at high S supply was studied, since the main objective of the study was the elucidation of the *V. dahliae*-induced accumulation of S (S^0) in the vascular tissues (see Figure 3 f) in relation to S-enhanced *V. dahliae* resistance. Hypocotyl sections were separated into cortex and vascular bundle tissue in the central cylinder using LMPC. Figure 5 a - f gives a sequential overview of the LMPC procedure. Light microscopy revealed the diverse tissue types of a typical tomato hypocotyl cross-section including vascular xylem and xylemparenchyma cells (Figure 5 a). The P.A.L.M. Robo software was used for labeling of relevant cell areas subjected to laser cutting along the green border line followed by laser catapulting of the complete pieces at each blue pressure point (Figure 5 b). The collection of a high number of uniform cell structures enabled the harvest of a homogenous tissue sample (Figure 5 c, d). LMPC-derived intact vascular cell layers were catapulted into buffer-containing caps (Zeiss, München, Germany) and stored directly at $-80\text{ }^{\circ}\text{C}$ until isolation of Poly(A)RNA (Figure 5 e). As a control, harvest of vascular cell structures from LMPC-treated tomato hypocotyl thin sections was monitored by light microscopy. The uniform arrangement of four collected tissue areas affirmed a successful application of the LMPC technique (Figure 5 f). In the cortex of the hypocotyl the expression of all genes except *LeMSt1* and *LeMSt2*, particularly *LeAPR* and *LeSiR*, were up-regulated in infected plants, however, this was not significant for *LeOastlp1*, *LeSultr4,1* and *LeGR2* owing to high confidence intervals of means (Figure 5 g). In contrast, the qRT-PCR analysis of laser-microdissected vascular tissue of the hypocotyl showed a different expression profile (Figure 5 h). Both Cys synthesis-related genes *LeSiR* and *LeOastlp1* were up-regulated in *V. dahliae*-infected vascular tissue. All other genes were down-regulated by the infection particularly the GSH synthesis-associated genes *LeGSH1*, *LeGSH2* and *LeGR2* which showed the most sensitive response with an on average 9-fold down-regulation.

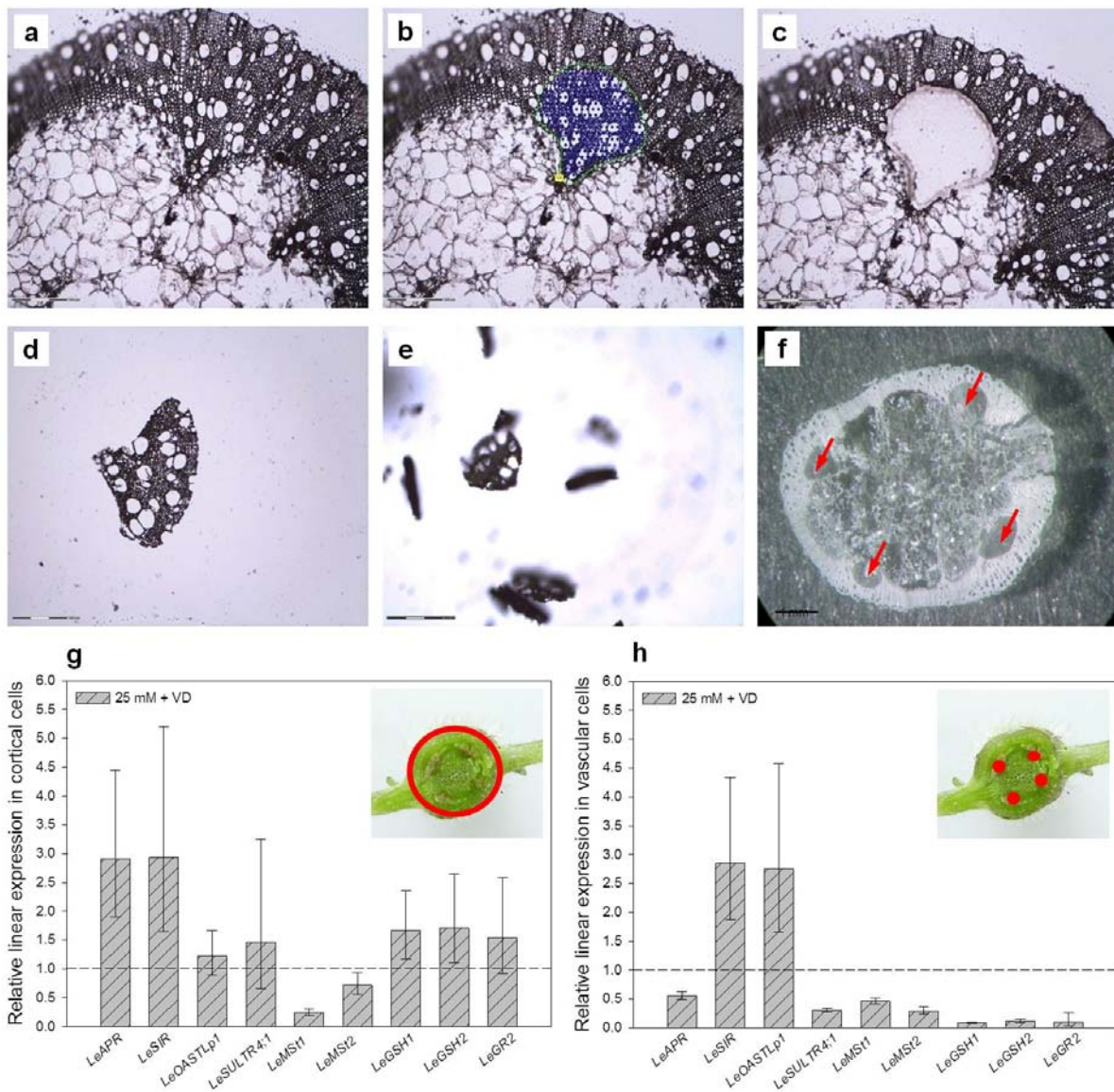


Figure 5 LMPC of xylem and xylemparenchyma-containing tissue areas in hypocotyl thin sections of the *V. dahliae* (VD)-resistant tomato genotype GCR 218 and expression of S metabolism-related genes in cortical tissue and in LMPC-isolated hypocotyl vascular bundles of the *V. dahliae*-resistant tomato genotype GCR 218 as affected by fungal infection. **a** Cross sections of hypocotyl tissue are used for the collection of vascular cell areas by LMPC. **b** With the P.A.L.M. Robo software cell structures subjected to LMPC were marked with a green line for laser dissection and blue dots for single catapulting events. **c** Cross-section after laser pulsing and pressure catapulting. **d** A LMPC harvested typical cell structure and **e** view into a collection tube containing typical pieces of harvested cell. Scale bar represents 800 μ m. **f** A complete hypocotyl thin section after quadruple LMPC procedure. Red arrows indicate harvested cell areas, scale bar represents 1 mm. The relative linear expression of nine selected S assimilation-related candidate genes was analyzed in hypocotyl cortical tissue **g** and in

hypocotyl vascular tissue **h** of the resistant tomato genotype GCR 218. The harvested cell areas are marked in red. Plants were pre-cultured for three weeks at 25 mM SO₄-S, root-inoculated and harvested at 7 dpi. From cortical tissue samples cDNA was synthesized including 1 µg total RNA. In LMPC samples RNA was *in-vitro* T7-amplified and cDNA was synthesized from 500 ng total aRNA. Expression was calculated using the $2^{-\Delta\Delta CT}$ method (Livak and Schmittgen, 2001). Uninfected plants of the resistant genotype at high S supply were set to '1' as the calibrator. Expression data represent mean values of four biological replicates. Error bars represent the 95 % confidence intervals.

Discussion

For the analysis of physiological and transcriptomic effects of an enhanced S supply on *V. dahliae* infection-induced protective SED mechanisms, two tomato genotypes differing in fungal susceptibility were cultivated at low and supra-optimal S supply. The S fertilization levels and the *V. dahliae* infection revealed a major influence on the plant phenotype in both tomato genotypes. The different S supplies caused different leaf and at a much lower level different hypocotyl S concentrations in both genotypes (Figure 1 a, b). Low S supply induced typical symptoms of a suboptimal plant S status characterized by leaf interveinal chlorosis and reduced leaf expansion and shoot growth (Figure 1 b, Figure 2 a). Leaf chlorosis can be explained by a decrease in chlorophyll and carotenoid contents, which is typical for S deficiency in tomato (Lopez et al., 1996; Zuchi et al., 2009) and other plant species (Nikiforova et al., 2005; Juszczuk and Ostaszewska, 2011). Changes in chlorophyll content are directly linked to limitations in Cys and methionine availability leading to a depression of the formation of S-adenosyl-methionine which is a precursor of chlorophyll synthesis (Nikiforova et al., 2005; Höfgen and Nikiforova, 2008). Reduced leaf expansion and plant growth could be the result of impaired photosynthesis in S-deficient leaves (Chapter I). S-starvation negatively affects plant photosynthesis lowering photosynthetic rates and reducing photosystem I and II and their efficiencies (Resurreccion et al., 2002; Höfgen and Nikiforova, 2008; Lunde et al., 2008). The *V. dahliae* infection caused clear wilting disease symptoms in both tomato genotypes (Figure 2 b). Shoot-growth depression was accompanied by wilting of single leaflets and whole leaves which was particularly severe in the sensitive genotype at high S supply. This appears surprising since in chapter I it was shown that high S supply clearly reduced the fungal colonization of the vascular hypocotyl tissue particularly in the sensitive genotype. However, the colonization and the number of infected suberized xylem vessels was still higher than in the resistant genotype even at low S supply. Thus the higher transpiration requirement of the high compared to low-S plants might lead to more severe wilting of the high S-supplied sensitive genotype.

In the xylem and xylemparenchyma cells the fungus *V. dahliae* induces a suberin-coating response attempting to block the further spread of the fungus as a kind of plant protective mechanism (Robb et al., 1989; Heinz et al., 1998; Fradin and Thomma, 2006). The number of suberized vascular bundle cells closely reflects the colonization of the xylem by the fungus and the genotypic differences in *V. dahliae* resistance of the two tomato genotypes studied (Chapter I). In addition, a special role of the pathogen-induced formation and deposition in

the xylem of the SDC S^0 has been implicated in the genotypic difference in *V. dahliae* resistance of these genotypes (Williams et al., 2002). The induction of S^0 formation in the hypocotyl central cylinder tissue by *V. dahliae* infection could be confirmed in an earlier study (Chapter I). However, in spite of clear differences in fungal colonization and suberization no clear differences in S^0 concentration existed between the genotypes which might be due to the fact that, in contrast to the study by Williams et al. (2002), we use much younger plants and a shorter infection period of 7 dpi. A high local accumulation of S has previously been detected by X-Ray and GC-MS analysis in scattered xylemparenchyma cells, xylem-vessel cell-walls and vascular gels of *V. dahliae*-infected *Theobroma cacao* and in vascular areas of *V. dahliae*-infected tomato plants (Cooper et al., 1996; Williams et al., 2002). In this study LA-ICP-MS allowed the localization of S across the hypocotyl (Figure 3). At supra-optimal S supply the *V. dahliae*-infection greatly increased the S concentration specifically in the vascular bundle (Figure 3 e, f) in agreement with higher S^0 concentrations previously detected in the central cylinder tissue (Chapter I). Since the 50 μ m diameter of the laser beam crater did not allow a resolution on the cellular level, we can only assume that the peak S concentrations are related to single xylem vessels. The number of peak S concentrations was particularly high in the vascular bundle of the infected resistant genotype. This might be an indication of a more localized accumulation of S^0 in these tissues particularly effective in controlling fungal spread. It thus appears that not the total S^0 concentration but rather its accumulation pattern in specific infected xylem vessels as proposed by Cooper et al. (1996), Williams et al. (2002), and Novo et al. (2007) is decisive for its fungicidal effectiveness which has been demonstrated for *V. dahliae* by Cooper and Williams (2004). Neither the exact localization nor the identity of the S accumulation can be revealed unequivocally by LA-ICP-MS. Thus it might also be possible that the identified S accumulations in the vascular bundles of *V. dahliae*-infected hypocotyls are S^0 precursors rather than S^0 . Enhanced synthesis of S^0 in *V. dahliae*-infected plants was accompanied by an increase in the GSH and Cys concentrations (Williams et al., 2002; Williams and Cooper, 2003; Novo et al., 2007). In the present pathosystem this could only be confirmed in the *V. dahliae*-sensitive genotype, whereas in the resistant genotype pathogen infection reduced the constitutively higher GSH and Cys concentrations in the hypocotyl vascular tissue (Chapter I). It thus appears that the metabolism of SDCs differs in response to fungal colonization between the *V. dahliae*-sensitive and resistant genotypes.

In order to get a better understanding of the synthesis of S-containing metabolites possibly leading to S^0 a transcriptomic analysis was initiated. The mechanism of S^0 synthesis is not known so far, but its production might be closely linked to several steps of the primary S assimilation pathway (Rausch and Wachter, 2005). To analyze differences in a possible enzymatic generation of S^0 in both tomato genotypes, a vacuolar S exporter, three candidate genes belonging to the reductive S assimilation pathway, three candidate genes related to GSH biosynthesis and reduction and two genes involved in S transfer reactions were selected for a detailed expression study (Table S1). The specific cellular distribution of the selected gene isoforms is schematically shown in Figure 4 a. Suitable primer pairs were developed (Table S2, Figure S1) and the effect of a variable S nutrition in combination with a *V. dahliae* infection was analyzed by relative qRT-PCR in intact tomato hypocotyls (Figure 4 b) in a first approach to get a general overview on transcription patterns.

APR is a key regulator of S assimilation and strongly induced by S starvation (Vauclare et al., 2002; Davidian and Kopriva, 2010; Kopriva et al., 2012). In tomato hypocotyls *LeAPR* was induced under S deficiency in both tomato genotypes (Figure 4 b I). The fungal colonization drastically decreased the transcription at low and slightly at supra-optimal S supply questioning a relevant contribution of *LeAPR* to SED against *V. dahliae* at the whole tissue level.

The exclusively plastid-localized enzyme SiR is encoded by a single-copy gene showing weak transcriptional control (Khan et al., 2010). In tomato hypocotyls *LeSiR* was down-regulated by fungal infestation at low S nutritional status, whereas at high S supply the transcription was not affected (Figure 4 b II). Thus, *LeSiR* seems not to be involved in SED against *V. dahliae*.

Oastl is part of the Cys-Synthase Complex (CS) which is decisive for Cys production (Heeg et al., 2008 Feldman-Salit et al., 2009). The minor changes in transcript amounts of the tomato plastidic isoform *LeOastlp1* in tomato hypocotyls in response to S deficiency and fungal colonization are in agreement with a generally weak transcriptional control of CS (Figure 4 b III). Thus, by focusing on the bulk hypocotyl tissue a contribution of *LeOastlp1* to SED appears to be unlikely.

A *V. dahliae*-mediated induction of a member of the group 1 high affinity sulfate transporters in vacuolar tissue of the *V. dahliae*-resistant genotype has been implicated in S^0 formation (Howarth et al., 2003). Since we assumed that the sulfate-S availability for S reduction and related S^0 formation is mainly controlled by transport of sulfate through the tonoplast the current study focused on group 4 vacuolar sulfate transporters. The tonoplast-localized gene *AtSultr4;1* encodes the major transporter isoform induced under S deficiency and facilitates sulfate efflux to the cytosol in the pericycle and xylemparenchyma cells of roots and hypocotyls (Kataoka et al., 2004). In tomato hypocotyls an increased abundance of *LeSultr4;1* mRNA at low S supply (Figure 4 b IV) confirmed its nutrient status-driven metabolic regulation. In contrast, in both tomato genotypes *LeSultr4;1* was down-regulated in relation to *V. dahliae* infestation particularly at a low plant S status. Therefore, an enhanced export of sulfate from the vacuoles to the cytoplasm facilitating and enhancing sulfate-S reduction may not be involved in S^0 synthesis and thus SED of the whole tomato hypocotyl tissue.

The *Arabidopsis* genome contains 20 putative sulfurtransferases (Str) divided into 6 groups, which generally transfer S from a donor to a suitable acceptor (Bartels et al., 2007; Mao et al., 2011). *AtStr1* is thought to be involved in plant disease-resistance establishment (Papenbrock et al., 2010). However, in tomato hypocotyls the expression of *LeMSt1* and *LeMSt2* was only slightly induced by S deficiency but repressed by *V. dahliae* colonization at both S levels (Figure 4 b V, VI). A direct participation of these genes in S^0 or SDC-mediated pathogen defence in intact hypocotyl tissue, therefore, cannot be assumed.

GSH is a major substrate for multiple cellular reactions including initiation of signal transduction, ROS scavenging and putatively also S^0 production (Mittler et al., 2004; Rausch and Wachter, 2005; Galant et al., 2011). As part of the reactive oxygen species (ROS) detoxification-system in plants, GSSG is recycled into its reduced form by NADPH-dependent GSH reductase (GR) (Noctor et al., 2012). Focusing on the tomato GSH synthesis-mediating genes *LeGSH1* and *LeGSH2* and the GSSG reduction-related gene *LeGR2* a clear responsiveness to S deficiency could not be detected (Figure 4 b VII - IX). However, these three genes were significantly induced by a *V. dahliae* infection in both genotypes particularly at deficient S supply. The transcription of plastid localized *LeGSH1* was nearly doubled in both tomato genotypes. This emphasizes the importance of GSH as an antioxidant involved in ROS scavenging in the presence of *V. dahliae*. The slightly higher induction of the three genes in the resistant genotype was also reflected by constitutively higher GSH concentrations

in resistant hypocotyl tissue (Chapter I). Since in *Arabidopsis* γ -glutamylcystein (γ -GC) is produced exclusively in plastids (Wachter et al., 2005), in tomato the fungus-mediated up-regulation of *LeGSH1* could result in elevated plastidic γ GC levels which might be transported into the cytosol for sufficient GSH formation and translocation. However, an increase in the GSH pool size was detected only in infected sensitive tomato plants especially under high S supply, whereas the resistant genotype seemed to have the ability to utilize its constitutively higher GSH reservoir in case of a fungal infestation (Chapter I).

In response to *V. dahliae* infection S^0 is specifically produced and deposited in the xylem and xylemparenchyma cells of the hypocotyl vascular bundles particularly by *V. dahliae*-resistant tomato plants at high S supply (Williams et al., 2002). A specific accumulation of S in these tissues areas in the resistant genotype at high S supply is also suggested by the LA-ICP-MS data shown in Figure 3. As a reference for cell-specific regulation of S metabolism-associated genes in non S^0 -producing plant tissue the cortex was analyzed (Figure 5 g). Comparable to the gene expression pattern in hypocotyl tissue the Cys synthesis-related transcription of *LeSiR* was induced but in contrast *LeOastlp1* remained unregulated. Similar to the total tissue analysis also in cortical tissue the fungus acted as inductor of the GSH biosynthesis-related genes. Particularly *LeGSH1* was up-regulated in a way comparable to its expression in bulk hypocotyl material. Thus, the broad pathogen-induced ROS scavenging function of GSH also prevails in tomato hypocotyl cortical cell layers whereas the promotion of Cys synthesis-related steps seem to be of minor importance especially in the presence of *V. dahliae*.

To specifically focus on the hypocotyl tissue targeted by the fungus, vascular cell areas were isolated by LMPC and the spatial gene expression of the nine S metabolism-related candidates was analyzed in infected high-S supplied resistant tomato xylem and xylemparenchyma cells (Figure 5 h). Compared to hypocotyl and cortical tissue significant changes could be observed in vascular cells. In the cortex and in vascular bundles *LeSiR*, *LeMSt1* and *LeMSt2* showed similar expression patterns after fungal colonization of plants. Although, changes in pool-size, redox-state and location of GSH have been considered to initiate SDC synthesis (Rausch and Wachter, 2005; Kruse et al., 2007), the strong down-regulation of all three GSH-related genes in vascular cells does not support a contribution to S-enhanced plant defence. GSH rather seems to facilitate a global ROS detoxification indicated by pathogen-based induction of the related genes in the bulk tomato hypocotyl tissue and the cortex. However, in the vascular bundle tissue *LeOastlp1* transcripts were

increased in presence of *V. dahliae*. This up-regulation suggests a transcriptomic contribution of *LeOastlp1* to vascular S-enhanced protective mechanisms. Processing of Cys is discussed as one way for SDC generation (Cooper and Williams, 2004; Kruse et al., 2007). Since OASTL is directly linked to Cys biosynthesis, it seems to be a key player in tomato SED mechanism on the cellular level. It can be assumed that the enhanced vascular *LeOastlp1* expression results in a local increased synthesis of Cys which offers a pool of metabolizable Cys for the production S^0 .

In conclusion the soil-borne phyto-pathogenic fungus *V. dahliae* commonly enters the vascular system of the host root through endodermis-free undifferentiated root tips and root wounds and spreads through the xylem vessels to systemically colonize the host-plant shoots (Heinz et al., 1998; Fradin and Thomma, 2006) (Figure 6 a). In an incompatible tomato-*Verticillium* interaction the fungitoxic character of S^0 induces a limitation of fungal growth directly at an early phase of plant-pathogen contact in the xylem. In the presence of the fungus the reductive S assimilation pathway is thought to deliver precursor metabolites for the efficient production of S^0 (Rausch and Wachter, 2005). The identification of cell-specific expression patterns for parts of the primary S metabolism revealed an S-enhanced supporting role of two candidate genes in local S-based defence and global anti-oxidative protection. In infected tomato vascular bundles the enhanced expression of *LeOastlp1* suggests a major role of Cys for the establishment of effective SED reactions (Figure 6 b). The rise in Cys synthesis seems to precede the enhanced formation of S^0 in xylem and xylemparenchyma cells. A second player implicated in defence against *V. dahliae* is GSH, which performs its ROS-scavenging activity through the continuous replenishment of its reduced form predominantly in non-vascular tissue areas. Increased *LeGSH1* expression in total hypocotyl tissue is accompanied by a reduction in vascular bundles. It thus appears that Cys and GSH are both involved in protection of tomato against *V. dahliae*, but each of the two S-containing metabolites with a different site and particular mode of action. Whereas GSH has a pivotal role as broad acting antioxidant in the entire tissue, Cys locally contributes to vascular SED mechanisms including the synthesis of the phytoalexin S^0 . To enable an effective defence, the global protective action of the antioxidant GSH supplements a Cys-promoted vascular SED mechanism in tomato plants infected by *V. dahliae*. The identification of two S metabolism-related genes responding to *V. dahliae* infection cell-specifically provides new insights into the early steps of S^0 synthesis in tomato vascular tissue.

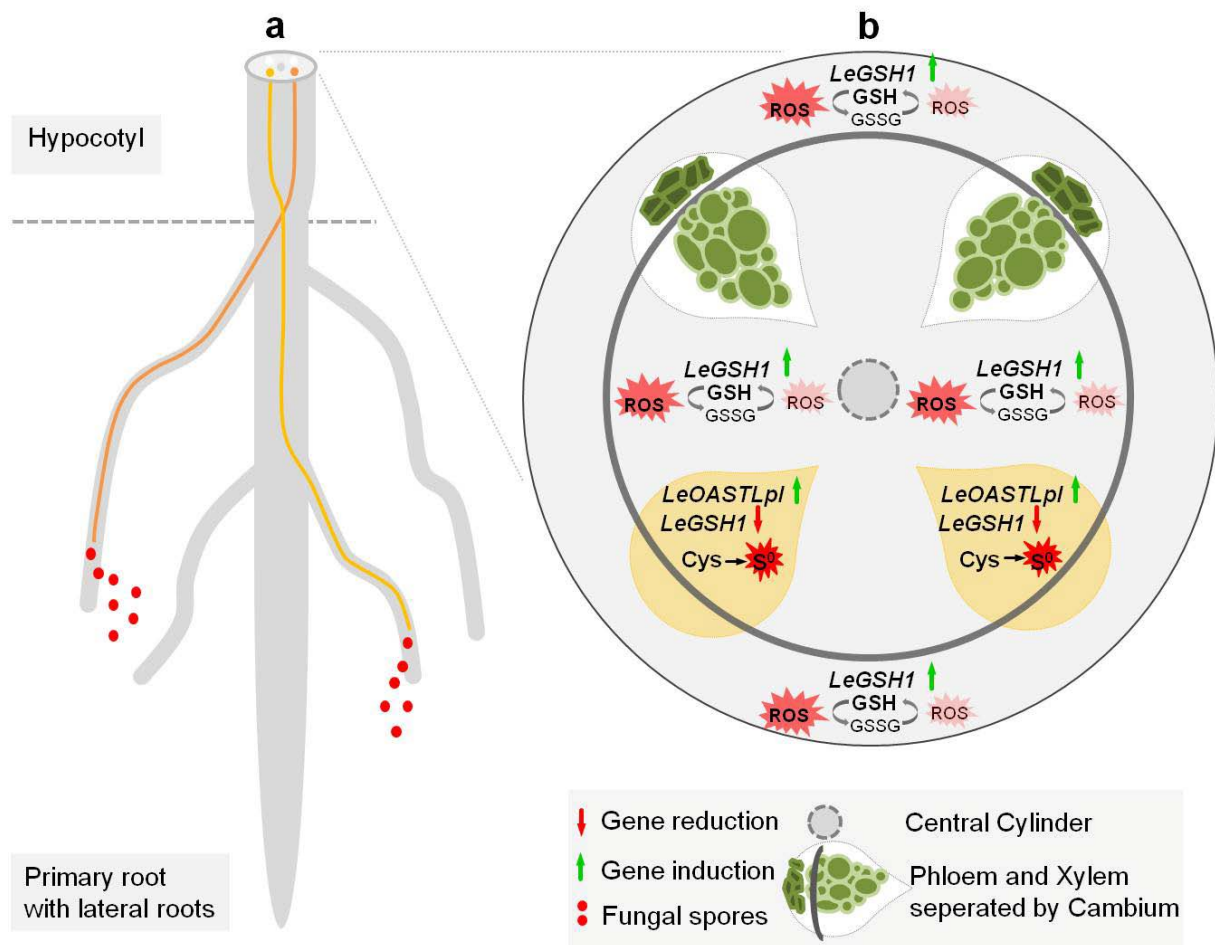


Figure 6 Schematic summary of *V. dahliae*-induced protective SED reactions in hypocotyl tissue of high S-supplied plants of the resistant tomato genotype. **a** The penetration of the root system at different sites results in fungal colonization of different parts of the vascular tissue. **b** S-containing key metabolites are involved in protection against the fungus. The enhanced synthesis of Cys through up-regulation of *LeOastlpl* and down-regulation of *LeGSH1* in the vascular bundle leads to formation of S⁰ in xylem vessels, and the enhanced synthesis of GSH through up-regulation of *LeGSH1* in the remaining tissue of the hypocotyl confers globally improved protection against fungus-induced formation of ROS in the hypocotyl.

Chapter III - Physiological and transcriptomic characterization of the response of *Solanum habrochaites* / *Solanum lycopersicum* introgression lines to *Verticillium dahliae* infection

Katharina, Bollig¹, André Specht¹, Mareike Bach¹ and Walter J. Horst¹

(1) Institute for Plant Nutrition, Faculty of Natural Science, Leibniz University Hannover, Herrenhäuserstraße 2, 30419 Hannover, Germany

To be submitted

Abstract

Verticillium-wilt disease is caused by the fungal pathogen *Verticillium dahliae* (*V. dahliae*), which infects a wide range of host plants including the solanaceous species tomato causing yield reduction. External plant disease control is difficult since chemical control reagents and non-chemical disease management show limited effectiveness. The application of disease-controlling strategies is of major interest. A promising consumer and environmental friendly mechanism already described in resistant tomato plants is the process of sulfur (S)-enhanced defence. The fungitoxic action of specific S-containing metabolites limits the fungal colonization of infected plants and can be further enhanced by high external S application. Besides, in tomato the expression of race-specific resistance genes is known to confer increased *V. dahliae* resistance. To identify tomato plants differing in *V. dahliae* resistance, an initial global screening was conducted with an introgression line (IL) population of wild type (WT) *Solanum habrochaites* in the background of the recurrent parent (RP) a cultivated *Solanum lycopersicum* genotype. On the basis of the hypocotyl tissue-concentration of fungal genomic DNA (gDNA) the sensitive IL 54 and the resistant IL 7 together with the WT donor and RP were selected for further physiological and transcriptomic analysis. For the characterization of *V. dahliae* resistance-promoting processes, measurements of fungal gDNA, total leaf S concentration and sugar phloem transport were combined with relative expression analysis of the race-specific receptor gene *Ve1* and the gene coding the signal-transduction supporting co-chaperon RAR1. The highly susceptible WT donor was shown to be incapable of efficient S-mediated defence and resistance (R) gene expression. The combined use of a strong S-enhanced defence together with R gene expression reduced fungal levels in the RP and the sensitive IL 54. The high fungal resistance of IL 7 was related to a strong induction of the R gene transcription. The current study using tomato ILs and their parents demonstrates a genotypic specific and differentially important defence strategy for the establishment of an incompatible tomato – *V. dahliae* interaction relying either on SED processes or an R gene-dependent action or both.

Keywords: Tomato introgression line, *Verticillium dahliae*, sulfur-enhanced defence, Resistance gene

Introduction

The plant pathogenic soil-borne ascomycete *Verticillium dahliae* (*V. dahliae*) is causing wilting disease in a huge number of host plants including also tomato as a member of the *Solanaceae* family worldwide (Pegg, 1984; Agrios, 2005). External plant disease control is difficult since the heterogeneous fungal genus *Verticillium* generates very robust and durable forms of resting structures in the soil (Pegg and Brady, 2002). The various application ways for a number of chemical control reagents including chemical products, fungicidal antibiotics, fungicides, growth retardants show limited effectiveness since many soil, climate and plant-dependent factors influence their performance and, additionally, they often proved to be environment and consumer-harmful (Goicoechea, 2009). Non-chemical disease management including grafting, crop rotation, soil solarisation, and especially the application of organic soil amendments also shows highly variable effectiveness and thus cannot guarantee appropriate pest suppression (Ochiai et al., 2008; Goicoechea, 2009). Therefore, there is a need of shifting the focus of pathogen elimination onto more efficient disease control strategies.

Today a popular approach in plant-disease research is the search for and identification and incorporation of a genomic source of resistance stably inherited in resistant plants. In tomato the genetic structure of *Verticillium*-disease resistance is described to be of monogenic nature. The decisive resistance (R) gene conferring increased monogenic resistance to *V. dahliae* race 1 strains is *Ve1* (*Verticillium* race 1), which encodes a cell surface receptor belonging into the family of extracellular leucin-rich repeat (eLRR) receptor-like proteins (RLPs) class of disease resistance proteins (Diwan et al., 1999; Kawchuk et al., 2001; Fradin et al., 2009). Together with the closely linked inversely orientated *Ve2* gene both R genes comprise the *Ve* locus located on the long arm of tomato chromosome 9. It was shown that only *Ve1* and not *Ve2* governs resistance against race 1 strains of *V. dahliae* and *V. albo-atrum* (Fradin et al., 2009). Several downstream-located candidate genes, already known to function in intensively studied disease signalling cascades, are thought to participate also in tomato defence against *Verticillium* species (Fradin et al., 2009; Fradin et al., 2010). Nevertheless, in tomato the molecular basis of signal-transduction following *Ve*-mediated pathogen recognition remains to be clarified.

An additional mechanism contributing to *in-planta* *Verticillium* disease-resistance is the sulfur (S)-enhanced defence (SED) response, which involves antifungal elemental S (S^0) to

constrain *V. dahliae* growth in colonized vascular tissue of resistant tomato plants (Chapter I; Chapter II; Williams et al., 2002). Besides the vascular tissue-specific up-regulation of S metabolism-associated genes (Chapter II), a high external S application could also stimulate the expression of known R genes and their associated signalling pathways. SED mechanisms might exhibit a complex interaction with the entirety of R genes involved in establishment of an incompatible tomato – *V. dahliae* interaction finally changing traditional monogenic resistance into a multifactorial process.

One possibility to identify and study specific genomic loci that might include single R genes or quantitative trait loci (QTL), which increase resistance against plant pathogens or participate in signal-transduction upon pathogen contact, is the use of a population originating from a cross between a susceptible and a resistant parent. Therefore, a common strategy is the development of a permanent mapping population through the interspecific crossing of a wild relative with a cultivar of a cultivated species (Rick, 1982; Eshed and Zamir, 1994; Finkers et al., 2007). The resulting population can represent a set of introgression lines (ILs) covering the whole or predominant part of the wild type (WT) parental genome. After repeated backcrossing of an interspecific hybrid with its recurrent parent (RP) the resulting ILs typically carry a single defined chromosome segment from the WT donor in the uniform genetic background of the RP (Monforte and Tanksley, 2000; Zamir, 2001). These ILs are nearly isogenic to the RP by containing major parts of the RP genome and observable phenotypic differences in comparison to the RP are often directly associated with one or multiple introgressed chromosome segments (Eshed and Zamir, 1995). Following identification of relevant resistance-linked single or multiple introgressed segments the genes or gene groups associated with these genomic regions can be examined, further characterized and cloned into susceptible genotypes. One IL library developed by Monforte and Tanksley (2000) in relation to the elucidation of disease resistance is composed of near isogenic lines (NILs) together with backcross recombinant inbred lines (BCRILs). After successful biparental crossing, the complete IL population represents the genome of the WT species *S. habrochaites* (*L. hirsutum*) accession LA1777 in the cultivated genetic background of *L. esculentum* cv. E6203 (Monforte and Tanksley, 2000). Each of the 98 lines contains one to several homozygous chromosome segments introgressed from *S. habrochaites* that are characterized by a specific set of genetic markers. The complete population covers at least 85 % of the WT species genome and seeds have been obtained from the Tomato Genetic Resource Centre (TGRC) (<http://tgrc.ucdavis.edu/>).

The objective of the current study was to screen the IL population of Monforte and Tanksley (2000) with an absolute qRT-PCR assay (Chapter I) for differences in the level of *V. dahliae* colonization of the hypocotyl after fulgal infection to identify and select specific *V. dahliae*-sensitive and resistant ILs carrying different WT donor introgressions. *Verticillium*-wilt disease-related physiological parameters were tested for the identified ILs, the WT donor and the RP elucidating the importance of SED mechanisms. Additionally, in a relative qRT-PCR approach the expression of *Verticillium*-wilt associated R genes was analyzed in the selected ILs and their parents to further characterization a possible S-dependency or SED linkage.

Material & Methods

Cultivation of plant material

A set of 90 near-isogenic introgression lines (ILs) containing at least 85 % of the wild type (WT) *S. habrochaites* LA1777 genome in a *L. esculentum* cv. E6203 recurrent parent (RP) genetic background (Monforte and Tanksley, 2000) was selected for this study. The ILs 24, 35 and 58 failed to germinate and finally a set of 87 ILs, the WT donor and the RP were used. Further analysis were performed with a selection of ILs and their parents. Plants were cultivated in a green house in summer 2011 and spring and summer 2012 under seasonal climate and light conditions. Two weeks after seeding, plants were transferred to peat moss (Klasmann-Deilmann GmbH, Geeste, Germany) limed with CaCO₃ to pH 5.0 in 1 L pots. Plants were pre-cultured for three weeks until fungal inoculation and harvested 7 dpi. During this four week cultivation period a full nutrient solution was applied every second day. The composition of the solution was: 7.00 mM KNO₃, 0.90 mM MgCl₂, 1.00 mM KH₂PO₄, 1.70 mM Mg(NO₃)₂, 0.10 mM NaCl, 5.00 mM Ca(NO₃)₂, 2.00 mM CaCl₂, 50 µM FeNaEDTA, 1.3 µM ZnSO₄, 24.5 µM H₃BO₃, 6.0 µM CuSO₄, 0.8 µM (NH₄)₂ MoO₄, 9.3 µM MnSO₄. Plants treated with low S supply did not receive additional S. To obtain a supra-optimal S supply plants were additionally supplied with 25.0 mM K₂SO₄.

Table 1 Tomato accession (TA) / *Lycopersicum* accession (LA) -based official and internal identification code for the tested set of 89 tomato ILs, the WT donor and the RP.

IL	TA	LA	IL	TA	LA	IL	TA	LA
1	TA1258	LA3913	32	TA1539	LA3944	64	TA1468	LA3978
2	TA523	LA3914	33	TA1545	LA3945	65	TA1630	LA3979
3	TA1229	LA3915	34	TA1546	LA3946	66	TA1290	LA3980
4	TA1127	LA3918	36	TA1303	LA3948	67	TA1116	LA3981
5	TA1223	LA3916	37	TA1304	LA3949	68	TA1631	LA3983
6	TA1128	LA3919	38	TA1547	LA3950	69	TA1632	LA3984
7	TA1538	LA3924	39	TA1312	LA3951	70	TA1306	LA3985
8	TA1537	LA3923	40	TA1315	LA3952	71	TA1309	LA3986
9	TA1266	LA3922	41	TA1316	LA3953	72	TA1318	LA3988
10	TA1105	LA3921	42	TA1548	LA3954	73	TA1319	LA3989
11	TA1473	LA3937	43	TA1320	LA3955	74	TA1560	LA3990
12	WT	LA1777	44	TA1324	LA3956	75	TA1326	LA3991
13	TA1111	LA3925	45	TA1325	LA3957	76	TA1635	LA3994
14	TA1276	LA3926	46	TA1330	LA3958	77	TA1553	LA3995
15	TA1277	LA3927	47	TA1331	LA3959	78	TA1120	LA3996

16	TA1540	LA3928	48	TA1550	LA3960	79	TA1563	LA3997
17	TA1541	LA3929	49	TA1551	LA3961	80	TA1638	LA3999
18	TA1133	LA3930	50	TA1552	LA3962	81	TA1557	LA4000
19	TA1280	LA3931	51	TA1337	LA3963	82	TA1644	LA4001
20	TA1562	LA3932	52	TA1339	LA3964	83	TA1645	LA4002
21	TA1542	LA3933	53	TA1555	LA3965	84	TA1648	LA4003
22	TA1459	LA3934	54	TA1554	LA3966	85	TA1649	LA4004
23	TA517	LA3935	55	TA1342	LA3967	86	TA1652	LA4005
25	TA1536	LA3936	56	TA1350	LA3968	87	TA1654	LA4006
26	TA1287	LA3938	57	TA1121	LA3969	88	TA1655	LA4007
27	TA1293	LA3939	59	TA1218	LA3970	89	TA1656	LA4008
28	TA1112	LA3940	60	TA1173	LA3071	90	TA1564	LA4009
29	TA1543	LA3941	61	TA1629	LA3975	91	TA1561	LA4010
30	TA1117	LA3942	62	TA1138	LA3976	92	RP	LA4024
31	TA1544	LA3943	63	TA1467	LA3077			

Cultivation of the fungal pathogen and inoculation method

The long-term cultivation of *V. dahliae* isolate TomIGZ (GU060637) mycelium was carried out on potato dextrose agar (PDA) (Duchefa, Haarlem, Netherlands) in the dark at 24°C. For the production of fungal inoculum six slices (\varnothing 1 cm) of mycelium were transferred into sucrose sodium nitrogen (SSN) medium and cultivated at 100 rpm and 26 °C for three weeks. The fungal spore concentration used for inoculation was diluted to $1 \cdot 10^{-7}$ spores mL⁻¹ with dH₂O in a hemocytometer. Three-weeks-old plants were carefully uprooted and roots were gently washed free of substrate in dH₂O. Then 1 / 3 of the total root mass were cut off and plant roots were inoculated by incubation in 80 ml spore suspension for 1 h at 110 rpm. After inoculation all plants were transferred into fresh CaCO₃-limed peat moss.

Analysis of physiological parameters

After analysis of plant height and fresh weight, leaves and hypocotyls were dried at 65 °C for 72 h. The dry weight was measured and samples were grinded and homogenized for the determination of total S using a Vario EL CNS analyzer (Dumas Elementar Analysensysteme GmbH, Hanau, Germany). The photosynthesis rate was measured with a portable gas-exchange system (LI-6400, LI-COR, Lincoln, NE, USA) at a photosynthetic photon flux density of 1000 $\mu\text{mol m}^{-2} \text{s}^{-1}$ and an incoming CO₂ concentration of 360 $\mu\text{mol mol}^{-1}$. Measurements included 6 cm² of the terminal leaflet from the youngest fully expanded leaf on each plant. Phloem exudates were collected according to Cakmak et al. (1994) using intact tomato shoots. Plants were cut off below the hypocotyl 4 h after the onset of the light period.

Immediately after recutting under dH₂O, plants were placed in 5 ml 20 mM Na-EDTA solution (pH 6.0). About 1 cm of the shoot was immersed in solution while plants were kept in the dark at high humidity. Phloem sap was sampled after 2 h and sugars were quantified with the anthrone method (Dreywood, 1946) in a μ Quant Scanning Microplate Spectrophotometer (BioTek, Bad Friedrichshall, Germany) at $\lambda = 620$ nm. A standard curve included 0, 25, 50, 100, 150, 200 $\mu\text{g ml}^{-1}$ D-glucose. The complete root systems were carefully washed out of substrate 7 dpi and the total root length was determined with the WinRHIZO Software (Regent Instruments Inc., Canada).

DNA extraction

Hypocotyls from both tomato genotypes were harvested 7 dpi and the hypocotyl tissue including plant vascular tissue was homogenized under liquid nitrogen. The isolation of gDNA followed a modified cetyltrimethylammonium bromide (CTAB) method including 200 mg (fresh weight) dissected hypocotyl tissue or 50 mg (fresh weight) homogenized fungal mycelia as described in Zahn et al. (2011). The DNA quantity and purity were determined spectrophotometrically (NanoPhotometer™, Implen GmbH, Munich, Germany). A quality control for the integrity of nucleic acids was additionally performed on 2 % (w / v) agarose gels stained with RotiSafe dye.

Absolute qRT-PCR conditions

The qRT-PCR-based absolute quantification of fungal gDNA within the plant tissue was performed in a CFX96™ Real-time detection system (BioRad Laboratories, Hercules, California, USA). A self-prepared SYBR Green-based master mix included the following components in a final volume of 25 μL : Hot-Start PCR buffer B1 (1 x), MgCl₂ (3.6 mM), SYBR Green-I (0.1 x) (Invitrogen GmbH, Darmstadt, Germany), dNTPs (200 μM each) (Fermentas, St. Leon-Roth, Germany), forward and reverse primer LeVD (252 nM each) (Chapter I), DCShot DNA polymerase (0.75 U) (DNA Cloning Service, Hamburg, Germany), 100 ng gDNA template. Thermal qRT-PCR cycling stages consisted of an initial denaturation at 95 °C (10 min), followed by 35 cycles at 95 °C (15 s), 60 °C (30 s), 72 °C (30 s) and a final melting curve analysis at 95 °C (10 s), 60 °C to 95 °C with a 0.5 °C 5 s⁻¹ increasing temperature gradient. Fluorescence signals were recorded during the primer annealing and strand elongation steps at 60 °C and 72 °C and during the melting curve phase at every 0.5 °C temperature ramp.

RNA extraction

Tomato hypocotyl material was frozen immediately in liquid nitrogen. For RNA isolation, samples were ground under liquid nitrogen and total RNA was isolated from 50 mg with the TRIsure® Reagent (Bioline, Luckenwalde, Germany) following the manufacturer's instructions. For the synthesis of cDNA 1 µg of total RNA was combined with random hexamer primer in the RevertAid™ H Minus First Strand cDNA Synthesis Kit (Fermentas, St. Leon-Roth, Germany) according to the manufacturer's instructions.

Primer design parameters

LeRAR1 primer pairs for the relative qRT-PCR assay were designed using the primer 3 plus software (Untergasser et al., 2007). Internal primer quality parameters included an amplicon size of 90 – 150 base pairs (bp), a melting temperature of 59 – 61 °C, a length of 20 – 24 nucleotides, and a GC content of 45 – 65 %. The primer pairs were initially tested for the amplification of predicted fragment sizes, primer dimerization, or multiple unspecific fragment amplification in a conventional PCR assay including the following components in a final volume of 25 µL: Hot-Start PCR buffer B1 (1 x), MgCl₂ (3.6 mM), dNTPs (200 nM each) (Fermentas, St. Leon-Roth, Germany), forward and reverse primer (252 nM each), DCSHot DNA polymerase (0.75 U) (DNA Cloning Service, Hamburg, Germany), 50 ng tomato cDNA template. The PCR parameters comprised an initial denaturation at 95 °C (10 min), followed by 30 cycles at 95 °C (15 s), 60 °C (30 s), 72 °C (30 s). PCR products were analyzed on a 2 % (w / v) agarose gel in 1 × TAE buffer with the Roti®-Safe GelStain (Carl Roth GmbH, Karlsruhe, Germany). The amplification efficiency was tested based on a standard curve method including a five-fold tomato cDNA triplicate serial dilution starting with 20 ng tomato cDNA. The qRT-PCR efficiency was calculated using the CFX Manager™ software (BioRad Laboratories, Hercules, California, USA).

Relative qRT-PCR analysis

Due to its consistent expression tested in nutrient and cold-stress experiments tomato elongation factor 1 α (*LeElf1a*, X14449) was used as internal reference gene (Løvdaal and Lillo, 2009). A self-prepared SYBR-Green I based master mix included 50 ng of tomato cDNA in the following 25 µL reaction mixture: Hot-Start PCR buffer B1 (1 x), MgCl₂ (3.6 mM), 1000 x SYBR Green-I (0.1 x) (Invitrogen GmbH, Darmstadt, Germany), dNTPs (200 nM each) (Fermentas, St. Leon-Roth, Germany), forward and reverse primer (252 nM each), DCSHot DNA polymerase (0.75 U) (DNA Cloning Service, Hamburg, Germany). Thermal

qRT-PCR cycling stages were performed in a CFX96™ Real-time detection system (BioRad Laboratories, Hercules, California, USA) and consisted of an initial denaturation at 95 °C (10 min), followed by 35 cycles of 95 °C (15 s), 60 °C (30 s), 72 °C (30 s) and a final melting curve analysis of 95 °C (10 s), 60 °C to 95 °C with a 0.5 °C 5 s⁻¹ increasing temperature gradient. For each target in the qRT-PCR three technical and three biological replicates were used. Relative transcript levels were calculated using the 2^{-ΔΔCT} method (Livak and Schmittgen, 2001) including a primer efficiency correction.

Statistical analysis

The design of the initial IL screening experiment had a randomization structure with two blocks nested in one greenhouse, while the three biological IL replicates were randomly arranged in each of the complete blocks. To account for this structure a mixed model was fitted, with the effects of lines in the fixed part and the effects of the greenhouse and blocks nested within the greenhouse in the random part. Pair-wise comparisons among all lines were performed, adjusting for multiple comparisons using the option adjust=Tukey in the lsmeans statements. For the statistical analysis, proc mixed (Littell et al., 2004) in version SAS 9.1 has been used. For all experiments including a selection of ILs a completely randomized design including three to five biological replicates was used. Analysis of variance was performed using the general linear model procedure of the statistical program SAS 9.1 (SAS Institute, Cary, NC, USA) testing for genotype, fertilization, infection and their interaction effects. Results of the absolute qRT-PCR analysis including the gDNA concentrations and appropriate standard deviations were calculated using the CFX Manager™ software (BioRad Laboratories, Hercules, California, USA). Significant relative qRT-PCR expression changes were indicated by non-overlapping of the 95 % confidence interval calculated with threshold cycle values given by the CFX Manager™ software (BioRad Laboratories, Hercules, California, USA).

Results

The set of 87 tomato ILs, originating from a cross of the WT donor *S. habrochaites* and the cultivated RP *S. lycopersicum* (Monforte and Tanksley, 2000), was cultivated in the greenhouse under natural climatic conditions and analyzed for *V. dahliae* resistance. The proportion of fungal gDNA in one ng of total gDNA isolated from intact tomato hypocotyl material was measured with the *V. dahliae*-specific primer pair LeVD (Chapter I) in an absolute qRT-PCR assay. According to the level of *V. dahliae* infection the whole IL population could be separated into four different groups (Figure 1).

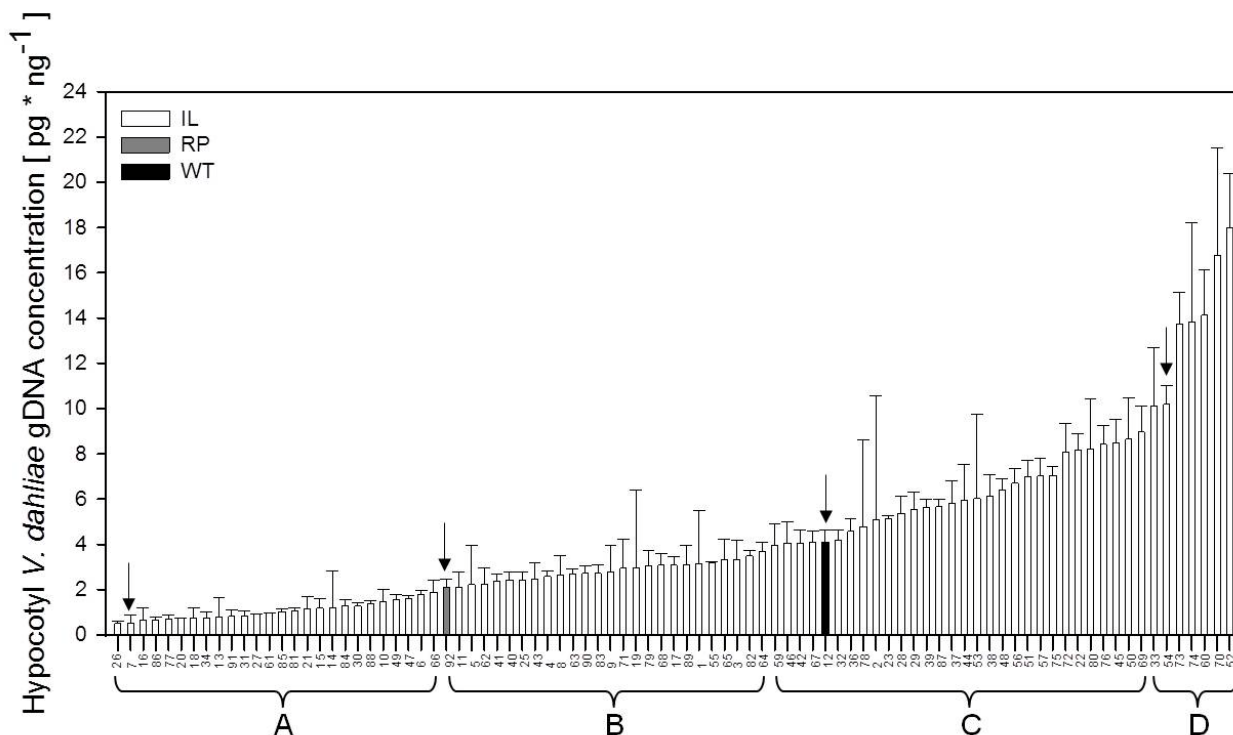


Figure 1 Concentration of fungal gDNA in hypocotyls of 87 *V. dahliae* (VD)-infected tomato ILs differing in fungal resistance and their parental lines. (After 3 weeks of pre-culture at 25 mM SO₄-S plants were root inoculated and harvested 7 dpi. Black arrows indicate the resistant IL 7 and the sensitive IL 54, the WT donor (black bar) and the RP (grey bar) selected for further characterization. ILs were grouped according to their level of *V. dahliae* infection. ILs within the group A and D were significantly more or less resistant against *V. dahliae* than the RP (group B) and the WT donor (group C). Data represent means \pm SD $n = 3$.)

The difference between the highly susceptible group A and the resistant group D was significant at $P \leq 0.05$. The values of the intermediate susceptible groups (B, C) were not significantly different from each other. Group A included resistant ILs with a fungal gDNA

concentration of $1.06 \pm 0.38 \text{ pg ng}^{-1}$. Intermediate group B ($2.81 \pm 0.44 \text{ pg ng}^{-1}$) included the *S. lycopersicum* cultivated RP (LA4024) which was classified as medium susceptible. In intermediate group C ($6.11 \pm 1.59 \text{ pg ng}^{-1}$) the WT accession *S. habrochaites* (LA1777) was among the more susceptible genotypes showing a higher fungal colonization level in comparison to the RP. Group D included seven sensitive ILs with highest *V. dahliae* concentrations of $13.82 \pm 2.98 \text{ pg ng}^{-1}$.

After four weeks of plant cultivation the supra-optimal S fertilization resulted in high plant tissue S concentrations in all genotypes of the tested IL population (Figure 2). The leaf S concentration was $14.87 \pm 1.46 \text{ mg g}^{-1}$ dry wt. and indicated a luxury S consumption for all 87 ILs and the cultivated RP. Although the ANOVA indicated highly significant genotypic differences the only major differences was observed for the WT donor with a leaf S concentration of $8.87 \pm 0.12 \text{ mg g}^{-1}$ dry wt. still reflecting a luxury but much lower plant S nutritional status.

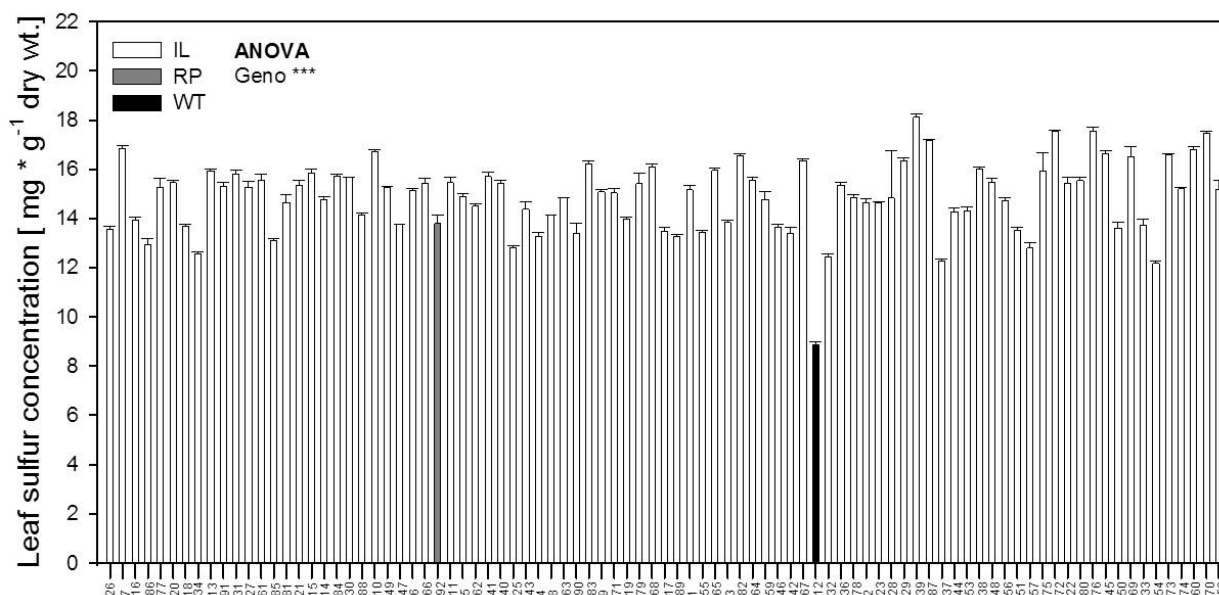


Figure 2 Effect of supra-optimal S supply on S concentrations in leaves of *V. dahliae* (VD)-infected tomato ILs differing in fungal resistance and their parental lines. The WT donor is indicated by a black bar and the cultivated RP by a grey bar. (After 3 weeks of pre-culture at 25 mM SO₄-S plants were root inoculated and harvested 7 dpi. Data represent means \pm SD $n = 3$. Results of the analysis of variance are given according to their level of significance as ***, for $P \leq 0.001$, n.s. non-significant.)

Based on the results of the absolute fungal gDNA quantification in the global *V. dahliae* screening approach, a *V. dahliae*-resistant and sensitive IL was selected for further analysis. Having a low fungal gDNA concentration of $0.53 \pm 0.36 \text{ pg ng}^{-1}$ in the hypocotyl tissue the IL 7 (Group A) was selected as a resistant line. The IL 54 (Group D) showed a significantly higher *V. dahliae* colonization level in hypocotyls with $10.19 \pm 0.85 \text{ pg ng}^{-1}$. Thus, IL 54 was selected as sensitive line. IL 7 carried an introgression on chromosome 2 including the marker TG353. The sensitive IL 54 carried one introgressed segment on chromosome 10 including the marker TG241 and TG233. Two additional large introgressions were located on chromosome 11 including marker TG286, TG36, TG393 and on chromosome 12 including marker TG296 and TG350.

In comparison to the cultivated phenotypic appearance of the RP plants, the WT donor plants typically had smaller dentate leaflets covered with sticky long hairs. These special WT phenotypic characteristics were not detectable within the tested set of 87 ILs, which completely resembled the RP phenotype. The low and high S fertilization caused different leaf S concentrations which resulted in visible differences of the leaf blade coloration of the selected ILs and their parental lines (Figure 3). Light green leaves with dark leaf veins indicated S-deficient growth conditions, whereas dark green leaves appeared on plants supplied with supra-optimal S and reflected a luxury S consumption.

Additionally, the low and high S supply caused differences in plant growth performance with S-deficient plants having a smaller shoot height. As a typical symptom indicating a *Verticillium*-induced disease course, the wilting of single leaflets but also whole leaves could be observed one week after fungal inoculation on infected tomato plants. Wilting symptoms followed a diurnal rhythm with more severe appearance at midday and symptom alleviation during the night. Infection-related shoot-growth reduction could be observed particularly on the low-S supplied WT donor plants.



Figure 3 Effect of low and high S supply on phenotypical appearance of the *V. dahliae* (VD)-resistant IL 7 and the sensitive IL 54 and their parental lines (WT donor and cultivated RP). (After 3 weeks of pre-culture at 25 mM or 0.016 mM $\text{SO}_4\text{-S}$ plants were root-inoculated and harvested 7 dpi.)

Under conditions of S-deficiency the selected ILs had leaf S concentrations of about 2 - 5 mg g^{-1} dry wt., a fungal infection did not cause significant changes (Figure 4 a). At high S supply IL 7 and the RP showed highest leaf S concentrations of about 28 mg g^{-1} dry wt.. IL 54 accumulated up to 22 mg g^{-1} dry wt. The WT donor plants showed the lowest accumulation of leaf S with 10 mg g^{-1} dry wt. The colonization of supra-optimal S fertilized plants by *V. dahliae* slightly reduced the leaf S concentrations in both ILs and their parents. Analysis of plant height, plant fresh weight and dry weight of the selected tomato ILs and both parents indicated no significant differences in relation to S supply or *V. dahliae* inoculation (data not shown). The resistant line IL 7 showed lowest fungal concentrations of about 0.1 pg ng^{-1} at both S supplies (Figure 4 b). In both parental lines a similar high level of fungal colonization of about 0.7 pg ng^{-1} could be detected at low S. The amount of fungal gDNA was substantially reduced by high S supply in the RP, whereas the WT donor even showed an increased fungal colonization under conditions of high S fertilization. The highest concentration of *V. dahliae* gDNA could be measured in hypocotyl material of the sensitive IL 54 at low S fertilization. However, supra-optimal S nutrition greatly reduced fungal gDNA levels in this line to a concentration of about 0.25 pg ng^{-1} .

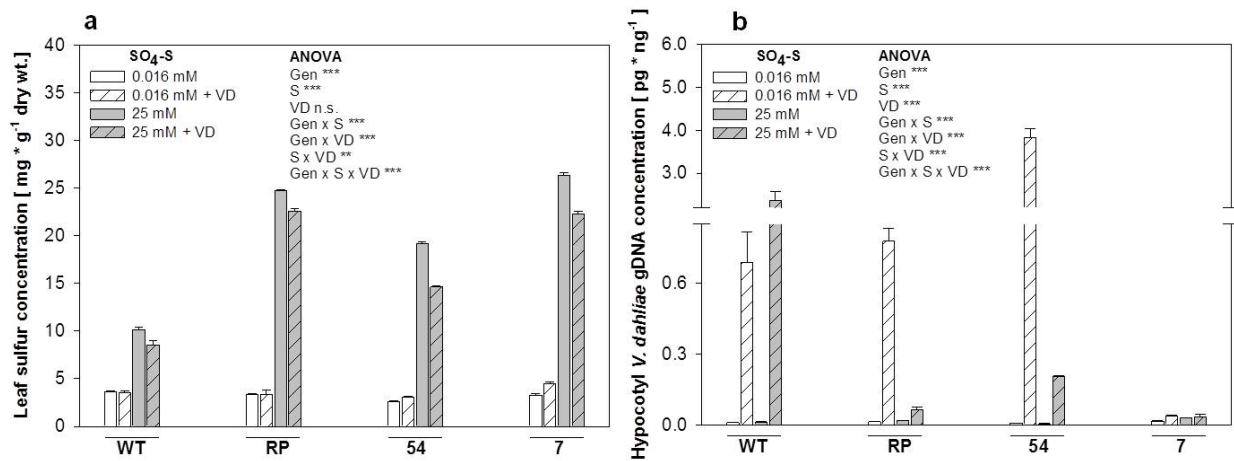


Figure 4 Leaf S concentration **a** and hypocotyl fungal gDNA **b** of the *V. dahliae* (VD)-resistant IL 7, the sensitive IL 54, and their parental lines (WT donor and cultivated RP) as influenced by low and high S fertilization and *V. dahliae* infection. (After 3 weeks of pre-culture at 0.016 mM or 25 mM SO₄-S plants were root inoculated and harvested 7 dpi. Data represent means \pm SD, $n = 3$. Results of the analysis of variance are given according to their level of significance as **, ***, for $P \leq 0.01$, 0.001, respectively, n.s. non-significant.)

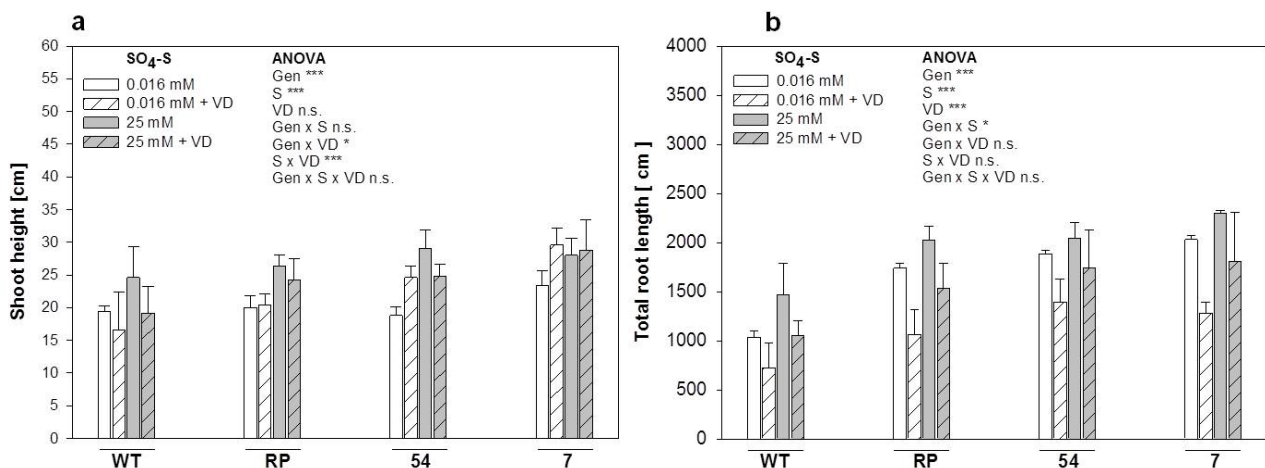


Figure 5 Effect of low and high S fertilization and *V. dahliae* (VD) infection on **a** shoot height and **b** total root length of the resistant IL 7, the sensitive IL 54 and their parental lines (WT donor and cultivated RP). (After 3 weeks of pre-culture at 25 mM SO₄-S plants were root-inoculated and harvested 7 dpi. Data represent means \pm SD, $n = 3$. Results of the analysis of variance are given according to their level of significance as *, ***, for $P \leq 0.05$ and 0.001, respectively, n.s. non-significant.)

Tomato shoot height was decreased by low S supply in both ILs and the parents (Figure 5 a). An infection reduced the shoot height of WT donor plants at both S levels but increased shoot

height of the RP and both ILs (significant Gen x VD interaction) particularly under low S fertilization (highly significant S x VD interaction). Total root length was more negatively affected by low S supply and *V. dahliae* infection than shoot length (Figure 5 b). All genotypes responded to S supply and *V. dahliae* infection principally in the same way and to the same extent.

In all genotypes, the photosynthetic rate of leaves was reduced at low S supply confirming S deficiency in these plants (Figure 6 a). *V. dahliae* colonization of plants caused a reduction of photosynthesis independent of genotype and S supply. An exception was the infected RP, which under high S supply exhibited a slight increase in the photosynthesis rate which may have contributed to the significant Gen x S interaction. The phloem sugar-transport rate was not consistently affected by S supply and *V. dahliae* infection among the genotypes (not significant S and VD effects, but significant Gen x S and Gen x VD interactions, Figure 6 b). The transport rate was lowest in the resistant IL 7 and was hardly affected by S supply and *V. dahliae* infection. In the WT donor plants high S supply enhanced assimilate transport rate which was further increased by *V. dahliae* infection. In the plants of the RP and the sensitive IL 54 high S supply and *V. dahliae* infection reduced the assimilate transport in the phloem.

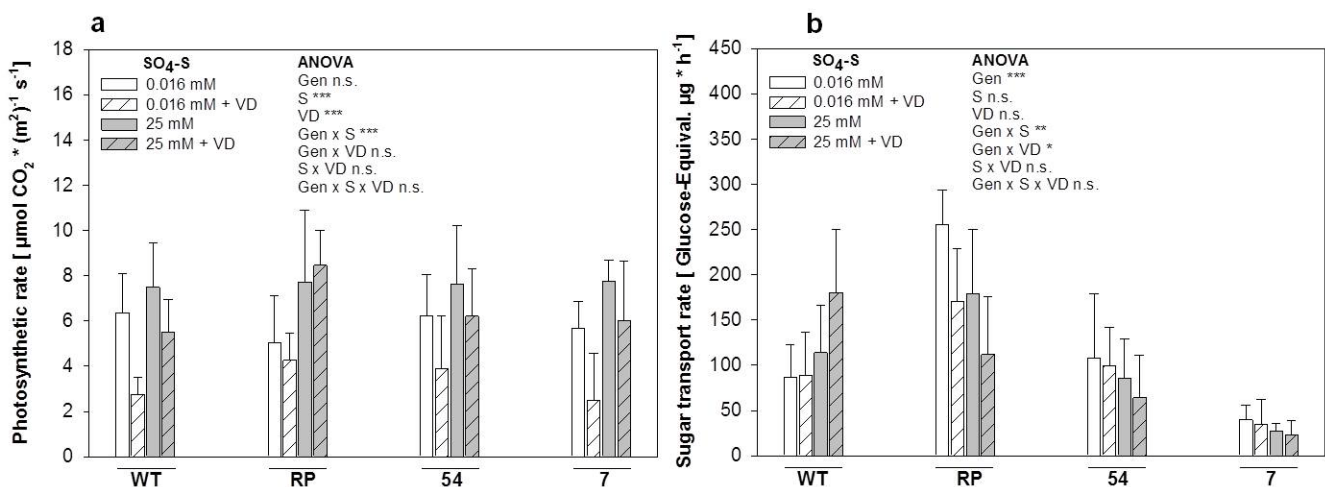


Figure 6 Photosynthetic rate of single leaflets on the youngest fully developed leaf **a** and sugar phloem transport rate in stem exudates collected after dissection of shoots **b**. (Plants of the resistant IL 7, sensitive IL 54 and their parental lines (WT donor and cultivated RP) were pre-cultured for 3 weeks at 25 mM or 0.016 mM $\text{SO}_4\text{-S}$ and then root-inoculated with *V. dahliae* (VD) and harvested 7 dpi. Data represent means \pm SD, $n = 3$. Results of the analysis of variance are given according to their level of significance as *, **, ***, for $P \leq 0.05, 0.01, 0.001$, respectively, n.s. non-significant.)

A comparison of the IL map with the high density genetic map “Tomato-EXPEN 2000” (Tanksley et al, 1992; Fulton et al., 2002) identified the molecular marker TG393 in both maps at position 103 cM on the long arm of tomato chromosome 11 directly linked to the At5g51700 locus. This locus encodes RAR1 (required for Mla12 (Mildew-resistance locus a 12) resistance) and a Blastn based search with the At5g51700 coding sequence (CDS) (Accession NM_124549) together with a taxonomy-report analysis revealed the homologue (E-value $6 \cdot 10^{-56}$) tomato cDNA sequence AK329648. A suitable *LeRAR1* primer pair (LeRAR1+ CAA AGG ATG GCA CAA CAG TG; LeRAR1- GTT GCA GAT GGA CCG AAA GT) was designed for the qRT-PCR analysis and dimerization products or multiple non-specific amplification products were not detectable in a conventional PCR.

Located on the short arm of chromosome 9 the *Ve* (*Verticillium* race 1) gene locus encodes the extracellular cell-surface receptor protein which confers resistance against *V. dahliae* race 1 strains. Based on the *LeVe1* CDS of the resistant tomato genotype GCR218 (Accession FJ464553), a primer pair from Fradin et al. (2009) was used for the qRT-PCR analysis (Ve1QPCRF2 AAC AGT TGT CAA AGC AAT GGC TCA GCC, Ve1QPCRR1 GAA AAC CAA AGC AAG CAT TTC TCC ATA TGC). In a conventional PCR assay no dimerization products or multiple non-specific amplification products were detectable.

The linear expression of the cell-surface receptor encoding gene *LeVe1* (Figure 7 a) and the resistance protein complex-associated gene *LeRAR1* (Figure 7 b) was analyzed by relative qRT-PCR measurement in control and infected resistant IL 7, sensitive IL 54 and both parents under low and high S supply. The constitutive expression of *LeVe1* was low at low S supply in all genotypes, particularly in the WT donor. High S supply enhanced the expression clearly in the *V. dahliae*-resistant IL 7, but decreased it in the *V. dahliae*-sensitive IL 54. *V. dahliae* infection greatly up-regulated *LeVe1* (up to 133-fold) with the exception of the WT donor which responded only at high S supply (22-fold). At high S supply the *LeVe1* expression was reduced under conditions of *V. dahliae* infection in the RP and even more in the *V. dahliae*-sensitive IL 54, but it was further enhanced in the *V. dahliae*-resistant IL 7. There was no significant effect of S supply and *V. dahliae* infection on the expression of *LeRAR1* in none of the genotypes. However, there was a trend of generally lowest *LeRAR1* expression in the WT donor and highest expression in the *V. dahliae*-resistant IL 7 (2 to 4-fold).

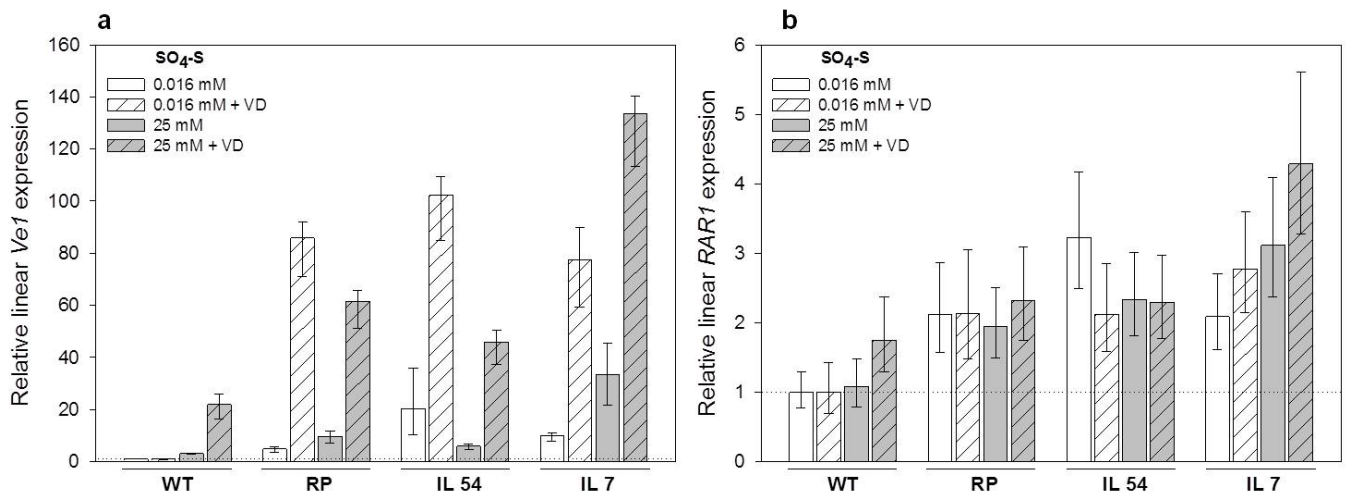


Figure 7 Relative linear expression of the R genes *LeVe1* **a** and *LeRAR1* **b** in hypocotyls of the *V. dahliae* (VD)-resistant IL 7, the *V. dahliae*-sensitive IL 54, the WT donor and cultivated RP as affected by S fertilization and fungal infection. Plants were pre-cultured for three weeks at 25 mM or 0.016 mM SO₄-S, root inoculated and harvested at 7 dpi. The cDNA was synthesized from 1 μg total RNA including random hexamer primer. Expression was calculated using the $2^{-\Delta\Delta CT}$ method (Livak and Schmittgen, 2001). Uninfected WT plants at low S supply were set to ‘1’ as the calibrator. Expression data represent mean values of five biological replicates. Error bars comprise the 95 % confidence intervals.

Discussion

The IL population of Montforte and Tanksley (2000), which was derived from a cross between the cultivated tomato genotype *L. esculentum* cv. E6206 and the *S. habrochaites* WT accession LA1777, was initially screened for variation in the *V. dahliae* hypocotyl colonization level which had proven to reflect genotypic differences in *V. dahliae* resistance (Chapter I). A set of 87 ILs was cultivated under greenhouse conditions in summer 2011 at supra-optimal S supply to activate and enhance SED-based fungus elimination reactions in ILs capable of this defence mechanism. The bulk-leaf S concentrations of tomato plants supplied with supra-optimal S showed a very high level with only minor differences between ILs (Figure 2). A marked exception was the WT donor plants which showed the lowest leaf S concentrations of all genotypes. This might be an indication that SED mechanisms, which were shown to effectively constrain the fungal growth in a resistant tomato line particularly under high S fertilization (Williams et al., 2002; Chapter I), are of less importance with regard to *V. dahliae* resistance in the WT genotype. After one week of inoculation the *V. dahliae* colonization level was quantified across the whole IL set with a previously established sensitive SYBR Green-based absolute qRT-PCR assay including the *V. dahliae*-specific primer pair LeVD (Chapter I). The screening approach revealed a uniform distribution of *V. dahliae* resistance with a nearly equal number of ILs developing a higher and lower fungal susceptibility in comparison to both parental lines (Figure 1). According to their level of fungal colonization the ILs were classified into four significantly different *V. dahliae* resistance groups (A to D). The *S. habrochaites* WT donor of the IL population showed a higher hypocotyl tissue concentration of *V. dahliae* when compared to the RT. This was unexpected, because most WT donor plants used for interspecific bi-parental crossings possess a wide spectrum of positive characteristics including biotic and abiotic stress resistance which after beneficial genetic integration improve the phenotype of their progeny (Eshed and Zamir, 1994, 1995; Gong et al., 2010; Li et al., 2011). Thus, the genome integration of single WT introgression associated with a specific trait improves the resulting ILs and further allows a more detailed identification of trait-associated single genes or QTLs. For the IL population of Monforte and Tanksley (2000) the WT accession *S. habrochaites* LA 1777 was identified as highly resistant against black leaf mold and late blight (Li et al., 2011; Zahn et al., 2011). Since the same WT donor plants were highly susceptible against *V. dahliae*, in the current study the contribution of WT introgressions to increased pathogen resistance of ILs seems to be unlikely in comparison to other major resistance-mediating factors possibly inherited by the cultivated RP.

Based on the initial global *V. dahliae* resistance screening of the IL population (Figure 1) the highly susceptible IL 54 (Group D) and the resistant IL 7 (Group A) were selected for further physiological and transcriptomic analysis in a second experimental approach. Both ILs, the WT donor and the cultivated RP were grown under greenhouse conditions in spring and summer 2012 at low and supra-optimal S supply. The low and high S fertilization caused total S concentrations in the range of 2 (clearly indicative of S deficiency) to 28 mg g⁻¹ dry wt. (clearly in the luxury consumption range) with significant differences in relation to genotype (Figure 4 a). S-deficient growth was reflected by a light green leaf color with dark leaf veins in comparison to dark green leaves at luxury plant S status (Figure 3). After one week of *V. dahliae* infection the level of fungal colonization was measured in tomato hypocotyl tissue with the previously established sensitive absolute qRT-PCR assay (Figure 4 b, Chapter I). Climatic conditions in this second experimental approach caused a slower *Verticillium*-disease development resulting in a less contrasting pathogenesis of tomato plants 7 dpi. However, the fungal gDNA concentrations reflected genotypic S effects comparable to the global IL screening. A significant reduction of fungal colonization levels was previously also detected in a *V. dahliae*-resistant and particularly a sensitive tomato genotype 7 dpi at supra-optimal S fertilization (Chapter I). A comparable S-enhanced containment of fungal growth could be observed for the RP and the sensitive IL 54 at high S supply (Figure 4 b). The RP obviously comprised a high SED capacity which seemed to be transferred to the sensitive IL 54. The luxury S nutrition possibly increased local fungitoxic SDC concentrations and thus promoted an elimination of the fungus in hypocotyl vascular tissue of IL 54 and the RP through enhancement of SED mechanisms. According to the initial global IL population screening, in the WT donor elevated S supply again did not confine the fungal pathogen but rather increased its spread causing highest *V. dahliae* gDNA concentrations. Possibly the combination of a constitutive lower SED capacity and the lack of additional resistance-mediating factors together with a S-enhanced transpiration rate and better growth rate (Figure 5 a, Figure 6 a) might benefit the stronger fungal colonization of WT donor plants. Reflecting results of the initial global screening, the resistant IL 7 exhibited a consistently low colonization level at both S supplies, indicating the existence of additional major factors contributing to its resistance against *V. dahliae* beside SED mechanisms.

The cyclic colonization pattern of the *Verticillium*-wilt disease-course with changes of fungal proliferation and elimination (Chen et al., 2004; Robb et al., 2007) caused a mild wilting of single leaflets within whole leaves 7 dpi in all genotypes (Figure 3). High S supply

significantly increased the shoot growth of all tested control tomato plants (Figure 5 a) confirming S deficiency at low S supply. A fungus-related clear growth reduction could only be detected in low and high S supplied WT donor tomato plants. After fungal infection the RP and the sensitive IL 54 showed an increased shoot length particularly under S-deficient growth conditions and the resistant IL 7 at both S levels. An elevated plant height was also observed in a tolerant tomato-*Verticillium* interaction 10 dpi after root-clip infection of high S-supplied tomato plants (Robb et al., 2007). A general down-regulation of ethylene biosynthesis associated genes, but also changes in the transcriptional control of gibberellin biosynthesis, were thought to account for this enhanced shoot length (Pierik et al., 2006; Robb et al., 2007). Root-length analysis displayed a clear S responsiveness in relation to S supply for all tested tomato plants with WT donor plants generally having the lowest total root length (Figure 5 b). The *V. dahliae* infection proved to be a strong biotic stress significantly inhibiting the recovery of tomato root growth. As already detected for a *V. dahliae*-infected resistant and sensitive tomato genotype (Chapter I) also in this study enhanced S supply did not alleviate the negative influence of the fungus on root growth. Therefore, SED mechanisms might not be effective in roots but rather be effective in the shoot.

High S supplied uniformly increased the photosynthetic rates of control plants (Figure 6 a). Except for the high S-fertilized RP, *V. dahliae* acted as a biotic stressor impairing leaf photosynthesis 7 dpi. Infected tomato plants initiate a self-protective suberin coating of invaded xylem vessel walls to prevent the fungal penetration of neighboring vessels thus limiting the systemic *in planta* spread of *V. dahliae* (Robb et al., 1989). The reduced diameter of conductive elements together with impeded root growth constrains water movement in the vascular tissue. As a result conditions similar to drought stress are established and major changes include a reduction in leaf diameter, stomata closure, reduced CO₂ diffusion through stomata and leaf mesophyll thus finally constricting leaf photosynthesis and its associated metabolic pathways (Nogués et al., 2002; Flexas et al., 2004; Chaves et al., 2009).

Directly linked to photosynthesis is the generation of photoassimilates, therefore, the pattern of phloem sugar-transport was determined (Figure 6 b). The WT donor plants showed an enhanced phloem sugar-transport rate orientated at satisfying the assimilate demand of the fungal pathogen. The WT accession showed highest *V. dahliae* levels particularly at high S supply and, therefore, initiated a sugar phloem flux for maintenance of the sink metabolism. Additionally, defence-related sink genes, that are responding to the local sugar (hexose) status

in incompatible plant-pathogen interactions (Berger et al., 2004; Scharte et al., 2005), might be activated. In a resistant tomato genotype the detection of a high assimilate transport to infected sink-tissue was linked to such protective sugar-sensing mechanisms (Chapter I). In contrast, in the resistant IL 7 the low fungal concentration could not notably deplete sugar pools hence a constant replenishment of metabolic reservoirs in infected tissue and a subsequent sugar-activation of protective sink-related genes were not required.

In addition to SED mechanisms a major participator involved in tomato resistance against *V. dahliae* race 1 strains is the *Ve1* gene. This genomic source of resistance was detected on the short arm of chromosome 9, cloned and sequenced from tomato. Many cultivated genotypes were shown to possess the *Ve* locus, which comprises two closely linked inversely orientated genes, *Ve1* and *Ve2* (Diwan et al., 1999; Kawchuk et al., 2001; Fradin et al., 2009). *Ve1* encodes an extracellular cell-surface receptor belonging to the family of eLRR RLPs, a major class of disease resistance-proteins (Wang et al., 2008). Only *Ve1* confers increase race-specific resistance against *V. dahliae* race 1 strains. In sensitive plants single nucleotide polymorphism analysis of *Ve1* revealed a deletion to cause a premature stop codon (Fradin et al., 2009). Thus the susceptibility of tomato plants against *V. dahliae* can be attributed to a truncated version of the *Ve1* protein. The relative quantification of the *LeVe1* transcript levels in both selected ILs and their parental lines as influenced by the fungus and S supply revealed the existence of the *Ve* locus in all tested plants and demonstrates a gene up-regulation after fungal penetration of plants, as already shown by Fradin et al. (2009). The qRT-PCR results present striking differences in the *LeVe1* expression patterns of *V. dahliae* sensitive and resistant tomato plants (Figure 7 a). WT donor plants showed lowest *LeVe1* transcript amounts which were slightly elevated in luxury S-supplied plants. This lack in *LeVe1* expression together with the previously assumed missing ability to perform SED mechanisms might explain the high level of fungal infection 7 dpi in WT donor plants. In the RP and the sensitive IL 54 S-deficient growth conditions dramatically increased the *LeVe1* expression. However this up-regulation did not contribute much to a reduction of low-S-favored fungal colonization (Figure 4 b). Only the luxury plant S nutritional status enabled the limitation of *V. dahliae* spread in the sensitive IL 54 and the cultivated RP, although the *LeVe1* transcript level was reduced (Figure 7 a). This clearly demonstrates the importance and considerable predominance of SED mechanisms over *LeVe1* expression in the cultivated parental line and the sensitive IL 54. In contrast low fungal colonization of the resistant IL 7 under both S supplies suggests that SED mechanisms are of minor importance for its *V. dahliae* resistance.

The responsiveness of the *LeVe1* expression in the resistant IL 7 to high S supply indicates that in this genotype, S acts on R gene expression rather than on classical SED mechanisms. Obviously, in IL 7 there is no need for SED because the *LeVe1* gene action makes SED mechanisms unnecessary.

The IL map from Monforte and Tanksley (2000) was developed from a cross between *S. habrochaites* accession LA1777 with *L. esculentum* cv. E6203. The resulting lines were characterized genotypically with 95 molecular markers evenly distributed along the tomato genome. In comparison, “Tomato-EXPEN 2000” is a more comprehensive high density genetic map. It was constructed on a F₂ population of 83 individuals derived from the crossing of *S. pennellii* (LA716) with *S. lycopersicum* (LA925) and includes 2586 molecular markers (Tanksley et al., 1992). The map is additionally assisted by molecular markers generated by a comparison of the tomato EST database to the *Arabidopsis* genome (Fulton et al., 2002). The molecular marker TG393 is located at position 103 cM on the long arm of tomato chromosome 11 in the map of IL 54 and in the tomato EXPEN 2000 map (Figure 8 a, b). Being in both mapping population located at the same place, the two markers are identical and linked to the *Arabidopsis* gene locus At5g51700. A subsequent Tair and Blastn analysis of the At5g51700 CDS region revealed that this locus comprises the *RAR1* gene, an R gene relevant in the context of pathogen recognition and pathogen-induced signal transduction. Binding of this co-chaperone together with other proteins to a heat-shock protein 90 family-member regulates the assembly of a resistance-protein complex, which includes an intracellular receptor for the subsequent initiation of signal transduction upon fungal effector perception (Schulze-Lefert, 2004; Seo et al., 2008). *RAR1* was also identified as a downstream signaling component of the Cf (*Cladosporium fulvum*)-mediated resistance in tomato (Thomma et al., 2005). However, virus-induced gene silencing did not confirm a major implication for *RAR1* in *Ve1*-mediated *Verticillium* defence-reaction of resistant tomato cv. Motelle (Fradin et al., 2009). In the current approach, except (in tendency) for the resistant IL 7 S responsiveness as well as fungal induction could not be detected in the *LeRAR1* expression level (Figure 7 b). This confirms a minor role of *LeRAR1* in *Ve1*-mediated *Verticillium* resistance of tomato, as already proposed by Fradin et al. (2009).

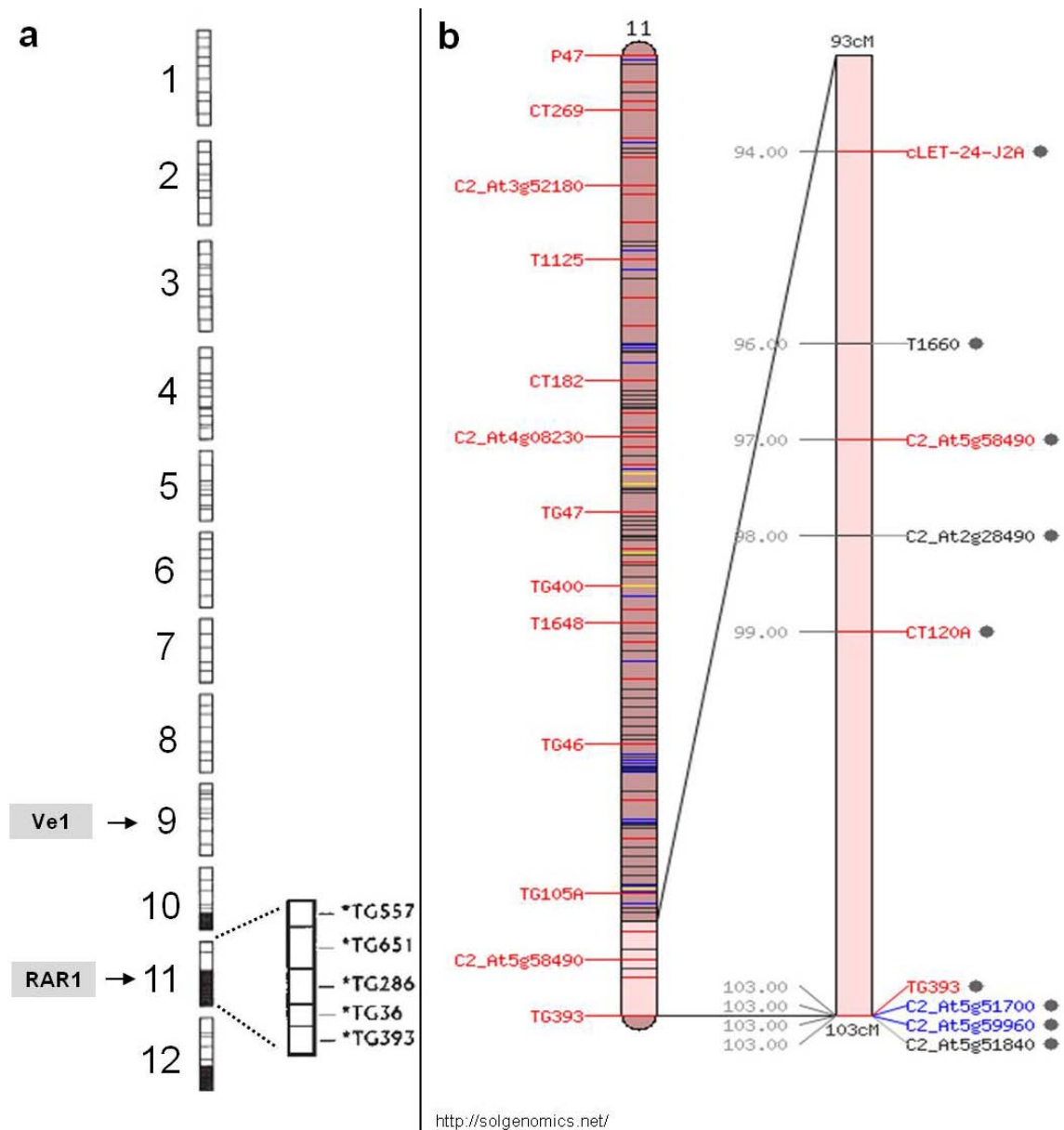


Figure 8 Chromosome map of tomato IL 54 (modified from Monforte and Tanksley, 2000) and partial close-up of tomato chromosome 11 long arm from the Tomato-EXPEN 2000 map (www.solgenomics.net). **a** Introgressed WT genomic regions in IL 54 are marked in black on chromosomes 10, 11 and 12. An overview of the molecular marker set on chromosome 11 is given. The chromosomal location of the gene loci for *Ve1* and *RAR1* is indicated for chromosomes 9 and 11, respectively. **b** The tomato high density genetic EXPEN 2000 map derived from a cross of the WT *S. pennellii* LA716 with the cultivated genotype *S. lycopersicum* LA925.

In the current study selected physiological parameters together with an analysis of selected R gene expression revealed differences between *V. dahliae*-sensitive and resistant ILs and their parental lines with regard to the relative importance of SED and R gene-based pathogen defence (Figure 9). WT donor plants appeared to be incapable of an effective SED-based *in planta* fungus restriction and additionally did not exhibit a strong R gene initiated protective response. The missing SED capacity and the minor role for R gene regulation finally render the WT donor highly susceptible towards *V. dahliae*. The sensitive IL 54 and the RP showed a combination of SED processes and R gene regulation for a significant limitation of *V. dahliae* colonization with a minor influence of R gene changes for the containment of *V. dahliae*. The existence and particularly the supra-optimal S-based enhancement of SED mechanisms seems to be of major importance for limitation of the fungal *in planta* spread in the RP and the sensitive IL 54. In the resistant IL 7 the R gene up-regulation in response to fungal infection seems to prevail the SED-mediated elimination of the fungal pathogen. Enhanced S nutrition stimulated the R gene transcription rather than induced classical SED processes. This underlines the predominance of an R gene-mediated pathogen restriction over classical SED mechanisms. Together with an early and specific pathogen recognition mediated by *Ve1*, a fungal effector-initiated signal-transduction chain seems to be activated for the start-up of a suitable defence response in resistant IL 7.

In conclusion, the present study suggests that SED mechanisms as well as R gene-mediated defence responses may be decisive for the establishment of an incompatible tomato–*V. dahliae* interaction. The relative importance of either mechanism depends on the genetic make-up of the tomato genotype. Thus, the assumption of tomato monogenic *Ve1* resistance solely limiting *V. dahliae* spread needs to be supplemented by a multifactorial *V. dahliae* defence process including SED. A tissue analysis of the concentration and plant tissue-specific spatial localization of specific SDCs (S^0) and S-containing precursor metabolites (Cys, GSH) might give further insights into the role of SED mechanisms in both ILs and their parental lines. Additionally, an expression analysis of primary S metabolism-associated genes might help identifying starting points and precursor metabolites for SDC synthesis in the selected genotypes. Also, an extended expression analysis of further R genes combined with a comparison of well-described R gene responses in other pathosystems (*Cf*-mediated resistance) may support a major importance of the R gene defence for an efficient pathogen restriction in specific *V. dahliae*-resistant ILs.

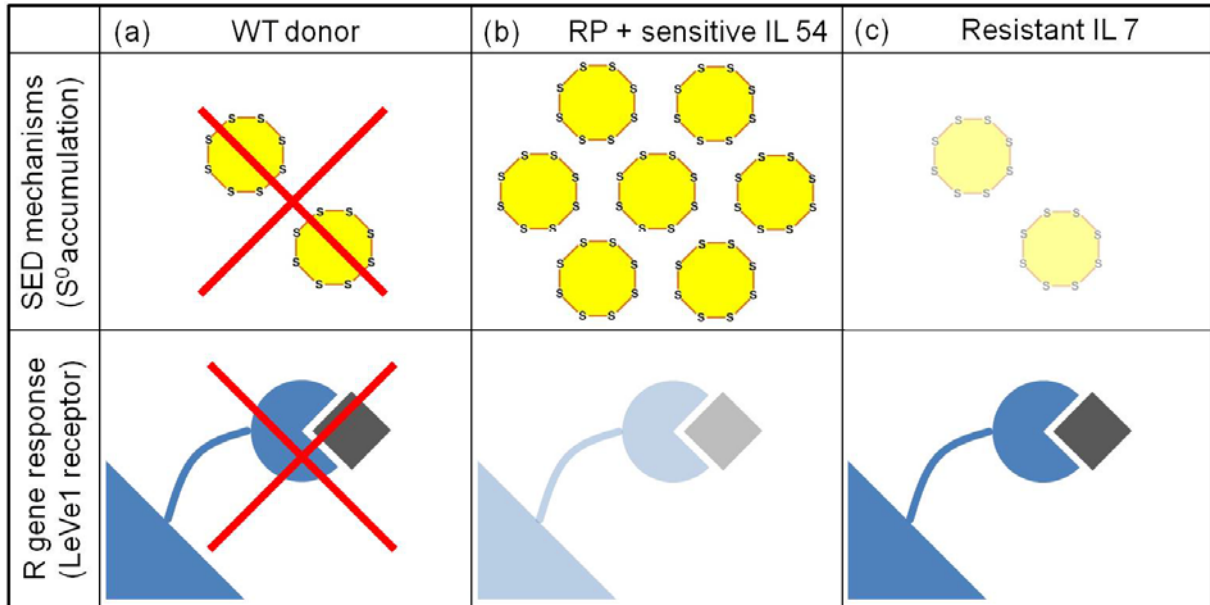


Figure 9 Proposed tomato IL-specific existence and utilization of S^0 -based SED mechanisms and Ve1 receptor-based R gene response for effective *V. dahliae* defence. **a** WT donor plants are incapable of S^0 -based fungal containment, and no R gene response is developed. **b** The RP and the sensitive IL 54 show strong S^0 -enhanced SED processes in combination with a weak R gene regulation. **c** The resistant IL 7 takes advantage of a strong R gene expression for fungal pathogen elimination while SED is of minor importance.

Chapter IV - Construction of binary T-DNA vector systems for the molecular characterization of sulfur-enhanced *Verticillium dahliae* plant defence mechanisms

Katharina, Bollig¹ and Walter J. Horst¹

(1) Institute for Plant Nutrition, Faculty of Natural Science, Leibniz University Hannover, Herrenhäuserstraße 2, 30419 Hannover, Germany

Abstract

Plant sulfur (S)-enhanced defence (SED) mechanisms are initiated in response to an invasion by plant pathogens. Under conditions of biotic stress the synthesis and rapid accumulation of specific S-containing defence compounds (SDCs) seems to be closely connected to the plant primary S metabolism. In a number of *Verticillium dahliae* (*V. dahliae*) resistant solanaceous plant species a contact with the vascular-localized fungal pathogen induced high transient levels of S, cysteine (Cys) and glutathione (GSH), which are either a part of the reductive S assimilation or a product of this pathway. At the same time, the fungitoxic SDC elemental S (S^0) accumulated at the place of fungal colonization. This coincidence indicates a special role of high S metabolite levels originating from the primary S metabolism for the generation and accumulation of S^0 . But so far, the exact mechanisms contributing to the synthesis of fungitoxic S^0 in the vascular plant tissue have not been characterized. Hence, a molecular analysis of specific S metabolism-related candidate genes, could uncover their role in the process of S^0 formation. An overexpression of the tomato-derived gene *LeSultr4;1* encoding a vacuolar sulfate exporter, is thought to enhance the primary S metabolism. Detection of higher vascular S^0 levels in *V. dahliae*-infected transgenic plants could prove the important role of reductive S assimilation for S^0 generation. An overexpression of the tomato-derived *LeGSH1*, which catalyzes the first step of GSH biosynthesis, could increase vascular S^0 level in *V. dahliae*-infected transgenic plants due to the consumption of an elevated GSH pool and raise the antioxidative buffer capacity in transgenic tissue. Therefore, in this study both S metabolism-related candidate genes were integrated into different binary transfer-DNA (T-DNA) vector systems for a chemical-inducible or a constitutive transgene overexpression analysis. Classical molecular techniques were adapted to guarantee the correct assembly of the constructs and their integration into bacterial cells. Novel transcriptomic methods were used to estimate the transgene copy number in host plant genomes. The expression capacity of the binary T-DNA vector systems was determined in plant model organism and the organogenesis efficiency of selected plant-model systems was tested.

Keywords: sulfur-enhanced defence, elemental sulfur, transgene overexpression, binary T-DNA vector systems

Introduction

The special relation between the plant sulfur (S)-metabolism and plant defence processes against pathogens is well known. The S-enhanced defence (SED) is a plant inherent protective mechanism limiting a colonization of resistant plants by biotic stressors, and the synthesis of participating antimicrobial S-containing defence compounds (SDCs) is supported by the reductive assimilation of S (Rausch and Wachter, 2005; Kruse et al., 2007). Several plant species are capable to form and accumulate specific SDCs as an induced stress-response in an incompatible interaction with bacterial and fungal plant pathogens (Williams and Cooper, 2003). In resistant cocoa, tomato and pepper genotypes high levels of the inorganic phytoalexin elemental S (S^0) were detected in the vascular tissue after infection with the soil borne fungus *Verticillium dahliae* (*V. dahliae*) (Cooper et al., 1996; Williams et al., 2002; Novo et al., 2007). However, neither the precise toxicity mechanism of S^0 acting on pathogens nor the biosynthetic pathway for S^0 generation is known. Up to now, the relevant candidate genes participating in the synthesis of S^0 still remain to be identified. An involvement of cysteine (Cys) but also glutathione (GSH) as S-containing precursor substances for the synthesis of S^0 is considered, since transient increases of these S metabolites were detected after fungal invasion of resistant tomato plants (Williams et al., 2002). Additionally, a spatial gene expression analysis of primary S metabolism-related candidate genes in *V. dahliae*-infected vascular tissue of a resistant tomato genotype indicated a role of Cys synthesis-associated steps for the synthesis of SDCs and particularly S^0 (Chapter II). An intensification of selected key reactions preceding the synthesis of Cys and GSH could generally demonstrate the involvement of the primary S metabolism and specifically prove the contribution of both thiols to an enhanced production of S^0 . Stimulation of the reductive S assimilation through an excess supply with reduced S could be used to enhance the Cys-dependent synthesis of S^0 . An appropriate starting point would be Sultr4;1, a tonoplast-localized sulfate exporter involved in balancing the storage and internal remobilization of S pools from vacuoles to the cytoplasm in root and hypocotyl pericycle and xylemparenchyma cells (Kataoka et al., 2004). To further test the contribution of GSH to the formation of S^0 , additional focus was laid on the first step of the GSH biosynthesis facilitated by exclusively plastid-localized γ -glutamylcystein-synthetase (GSH1) (Wachter et al., 2005). Intensification of this rate limiting step could generate excess GSH to promote a GSH-depend S^0 synthesis.

A common way for the identification and further characterization of a specific candidate gene function is the integration and overexpression of transgenes in a model plant system. One frequently used strategy for a stable integration of candidate genes into plant genomes is the method of *Agrobacterium*-mediated genetic transformation. *Agrobacterium tumefaciens* (*A. tumefaciens*) is a soil-borne bacterium, which naturally manipulates host plant tissue to induce tumor structures for the synthesis of energy-delivering opines (Tzfira and Citovsky, 2006). The basic steps of this process are today used for the generation of transgenic plants and today most commonly disarmed transfer-DNA (T-DNA) vector systems serve to shuttle candidate genes or reporter genes into the plant genome. A disarmed binary vector system is characterized through the split of an original (tumor-inducing) Ti-plasmid into the T-DNA region and the virulence (*vir*) gene region on two separate replicons (Lee and Gelvin, 2008; Komori et al., 2007). Only the coexistence of both plasmids in one agrobacterial cell enables the processing of the T-DNA located on the binary vector through the *vir* genes-containing helper plasmid. In the current study two kinds of disarmed binary T-DNA vector systems were used for the overexpression of transgenes. The binary pER8 T-DNA vector is under chemical control and the transcription of the T-DNA region can be induced by the hormone 17 β -estradiol, which allows a time-directed initiation and termination of the candidate gene expression (Zuo et al., 2000). The binary p9 T-DNA vector allows a constitutive gene expression, which assures a continuously high level of candidate gene products to guarantee the enhancement of related pathways.

The aim of this study was the construction and verification of molecular tools and mechanisms needed for a chemical-inducible and constitutive overexpression of the tomato-derived *LeSultr4;1* and *LeGSH1* candidate genes. This comprised the complementation of different disarmed T-DNA vector systems with both S metabolism-related transgenes. Commonly accepted molecular techniques were used to prove the correct assembly of all vector constructs and transgenes and a successful transfer into bacterial cells. Novel transcriptomic methods including a fluorogenic probe-based quantitative Real-Time polymerase chain reaction (qRT-PCR) assay were adapted to estimate the number of transgenes integrated into the host plant genome. The expression capacity of both disarmed T-DNA vector systems was determined in plant model organism by qRT-PCR and reporter gene visualization. Finally, the organogenesis efficiency of explants produced from selected plant-model systems was tested.

Material & Methods

Molecular methods

Bacterial strains

The *Escherichia coli* (*E. coli*) K12 derivative strain XL1-Blue (*recA1 endA1 gyrA9 thi-1 hsdR17 supE44 relA1 lac* [F' *proAB lacIqZAMI5 Tn10* (Tet^R)] (Agilent Technologies, Böblingen, Germany) with a tetracycline resistance (Tet^R) on its F'-episome was used for molecular cloning. Additionally, the *A. tumefaciens* strain GV2260 (Dr. Köhl, MPI for Molecular Plant Physiology, Potsdam, Germany) with a rifampicin resistance (Rif^R) on its C58 chromosomal background and a carbenicillin resistance (Carb^R) on its Ti-Plasmid (pTiB6S3DT-DNA) was used for molecular cloning.

Vector systems

The T / A cloning vector pGEM[®]-T-Easy (bacterial marker: ampicillin (*Amp*^R)) was obtained from Promega Corporation (Madison, USA). The chemical-inducible binary pER8 T-DNA vector (AF309825) (bacterial marker: spectinomycin (*Spec*^R), plant marker: hygromycin (*Hyg*^R)) was obtained from Prof. Nam-Hai Chua (Laboratory of Plant Molecular Biology, Rockefeller University, New York, USA). The helper plasmid pPK2013 (bacterial marker: kanamycin (*Kan*^R)) carried the *vir*-gene region for T-DNA processing. The binary p9 T-DNA vector (bacterial marker: *Spec*^R, plant marker: *Kan*^R), p9:eGFP (bacterial marker: *Spec*^R) and p9:GUSi (bacterial marker: *Spec*^R) were obtained from DNA Cloning Service e. K. (Hamburg, Germany). The Ti-Plasmid pTiB6S3DT-DNA (*Carb*^R) carried the *vir*-gene region for T-DNA processing.

Candidate genes

The coding sequence (CDS) of the gene *DsRed* (drFP583), encoding the red fluorescent protein originating from *Discosoma* sp., was amplified from the pRedRoot binary vector (Limpens et al., 2004) and used for *in vivo* expression monitoring. The CDS of the tomato vacuolar sulfate exporter gene *LeSultr4;1* (AK320538) and the CDS of the tomato gene *LeGSH1* (AF017983), facilitating the first step of glutathione (GSH) biosynthesis, were used for a chemical-inducible and a constitutive overexpression analysis.

Production of chemical competent *E. coli* XL1-Blue and *A. tumefaciens* GV2260 cells

For the production of chemical competent cells according to Inoue et al. (1990), initially 20 μL competent *E. coli* XL1-Blue cells were plated onto solid lysogeny broth Lennox (LB) medium (Tet 50 μg / mL) (Table S10) and cultivated at 37 °C overnight. A single colony was transferred into 4 mL liquid LB medium (Tet 50 μg / mL) and cultivated at 180 rpm and 37 °C overnight. Then, 2.5 mL of the liquid culture were added to 200 mL super optimal broth (SOB) medium (Carl Roth GmbH, Karlsruhe, Germany) and grown at 180 rpm and 18 °C until an optical density at 600 nm (OD_{600}) of 0.6 was reached. The 200 mL bacterial SOB solution were cooled down on ice for 10 min, transferred into 50 mL pre-cooled falcon tube and centrifuged at 3,500 rpm and 4 °C for 10 min (Heraeus Multifuge 3SR, Thermo Fisher Scientific, Dreieich, Germany). The supernatant was discarded. Each pellet was overlaid with 15 mL terrific broth (TB) buffer (Table S13) and cooled at 4 °C for 10 min. Then, each pellet was carefully resuspended, the solutions were collected in two falcon tubes and centrifuged at 3,500 rpm and 4 °C for 10 min. The supernatant was discarded, both pellets were carefully resuspended in 10 mL TB buffer and combined. The 20 mL solution was mixed with 1.4 mL dimethylsulfoxid and cooled at 4 °C for 10 min. Finally, 200 μL aliquots were transferred into pre-cooled steril 1.5 mL reaction tubes and long-term stored at -86 °C. Chemical competent *A. tumefaciens* GV2260 cells were produced with a modified protocol according to Weigel and Glazebrooke (2002). Initially, a single colony was transferred into 4 mL liquid LB medium (Rif 5 μg / mL; Carb 50 μg / mL) and cultivated at 200 rpm and 28°C overnight. Then, 2.5 mL of the liquid culture were added to 200 ml liquid LB medium and grown at 200 rpm and 28°C until an OD_{600} of 0.5 - 0.8 was reached. The bacterial solution was transferred into 4· 50 mL falcon tube and centrifuged at 5,000 rpm and room RT for 10 min. The bacterial pellet was resuspended in 20 mL liquid LB medium. Aliquots of 200 μL were transferred into sterile 1.5 mL reaction tubes, short-term frozen in liquid nitrogen (N_2) and long-term stored at -86°C.

Isolation of total RNA and synthesis of cDNA

For the isolation of total RNA N_2 -homogenized 100 mg fresh weight plant tissue was mixed with 1 mL Trizol[®] Reagent (Invitrogen, Darmstadt, Germany) and incubated for 5 min at RT. Then, 200 μL of chloroform were added, samples were inverted several times and incubated at RT for 3 min. The samples were centrifuged at 12,000 g for 15 min at 4°C (Heraeus Biofuge Primo R, Thermo Fisher Scientific, Dreieich, Germany). The entire upper aqueous phase was transferred into a sterile 1.5 mL reaction tube and mixed with 500 μL isopropyl

alcohol (4 °C). The samples incubated at RT for 10 min and were centrifuged at 12,000 g for 10 min at 4 °C and the supernatant was removed. The RNA pellet was washed with 1 mL 75 % (v / v) ethanol. Samples were centrifuged at 7,500 g for 5 min at 4 °C and the supernatant was discarded. The RNA pellet was dried for 2 min, dissolved in 50 µL RNase-free dH₂O and finally stored at -86°C. The concentration of each isolated total RNA sample was determined spectrophotometrically (NanoPhotometer™ Implen, Munich, Germany) at $\lambda = 260$ nm with dH₂O as reference. The integrity of the isolated total RNA was controlled by native electrophoretic separation. Therefore, 10 µL of total RNA were mixed with 2 µL of 6 x loading dye (Fermentas, St. Leon-Roth, Germany) and loaded on a 1.6 % (w / v) agarose-gel supplemented with Roti[®]-Safe GelStain (Carl Roth GmbH, Karlsruhe, Germany) and the GeneRuler 1 kb ladder (Fermentas, St. Leon-Roth, Germany). All samples were separated in 1 x TAE buffer (Table S9) at 100 V for 40 min (Gelsystem Polymer, Landgraf, Hannover, Germany). DNA fragments were analysed under a UV transilluminator (Gel Imager, Intas, Göttingen, Germany). For the synthesis of cDNA 1 µg of total RNA was combined with 1 µL oligo(dT)₁₈ primer (0.5 µg / µl) in the RevertAid™ H Minus First Strand cDNA Synthesis Kit (Fermentas, St. Leon-Roth, Germany) according to the manufacturer's instructions.

Amplification of candidate genes

For the identification of candidate gene CDS regions a 50 µl proof-read PCR reaction was set up including iProof HF buffer (1 x), dNTPs (200 nM each) (Fermentas, St. Leon-Roth, Germany), iProof HF Polymerase (5 U) (BioRad Laboratories, Hercules, USA), forward and reverse Primer (400 nM each; Table S1), and 50 ng of tomato cDNA. The PCR parameters comprised an initial denaturation at 98 °C (30 s), followed by 33 cycles at 98 °C (10 s), 60 °C (30 s) and 72 °C (90 s), and a final elongation step at 72 °C (7 min), in a peqSTAR 2x thermocycler (PEQLAB Biotechnologie GMBH, Erlangen, Germany). PCR reactions were separated electrophoretically on a 1.2 % (w / v) agarose-gel and cleaned-up with the GeneJET™ Gel Purification Kit (Fermentas, St. Leon-Roth, Germany) according to the manufacturer's instructions.

A-tailing and ligation of candidate genes into the pGEM[®]-T-Easy T / A cloning vector

A 25 µL A-tailing reaction included Hot-Start PCR buffer B1 (1 x), MgCl₂ (3.6 mM), dATPs (200 nM each) (Fermentas, St. Leon-Roth, Germany), DCSHot DNA polymerase (0.75 U) (DNA Cloning Service, Hamburg, Germany), and 200 ng proof-read PCR product. The PCR parameters consisted of an initial denaturation at 95 °C (10 min), followed by 72 °C (15 min).

The amount of proof-read PCR product used for a ligation reaction was calculated for a molar 3:1 insert:vector ratio as described in the pGEM[®]-T Easy technical manual. A standard ligation reaction was set up on ice and included Rapid Ligation Buffer (2 x), T4 DNA Ligase (3 U) (Promega, Madison, USA), 50 ng pGEM[®]-T-Easy Vector (Promega, Madison, USA), the calculated volume of proof-read PCR Product and dH₂O up to a volume of 10 µL. The reactions were mixed gently and incubated for 12 h at 4 °C.

Heat-shock transformation and Blue-white screening of *E. coli* XL1-Blue cells

Chemical competent *E. coli* XL1-Blue cells were placed on ice until just thawed. Then 10 µL of a ligation reaction were added and the mixture incubated at 4 °C for 5 min. The bacterial cells were heat-shocked for 30 s at 42 °C. The reaction tubes rested on ice for 2 min and were then supplied with 200 µL SOC medium (Table S12). The samples were incubated at 37 °C for 1 h. From each transformed sample 25 µL and 50 µL were transferred onto blue-white screening LB agar plates (Amp 50 µg / mL) and incubated overnight at 37 °C. Prior to use, 100 µL isopropyl-β-D-thiogalactopyranosid (IPTG) (0.1 M) (Carl Roth GmbH, Karlsruhe, Germany) and 20 µL of 5-bromo-4-chloro-3-indolyl-β-D-galactoside (x-Gal) (50 mg / mL) (Sigma Aldrich, St. Louis, Missouri, USA) were spread over the plate surface and allowed to absorb for 30 min at 37 °C.

Isolation of plasmid DNA

To control the ligation of the candidate genes into pGEM[®]-T-Easy putative positive white colonies were picked and cultivated in 5 mL liquid LB medium (Amp 50 µg / mL) at 180 rpm and 37 °C overnight. For the preparation of a permanent culture 500 µL bacterial solution were mixed with 500 µL sterile 86 % (v / v) glycerol (Carl Roth GmbH, Karlsruhe, Germany) and long-term stored at -86 °C. For the isolation of high purity plasmid DNA, 4 mL of the bacterial solution were centrifuged at 8,000 g for 1 min and the supernatant was discarded. The bacterial pellet was handled in the GeneJET[™] Plasmid Miniprep Kit (Fermentas, St. Leon-Roth, Germany) according to the manufacturer's instructions. A control digest included EcoRI Buffer (1 x), EcoRI (10 U), 200 ng plasmid DNA, and dH₂O up to a final volume of 10 µL. The reaction incubated at 37 °C for 2 h and was electrophoretically separated on a 2 % (w / v) agarose-gel.

Custom Sequencing

From each positive tested clone 20 μL isolated plasmid DNA (30 – 100 ng / μL) were send for custom DNA sequencing to GATC Biotech AG (Konstanz, Germany). The pUC / M13 forward standard primer (5'-TGTAACGACGGCCAGT-3') was used for plasmid sequencing. All sequences were screened for nucleic acid segments of vector origin with the VecScreen software (www.ncbi.nlm.nih.gov/VecScreen/VecScreen.html). Decontaminated sequences were searched against a nucleotidedatabase on the Basic Local Alignment Search Tool (BLAST) Server (Altschul et al., 1990).

Candidate gene modification and integration into the binary pER8 / p9 T-DNA vector

For the directed ligation of candidate genes into both binary T-DNA vectors, a proof-read PCR for the addition of restriction sides to the candidate gene CDS was performed with the appropriate primer pairs (Table S2) in a 50 μl proof-read PCR reaction including the iProof HF Polymerase with 50 ng of tomato cDNA as described above. All PCR reactions were electrophoretically separated on a 1.2 % (w / v) agarose-gel and cleaned-up with the GeneJET™ Gel Purification Kit (Fermentas, St. Leon-Roth, Germany) according to the manufacturer's instructions. For the isolation of the empty binary T-DNA vectors, 5 mL liquid LB medium (Spec 50 μg / mL) were mixed with 10 μl permanent culture and cultivated at 180 rpm and 37 °C overnight. Empty binary pER8 and p9 T-DNA vectors were isolated from 4 mL bacterial solution with the GeneJET™ Plasmid Miniprep Kit (Fermentas, St. Leon-Roth, Germany) according to the manufacturer's instructions. The cleaned PCR Products and empty binary vector systems were separately digested in a final volume of 20 μL at RT overnight. The specific composition of each digest reaction was determined with the DoubleDigest™ software (Fermentas, St. Leon-Roth, Germany) and included two restriction enzymes, restriction buffer (1 x) and the appropriate gel-extracted template up to a final volume of 20 μL . Reactions were cleaned-up with the GeneJET™ PCR Purification Kit (Fermentas, St. Leon-Roth, Germany) according to the manufacturer's instructions. A ligation reaction included T4 ligation buffer (1 x), T4 DNA Ligase (10 U) (Fermentas, St. Leon-Roth, Germany), 50 ng empty binary T-DNA vector, and 500 ng digested and cleaned PCR product, in dH₂O up to a final volume of 20 μL . A heat-shock transformation of *E. coli* XL1-Blue cells was carried out with 20 μL of the ligation reaction as described above. From each transformed sample 25 μL were transferred onto LB agar plates (Spec 50 μg / mL) and incubated overnight at 37 °C. Single colonies were picked and cultivated in 5 mL liquid LB medium (Spec 50 μg / mL) at 180 rpm and 37 °C overnight. For the preparation of a permanent culture

500 μL bacterial solution were mixed with 500 μL sterile 86 % (v / v) glycerol (Carl Roth GmbH, Karlsruhe, Germany) and long-term stored at $-86\text{ }^{\circ}\text{C}$. For the isolation of high purity plasmid DNA, 4 mL of the bacterial solution were used in the GeneJET™ Plasmid Miniprep Kit (Fermentas, St. Leon-Roth, Germany) according to the manufacturer's instructions.

Control of directed candidate gene integration into the binary pER8 / p9 T-DNA vector

A conventional 25 μL PCR reaction was set up including Hot-Start PCR buffer B1 (1 x), MgCl_2 (3.6 mM), dNTPs (200 nM each) (Fermentas, St. Leon-Roth, Germany), primer Spec + / - (400 nM each) (Table S3, Table S4), specific primer pair combination for candidate gene detection (400 nM) (Table S3, Table S4), DCSHot DNA polymerase (0.75 U) (DNA Cloning Service, Hamburg, Germany), 200 ng plasmid DNA. The PCR parameters consisted of an initial denaturation at $95\text{ }^{\circ}\text{C}$ (10 min), followed by 33 cycles of $95\text{ }^{\circ}\text{C}$ (15 s), $60\text{ }^{\circ}\text{C}$ (30 s), $72\text{ }^{\circ}\text{C}$ (30 s), and a final elongation step of $72\text{ }^{\circ}\text{C}$ (7 min). Each PCR reaction was electrophoretically separated on a 2 % (w / v) agarose-gel at 100 V for 40 min.

Freeze transformation of *A. tumefaciens* GV2260

Chemical competent *A. tumefaciens* GV2260 cells were placed on ice until just thawed and mixed with 10 μL of the appropriate vector construct. The samples were placed into liquid N_2 for 5 min and subsequently incubated at $37\text{ }^{\circ}\text{C}$ for 5 min. Then 1 mL liquid LB was added and each sample incubated for 4 h at $28\text{ }^{\circ}\text{C}$. From each transformed sample 25 μL were transferred onto LB agar plates (Spec 50 μg / mL and Kan 50 μg / mL or Spec 50 μg / mL and Carb 50 μg / mL) and incubated at $28\text{ }^{\circ}\text{C}$ for 48 h. Single colonies were picked and cultivated in 5 mL liquid LB medium (Spec 50 μg / mL and Kan 50 μg / mL or Spec 50 μg / mL and Carb 50 μg / mL) at 200 rpm and $28\text{ }^{\circ}\text{C}$ overnight. For the preparation of a permanent culture 500 μL bacterial solution were mixed with 500 μL sterile 86 % (v / v) glycerol (Carl Roth GmbH, Karlsruhe, Germany) and long-term stored at $-86\text{ }^{\circ}\text{C}$. For the isolation of high purity plasmid DNA, 4 mL of the bacterial solution were used in the GeneJET™ Plasmid Miniprep Kit (Fermentas, St. Leon-Roth, Germany) according to the manufacturer's instructions. For the control of correct integration into bacterial cells a conventional 25 μL PCR reaction was set up including 200 ng plasmid DNA, and a conventional PCR and electrophoretic separation were performed on a 2 % (w / v) agarose-gel at 100 V for 40 min as described above.

Plant transformation work

Plant cultivation

The *A. thaliana* C24 genotype, the near-isogenic *V. dahliae*-sensitive *S. lycopersicum* GCR 26 genotype, the *S. lycopersicum* cv. MicroTom, and *N. tabacum* cv. Samsun NN (SSN) were used in the current study.

For ‘floral dip’ transformation, *A. thaliana* C24 plants were initially cultivated in a climate chamber, with a short-day 8 / 16 h regime, at 20 °C and 70 % relative air humidity and a photon flux density of 200 mmol m⁻² s⁻¹ at the plant canopy. One week after seeding plants were transferred into a mixture (1:3) of Einheitserde type P (Balster Einheitserdewerk GmbH, Fröndenberg, Germany) and sand. After 6 weeks plants were transferred into a long-day 16 / 8 h regime until the primary inflorescence was visible. The primary inflorescence was removed and about one week later plants had developed a high number of secondary inflorescences in a developmental stadium ready for transformation. For the production of seeds, transformed *A. thaliana* C24 plants were cultivated in a climate chamber under long-day conditions and watering was stopped after seed maturity. For the organogenesis assays, the Hyg B resistance-test, the copy number determination and transgene expression analysis, all seeds were surface sterilized for 1 min with 0.5 % (v / v) NaClO, washed for 1 min with dH₂O three times and transferred to solid MS medium (Table S16) for germination. Seedlings were kept in a climate cabinet with a long-day 16 / 8 h regime under white light at 25 °C. For *Agrobacterium*-mediated leaf infiltration, tobacco cv. SSN was cultivated in a greenhouse under natural climatic conditions in summer 2012. One week after germination in seedlings substrate plants were transferred into CaCO₃-limed (pH 5.0) peat substrate and further cultivated for six weeks.

***Agrobacterium*-leaf infiltration of tobacco**

For the *A. tumefaciens* GV2260 infiltration solution, 10 µL of an *A. tumefaciens* GV2260 permanent culture (p9:DsRed, p9:eGFP, p9:GUSi) were mixed with 40 µL dH₂O, plated onto solid LB plates (Spec 50 µg / mL, Carb 50 µg / mL) and cultivated for 24 h at 28 °C. A single bacterial colony was transferred into 50 mL liquid LB (Spec 50 µg / mL, Carb 50 µg / mL) and cultivated at 28 °C until an OD₆₀₀ of 0.5 was reached. Agrobacterial cells were centrifuged at 1,000 g for 10 min and resuspended in 2 mL infiltration medium (Table S14). The four youngest leaves of each tobacco plant were partially infiltrated with a sterile 10 mL

syringe according to Sparkes et al. (2006). The plunger was pressed down gently onto the abaxial side while the upper leafside was directly supported until the liquid visibly filled the mesophyll air spaces. After an incubation period of 72 h the fluorescence emitted by the reporter genes was examined in infiltrated leaves areas with a Leica MZ10 F stereomicroscope (Leica Microsystems GmbH, Wetzlar, Germany).

GUS staining

Agrobacterium-infiltrated leaf areas were cut out of the leaf lamina at 3 dpi. Samples were vacuum-infiltrated with GUS-staining solution (Table S15) for 1 min and incubated in GUS-staining solution at 37 °C overnight. Samples were destained twice by vacuum-infiltration for 2 min in 70 % (v / v) ethanol.

‘Floral dip’ transformation of *A. thaliana* C24 T₀

The ‘floral dip’ transformation of *A. thaliana* C24 T₀ plants was modified according to Logemann et al. (2006). Therefore, 50 µL from an *A. tumefaciens* GV2260 permanent culture (pER8, pER8:LeSultr4;1) were mixed with 50 µL dH₂O and plated onto solid YEP medium (Spec 50 µg / mL and Kan 50 µg / mL) (Table S11) at 28 °C for 48 h. The bacterial mass was carefully covered with 5 mL liquid YEP medium and dissolved by scraping with a glass spatula. Bacteria were transferred into 50 ml falcon tubes and mixed with liquid YEP medium until an OD₆₀₀ of 2.0 was reached. For transformation 120 mL of a 5 % (w / v) sucrose solution containing 0.03 % (v / v) Silwet L-77 (Lehle Seeds, Round Rock, Texas, USA) were mixed with the bacterial suspension and poured into a disposable plastic bag. Plant inflorescences were dipped into the transformation solution several times until coated with a visible liquid film. Dipped plants were placed under a dark cover for 24 h and then transferred into a climate chamber. *A. thaliana* C24 T₀ plants were further cultivated until maturation and harvest of seeds.

Selection of Hyg B-resistant *A. thaliana* C24 T₁

Seeds harvested from *A. thaliana* C24 T₀ plants were surface sterilized and placed onto solid MS medium (Hyg B 25 µg / mL) for a rapid selection according to Harrison et al. (2006). After an initial stratification period of two days in the dark at 4°C, the seeds were placed for 6 h at 25 °C under white light to stimulate and synchronize the germination. All seed were then placed in the dark for additional two days. Following a final 24 h light period, the transformed and Hyg B-resistant *A. thaliana* C24 T₁ seedlings were identified by a clear

elongation of their hypocotyls. All selected *A. thaliana* C24 T₁ plants were further cultivated until maturation and harvest of seeds.

Transgene detection in *A. thaliana* C24 T₂

The isolation of genomic DNA (gDNA) included N₂-homogenized 100 mg fresh weight *A. thaliana* C24 T₂ tissue in the GeneJET Plant Genomic DNA Purification Kit (Fermentas, St. Leon-Roth, Germany) according to the manufacturer's protocol. Integration of the *LeSultr4;1* transgene as well as the empty pER8 T-DNA was initially checked by conventional PCR. For confirmation of transgene integration the primer pair pER8 35S A+ / *LeSultr4;1* A – was used (Table S3). The primer pair LexA Op + / - was used for the detection of the integrated empty pER8 T-DNA region (Table S3). A 25 µl conventional PCR assay included Hot-Start PCR buffer B1 (1 x), MgCl₂ (3.6 mM), dNTPs (200 µM each) (Fermentas, St. Leon-Roth, Germany), forward and reverse primer (252 nM each), DCSHot DNA polymerase (0.75 U) (DNA Cloning Service, Hamburg, Germany), 100 ng *A. thaliana* C24 T₂ gDNA or 100 ng *A. thaliana* C24 WT gDNA as a negative control, or dH₂O as a no-template control. Thermal PCR cycling stages consisted of an initial denaturation at 95°C (10 min), followed by 33 cycles at 95°C (15 s), 60°C (30 s), 72°C (30 s) and a final elongation at 72°C (7 min). Samples were electrophoretically separated on a 2 % (w / v) agarose-gel at 100 V for 40 min.

Transgene copy number estimation in *A. thaliana* C24 T₂

The transgene copy number was estimated in *A. thaliana* C24 T₂ plants by absolute qRT-PCR quantification. A fluorogenic twice dyed probe (TDP) (Biolegio, Nijmegen, Netherlands) was designed on the basis of the transgene CDS using the free available primer 3 plus software (Untergasser et al., 2007). The TDP (Table S5) represented an oligonucleotide with the 5'-reporter dye 6-Carboxyfluorescein (6-FAM) and the 3'-quencher dye Black Hole Quencher™ (BHQ-1™). The TDP was located in between the primer pair *LeSultr4;1* qRT-PCR + / - (Table S5). In order to prepare a dilution series for the absolute quantification the number of pER8:*LeSultr4;1* copies was calculated in an isolated plasmid DNA sample according to Gadaleta et al. (2011):

- $\text{Copies} / \mu\text{L} = [\text{DNA} (\text{g} / \text{L}) / \text{pER8}:\text{LeSultr4;1} (\text{g} / \text{mol})] \cdot (6.022 \cdot 10^{23} \text{ mol}^{-1}) \cdot 10^{-6}$
- Molecular weight of pER8:*LeSultr4;1* = ((309 bp · 2) · 13962 bp)

An eight point serial dilution was prepared for pER8:LeSultr4;1 with dH₂O and included ≤ 1 copy in the last dilution point. A 25 μ l mix included Hot-Start PCR buffer B1 (1 x), MgCl₂ (3.6 mM), dNTPs (200 nM each) (Fermentas, St. Leon-Roth, Germany), primer pair LeSultr4;1 qRT-PCR + / - (252 nM each), TDP (252 nM), DCSHot DNA polymerase (0.75 U) (DNA Cloning Service, Hamburg, Germany), 100 ng gDNA of *A. thaliana* C24 T₂. Thermal qRT-PCR cycling stages were performed in a CFX96™ Real-Time detection system (BioRad Laboratories, Hercules, USA) and consisted of an initial denaturation at 95°C (10 min), followed by 30 cycles at 95°C (15 s), 60°C (30 s), 72°C (30 s) and a final melting curve analysis from 60°C to 95°C with a 0.5°C · 5 s⁻¹ increasing temperature gradient.

Transgene expression analysis in *A. thaliana* C24 T₂

For the analysis of the pER8:LeSultr4;1 expression level plants from the *A. thaliana* C24 T₂ line 10 were cultivated on solid MS medium for two weeks. An expression of the transgene was initiated with 17 β -Estradiol (5 μ M) (Sigma Aldrich, St. Louis, Missouri, USA). Plants were harvested after 24 h. Total RNA was isolated and cDNA was synthesized as describe above. A relative qRT-PCR quantification included the primer pair LeSultr4;1 qRT + / - and the TDP. Due to its consistent expression tested in nutrient and cold-stress experiments, tomato elongation factor 1 α *LeElf1a* (X14449) was used as internal reference gene (Løvda and Lillo, 2009). A 25 μ l mix included Hot-Start PCR buffer B1 (1 x), MgCl₂ (3.6 mM), dNTPs (200 nM each) (Fermentas, St. Leon-Roth, Germany), primer pair LeSultr4;1 qRT + / - (252 nM each), TDP (252 nM), SYBR Green-I (0.1 x) (Invitrogen GmbH, Darmstadt, Germany), DCSHot DNA polymerase (0.75 U) (DNA Cloning Service, Hamburg, Germany), 50 ng cDNA of *A. thaliana* C24 T₂ line 10. Thermal qRT-PCR cycling stages were performed in a CFX96™ Real-Time detection system (BioRad Laboratories, Hercules, USA) as described above.

Tomato and tobacco organogenesis

For the organogenesis assay two week old cotyledons from the tomato genotype GCR 26 and from the tomato cv. MicroTom were cut with a scalpel into two to four pieces. For two days explants were placed with the adaxial side onto feeder layer plates prepared from a tobacco cell-suspension culture in MS-SSN medium (Table S17) as described by Ling et al. (1998). The tobacco cell-suspension culture was prepared from a durable tobacco cv. SSN tissue culture on solid MS medium. Next, all explants were placed with the adaxial side onto shoot-induction medium (MS-S) (Table S18) containing either trans-zeatin riboside (Zea) 0.5, 1.0,

1.5, 2.0 mg / L; or 6-benzylaminopurine (BAP) / indole-3-acetic acid (IAA) 1.0 / 0.2 mg / L, 2.0 / 0.2 mg / L; or 2,4-Dichlorophenoxyacetic acid (2,4-D) 2.0 mg / L.

Four week old tobacco cv. SSN cotyledons were cut with a scalpel into two pieces and placed with the adaxial side onto MS-S medium containing Zea 2.0 mg / L. After four weeks newly initiated tobacco shoots were cut and placed into MS-S medium for further growth. Two weeks later all shoots were transferred into hormone free solid MS medium for the induction of roots on the cut surface. Plants were cultured for four weeks on hormone-free solid MS medium until sufficient root development was detectable. All plants were then transferred into Einheitserde type P (Balster Einheitserdewerk GmbH, Fröndenberg, Germany) and placed into a climate cabinet at 25°C under long-day conditions. To reduce the transpiration and to enhance the adaption of plantlets to substrate culture and lower humidity all pots were covered with transparent foil for four weeks.

Results

The pGEM[®]-T-Easy T / A cloning vector system

The *DsRed* gene encodes a red fluorescent protein originating from coral *Discosoma* sp., and was integrated into the chemical-inducible binary pER8 T-DNA vector and the constitutive binary p9 T-DNA vector. The *DsRed* CDS was initially amplified in a proof-read PCR from the pRedRoot vector system and comprised a length of 690 bp (Figure 1). For a chemical-inducible and a constitutive overexpression of candidate genes related to the primary S metabolism the *Arabidopsis* full-length CDS of the vacuolar tonoplast-localized sulfate transporter *AtSultr4;1* and the plastid-localized γ -glutamylcysteine synthetase *AtGSH1* were obtained from the TAIR gene database (www.arabidopsis.org). Both sequences were searched against the nucleotide database of the BLAST Server (Altschul et al., 1990). A taxonomy report revealed highest sequence similarity for the following two tomato-derived CDS results: vacuolar sulfate transporter *LeSultr4;1* (AK320538) with a length of 2452 bp and plastidic *LeGSH1* (AF017983) with a length of 2089 bp. The CDS of both genes was amplified in a proof-read PCR including cDNA synthesized from total tomato RNA (Figure 1).

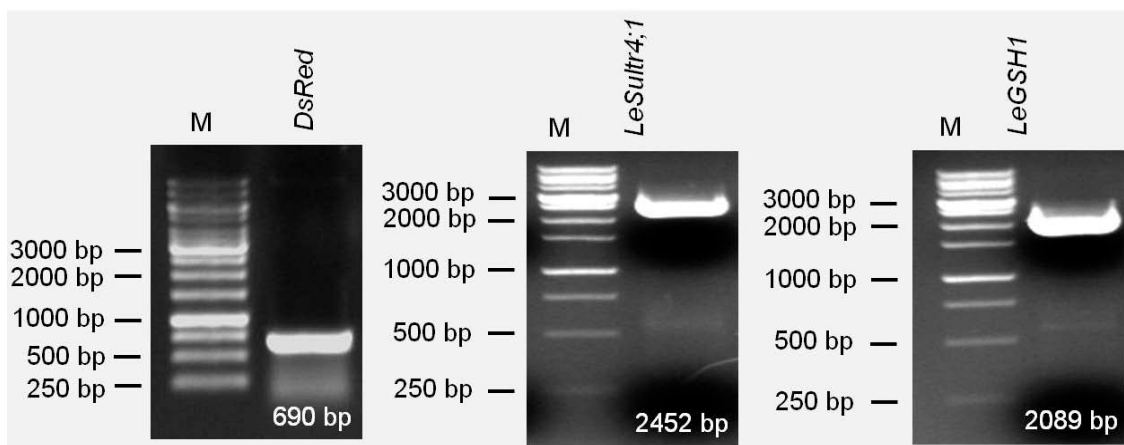


Figure 1 Proof-read PCR products of the reporter gene *DsRed*, the candidate gene *LeSultr4;1* and the candidate gene *LeGSH1* after amplification with primer pairs spanning the complete CDS regions. Samples were separated on a 1.2 % (w / v) agarose-gel at 100 V for 40 min. (M: marker GeneRuler 1kb ladder).

Following the A-tailing process, the CDS of the *DsRed* reporter gene, the CDS of the candidate genes *LeSultr4;1* and the *LeGSH1* were ligated into the multiple cloning side (MCS) of the pGEM[®]-T-Easy T / A cloning vector (Figure 2). The MCS contained multiple restriction sites and was flanked by recognition sites for the restriction enzyme EcoRI to provide a single-enzyme digestion for release of an integrated insert. The high-copy pGEM[®]-T-Easy T / A cloning vector further contained the α -peptide coding region of the enzyme β -galactosidase. By cleaving the synthetic lactose analogue x-Gal, blue colonies appeared on the LB screening agar plates. Positive recombinant clones were identified after insertional inactivation of the coding region of the α -peptide, which resulted in an inhibition of the substrate cleavage and led to the formation of white colonies.

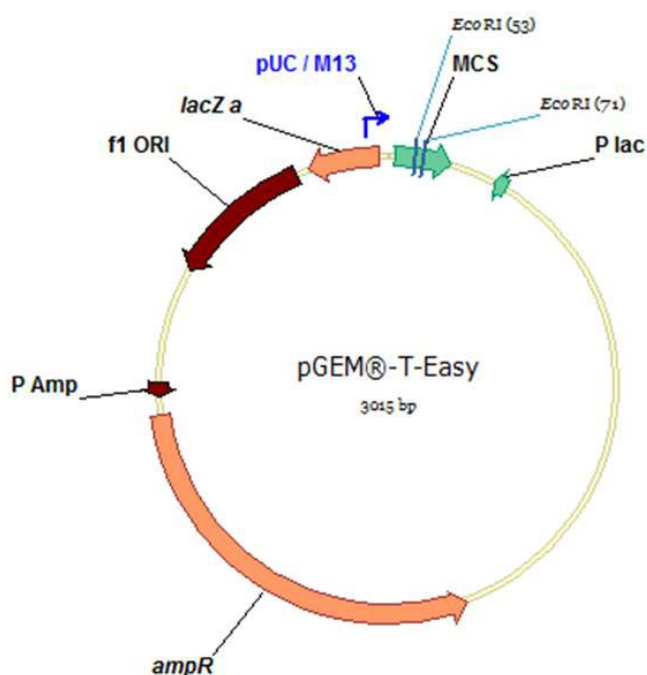


Figure 2 The pGEM[®]-T-Easy T / A cloning vector. The pUC / M13 forward sequencing primer enabled the sequencing of integrated sequences (P lac: promoter lac operon; lacZ a: partial CDS of β -galactosidase; f1 ORI: replication origin phage f1; P Amp: promoter β -lactamase; ampR: CDS of β -lactamase).

To ensure the identity of all three amplified CDS regions, the puC / M13 forward primer was used for custom sequencing of integrated sequences in the pGEM[®]-T-Easy T / A cloning vector. Additionally, an EcoRI control digest was performed to check the integrity of the *DsRed*, *LeSultr4;1* and *LeGSH1* CDS after ligation into the pGEM[®]-T-Easy T / A cloning vector (Figure 3). After electrophoretic separation of the digested samples the empty vector with a length of 3015 bp and specific CDS digestion patterns were detected. The intact CDS of the reporter gene *DsRed* comprised 690 bp. The CDS of the candidate gene *LeSultr4;1* included an EcoRI recognition site at position 1829 bp, giving a two band digestion pattern of 1829 bp and 640 bp. For *LeGSH1* a single band of 2089 bp was detected.

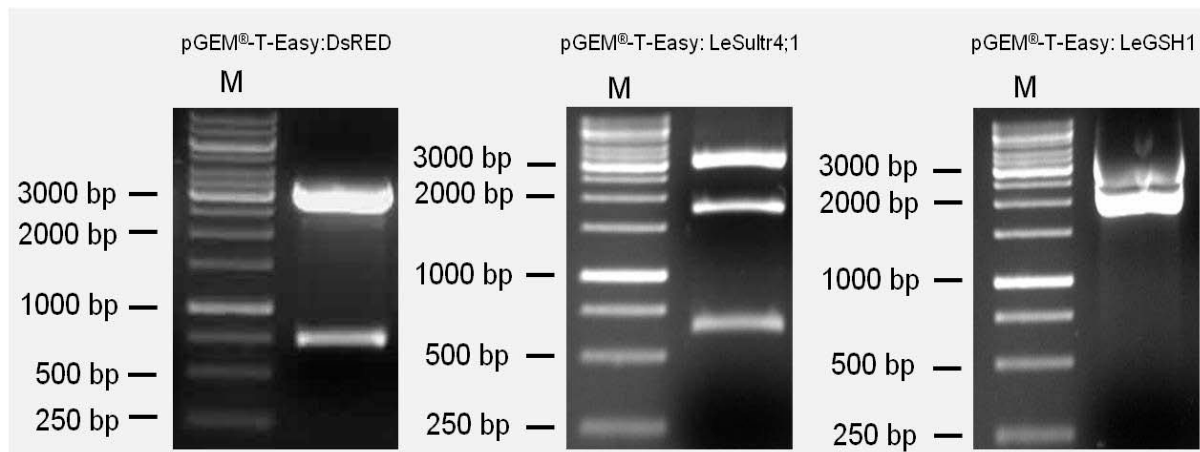


Figure 3 EcoRI control digest of the CDS regions from the reporter gene *DsRed*, the candidate genes *LeSultr4;1* and *LeGSH1* ligated into the pGEM[®]-T-Easy T / A cloning vector. Samples were separated on a 2 % (w / v) agarose-gel at 100 V for 40 min. (M: marker GeneRuler 1kb ladder).

The chemical-inducible binary pER8 T-DNA vector system

For the establishment of the chemical-inducible overexpression constructs in a first cloning approach the binary pER8 T-DNA vector was used (Figure 4). This vector system was combined with the helper-plasmid pPK2013, which carried the relevant *vir* genes necessary for T-DNA integration after *Agrobacterium*-mediated explant transformation. The binary pER8 T-DNA vector represents an estrogen receptor-based chemical-inducible system with a length of 11522 bp (Figure 4).

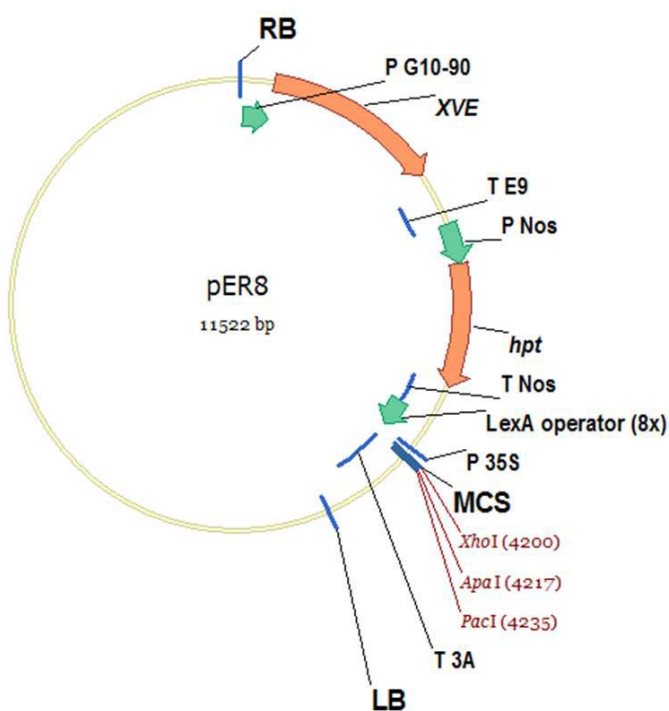


Figure 4 The chemical-inducible binary pER8 T-DNA vector system (AF309825). (P G10-90: synthetic promoter; XVE: CDS of chimeric transcription activation fusion gene; T E9: pea terminator E9 poly(A) sequence; P Nos: promoter nopaline synthase; *hpt*: CDS of hygromycin phosphotransferase; T Nos: terminator nopaline synthase poly(A) sequence; P 35S: minimal CaMV 35S promoter; T 3A: pea terminator 3A poly(A) sequence).

In a first transcriptional unit the strong synthetic constitutive promoter P G10-90 controls the chimeric transcription activation *XVE* fusion gene. *XVE* encodes the DNA-binding domain of the bacterial repressor LexA (X), the acidic transactivation domain of VP16 (V), and the carboxyl part of the human estrogen receptor (E). In a second transcription unit eight copies of the strong LexA operator are fused to parts of the minimal cauliflower mosaic virus (CaMV) 35S promoter for transcription of candidate genes integrated into the MCS. Both transcription units are separated by the plant selectable marker gene *hpt* which encodes the hygromycin phosphotransferase II. After successful sequencing of the *DsRed*, *LeSultr4;1* and *LeGSH1* CDS regions, specific recognition sites for restriction enzymes present in the MCS of the binary pER8 T-DNA vector were added to all three sequences (Figure 5).

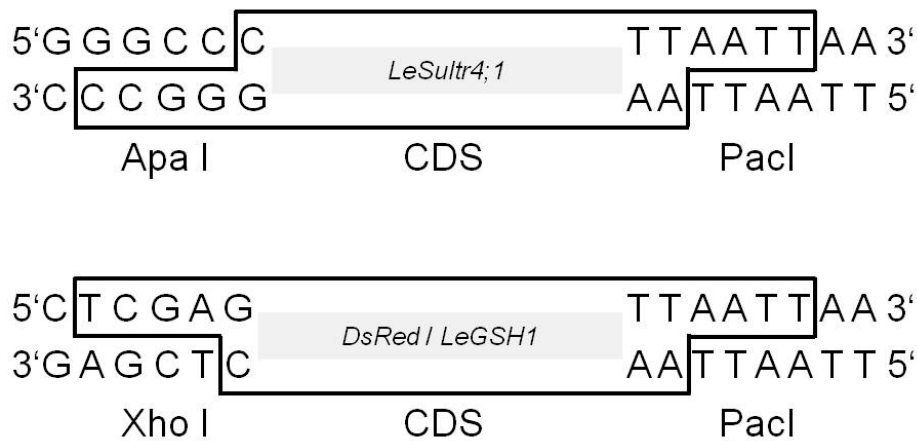


Figure 5 CDS modification of *DsRed* and the two candidate genes *LeSultr4;1* and *LeGSH1* with specific recognition sites for restriction enzymes included in the MCS of the binary pER8 T-DNA vector.

A proof-read PCR with primer pairs including the specific recognition sites at their 5'-end was performed. The *LeSultr4;1* CDS was extended by addition of the recognition sites for the restriction enzymes ApaI and PacI and the *DsRed* and *LeGSH1* CDS was extended by addition of the recognition sites for the restriction enzymes XhoI and PacI. This allowed a directed integration of the *DsRed* red fluorescent reporter gene and the two S metabolism-related candidate genes *LeSultr4;1* and *LeGSH1* into the MCS of the binary pER8 T-DNA vector. The three new binary T-DNA constructs are shown in Figure 6 with pER8:DsRed comprising a size of 12187 bp, pER8:LeSultr4;1 with a size of 13962 and pER8:LeGSH1 with a size of 13586 bp.

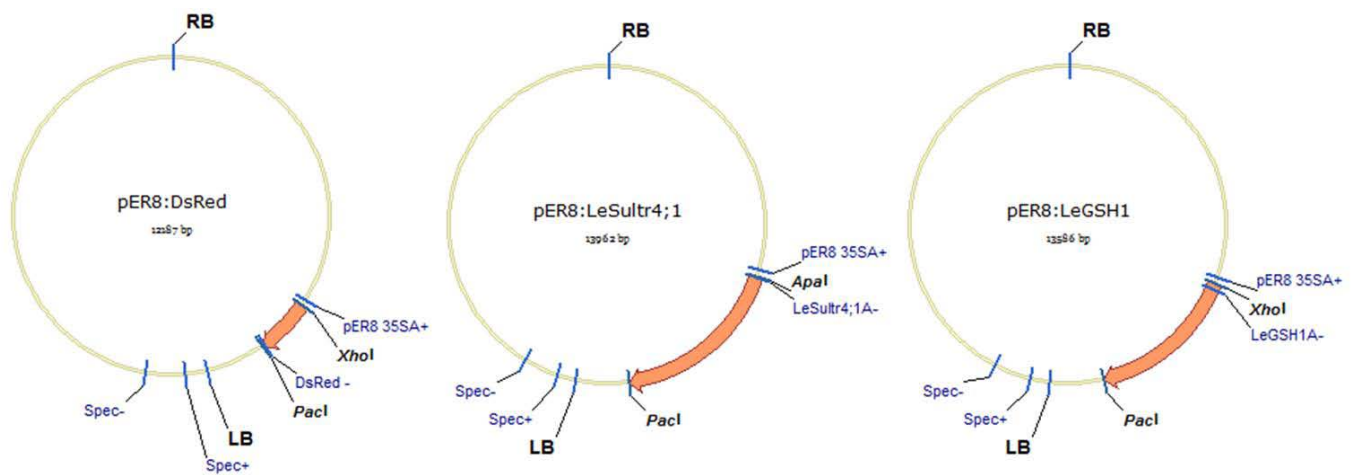


Figure 6 Directed integration of the *DsRed*, *LeSultr4;1* and *LeGSH1* CDS regions into the binary pER8 T-DNA vector. Restriction-enzyme positions for the integration of modified CDS regions are marked in red. Specific primer-pair combinations for a simultaneous detection of candidate genes and binary vector are indicated in blue.

Following the heat-shock transformation into *E. coli* *XII*-Blue cells and the N_2 -freeze transformation into *A. tumefaciens* GV2260 cells, plasmid DNA was isolated from *A. tumefaciens* GV2260 cells. To test the successful integration and the presence of the candidate genes in the binary pER8 T-DNA vector a control duplex PCR including two primer pairs was performed (Figure 7). A first primer pair annealed to the *Spec^R* gene located on the vector backbone. A second primer pair consisted of a forward primer binding to the minimal CaMV 35S promoter sequence present in the binary pER8 T-DNA vector, and a reverse primer binding in the integrated candidate gene sequence.

In all three samples the binding of the first primer pair to the *Spec^R* CDS resulted in a distinct 500 bp band. For pER8:DsRed the candidate gene-specific primer pair combination caused a 771 bp distinct band. A 118 bp band was detected for the binary pER8:LeSultr4;1 construct and a 198 bp band for the binary pER8:LeGSH1 construct.

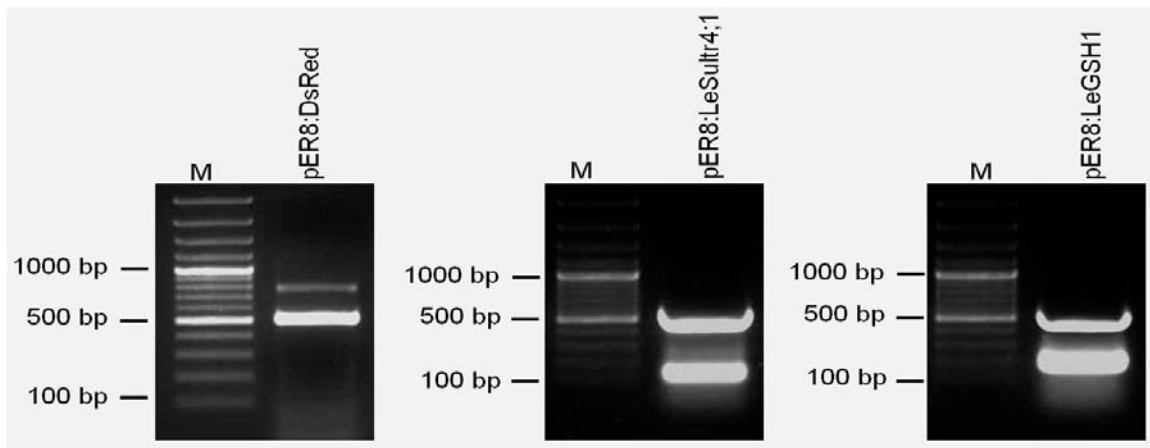


Figure 7 Control duplex PCR including the binary pER8 T-DNA vector with integrated candidate genes isolated from *A. tumefaciens* GV2260 cells. Samples were separated on a 2 % (w / v) agarose-gel at 100 V for 40 min. (M: marker GeneRuler 100 bp ladder).

The constitutive binary p9 T-DNA vector system

For the establishment of constitutive overexpression constructs in a second cloning approach the binary p9 T-DNA vector was used (Figure 8). This vector system was combined with the agrobacterial Ti-Plasmid pTiB6S3DT-DNA (Carb^R). The T-DNA region included a CaMV 35S promoter and CaMV 35S terminator framed plant-selectable marker gene for neomycine phosphotransferase II and the CaMV 35S promoter and CaMV 35S terminator framed CDS. An origin for replication in *E. coli* cells and in *A. tumefaciens* cells was located on the vector backbone. Additionally, the bacterial selection marker gene *nptII* encoding neomycine phosphotransferase II was located in front of the left border sequence.

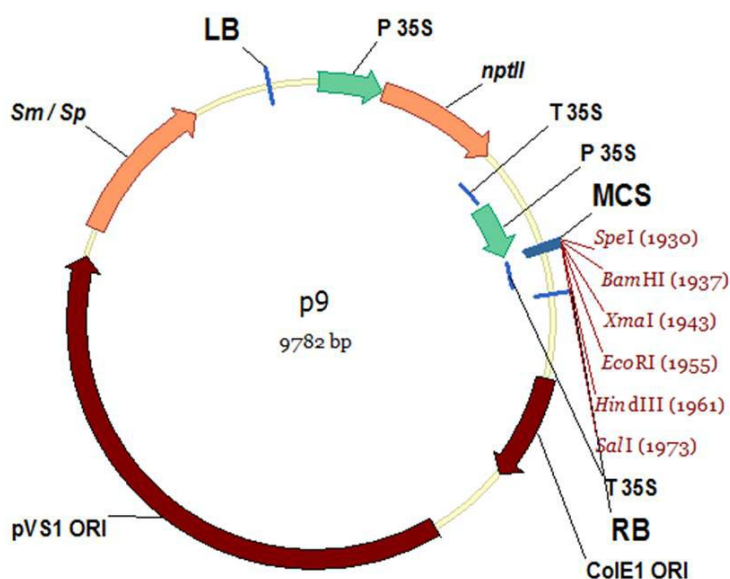


Figure 8 The constitutive binary p9 T-DNA vector system (LB: left border; P 35S: CaMV 35S promoter; *nptII*: CDS of neomycine phosphotransferase II; T 35S: CaMV 35S terminator; RB: right border; CoIE1 ORI: replication origin *E. coli*; pVS1 ORI: replication origin *A. tumefaciens*; *Sm / Sp*: CDS of Spec / Strep).

After successful sequencing of the *DsRed*, *LeSultr4;1* and *LeGSH1* CDS region, specific recognition sites for restriction enzymes present in the MCS of the binary p9 T-DNA vector were added to all three sequences (Figure 9). A proof-read PCR with primer pairs including these recognition sites at their 5'-end was performed. The *LeSultr4;1* and the *DsRed* CDS regions were extended by addition of the recognition sites for the restriction enzymes BamHI and XmaI. The *LeGSH1* CDS was extended by addition of the recognition sites for the restriction enzymes XmaI and EcoRI.

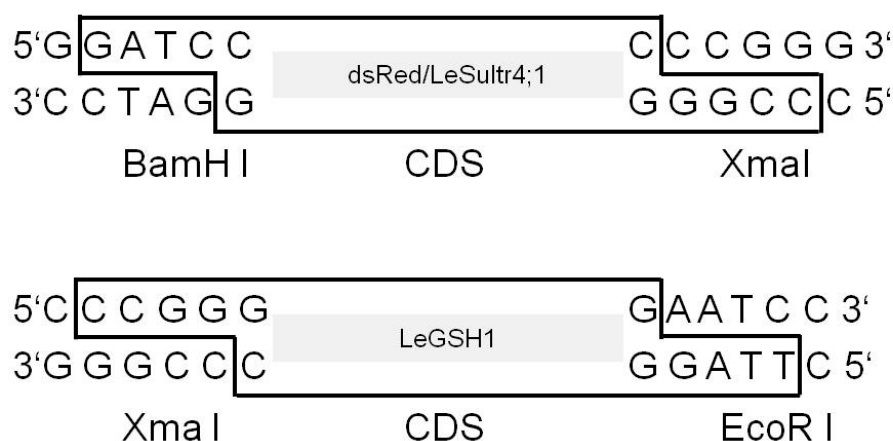


Figure 9 CDS modification of *DsRed* and the two candidate genes *LeSultr4;1* and *LeGSH1* with specific recognition sites for restriction enzymes included in the MCS of the constitutive binary p9 T-DNA vector.

This allowed a directed ligation of the *DsRed* red fluorescent reporter gene and the two S metabolism-related candidate genes *LeSultr4;1* and *LeGSH1* into the MCS of the binary p9 T-DNA vector (Figure 10). With a total size of 10469 bp p9:DsRed was the smallest construct followed by p9:LeGSH1 with a size of 11865 bp and p9:LeSultr4;1 with a size of 12231 bp (Figure 10). The three new vector constructs were heat-shock transformed into *E. coli* XLI-Blue cells and afterwards N₂-freeze transformed into *A. tumefaciens* GV2260 cells. The plasmid DNA was isolated from *A. tumefaciens* GV2260 cells.

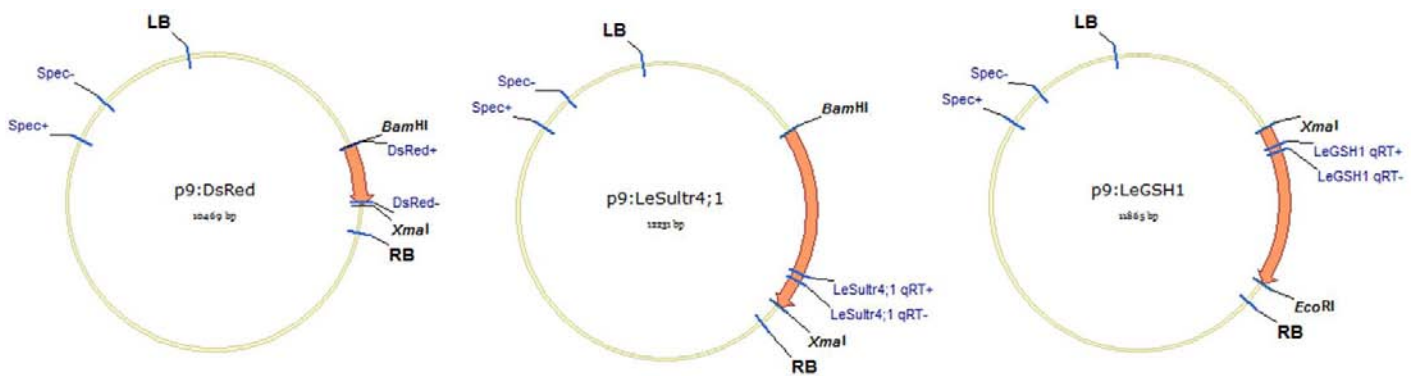


Figure 10 Directed integration of the *DsRed*, *LeSultr4;1*, *LeGSH1* CDS region into the binary p9 T-DNA vector. Restriction enzyme positions for the integration of modified CDS regions are marked in black. Specific primer pair combinations for a simultaneous detection of partial candidate genes CDS regions and binary vector are indicated in blue.

To test the successful integration and the presence of the candidate gene in the binary p9 T-DNA vector a control duplex PCR including two primer pairs was performed (Figure 11). A first primer pair annealed to the *Spec^R* gene located on the vector backbone. For the detection of the entire *DsRed* CDS as a second primer pair cDsRed + / - was used. For the partial detection of the *LeSultr4;1* CDS and the *LeGSH1* CDS the primer pair LeSultr4;1 qRT + / - and LeGSH1 qRT + / - were used. In all three samples the binding of the first primer pair to the *Spec^R* CDS resulted in a distinct 500 bp band. For p9:DsRed the specific primer pair combination caused a 690 bp distinct band. A 137 bp band was amplified for the p9:LeSultr4;1 construct and a 108 bp for the p9:LeGSH1 construct.

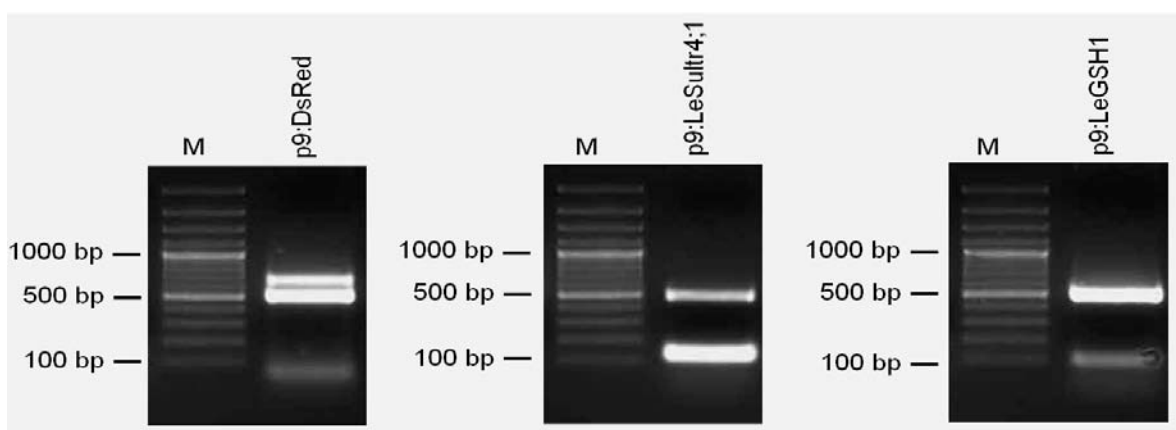


Figure 11 Control duplex PCR including the binary p9 T-DNA vector with integrated candidate genes isolated from *A. tumefaciens* GV2260 cells. Samples were separated on a 2 % (w / v) agarose-gel at 100 V for 40 min. (M: marker GeneRuler 100 bp ladder).

***Agrobacterium* leaf-infiltration of tobacco with the binary p9 T-DNA vector system**

The constitutive expression level of the binary p9 T-DNA vector was tested by an *Agrobacterium* leaf-infiltration of tobacco plants using the p9:DsRed vector and the p9:GUSi and p9:eGFP vector (Figure 12). All three reporter-gene constructs were N₂ freeze-transformed into competent *A. tumefaciens* GV2260 cells and positive colonies were selected based on their antibiotic resistance.

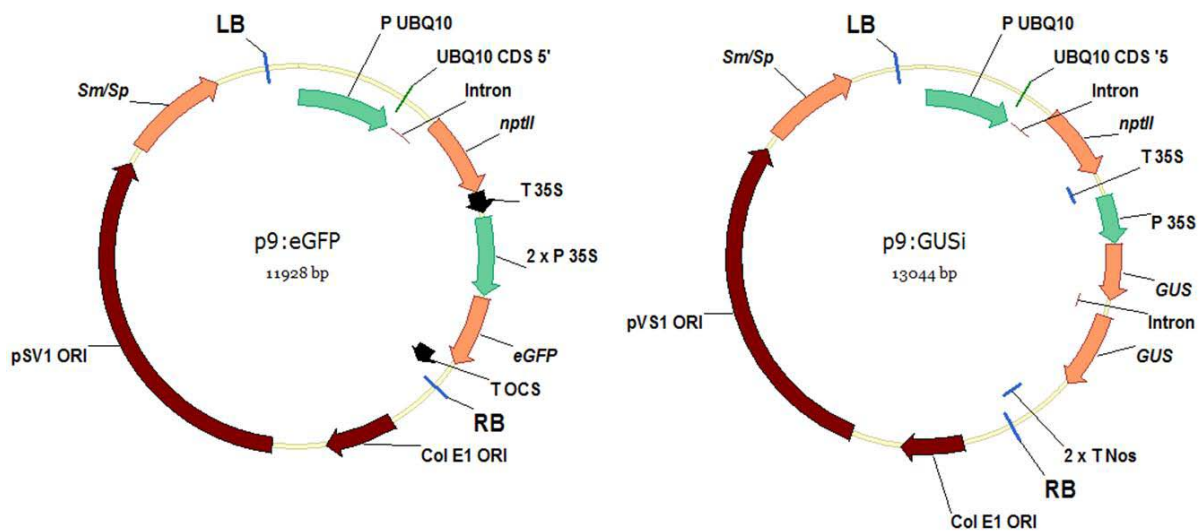


Figure 12 The constitutive binary p9 T-DNA vector system including the reporter gene *eGFP* and *GUSi* (LB: left border; P UBQ10: promoter ubiquitin; UBQ10 CDS 5': 5' sequence ubiquitin; *nptII*: CDS for neomycine phosphotransferase II; T 35S: CaMV 35S terminator, P 35S: CaMV 35S promoter, *eGFP*: CDS for enhanced green fluorescent protein; *GUSi*: CDS for beta-glucuronidase with intron; T Nos: terminator nopaline synthase; T OCS: terminator octopine synthase; RB: right border; ColE1 ORI: replication origin *E. coli*; pVS1 ORI: replication origin *A. tumefaciens*; *Sm/Sp*: CDS of Spec / Strep).

Three days after infiltration tobacco leaf areas previously filled with the agrobacterial solution appeared as light green patches (Figure 13 a, b). All three constructs were injected into the lamina of tobacco leaves and the level of p9:DsRed and p9:eGFP CaMV 35S-based transient expression was monitored microscopically. The level of CaMV 35S-based transient GUSi expression was analyzed after GUS staining of excised infiltrated tobacco tissue areas (Figure 13 c). A light blue coloration was detectable on the border sides of infiltrated tissue areas. The integration of the *DsRed* transgene resulted in transformed tobacco leaf areas with a slightly stronger red fluorescence in comparison to non-infiltrated border areas, which comprised a

high red auto-fluorescence (Figure 13 d). Dense accumulation spots of particles with an intense red fluorescence were detectable only in infiltrated tissue areas. The transient expression of the *eGFP* transgene resulted in a strong green fluorescence of infiltrated tobacco tissue areas whilst non-infiltrated areas exhibited a clearly weaker green auto-fluorescence (Figure 13 e). Distinct intense green fluorescent structures were detectable in infiltrated tobacco leaf areas which represented transient transformed single tobacco leaf epidermal cells with a high expression level.

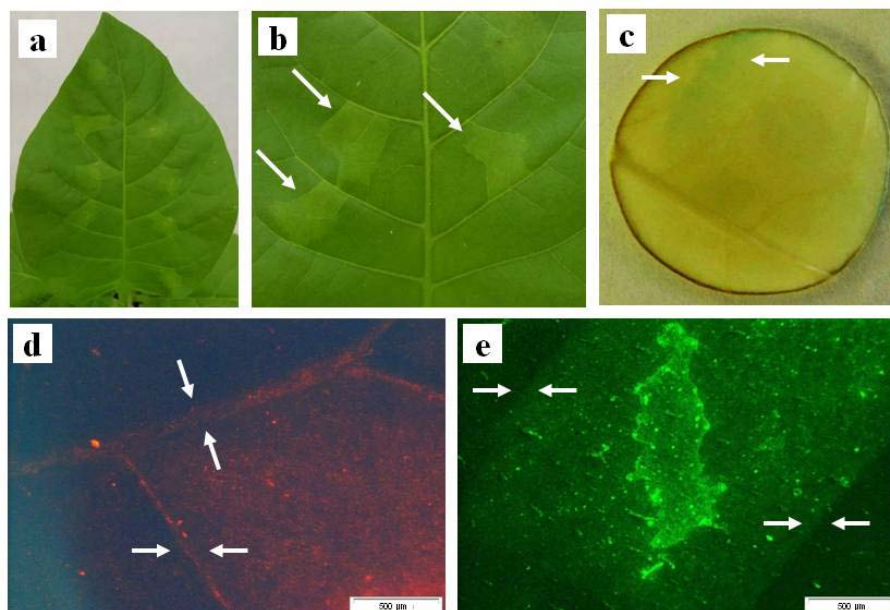


Figure 13 *Agrobacterium* leaf-infiltration of tobacco cv. SSN with the binary p9:DsRed, p9:eGFP and p9:GUSi construct at 3 dpi. **a, b** Light green patches appeared on infiltrated tobacco leaf areas. White arrows indicate infiltration spots. Constitutive CaMV 35S promoter-driven expression of **c** *GUSi*, **d** *DsRed*, **e** *eGFP* reporter genes. Bar represents 500 µm. White arrows indicate borders of p9:DsRed and p9:eGFP infiltration areas and light-blue staining in p9:GUSi infiltrated leaf discs.

***A. thaliana* ‘floral-dip’ transformation, copy number estimation and promoter-induction assay with the binary pER8 T-DNA vector system**

Nine week old *A. thaliana* C24 plants were ‘floral dip’ transformed following a method developed by Logemann et al. (2006) with *A. tumefaciens* GV2260 containing the empty binary pER8 T-DNA vector or the binary pER8:LeSultr4;1 construct. After maturation, seeds were harvested from *A. thaliana* C24 T₀ plants, surface sterilized and subjected to a rapid 3.25

days germination process according to Harrison et al. (2006) on MS medium containing Hyg B (25 $\mu\text{g} / \text{mL}$). After a final 24 h light period all seedlings were green. Hyg B-resistant seedlings had an average hypocotyl length of 0.8 cm whereas Hyg B-susceptible seedling had an average hypocotyl length of 0.4 cm (Figure 14). 20 *A. thaliana* C24 T₁ were selected based on the phenotype of an elongated hypocotyl and further cultivated for the production of seeds.



Figure 14 Selection of Hyg B-resistant transgenic *A. thaliana* C24 T₁ seedlings. Seeds were obtained from T₀ plants subjected to ‘floral dip’ transformation with the GV2260 *A. tumefaciens* strain containing the empty binary pER8 T-DNA vector and the binary pER8:LeSultr4;1 construct. Seeds were grown on 1 % (w / v) MS agar including Hyg B (25 $\mu\text{g} / \text{mL}$). Scale represents 1 cm.

For the control of a positive genomic *LeSultr4;1* transgene integration and to check the effect of an empty vector transformation, seeds from *A. thaliana* C24 T₁ plants were cultivated in a climate cabinet. The gDNA was isolated from 100 mg fresh weight leaf material originating from the *A. thaliana* C24 T₂ plants. For the detection of the binary pER8:LeSultr4;1 construct a conventional PCR assay was performed with a primer pair binding on the vector sequence and the transgene (Figure 15 a, Table S3).

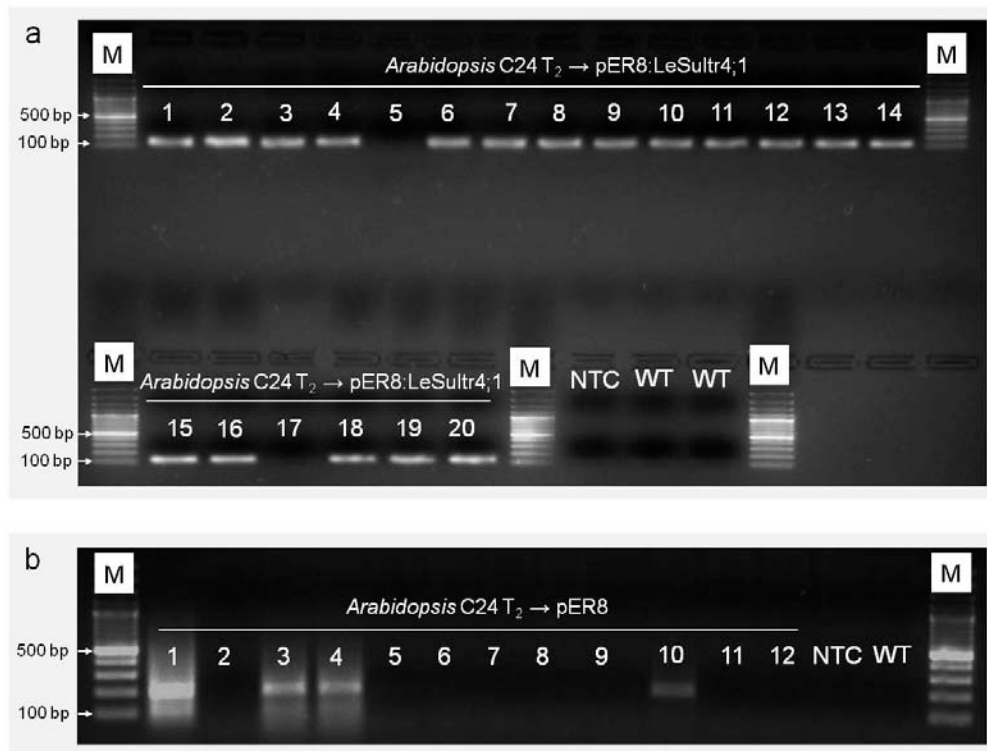


Figure 15 Detection of **a** the binary pER8:LeSultr4;1 construct and **b** the empty binary pER8 T-DNA vector in *A. thaliana* C24 T₂ plants. A conventional PCR assay with appropriate detection primer pairs was set up including 100 ng *A. thaliana* C24 T₂ gDNA, 100 ng *A. thaliana* C24 WT gDNA as a negative control (WT), or dH₂O for the no template control (NTC). Samples were separated on a 2 % (w / v) agarose-gel at 100 V for 40 min. (M: marker GeneRuler 100 bp ladder).

The forward primer pER8 35S A⁺ annealed to the LexA operator sequence of the CaMV 35S promoter in the binary pER8 T-DNA vector. The reverse primer LeSultr4;1 A⁻ was placed into the CDS of the transgene amplifying a 115 bp amplicon in 18 transgenic *A. thaliana* C24 T₂ plants. Additionally a conventional PCR approach for the detection of the empty binary pER8 vector T-DNA region included the LexA Op + / - primer pair, which span the MCS region of the binary pER8 T-DNA vector, thus giving a 185 bp product in four transgenic *A. thaliana* C24 T₂ plants (Figure 15 b). No phenotypic differences could be observed between *A. thaliana* C24 T₂ plants carrying the binary pER8:LeSultr4;1 construct or the empty binary pER8 T-DNA vector.

The *LeSultr4;1* copy number was determined in 18 *A. thaliana* C24 T₂ plants, which were positively tested in the previous conventional PCR transgene detection approach. A

fluorogenic TDP was designed and dual-labeled by the 5'-reporter dye 6-FAM and the 3'-quencher dye BHQ-1™. An absolute qRT-PCR assay comprised an eight point dilution series down to ≤ 1 transgene copy calculated according to Gadaleta et al. (2011). The TDP was located in between the LeSultr4;1 qRT+ / - primer pair. The number of detected *LeSultr4;1* transgene copies was highly variable between the tested 18 *A. thaliana* C24 T₂ plants (Figure 16). Highest copy numbers were detected in line 7 (66.9) and line 17 (86.3). In line 1 (1.3), line 8 (2.4), line 10 (2.6) and line 16 (2.7) less than three transgene copies could be detected.

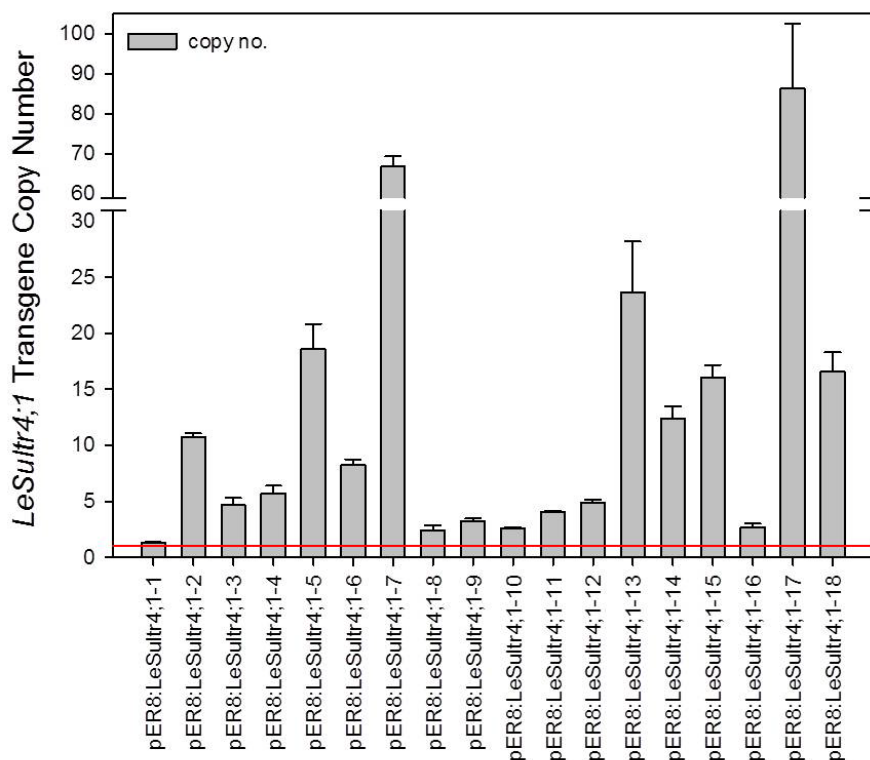


Figure 16 Analysis of *LeSultr4;1* transgene copy number in *A. thaliana* C24 T₂ plants. A dual-labeled fluorogenic TDP was used together with the LeSultr4;1 qRT + / - primer pair in an absolute qRT-PCR assay including 100 ng *A. thaliana* C24 T₂ gDNA.

The low copy *A. thaliana* C24 T₂ plant line 10 was tested for the chemical-inducible expression capacity of the binary pER8:LeSultr4;1 construct. For the activation of the XVE transcription unit on the pER8 T-DNA, plants were grown for 24 h on solid MS medium containing 17 β -Estradiol (5 μ M). Complete seedlings were harvested for the isolation of total RNA and the synthesis of cDNA. A relative qRT-PCR test was performed including the TDP. The 17 β -Estradiol-based induction of the transcription of the XVE activation unit resulted in an average six-fold higher transcript level of the *LeSultr4;1* transgene (Figure 17).

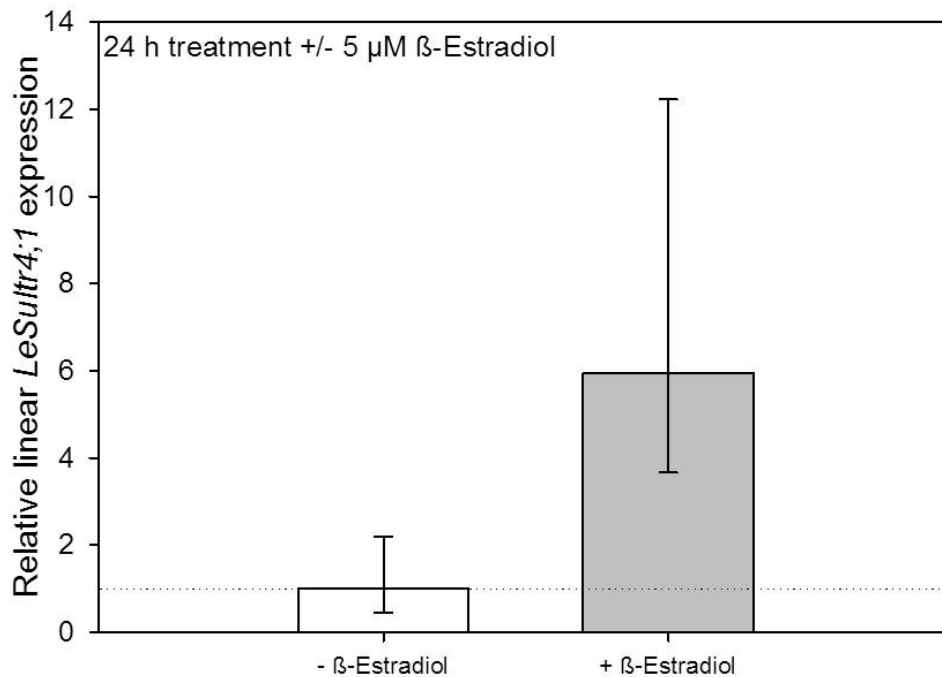


Figure 17 Determination of the relative linear *LeSultr4;1* transgene expression in *A. thaliana* C24 T₂ plants of the low copy line 10. A TDP-based relative qRT-PCR included 50 ng *A. thaliana* C24 T₂ line 10 cDNA. Plants were pre-cultured for two weeks on solid MS medium, and harvested after 24 h of 17β-Estradiol (5 μM) treatment. The cDNA was synthesized including 1 μg total RNA. Expression was calculated using the $2^{-\Delta\Delta CT}$ method (Livak and Schmittgen, 2001). Non-treated *A. thaliana* C24 T₂ line 10 plants were set to '1' as the calibrator. Expression data represent mean values of four biological replicates. Error bars represent the 95 % confidence intervals.

Tomato and tobacco organogenesis assay

For the tomato genotype GCR 26 and the tomato cv. MicroTom organogenesis assay cotyledonary explants were cut from two week old in-vitro grown seedlings. For two days explants were placed with the adaxial side onto tobacco feeder layer plates. Afterwards all explants were placed with the adaxial side onto phytohormone supplied MS-S medium for the initiation of shoot development. Different kinds of cytokinins and mixtures of cytokinins and auxins were added to the MS medium for an evaluation of the shoot induction frequency (Table 1). Explants prepared from the tomato genotype GCR 26 failed to induce and generate complete shoots. The organogenesis resulted in the formation of single leaves on MS-S medium containing 4 mg / L Zea six weeks after cotyledon cutting. After four to six weeks 6.6 % of the explants prepared from the tomato cv. MicroTom showed a development of

shoots buds on MS-S medium with a Zea concentration of 4 mg / L. Two different combinations of the cytokinin BAP and the auxin IAA did not lead to the formation of shoots on cutting sides of the explants. As a single auxin 2.4-D was effective at a MS-S medium concentration of 2 mg / L with on average 10.9 % explants showing a shoot induction. Additionally, an organogenesis assay was performed with four week old in-vitro grown tobacco cv. SSN seedlings. The explants were cut and directly placed with their adaxial side onto MS-S medium containing 2 mg / L Zea (Table 1). Shoots were induced four weeks after cotyledon cutting at on average 97 % of the tobacco explants.

Table 1 Shoot induction frequency of the tomato genotype GCR 26, tomato cv. MicroTom and tobacco cv. SSN, cultivated on MS-S medium with different phytohormones.

Phytohormone	Concentration [mg / L]	Shoot induction		
		Tomato genotype GCR 26 [%]	Tomato cv. MicroTom [%]	Tobacco cv. SSN [%]
Zea	0.5	0	0	nt
	1	0	0	nt
	2	0	0	97
	4	0 (single leaves)	6.6	nt
BAP / IAA	1.0 / 0.2	0	0	nt
	2.0 / 0.2	0	0	nt
2.4-D	2	0	10.9	nt

nt = not tested

For the tomato genotype GCR 26 the formation of callus tissue and the limited generation of single leaves on MS-S medium containing Zea (4 mg / L) is shown in Figure 18. One week after explant preparation following the tobacco feeder layer, white and soft callus structures developed on one cutting side (Figure 18 a, b). This fresh callus tissue started to transform into a compact green tissue mass at about two to four weeks after explant preparation (Figure 18 c, d). During the whole organogenesis assay tomato GCR 26 explants did not expand their size. Six weeks after explants cutting the callus tissue turned into a compact cell accumulation with a limited induction of single leaves (Figure 18 e, f).

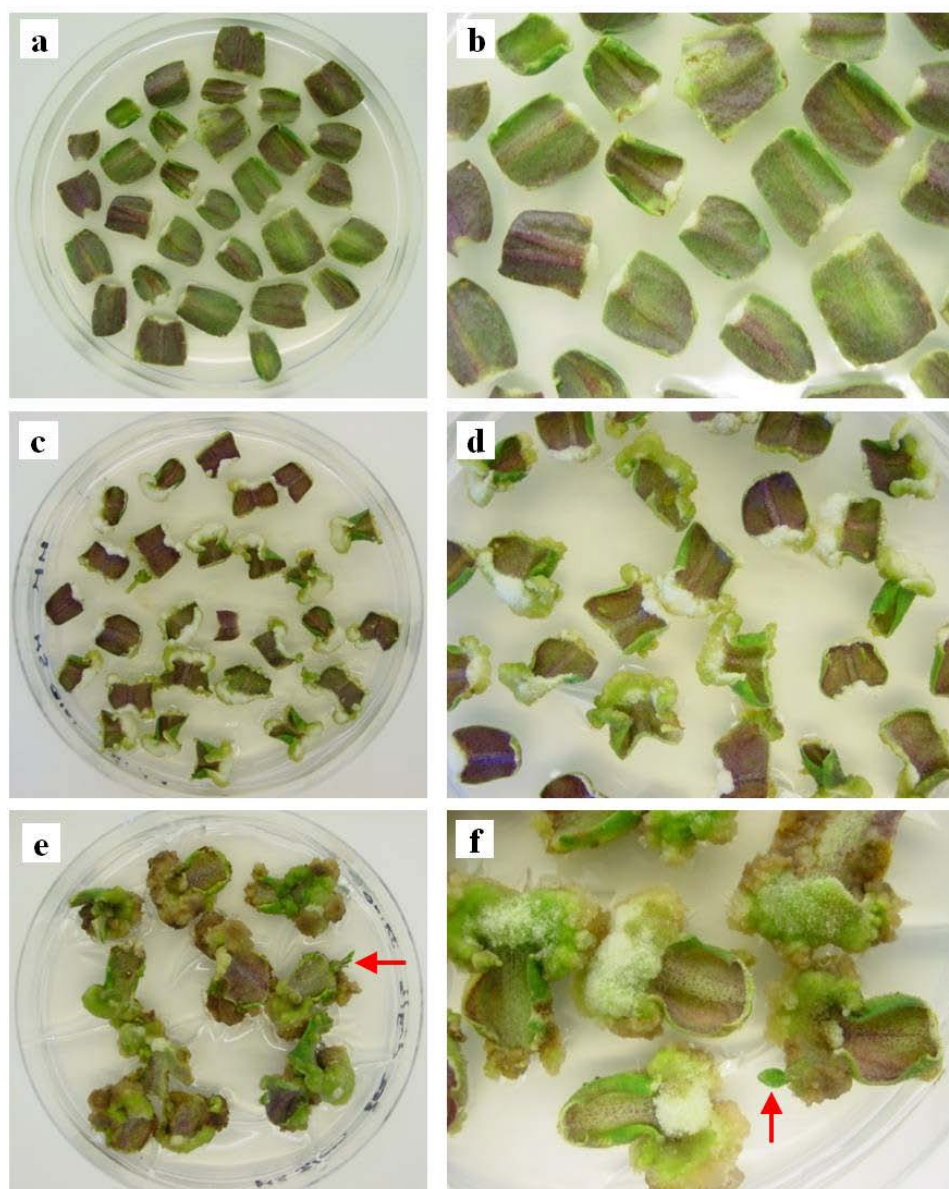


Figure 18 Callus formation and single leaf induction on explants of the tomato genotype GCR 26. **a, b** Cotyledonary explants were prepared from two week-old in-vitro grown seedlings and cultured on MS-S medium (Zea 4 mg / L). After one week white callus cells started to form at one cutting side on each explant. **c, d** Callus cells formed a dense green cell accumulation on two to four week-old explants. **e, f** Single leaves were induced and started to grow on compact green callus structures after six weeks (Red arrows indicates single leaves).

One week after cutting and tobacco feeder layer culture, the formation of white and soft callus tissue could be detected on one side of each explant prepared from the tomato cv. MicroTom. The callus cell production stopped at about two to four weeks after explant preparation. Cotyledonary explants did not expand their size but single shoot buds started to develop on

four to six week-old explants (Figure 19 a – f). The single shoot buds did not grow further and necrotic areas appeared on leaf tips. Additionally, some explants started to develop necrotic border areas.

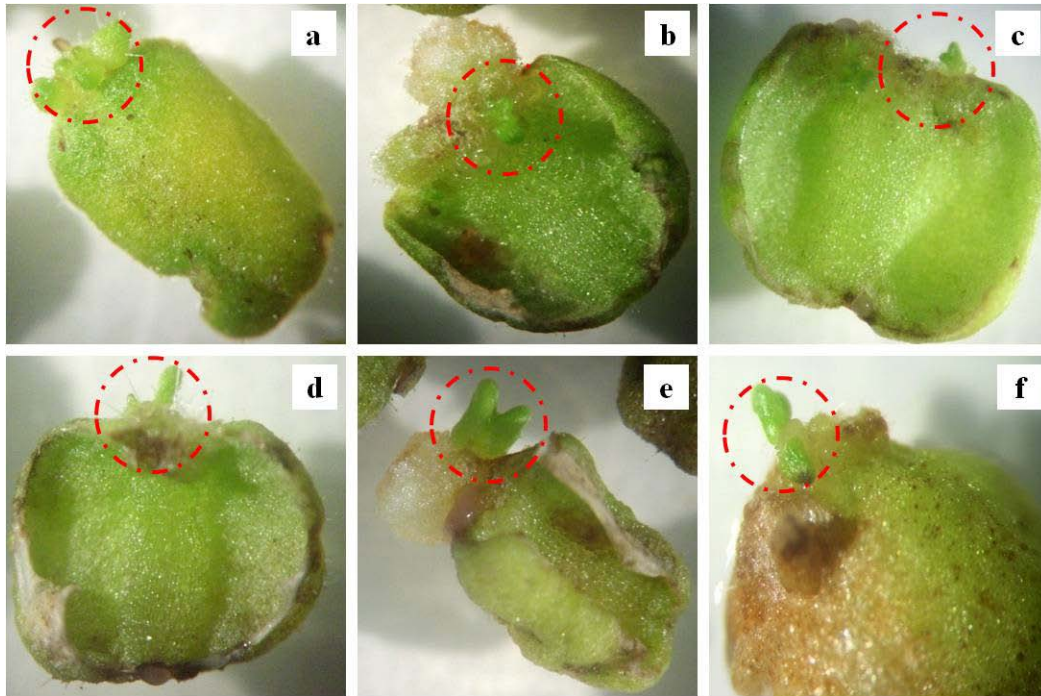


Figure 19 Shoot induction on explants of the tomato cv. MicroTom. Cotyledonary explants were prepared from two week old *in-vitro* grown seedlings and cultured on MS-S medium (Zea 4 mg / L). After one week small white callus structures started to form at one cutting side on each explant. **a - f** Single shoot buds appeared on four to six week-old explants (Red circles highlight newly induced shoots).

The progress of tobacco organogenesis is shown in Figure 20. Cotyledonary explants were prepared from four week-old *in-vitro* grown seedlings and cultured on MS-S medium. Soft white callus formed on one week-old explants (Figure 20 a). Multiple shoots were induced up to four weeks after explants preparation (Figure 20 b). These shoots were separated from explants and placed onto fresh MS-S medium (Figure 20 c, d). Leaves emerging from axillary buds were removed several times (Figure 20 e, f) and two week-old shoots were transferred on to hormone-free MS medium. A defined new root system was induced on the cutting side of shoots (Figure 20 g). Fully developed young plantlets were removed from the *in-vitro* culture and further cultivated under low humidity conditions in substrate covered with transparent foil (Figure 20 h, i).

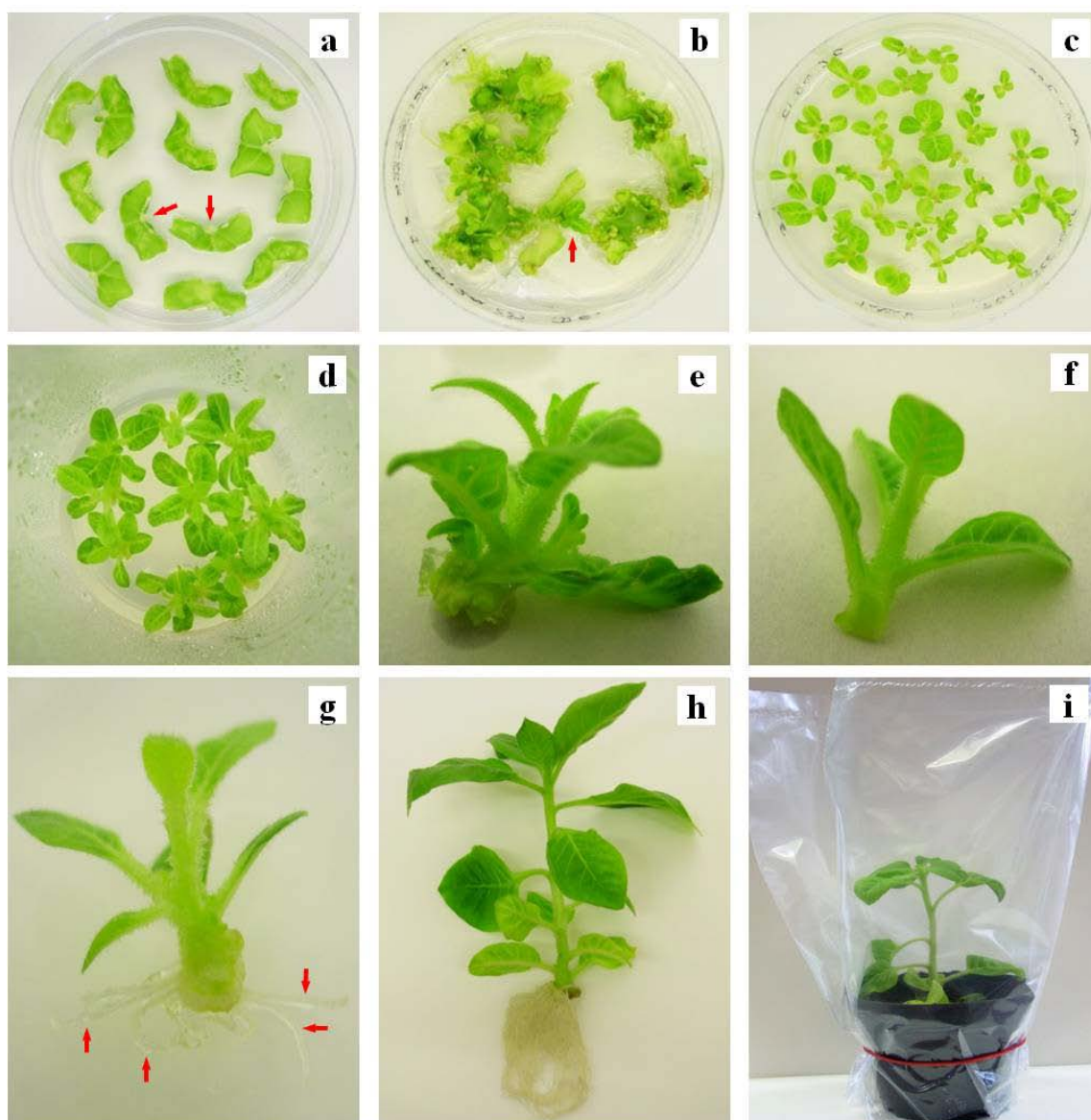


Figure 20 Different stages of the tobacco cv. SSN organogenesis. **a** White callus cells started to form at the cutting sides of one week old explants (Red arrows indicated callus). **b** Up to four weeks after explants cutting multiple shoots were induced by Zea (2 mg / L) and started to grow on the callus tissue (Red arrow indicates developing shoot). **c, d** Growing shoots were separated from explants and weekly transferred into fresh MS-S medium. **e, f** Axillary leaves were weekly removed from growing shoots. **g** Two week old shoots were placed into hormone-free MS medium, and defined single roots started to developed. **h, i** Six week old tobacco plantlets with well developed roots were transferred into Einheitserde type P. For substrate and low humidity acclimation young tobacco plantlets were kept under transparent foil for four weeks.

Discussion

The uptake, activation and reduction of sulfate has a pivotal role in the overall metabolism of plants. As the major product of the primary reductive S assimilation pathway Cys is the first organic reduced S compound being directly incorporated into a number of primary and secondary S metabolites via numerous downstream biosynthetic pathways (Droux, 2004). In the context of biotic stress, Cys and also its follow-up product GSH are thought to be relevant precursors for the synthesis of specific SDCs, which are directly involved in SED processes against phyto-pathogens (Rausch and Wachter, 2005; Kruse et al., 2007). Increased contents of sulfate, Cys, and GSH were detected in a *V. dahliae*-infected resistant tomato genotype (Williams et al., 2002; Chapter I), which was shown to be capable of S⁰ formation in its colonized vascular tissue. This further suggests a role of both thiols for the synthesis of specific SDCs including S⁰. During the last ten years several plant species were shown to internally accumulate S⁰ in the vascular tissue in response to a *V. dahliae* infection and thus to be capable of S⁰-based SED against the fungal pathogen (Williams and Cooper, 2004). Up to now the *in planta* phytotoxic mechanism of S⁰ and its biosynthetic pathway are not completely elucidated, and the participation of sulfate, Cys and GSH remains to be clarified. Therefore, the current study aimed at providing molecular gene overexpression tools for the characterization of primary S metabolism-associated steps in relation to their contribution for the tissue inherent S⁰ synthesis in tomato plants after infection with the fungal pathogen *V. dahliae*.

One focus is thereby on the intracellular sulfate remobilization by sulfate transporters (Sultr). In *Arabidopsis* phylogenetic analysis showed that the family of high and low affinity sulfate transporters and related homologue proteins is comprised of 14 genes which are sub-divide into five groups (Buchner, 2004; Kopriva et al., 2009). The group four of vacuolar sulfate transporters contains the two gene isoforms *AtSultr4;1* and *AtSultr4;2* (Buchner, 2004), with a tissue-specific localization in tonoplast membranes of root and hypocotyl pericycle and xylemparenchyma cells (Kataoka et al., 2004). Both transporters respond to plants S availability by a demand-driven regulation and the vacuolar sulfate transporter *AtSultr4;1*, as the major isoform, predominantly mediates the export of sulfate out of the vacuolar lumen (Kataoka et al., 2004). The homologous overexpression of the tomato-derived *LeSultr4;1* should thus enhance the export of sulfate into the cytoplasm. Increased cytosolic sulfate levels are than thought to enhance the reductive S assimilation resulting in a rapid turnover of cytosolic free sulfate. Subsequently, elevated Cys contents might be converted to enhance the

biosynthetic process of SDCs formation leading to higher vascular levels of S^0 after a *V. dahliae* colonization of transgenic tomato plants.

A second primary S metabolism-associated focus is on the two step adenosine-triphosphate (ATP)-dependent biosynthesis of GSH. In the first plastid-localized rate limiting step GSH1 catalyzes the formation of γ -glutamylcysteine and in the second predominantly cytosol-localized step glutathione synthetase mediates the formation of GSH (Wachter et al., 2005; Noctor et al., 1998). In plants GSH is the major pool for reduced organic sulfur being translocated via the phloem and accumulates to millimolar intracellular concentrations in its reduced state with variations depending on the sub-cellular compartments (Noctor et al., 2012). Major factors influencing the GSH biosynthesis are the Cys availability, GSH1 activity but also glycine and ATP availability. Additionally, under optimal S nutritional status, GSH leaf-tissue concentrations can be substantially increased in diverse plant species by homo – and heterologous overexpression strategies mainly focusing on GSH1 (Creissen et al., 1999; Xiang et al., 2001; Liedschulte et al., 2010). The homologous overexpression of tomato-derived *LeGSH1* is, therefore, expected to increase cellular pools of reduced GSH. Since a major metabolic function of GSH is antioxidative defence under conditions of biotic stress (Foyer and Noctor, 2011), in genetically-modified plants after fungal infection elevated levels of this redox buffer might either improve a detoxification of reactive oxygen species (ROS) or enhance the synthesis of S^0 .

In the current study for the future purpose of an *Agrobacterium*-mediated transformation of cotyledonary explants and a subsequent in-depth molecular characterization of *in vitro* grown genetically modified transgenic plants, the two tomato-specific candidate genes *LeSultr4;1* and *LeGSH1* were inserted into two different kinds of transgene overexpression systems. Both transgenes were integrated either into the chemical-inducible binary pER8 T-DNA vector or the constitutive CaMV 35S-based binary p9 T-DNA vector. These disarmed overexpression systems consist of an autonomous T-DNA binary vector and the appropriate Ti-plasmid, which *in cis* carries the *vir* genes required for processing and integration of the agrobacterial T-DNA into the nuclear host plant genome (Tzfira and Citovsky, 2006). The resulting T-DNA vector constructs were then heat-shock transformed into cells of the *A. tumefaciens* GV2260 strain, which belongs into the octopine class of agrobacterial strains with a C58 chromosomal background (Hellens et al., 2000).

The constitutive transgene overexpression causes very high levels of gene expression, thus establishing high gene product levels at all developmental stages and a suitable constitutive promoter commonly used for the transformation of dicotyledonous plant species is the CaMV 35S promoter (Benfey and Chua, 1990). This promoter was found to transcribe a major 35S RNA, which represented a complete transcript of the circular viral genome of the double-stranded DNA plant pathogenic cauliflower mosaic virus isolated from turnip leaves (Guilley et al., 1982). In this study as a constitutive overexpression system the CaMV 35S promoter-based binary p9 T-DNA vector was used and included next to the left border sequence the plant selectable marker gene encoding neomycin phosphotransferase II framed by a strong CaMV 35S promoter and terminator. Additionally, a MCS used for transgene overexpression was framed by a strong CaMV 35S promoter and terminator and located near the right border sequence.

To control the functioning of the constitutive CaMV 35S-based transgene overexpression, tobacco plants were transiently transformed by an *Agrobacterium*-mediated leaf infiltration with *A. tumefaciens* GV2260 cells harboring the binary p9:DsRed, p9:eGFP and p9:GUSi construct. The expression of the three reporter genes was monitored after 72 h (Figure 13). The leaf infiltration of tobacco with the binary p9:GUSi construct did not allow a clear differentiation of transformed leaf areas. The GUS-staining assay failed to indicate a sufficient infiltration by a clear blue tissue coloration (Figure 13 c). When compared to non-infiltrated leaf areas, parts infiltrated with the binary p9:DsRed construct did show a slightly higher *DsRed* expression level in form of a more intense red-fluorescence (Figure 13 d). Since tobacco leaf tissue exhibited a high red auto-fluorescence and the origin of dense particle accumulation spots in infiltrated leaf parts remained unknown, a satisfactory differentiation between transformed tissue and non-transformed tissue was not possible with the *DsRed* reporter gene. In contrast, the leaf infiltration of tobacco with the *eGFP* reporter gene caused a high green-fluorescence in transformed leaf areas. Distinct green-fluorescent cell structures were present only in infiltrated leaf parts, indicating a local high level of *eGFP* expression (Figure 13 e). Therefore, the eGFP reporter gene could be used to demonstrate the high constitutive overexpression capacity of the CaMV 35S-based binary p9 T-DNA vector system.

In contrast, the chemical control of expression is thought to enable a precise temporal, spatial and quantitative expression of selected transgenes (Wang et al., 2003). Critical factors for a reliable chemical-inducible system include a low basal expression but high inducibility, a high range of applicable inducer concentrations, a rapid activation by an inducer with low toxicity and high specificity naturally not occurring in plants and a rapid turn-off after inducer application (Padidam, 2003). The binary pER8 T-DNA vector represents a chemical-regulated expression systems belonging into the class of steroid receptor-based transcription activation systems (Padidam, 2003; Wang et al., 2003). The T-DNA region includes two transcription units. The first transcription unit harbors a strong constitutive promoter in front of the XVE fusion gene, which consists of a DNA-binding domain (X), a transactivation domain (V), and the human estrogen receptor (E). The second transcription unit includes a LexA operator sequence and a minimal CaMV 35S promoter in front of the MCS (Zuo et al., 2000). Both units are separated by an expression cassette carrying the plant selectable marker gene *hpt*. The hormone 17 β -estradiol was shown to functionally bind in a wide concentration range (8 nM to 5 μ M) to the regulatory part of the human estrogen receptor (Zuo et al., 2000). The XVE fusion gene product is then transferred into an active form and binds to the operator part in the second transcription unit to induce the minimal part of the CaMV 35S promoter for a chemical-controlled activation of the transgene expression.

To assess the potential of the targeted chemical transcription induction the *A. thaliana* C24 genotype was subjected to a 'floral-dip' transformation according to Logemann et al. (2006) with *A. tumefaciens* GV2260 cells harboring the pER8 and pER8:LeSultr4;1. Seeds were obtained from T₀ plants and transgenic *A. thaliana* C24 T₁ seedlings were selected based on their Hyg-B resistance in a rapid screening approach according to Harrison et al. (2006). Transgenic *A. thaliana* C24 T₁ seedlings could be identified based on a distinct elongation of the hypocotyl in comparison to non-transformants (Figure 14). Additionally, a conventional PCR assay including a primer pair positioned on the binary pER8 T-DNA vector, and the *LeSultr4;1* transgene to amplify a 115 bp product was used to control a correct T-DNA integration into the *A. thaliana* C24 T₂ genome (Figure 15 a). A total number of 18 transgenic *A. thaliana* C24 T₂ plants was identified to carry the *LeSultr4;1* transgene. A second conventional PCR approach for the detection of the empty T-DNA region included a primer pair, which span the MCS region to amplify a 185 bp product (Figure 15 b). Genetically modified plants must be tested for single or multiple transgene integrations to clearly differentiate homozygous from heterozygous transgenic plant material. Only homozygous

plants, which typically exhibit a very low number of transgene integrations, offer a stable and high expression of the candidate gene (Yi et al., 2008). Additionally, multiple random integrations into several chromosomal locations often cause gene silencing (Yang et al., 2005). Therefore, an absolute qRT-PCR assay including a dual-labeled fluorogenic TDP was established to estimate the number of transgene copies included in the genome of single *A. thaliana* C24 T₂ plants. Compared to classical nucleic acid blotting techniques like southern blot hybridization, this novel qRT-PCR approach enables a rapid, accurate and save determination of single or multiple transgene insertions and, with a minimal input of transgenic plant material, was most reliable particularly in the case of low-copy identification (Ingham et al., 2001; Gadaleta et al., 2011). In the present work the absolute quantification test revealed a homogeneous distribution of high and low copy number transgenic *A. thaliana* C24 T₂ plants (Figure 16). From 18 plants, previously identified to carry the *LeSultr4;1* candidate gene, four plants were tested to obtain three to one transgene integration. Thus, the absolute qRT-PCR assay including a fluorogenic probe can be used in future experiments to reliably determine the integration and number of transgenic copies in genetically modified plant material. The *A. thaliana* C24 T₂ low copy line 10 was selected to assess the potential of a targeted chemical-directed transcription induction. Since the optimal 17 β -estradiol inducer concentration was in the range of 8 nM to 5 μ M and the optimal treatment time was 12 h to 48 h (Zuo et al., 2000) in the present study the *LeSultr4;1* transgene was induced with 5 μ M 17 β -estradiol for 24 h. The *A. thaliana* C24 T₂ low copy line 10 showed an on average six fold linear *LeSultr4;1* expression (Figure 17). Therefore, a pER8-mediated chemical-induction of S metabolism-related candidate genes proved to be applicable for a targeted transgene overexpression in upcoming physiological tests.

To further elucidated the synthesis of S⁰ and to assess the possible contribution of the primary S assimilation pathway, different tomato genotypes and tobacco were designated for an overexpression analysis of the two S metabolism-related genes *LeSultr4;1* and *LeGSH*. In this context, a preferred method for the generation of transgenic plants is the *Agrobacterium*-mediated transformation of cotyledonary explants. The basic steps of this procedure comprise: the cutting of *in vitro* grown young cotyledons, the infection and co-cultivation of explants with agrobacterial cells carrying the transgene, the elimination of agrobacterial cells, the chemical-based induction of shoots from callus tissue, and the generation of roots (Sun et al., 2006; Sarker et al., 2009). Thereby, many factors including e.g. age and treatments of explants, time and temperature of co-cultivation, bacterial strains, vector constructs, type and

concentration of hormones can influence the efficiency of the *Agrobacterium*-mediated transformation (Gao et al., 2009). Thus, it is most important to initially optimize all relevant factors in a first test for the generation of new transplants from *in vitro* grown seedlings in the absence of agrobacterial cells. In the current study the *in vitro* organogenesis capability of the *V. dahliae*-sensitive tomato genotype GCR 26, the tomato model cv. MicoTom and tobacco cv. SSN was determined. The tomato genotype GCR 26 is only insufficiently capable of a fungitoxic S^0 production in response to a *V. dahliae* infection (Williams et al, 2002; Chapter I). Thus, it was selected to analyze the effect of an overexpression of both S metabolism-related candidate genes on the S^0 accumulation in the presence of the fungus. The tomato cv. MicroTom is often used in plant diseases studies and due to its small size, short life cycle, small genome size and highly efficient transformation ability (Dan et al., 2006) this plant model system was also selected to analyze mechanisms involved in S^0 synthesis. During the organogenesis assay, the variable cytokinin or auxin treatment of explants prepared from cotyledons of the tomato genotype GCR 26 caused callus growths but failed to induce complete shoots (Figure 18). Only single leaves were visible after six weeks of Zea treatment (Figure 18 e, f). Additionally, a variable cytokinin treatment caused callus formation on cotyledonary explants of the model cv. MicroTom, but shoot buds only appeared after four to six weeks of 2,4-D auxin treatment and finally died off (Figure 19). Since multiple attempts for the tomato organogenesis failed to produce vital young plantlets, the *A. tumefaciens* strain GV2260 including the binary p9:LeSultr4;1 construct and binary p9:eGFP construct were sent to the Max Planck Institute of Molecular Plant Physiology (Potsdam, Germany) for an *Agrobacterium*-mediated transformation of cotyledonary explants from the tomato cv. Moneymaker. Tobacco as a member of the *Solanaceae* family might also be capable of relevant S^0 synthesis after overexpression of S metabolism-related transgenes. Additionally, tobacco is known to give high transformation efficiencies (Sparkes et al., 2006). Therefore, tobacco was thus also chosen to study S^0 synthesis mechanisms. Cotyledonary explants were prepared from tobacco and treated with Zea for an induction of a high number of shoots (Figure 20 a - c). These shoots were further cultivated without hormones to form a new root system, and fully developed young plantlets were finally transferred into substrate (Figure 20 d - i). Additionally, following the successful tobacco organogenesis test, the *Agrobacterium*-mediated transformation of tobacco cotyledonary explants was initiated with GV2260 cells harboring the binary p9 T-DNA vector and the binary p9:LeSultr4;1 construct.

In the present work the two tomato-derived candidate genes *LeSultr4;1* and *LeGSH1* from the primary S assimilation pathway were successfully integrated into the chemical-inducible binary pER8 and the constitutive binary p9 T-DNA vector system and transferred into suitable agrobacterial cells. Conventional PCR, restriction digestion and sequencing were adapted to control the correct assembly of all constructs and to verify their presence in different bacterial cells. Additionally, conventional PCR methods and qRT-PCR methods including a fluorogenic probe were tested to further verify the successful integration of candidate genes into the host plant genome and to determine the exact number of integrated transgene copies. The functioning and expression capacity of both vector systems was determined either with a fluorogenic probe-based absolute qRT PCR after *floral-dip* transformation of plants or by reporter genes expression monitoring after *Agrobacterium*-mediated leaf infiltration of plants. Therefore, all molecular requirements are fulfilled for the production of transgenic plant material which can be used to characterize the contribution of primary S metabolism-associated steps to the vascular tissue-inherent S^0 synthesis initiated in the presence of the fungal pathogen *V. dahliae*. Future analysis of transgenic tomato plants cv. Moneymaker, transgenic tomato plants cv. GCR 26 and transgenic tobacco plants cv. SSN constitutively overexpressing the *LeSultr4;1* gene which encodes the tonoplast-localized sulfate export, will focus on the concentration measurement of different SDC including Cys, GSH, and S^0 . An increase in specific SDC concentrations is expected after colonization of genetically modified plants with *V. dahliae* and might be verified with previously established methods (Chapter I).

General Discussion

Verticillium-wilt is a detrimental fungal disease annually causing severe crop harvest losses on a worldwide level, which finally leads to high financial penalties for farmers and companies (Pegg and Brady, 2002). The phyto-pathogenic fungus *V. dahliae* globally infects host plants especially in temperate and subtropical areas (Fradin and Thomma, 2006). Common disease management strategies include the external application of fungicides which is questionable in terms of consumer and environment safety and offers only limited protection against the internal colonization of plant vascular tissue (Goichoecea, 2009). In different plant taxa, the tissue-inherent process of SED constitutes a supplementary protective approach and an effective alternative for a significant *in planta* limitation of the *Verticillium*-wilt disease level (William and Cooper, 2004). Resistant tomato plants were shown to accumulate S^0 as a specific SDC in xylem and xylemparenchyma cells to constrain the systemic spread of the fungus (William et al., 2002; Chapter I). In the presented work the plant protective mechanism of SED was studied using physiological and transcriptomic approaches aiming at a better understanding of the role of SDCs in the tomato - *V. dahliae* interaction. The study confirmed that a supra-optimal S nutritional status increases the resistance of tomato against *V. dahliae*, provides new insights into the pathway of S^0 synthesis, and reveals a genotypic connection of SED and R gene defense in tomato. The most important results are summarized and discussed here in an integrative way.

Enhanced S fertilization activates SED mechanisms and limits the spread of *V. dahliae* in tomato plants

In the vascular stage of the *Verticillium*-wilt disease the fungal pathogen enters into xylem and xylemparenchyma cells and starts in a cyclic manner the invasion of plants (Chen et al, 2004; Robb et al., 2007). A rapid plant response after initial vascular contact with the pathogen is the deposition of suberin on the vessels walls to prevent the penetration of fungal hyphae into neighboring cells. This coating reaction represents a most important physical barrier to close infected vessels and thus constrict a vertical spread of the fungus (Robb et al., 1989; Heinz et al. 1998). To characterize the influence of a variable S nutrition on the disease course and thus to further elucidate the S-stimulation of SED for tomato protection against the fungal vascular wilt pathogen, *V. dahliae*-sensitive and resistant tomato genotypes were grown either with luxury or low S nutrition. The cell-wall coating-response of host plants, as

reflected by the number of suberized xylem vessels, was evaluated after fungal infection of the tomato root systems. The excess application of S reduced the suberization of vascular vessels in sensitive tomato genotypes as well as in resistant genotypes (Chapter I, Figure 3 a). This on the one hand outlines the general importance of S nutrition for an effective internal plant defense against the vascular wilt pathogen *V. dahliae*. An optimal supply with S is known to reduce the susceptibility of plants towards biotic stressors (Klikocka et al. 2005; Höller et al. 2010). Moreover, this clearly confirms the potential of particularly high S supply to effectively activated S-based fungal elimination processes.

Additionally, a high S supply affected the fungal pathogen illustrated by a clear decline of *V. dahliae* gDNA and thus colonization in hypocotyls of luxury S-supplied sensitive tomato plants (Chapter I, Fig. 8). The results suggest an implication in SED of an increased formation of specific SDCs in the presence of the fungus. Cys and GSH pools, which are both frequently mentioned as possible precursor S metabolites in S^0 synthesis (Rausch and Wachter, 2005; Kruse et al., 2007), were increased in *V. dahliae*-infected sensitive tomato plants after an enhanced S fertilization (Chapter I, Figure 9 a). This confirms the well known strong dependency of these thiols on the plant S nutritional status (Schnug et al. 1995; Bloem et al. 2010). Additionally, the supra-optimal S nutritional status seemed to allow a surplus production of reduced GSH possibly needed for antioxidative protection in the presence of *V. dahliae* particularly in resistant plants (Chapter I, Figure 9 b). These observations suggest the efficacy of SDCs to effectively promote already existing protective SED mechanisms in an incompatible pathosystem. Additionally, a high sulfate-S supply proved to be an effective way to overcome constitutive compatible pathosystems with low *V. dahliae* resistance by decreasing the *in planta V. dahliae* colonization levels using an effective SED.

In the presented study the induction of S^0 formation in four week-old hypocotyl central cylinder tissue enhanced by *V. dahliae* infection could be confirmed by HPLC analysis (Chapter I) and reflect the genotypic differences in tomato S^0 formation described by Williams et al. (2002) in 11 week-old infected plants. At supra-optimal S supply the *V. dahliae*-infection greatly increased the S concentration in the vascular bundle. The application of LA-ICP-MS enabled the detection of a number of particularly high S concentration peaks in the vascular bundle of the infected resistant genotype (Chapter II, Figure 3 f). This specific local accumulation pattern in infected xylem vessels as proposed by Cooper et al. (1996), Williams et al. (2002), and Novo et al. (2007) seems to be a decisive factor for the fungicidal

impact of S^0 which was demonstrated for *V. dahliae* in different plant species (Cooper and Williams, 2004). However, the exact identity of detected local S accumulations remains to be analyzed since the vascular peak S concentrations might represent S^0 or precursor S substances involved in SDC generation.

***V. dahliae*-initiates a tissue-specific expression of S metabolism-related genes**

To analyze genotypic differences in SED mechanisms and the corresponding formation of S^0 a group of candidate genes related to the reductive S assimilation pathway and genes involved in the biosynthesis and recycling of GSH were selected for a detailed qRT-PCR-based expression study (Chapter II, Figure 4 a). As part of the primary S metabolism the tonoplast-localized S exporter *LeSultr4;1*, the plastidic key regulator *LeAPR*, plastidic single gene encoded *LeSiR* and Cys-Synthase complex forming plastidic *LeOastlp1* were selected (Kataoka et al., 2004; Kopriva et al., 2012; Khan et al., 2010; Heeg et al. 2008). Involved in GSH biosynthesis and reduction plastidic *LeGSH1*, plastidic and cytosolic *LeGSH2* and plastidic *LeGR2* were chosen (Wachter 2005; Noctor et al., 2012). Thereby, a special focus was on the bulk hypocotyl tissue of tomato plants colonized by *V. dahliae* and on infected vascular cell areas as the initial place of S^0 accumulation, which were isolated with the LMPC technique. Subsequently, the spatial gene expression of the S metabolism-related candidates was analyzed in infected high-S supplied resistant tomato plants.

The analysis of bulk hypocotyl tissue revealed an S demand-driven gene regulation pattern for *LeSultr4;1*, *LeAPR*, and *LeSiR*, which either resupply the primary S metabolism with sulfate or facilitate the early steps of the reductive S assimilation. The strong induction of sulfate uptake and the first steps of the S assimilation pathway under S-limiting conditions has been well established (Davidian and Kopriva, 2010; Takahashi et al., 2011). Fungal pathogen infection strongly down-regulated all these steps related to the primary S metabolism (Chapter II, Figure 4 b). Therefore, a contribution of these genes to an S assimilation-based induction of SED mechanisms or the synthesis of specific SDCs appears unlikely in the bulk hypocotyl tissue. In contrast, the two-step process of GSH biosynthesis was not responsive to enhanced S supply, but the first rate-limiting reaction involving *LeGSH1* was clearly up-regulated by the fungal pathogen particularly in the *V. dahliae*-resistant tomato genotypes (Chapter II, Figure 4 b). This suggests a need for GSH possibly necessary for infection-induced scavenging processes. GSH is the major redox-buffer present in almost all plant cells (Mittler

et al., 2004; Galant et al., 2011) and scavenging processes for the detoxification of pathogen-derived ROS seem to be best managed in the entire hypocotyl tissue of pathogen resistant plants. In the presence of *V. dahliae* vascular cell-specific expression patterns for genes related to the primary S metabolism revealed an S-enhanced induction of steps directly associated with Cys synthesis (Chapter II, Figure 5 b). An enhanced vascular *LeOastp1* expression is expected to cause a locally increased synthesis of Cys which could be a prerequisite for an enhanced production of S^0 . Thus Cys appears to play a major role for the establishment of effective SED reactions and the synthesis of specific SDCs in tomato vascular tissue. Additionally, the strong down-regulation of genes related to GSH biosynthesis and recycling in tomato vascular bundles cells does not suggest a major role of local antioxidative function of this S metabolite in *V. dahliae* resistance. The results thus support the conclusion that Cys enables a vascular tissue-localized SED response after fungal infection and serves as a precursor for the synthesis of specific SDCs including S^0 . Following the pathogen infestation, GSH facilitates a global ROS detoxification in the bulk hypocotyl tissue. Therefore, the local tissue-specific Cys-based defense against *V. dahliae* in tomato plants is supported by a global GSH-based antioxidative protection mechanism.

Sulfur-enhanced and R gene-mediated defense differentially contribute to *V. dahliae* resistance in tomato genotypes

To identify the relative importance and connection of SED mechanisms and R gene-based pathogen defence in tomato plants, selected physiological parameters together with qRT-PCR-based gene expression analysis were evaluated to find differences between *V. dahliae*-sensitive and resistant ILs and their parental lines. Therefore, an IL population, originating from a cross between the cultivated tomato genotype *L. esculentum* cv. E6206 and the WT accession *S. habrochaites* LA1777 was screened for variation in the hypocotyl *V. dahliae* colonization level (Montforte and Tanksley, 2000). This IL set had been successfully used in a black leaf-mold analysis to characterize the parental lines and to identify sensitive and resistant ILs (Zahn et al., 2011). According to their level of fungal colonization in the current work the whole IL population was classified into four *V. dahliae* resistance groups (Chapter III, Figure 1) and a selection of *V. dahliae*-sensitive and resistant ILs, the WT donor, and the cultivated RP were further grown at variable S supply. An S-enhanced containment of fungal growth was detected for the RP and the sensitive IL, whereas highest *V. dahliae* gDNA concentrations in the WT donor proved that elevated S supply did not have any limiting effect

on the fungal *in planta* spread (Chapter III, Figure 4 b). A highly resistant IL showed a consistently low colonization level independent of the applied S fertilization level (Chapter III, Figure 4 b). The detected differences in the S-based stimulation of SED mechanisms seem to determine the level of *V. dahliae* resistance in tomato plants. The beneficial effect of enhanced S nutrition again empathizes the S-responsiveness of SED mechanism as already shown in chapter I (Figure 3 a; Figure 8). The missing S-responsiveness of highly resistant plants indicates the existence of further processes, which can complement SED mechanisms or can alone confer a high level of resistance against *V. dahliae*.

As well established, a genomic source of resistance is the R gene-mediated pathogen recognition and signal transduction, which also determines the *V. dahliae* resistance of tomato plants (Fradin et al. 2009). An important R gene needed to establish an incompatible tomato-*Verticillium* interaction is *Ve1* (*Verticillium* race 1). In many cultivated resistant tomato plants the *Ve* locus encodes a functional cell-surface receptor belonging to the family of extracellular leucine-rich repeat (eLRR) receptor-like proteins (RLP), which enables the recognition of fungal elicitor molecules (Diwan et al. 1999; Kawchuk et al. 2001; Wang et al., 2008). Although the exact mechanisms of the subsequent signal-transduction pathways are not completely analyzed yet, the mature *Ve1* receptor as a disease-resistance protein is known to confer increased resistance against race 1 strains of different *Verticillium* species (Fradin et al. 2009, 2010). In this study the relative quantification of *Ve1* transcript levels as influenced by the fungus and variable S supply confirmed the existence of the *Ve* locus in all tested lines and demonstrated a pathogen-elicited gene up-regulation after infection of the plants (Chapter III, Fig. 7 A). WT donor plants had lowest *Ve1* transcript amounts combined with a weak response to high S. In the RP and the sensitive IL, S deficiency strongly increased the *LeVe1* expression, and the resistant IL responded to enhanced S fertilization with strongly increased *Ve1* transcript levels, which shows that S can also act on R gene expression in addition to an activation of SED mechanisms. This clearly indicates that SED mechanisms and an R gene-mediated defence response may be both crucial for the establishment of an incompatible tomato-*V. dahliae* interaction, but the genetic constitution of the tomato genotype seems to determine the relative contribution of either mechanism to increased resistance against *V. dahliae*. Thus, in resistant tomato plants monogenic *Ve1* resistance can either prevail SED, or both defence strategies complement each other.

Outlook

Physiological methods were applied in the current work to clarify the role of enhanced plant S nutrition for an activation of SED mechanisms in tomato plants infected with the *Verticillium*-wilt pathogen *V. dahliae*. Transcriptomic approaches were used to elucidate the influence of excess S on the spatial expression of S metabolism-associated steps and to focus on the role of Cys or GSH for the synthesis pathway of specific SDCs including S⁰.

One part of the future experimental approaches will focus on the linkage of previous physiological and transcriptomic findings in connection with forward genetics molecular tools. A major goal is the in-depth characterization of selected primary S metabolism-associated steps in relation to their role in tissue-inherent S⁰ synthesis in *V. dahliae*-colonized tomato plants. Therefore, specific candidate genes related to the primary S assimilation were already integrated into different kinds of transgene overexpression systems. The CDS regions of the tonoplast-localized vacuolar sulfate exporter *LeSultr4;1* and *LeGSH1*, facilitating the first step of GSH biosynthesis, were integrated into the binary chemical-inducible pER8 vector system and the binary CaMV 35S-based constitutive p9 vector system. The binary constructs were transferred into the *A. tumefaciens* strain GV2260, and functional tests revealed the *in vivo* activation in *Arabidopsis* and tobacco. For an *Agrobacterium*-mediated transformation of cotyledonary tomato explants of cv. Moneymaker, the p9:LeSultr4;1 construct and binary p9:eGFP constructs were sent to the Max Planck Institute of Molecular Plant Physiology (Potsdam, Germany). Additionally, an *Agrobacterium*-mediated transformation of cotyledonary tomato explants of cv. GCR 26 (*V. dahliae*-sensitive) and of tobacco cv. SSN will be performed including the binary p9:LeSultr4;1 construct and the binary p9:LeGSH1 construct. Different *in vitro* regeneration strategies will be tested to generate genetically modified transgenic tomato and tobacco plants. Previously tested conventional PCR methods and qRT-PCR methods including a fluorogenic probe will be used to verify the successful integration of all candidate genes into the host plant genome and to determine the exact number of integrated transgene copies. The distinct transformation and regeneration of particularly *V. dahliae*-sensitive tomato plants is thought to give new insights into the activation capacity of classical SED mechanism. An overexpression of the S metabolism-related candidate genes is expected to improve the S-based defense particularly in pathogen-sensitive tomato plants. Subsequently, a major focus will be on the physiological

and transcriptomic analysis of transgenic tomato and tobacco plants grown at low and high S supply in comparison to the wild types after infection with the fungus *V. dahliae*.

Vacuoles are major sulfate storage cell compartments, and thus the overexpression of the tonoplast-localized sulfate exporter *LeSultr4;1* is thought to remobilize stored sulfate into the cytoplasm. An excess release of sulfate to the cytosol should promote a direct consumption of sulfate through the reductive S assimilation pathway. Since cytosolic Cys concentrations are generally on a relatively low level, a metabolization of excess Cys and the synthesis and accumulation of SDCs is expected to be promoted in transgenic plants. The beneficial impact of a supra-optimal plant S nutritional status could be demonstrated in the present study and clearly affected a restriction of the *in planta* fungal growth. This fungitoxic action of high S nutrition was combined with an S-enhanced formation of Cys and GSH in the presence of the fungus. Therefore, the *V. dahliae* colonization level should be lowest in transgenic tomato plants, which should have acquired the ability to perform an enhanced synthesis of GSH and S^0 . Since GSH was shown to function as a global antioxidant against biotic stress in the entire tissue, the overexpression of *LeGSH1* might increase the redox capacity of the entire plant tissue enabling a better compensation of ROS development in transgenic plants. This increase in GSH concentrations is expected to be enhanced after colonization of genetically modified plants by *V. dahliae*. Additionally, the application of supra-optimal S might further increase SDC formation finally causing high levels of GSH and fungitoxic S^0 in transgenic tomato plants. Previously established HPLC methods will be used to determine the levels of Cys, GSH and S^0 . A vascular-tissue specific induction of steps belonging to the synthesis of Cys was confirmed in the current work and linked to the formation and accumulation of S^0 or its precursor SDCs in xylem and xylemparenchyma vessels of an incompatible tomato - *V. dahliae* interaction. Thus, a spatial LA-ICP-MS S analysis is expected to demonstrate a high S supply enhanced elevated SDC accumulation in transgenic plant vascular tissue after fungal infection.

A further emphasis of future experimental approaches should be a detailed physiological and transcriptomic analysis of selected *V. dahliae*-sensitive and resistant ILs and their parental lines. This approach will allow acquiring further information on the relative importance of SED and R gene-based defense and their interconnection. HPLC and LA-ICP-MS analysis of the concentrations and spatial localization of Cys, GSH and S^0 might give more insights into the importance of SED mechanisms in the ILs. A qRT-PCR based expression analysis of S

Outlook

assimilation-associated genes might pinpoint starting points and precursor metabolites for SDC synthesis in the selected genotypes. Additionally, a comparison of well-described R gene responses in other pathosystems (*Cf*-mediated resistance) (Thomma et al., 2005) together with an expression analysis of down-stream components complementing the *Ve1* signalling-cascade, may give more insights on the importance of the R gene transcription for efficient pathogen elimination in *V. dahliae*-resistant ILs.

Supplementary Materials

Supplementary Material for Chapter I

Sulfur supply impairs spread of *Verticillium dahliae* in tomato

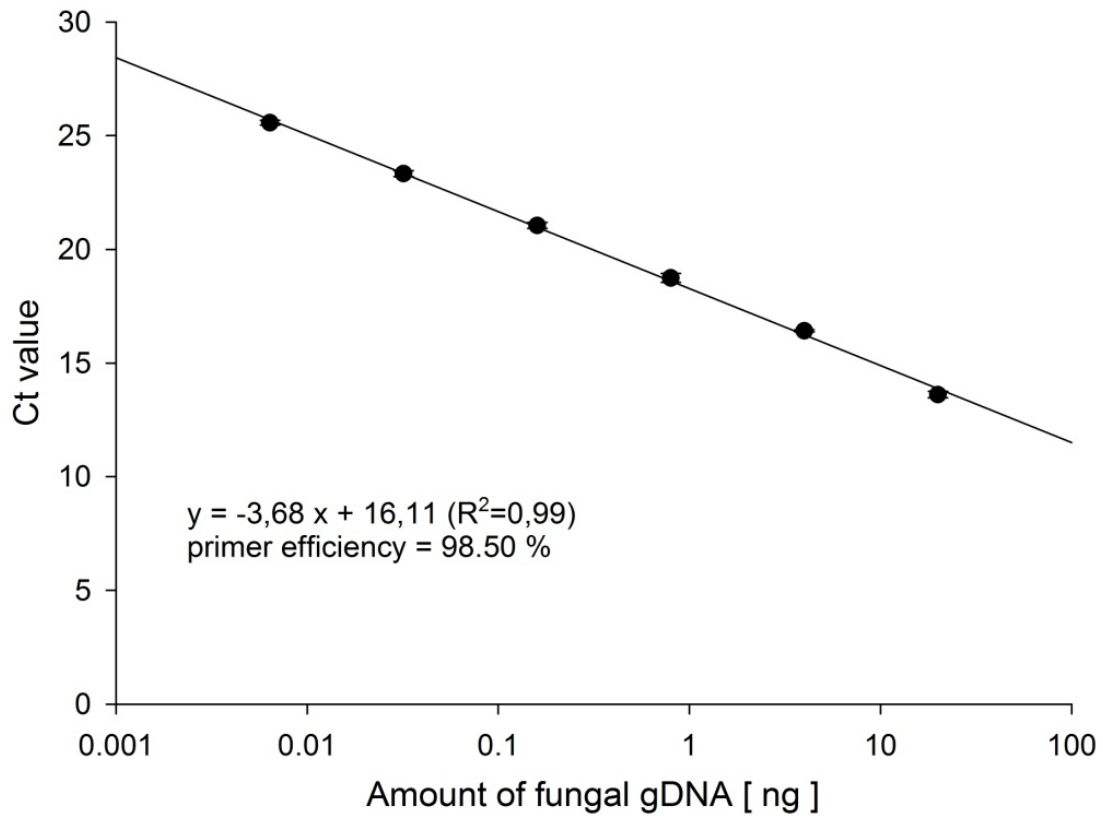


Figure S1 Regression line showing the obtained cycle threshold values plotted against the serial-dilution of *V. dahliae* gDNA using the LeVD primer pair. Values represent means \pm SD of $n = 3$.

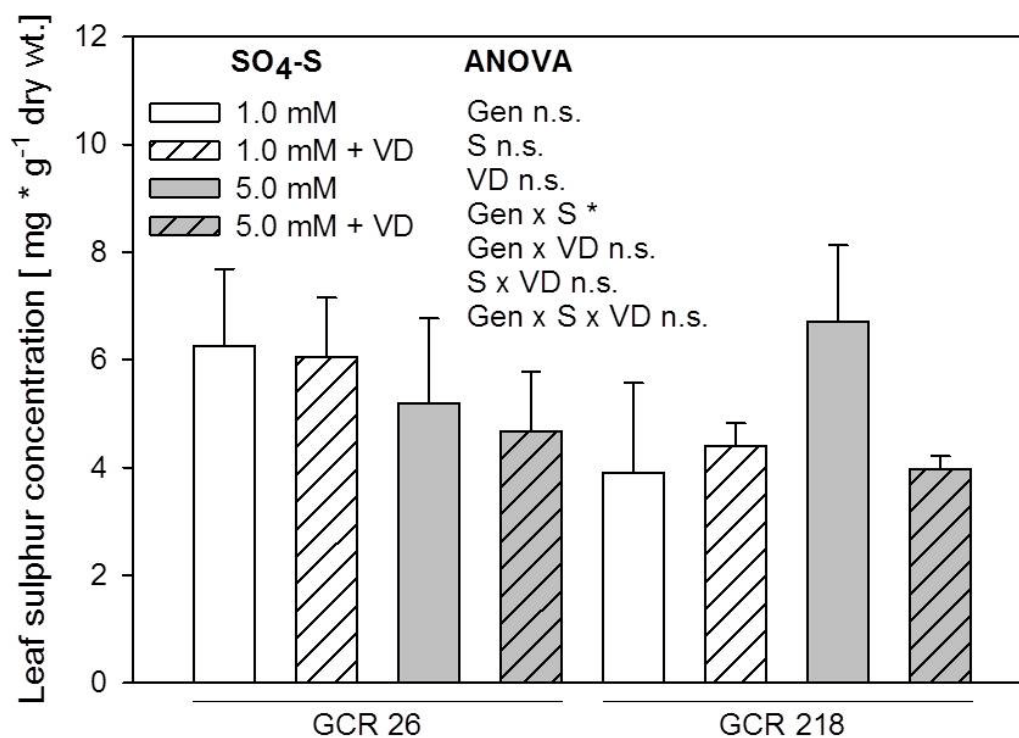


Figure S2 Effect of S supply on S concentrations in leaves of *V. dahliae*-infected tomato genotypes. (After 3 weeks of pre-culture at 5 mM or 1 mM SO₄-S plants were root inoculated and harvested 7 dpi. Data represent means \pm SD $n = 3$. Results of the analysis of variance are given according to their level of significance as *, **, ***, for $P \leq 0.05$, 0.01, 0.001, respectively, n.s. non-significant.)

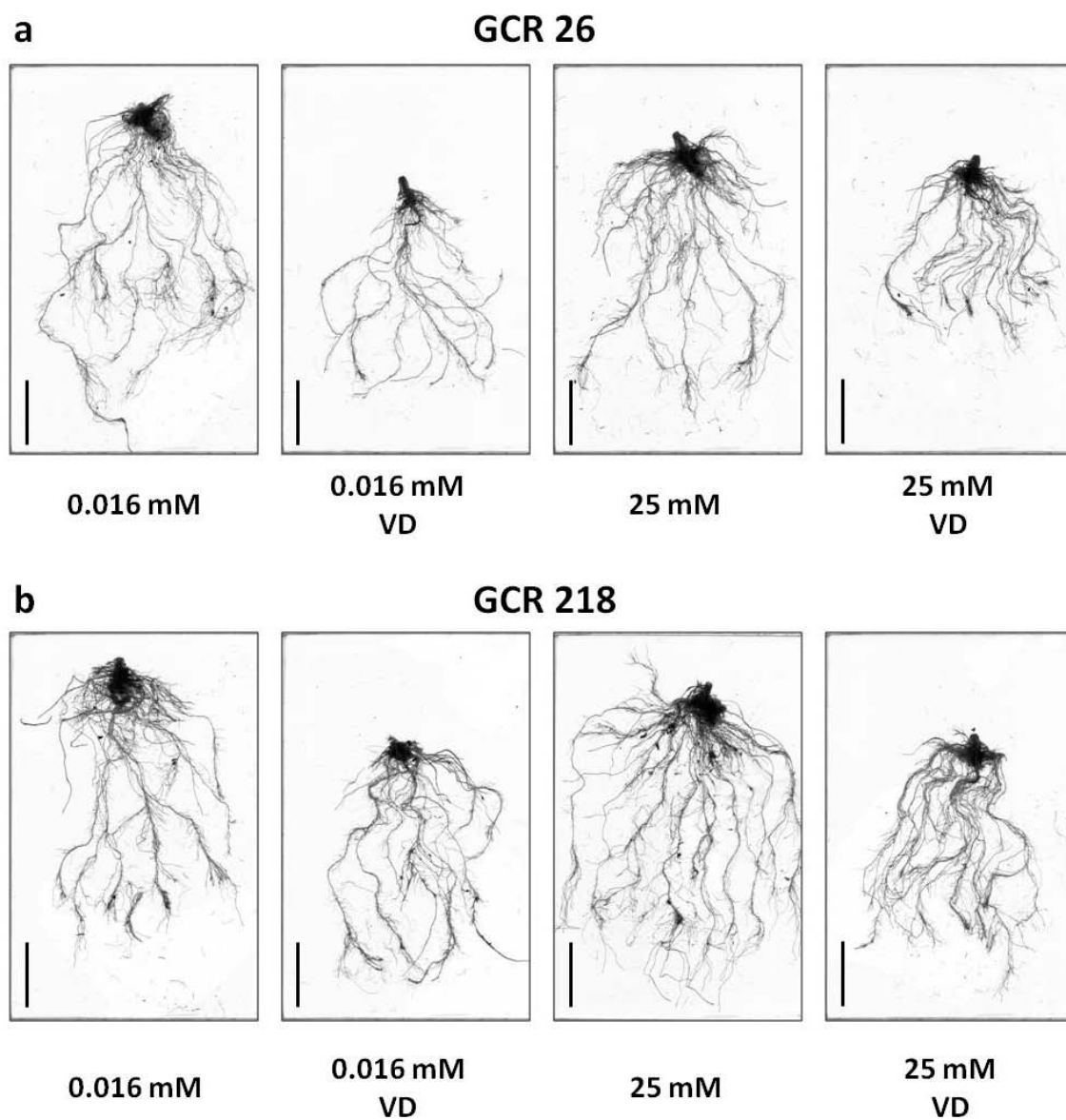


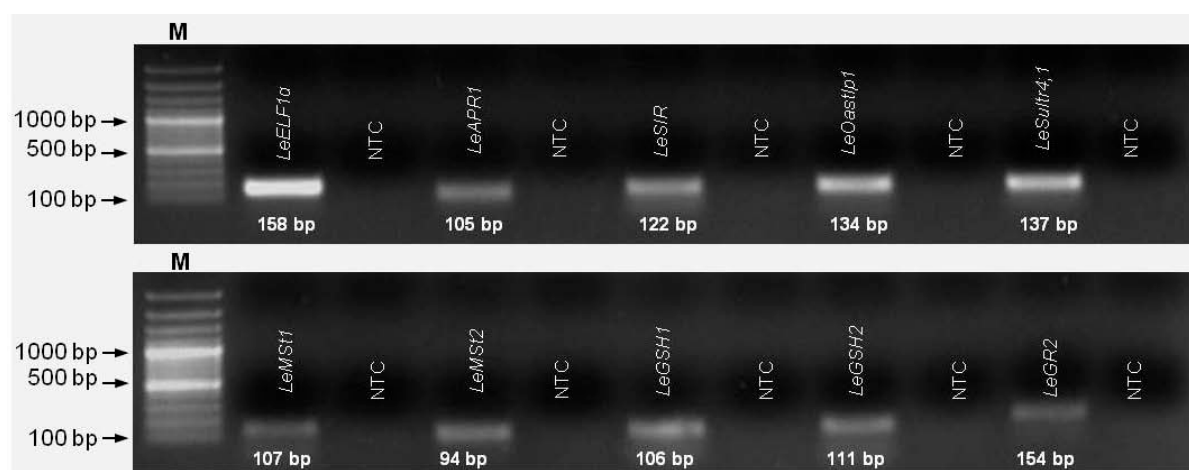
Figure S3 Total root systems of **a** the sensitive tomato genotype GCR 26 and **b** the resistant tomato genotype GCR 218. Root systems were washed out of substrate and total root length was determined with the WinRHIZO Software (Regent Instruments Inc., Canada). Bar represents 5 cm.

Supplementary Material for Chapter II**Spatial expression analysis of sulfur metabolism-related genes in hypocotyl tissues of tomato genotypes differing in *Verticillium dahliae* resistance****Table S1** Blastn derived nucleotide sequence alignment parameters of nine selected S assimilation-related candidate genes.

Gene Name	Gene Locus (<i>A. thaliana</i>)	Accession (<i>S. lycopersicum</i>)	Query Coverage [%]	E-Value	Maximum Identity [%]
<i>LeSultr4;1</i>	At5g13550 / NM_121358	AK320538	78	0.0	73
<i>LeAPR</i>	At4g04610 / NM_116699	AK320536	62	0.0	74
<i>LeSiR</i>	At5g04590 / NM_120541	DB698163	66	$2 \cdot 10^{-80}$	72
<i>LeOastlp1</i>	At2g43750 / NM_129937	BT014392	62	0.0	75
<i>LeGR2</i>	At3g54660 / NM_115323	NM_001247314	66	0.0	76
<i>LeGSH1</i>	At4g23100 / NM_118439	AF017983	64	0.0	77
<i>LeGSH2</i>	At5g27380 / NM_122620	AF017984	64	0.0	71
<i>LeMSt1</i>	At1g79230 / NM_106574	FJ711706	57	0.0	78
<i>LeMSt2</i>	At1g16460 / NM_101511	FJ711707	59	$6 \cdot 10^{-160}$	75

Table S2 Primer sequences and PCR parameters of nine *S* assimilation-related genes of interest and the selected internal reference gene.

Gene Name	Accession (<i>S. lycopersicum</i>)	Forward Primer (5'→3')	Reverse Primer (5'→3')	Efficiency (%)	Amplicon (bp)
<i>LeElf1a</i> ^a	X14449	GGAACCTTGAGA AGGAGCCTAAG	CAACACCAACAGC AACAGTCT	102.5	158
<i>LeSultr4;1</i>	AK320538	TAGCCATTTCCTAATC CCAAC	TAACCGCTGAACA TGCTGAA	93.3	137
<i>LeAPR</i>	AY568717	GAACCCGGAGACAT ACCAATTA	GTCCTAACCAACG CCTGAACT	101.1	105
<i>LeSiR</i>	DB698163	GGACTACTCCGTTTG ACAACA	GTCACCACATGCA CCAAGAG	100.5	122
<i>LeOast1p1</i>	BT014392	GCAGTATCTGTGCC AACGAA	GCAATGTTTGCAAC ACAACC	99.8	134
<i>LeGR2</i>	AF017983	AGGCAGGTTCTTCA CATTGC	CAAAGCATATCTCC CGCATT	99.0	108
<i>LeGSH1</i>	AF017984	ATTTTTGGAACCCC ATCTCC	GGTTTCGCAGAATC TTCCAG	98.5	111
<i>LeGSH2</i>	EU285581	TGAGGAGAGTTGTG GTTTTGG	CCGCCCTTCTATCA GAGTGA	100.7	154
<i>LeMSt1</i>	FJ711706	AAACATCAGAGACC CCGACT	TGCAAGCGACCTG ATACTCC	101.7	107
<i>LeMSt2</i>	FJ711707	AAACATCAGAGACC CCGACT	GGAGTATCAGGTC GCTTGCA	98.6	94

^a Løvdaal and Lillo (2009)**Figure S1** Gelelectrophoretic separation of PCR products amplified with selected primer pairs for genes related to the plant *S* metabolism and the endogenous reference gene. In a conventional PCR 50 ng of tomato cDNA were used to check the primer quality parameters (M: Molecular Marker, NTC: no-template control).

Supplementary Material for Chapter IV**Construction of binary T-DNA vector systems for the molecular characterization of sulfur-enhanced *Verticillium dahliae* plant defence mechanisms****Table S1** Oligonucleotides for the amplification of candidate gene CDS regions

Primer	Sequence [5' – 3']	Length [bp]	GC content [%]	TM [°C]
cLeSultr4,1 +	GCAGTTTATAGTTTTCCGCCAAT	24	37.5	61.7
cLeSultr4,1 -	ATCAACAATATGCTTTTCTTTTATTCC	28	25.0	60.3
cLeGSH1 +	AGATTCTTTTTCATTCAATCTGCT	24	29.2	57.7
cLeGSH1 -	GGTCAGCCAATAGATTCATT	21	38.1	55.8
cDsRed +	ATGGTGCGCTCCTCCAAG	18	61.1	62.4
cDsRed -	CTAAGATCTGAGCAGGAACAGG	22	50.0	58.2

Table S2 Oligonucleotides for the amplification of modified candidate gene CDS regions

Primer	Sequence [5' – 3']	Length [bp]	GC content [%]	TM [°C]
cLeSultr4,1 pER8 +	CCGGGGCCCGCAGTTTATAGTTTTTC CGCCAAT	33	54.5	67.7
cLeSultr4,1 pER8 -	CCTTAATTAATCAACAATATGCTTT TCTTTTATTCC	38	23.7	55.4
cLeGSH1 pER8 +	CCGCTCGAGAGATTCTTTTTCATTCA ATCTGCT	33	42.4	61.6
cLeGSH1 pER8 -	CCTTAATTAAGGTCAGCCAATAGATT CATT	31	32.3	55.7
cDsRed pER8 +	CCGCTCGAGATGGTGCGCTCCTCCAA G	27	66.7	67.8
cDsRed pER8 -	CCTTAATTAATAAGATCTGAGCAGG AACAGG	32	40.6	58.2
cLeSultr4,1 p9 +	CCGGGATCCGCAGTTTATAGTTTTTC CGCCAAT	33	48.5	64.6
cLeSultr4,1 p9 -	CCCCCGGGATCAACAATATGCTTTTC TTTTATTCC	36	41.7	62.0
cLeGSH1p9 +	CCGCCCGGGAGATTCTTTTTCATTCA ATCTGCT	33	48.5	64.6
cLeGSH1 p9-	CCGAATCCGGTCAGCCAATAGATTCA TTT	29	44.8	60.5
cDsRed p9 +	CCGGGATCCATGGTGCGCTCCTCCAA G	27	66.7	68.1
cDsRed p9-	CCCCCGGGCTAAGATCTGAGCAGGA ACAGG	30	63.3	67.7

Table S3 Oligonucleotides for a control of transgene integration into binary pER8 T-DNA vector

Primer	Sequence [5' – 3']	Length [bp]	GC content [%]	TM [°C]
pER8 35SA +	ATCTTCGCAAGACCCTTCCT	20	50	60.2
LeSultr4;1 A-	GGTGATTGGCGGAAAAACTA	20	45	59.9
LeGSH1 A-	AGGATTTTGGTGTGCTGAGG	20	50	60.1
LexA Op +	ATCATCCCCTCGACGTA CTG	20	55	60.0
LexA Op -	CCATATCTAATCTTACCTCGACTGC	25	44	59.6
Spec +	CGGGCACGAACCCAGTG	17	70.6	64.9
Spec -	CCAGGGGAAGCCGAAGTT	18	61.1	62.5

Table S4 Oligonucleotides for a control of transgene integration into binary p9 T-DNA vector

Primer	Sequence [5' – 3']	Length [bp]	GC content [%]	TM [°C]
LeSultr4;1 qRT +	TAGCCATTTCCAATCCCAAC	20	45	59.8
LeSultr4;1 qRT -	TAACCGCTGAACATGCTGAA	20	45	60.4
LeGSH1 qRT +	AGGCAGGTTCTTCACATTGC	20	50	60.3
LeGSH1 qRT -	CAAAGCATATCTCCCGCATT	20	45	60.1
Spec +	CGGGCACGAACCCAGTG	17	70.6	64.9
Spec -	CCAGGGGAAGCCGAAGTT	18	61.1	62.5

Table S5 Oligonucleotides for the transgene copy number estimation and expression analysis in the binary pER8 T-DNA vector

Primer	Sequence [5' – 3']	Length [bp]	GC content [%]	TM [°C]
LeSultr4;1 qRT +	TAGCCATTTCCAATCCCAAC	20	45	59.8
LeSultr4;1 qRT -	TAACCGCTGAACATGCTGAA	20	45	60.4
TDP	CTAGCTAAAGCTGGTGTGGTTGACCTGA	39	50	68.4
LeElf1a +	GGAACCTTGAGAAGGAGCCTAAG	22	50	58.7
LeElf1a -	CAACACCAACAGCAACAGTCT	21	47.6	58.8

Table S6 List of restriction enzymes

Restriction enzyme	Recognition side (5' - 3')	Stock concentration	Manufacturer
Apal	GGGCC C	(10 U / μ L)	Fermentas, Germany
BamHI	G GATCC	(10 U / μ L)	Fermentas, Germany
EcoRI	G AATTC	(10 U / μ L)	Fermentas, Germany
PacI	TTAAT TAA	(10 U / μ L)	Fermentas, Germany
XhoI	C TCGAG	(10 U / μ L)	Fermentas, Germany
XmaI	C CCGGG	(10 U / μ L)	Fermentas, Germany

Table S7 List of antibiotics

Antibiotic	Stock concentration [mg / mL]	Bacteria selection [μ g / mL]	Plant selection (μ g / mL)	Company
Amp	50 in dH ₂ O	50	-	Applichem, Germany
Carb	250 in Ethanol:dH ₂ O (1:1)	50	-	Duchefa, Netherlands
Hyg B	250 in dH ₂ O	-	25	Duchefa, Netherlands
Kan	50 in dH ₂ O	50	-	Applichem, Germany
Rif	20 in DMSO	5	-	Carl Roth GmbH, Germany
Spec	100 in dH ₂ O	50	-	Applichem, Germany
Tet	50 in dH ₂ O	50	-	Applichem, Germany

Table S8 List of phytohormones

Phytohormone	Stock concentration [mg / mL]	Company
BAP	1	Sigma Aldrich, USA
IAA	0.2	Sigma Aldrich, USA
2,4-D	2	Sigma Aldrich, USA
NAA	0.1	Sigma Aldrich, USA
Zea	0.5	Sigma Aldrich, USA

Table S9 50 x TAE buffer (1 L), autoclave at 121 °C for 20 min, storage at RT

Chemical	Use concentration	Stock concentration	Company
Tris Base	242 g	-	Applichem, Germany
Glacial Acetic Acid	57.1 mL	-	Sigma Aldrich, USA
EDTA	50 mM	0.5 M, pH 8.0	Applichem, Germany

Table S10 1 x liquid / solid lysogeny broth (LB) Lennox medium (1 L), autoclave at 121°C for 20 min, storage at RT

Chemical	Use concentration	Stock concentration	Company
Yeast Extract	5 g	-	Carl Roth GmbH, Germany
Trypton form Casein	10 g	-	Carl Roth GmbH, Germany
NaCl	5 g	-	Carl Roth GmbH, Germany
(Agar-Agar Kobel)	15 g	-	Carl Roth GmbH, Germany
adjust pH to 7.0 with 1M NaOH			

Table S11 1 x liquid / solid YEP (1 L), autoclave at 121 °C for 20 min, storage at RT

Chemical	Use concentration	Stock concentration	Company
Yeast Extract	10 g	-	Carl Roth GmbH, Germany
Peptone from Casein	10 g	-	Carl Roth GmbH, Germany
NaCl	5 g	-	Carl Roth GmbH, Germany
(Agar-Agar Kobel)	15 g	-	Carl Roth GmbH, Germany
adjust pH to 7.0 with 1M NaOH			

Table S12 1 x SOC Medium (1 L), filtersterilisation, storage at -20 °C

Chemical	Use concentration	Stock concentration	Company
SOB	26.64 g	-	Carl Roth GmbH, Germany
α -D-Glucose	3.6 g	-	Carl Roth GmbH, Germany

Table S13 1 x TB buffer (1 L), filtersterilisation, storage at 4°C

Chemical	Use concentration	Stock concentration	Company
KCl	250 mM	-	Carl Roth GmbH, Germany
CaCl ₂	15 mM	-	Carl Roth GmbH, Germany
PIPES	10 mM	0.5 M	Applichem, Germany
pH adjusted to 6.7 with 1M KOH			
MnCl ₂	55 mM	-	Sigma Aldrich, USA

Table S14 1 x Infiltration medium (50 mL), filtersterilisation, storage at 4°C

Chemical	Use concentration	Stock concentration	Company
α-D-Glucose	250 mg	-	Carl Roth GmbH, Germany
MES	10 mM	500 mM	Carl Roth GmbH, Germany
Acetosyringone	20 mM	1M	Carl Roth GmbH, Germany

Table S15 1 x GUS staining solution (250 mL), storage at -20 °C

Chemical	Use concentration	Stock concentration	Company
x-Gluc	1 mM	10 mM in DMSO	Applichem, Germany
NaPO ₄	50 mM	0.5 M Na ₂ HPO ₄ , pH 7.0 0.5 M NaH ₂ PO ₄ , pH 7.0	Carl Roth GmbH, Germany
Triton-x-100	0.5 %	-	Sigma Aldrich, USA
K ₃ [Fe(CN) ₆]	0.5 mM	-	Sigma Aldrich, USA
K ₄ [Fe(CN) ₆] · 3H ₂ O	0.5 mM	-	Sigma Aldrich, USA

Table S16 1 x solid / liquid MS medium (1 L), autoclave at 121 °C for 20 min, storage at RT

Chemical	Use concentration	Stock concentration	Company
MS salts	4.4 g	-	Duchefa, Netherlands
MS vitamins	103 mg / L	103 mg / mL	Duchefa, Netherlands
MES	0.25 g	-	Carl Roth GmbH, Germany
Sucrose	3 % (w / v)	30 % (w / v)	Carl Roth GmbH, Germany
(Phytoagar)	7.0 g	-	Duchefa, Netherlands
pH adjusted to 5.7 with 1M NaOH			

Table S17 1 x MS-SSN medium (1 L), autoclave at 121 °C for 20 min, storage at RT

Chemical	Use concentration	Stock concentration	Company
MS salts	4.3 g	-	Duchefa, Netherlands
MS vitamins	103 mg / L	103 mg / mL	Duchefa, Netherlands
Sucrose	3 % (w / v)	30 % (w / v)	Carl Roth GmbH, Germany
(Phytoagar)	8.0 g	-	Duchefa, Netherlands
pH adjusted to 5.8 with 1M NaOH			
NAA	0.1 mg / L	0.1 mg / mL	Sigma Aldrich, USA
BAP	1.0 mg / L	1.0 mg / mL	Sigma Aldrich, USA

Table S18 1 x MS-S medium (1 L), autoclave at 121 °C for 20 min, storage at RT

Chemical	Use concentration	Stock concentration	Company
MS salts	4.4 g	-	Duchefa, Netherlands
MS vitamins	103 mg / L	103 mg / mL	Duchefa, Netherlands
MES	0.25 g	-	Carl Roth GmbH, Germany
Sucrose	3 % (w / v)	30 % (w / v)	Carl Roth GmbH, Germany
(Phytoagar)	7.0 g	-	Duchefa, Netherlands
pH adjusted to 5.7 with 1M NaOH			
Zea	0.5 - 4 mg / L	0.5 mg / mL	Sigma Aldrich, USA
BAP / IAA	1 - 2 mg / L; 0.2 mg / L	1.0 / 0.2 mg / mL	Sigma Aldrich, USA
2,4-D	2.0 mg / L	2.0 mg / mL	Sigma Aldrich, USA

pGEM-T-Easy:DsRed

ANGGCGATTGGGCCGACGTCGCATGCTCCCGGCCGCCATGGCGGCCGCGGGAATTCGATTCTAAGA
 TCTGAGCAGGAACAGGTGGTGGCGGCCCTCGGTGCGCTCGTACTGCTCCACGATGGTGTAGTCCTC
 GTTGTGGGAGGTGATGTCCAGCTTGGAGTCCACGTAGTAGTAGCCGGGCAGCTGCACGGGCTTCTT
 GGCCATGTAGATGGACTTGAACCTCACCAGGTAGTGGCCGCCGCTCCTCAGCTTCAGGGCCTTGTG
 GATCTCGCCCTCAGCACGCCGTCGCGGGGGTACAGGCGCTCGGTGGAGGCCTCCAGCCCATGGT
 CTTCTTCTGCATTACGGGGCCGTCGGAGGGGAAGTTCACGCCGATGAACTTCACCTTGTAGATGAA
 GCAGCCGTCCTGCAGGGAGGAGTCTGGGTCACGGTCACCACGCCGCCGCTCCTCGAAGTTCATCAC
 GCGTCCCACCTTGAAGCCCTCGGGGAAGGACAGCTTCTTGTAGTCGGGGATGTCGGCGGGGTGCTT
 CACGTACACCTTGGAGCCGTAAGTGGAACTGGGGGGACAGGATGTCCAGGCCGAAGGGCAGGGGGC
 CGCCCTTGGTCACCTTCAGCTTCACGGTGTGTGGCCCTCGTAGGGGCGGCCCTCGCCCTCGCCCTC
 GATCTCGAACTCGTGGCCGTTACGGTGCCCTCCATGCGCACCTTGAAGCGCATGAACTCCTTGAT
 GACGTTCTTGGAGGAGCGCACCATAACTACTAGTGAATTCGCGGCCCGCTGCAGGTCGACCATATG
 GGAGAGCTCCCAACGCGTTGGATGCATAGCTTGTAGTATTCTATAGTGTACCTAAATAGCTTGGCG
 TAATCATGGTCATAGCTGTTTCTGTGTGAAATTGTTATCCGCTCACAATTCCACACAACATACGAG
 CCGGAAGCATAAAGTGTAAGCCTGGGGTGCCTAATGAGTGAGCTAACTCACATTAATTGCGTTGC
 GCTCACTGCCCGCTTCCAGTCGGGAAACCTGTCGTGCCAGCTGCATTAATGAATCGGCCAACGCN
 CGGGGAAGAGGCGGTT

pGEM-T-Easy:LeSultr4;1

AANNTGGGCCCGACGTCGCATGCTCCCGGCCGCCATGGCGGCCGCGGGAATTCGATTGCAGTTTAT
 AGTTTTTCCGCCAATCACCATTTTTCTTCTTCTGACACTTCCCGGTGGGCGCCACCTTACGCCGCC
 GTTCGCCGCCGTAATCCGCCATGGACAGAACCTATGCTTCTCCGAGCTCCCAAAACCTTACGGCTAT
 AACAACTAATTCTGTAGATTCGCTTCATCTTCTTCTCCTTCTCCAACCTCCATGTGCGACCGGCGGTA
 GCCGTGCCGTGAAAATCATCCCGCTGGAGCATCCGTCTGCTACGGCATCGTCTACGTCGGCGACGG
 CGTCTGCTTCGGCATCTGTGATCGAAATGGAGGGCGAGGATGAAGGGGATGACGTGGAAGGAA
 TGGATTGAGCTATTTTTCTTGTATCGATGGATGCGAACGTATAAAGTGCGTGAGTACTTGCAAT
 CTGATCTCATGGCTGGTATCACAGTCGGTATCATGCTTGTTCCTCAGATTCTGGTTTCATCCCTATAT
 TTGTCTACACCATATTTGGGTCATCTCGTCAGCTGGCAATTGGTCCAGTTGCATTGACGTCCCTTCT
 AGTCTCAAATGTCTTGAGCAGCATAGTTGAACCATCAGACAAGTTATACACAGAGCTCGCTATACT
 ATTAGCACTTATGNTTGGCATCTTGGAAATGCATAAT

pGEM-T-Easy:LeGSH1

TANGCGATTGGGCCGACGTCGCAGGCTCCCGGCCGCCATGGCGGCCGCGGGAATTCGATTGTCAG
 CCAATAGATTCATTTATTACTTTAGCATTGCTATGTTACTTTTCTGGGGAAAATGTATACAAATGCT
 ATCTGGAACCAGATTGATCACATCCCAAGGGGAGAGAGCTACATATGACGTTTTTCGAGCCATAGAT
 ACATGTAACATATCTTAATCTAGCTAGCTAGATTATTTGTCTAACGATGGAAAAATCGGCTGATAT
 AACTCTCAATGAAATTGAGAAATCATTTACAACACAGGAAAAAGACAGAATTGAAATTGCACTCTC
 AAACAACCTCAGTAGAGAAGCTCCTCAAAGATAGGATCCACACTTTGTCCCACTTCCCATGGTAC
 AATTCCAGTAGCTTCTCAGCTGGTGTACACCTGTTTTAACAACTCGGCTACTTCGTTTCAGAAATC
 CTGTTTCTTAAAGCCTTCTTTTCCAAGCCTTCTTTGCCAACCTTGACAACATCTTGAGCAACATGC
 ATAAGCAATCCATCTCGAAATGGTGTCTTTCAGACCACTTTTTGGCACCTTATTCCTTAACATGTCTC
 TTTCTTCTGAGTCCAATCAAATGTCATGTCCAAAACGCTTTGCAAAGACCCCTCATCGTAGAGTAT
 ACCCACCCAGAATGCAGGCAATGCGCATAACCGTCTCCAAGGCCCTCCATCAGCACCTCTCATTTTC
 CAGATATCTTTGAGTCTGACCTCAGGAAATATTGTTGTGAGATGATTCTCCCAATCATTAAGAGTA
 GGGTATTCGCCGGAANGGGCGGAAGTTTTCCATTCATGAAGTCCCGGAAAGACAATCCAGTACA
 ATCAACATACTTCTTCTCCGATAGACAAAATACATTGGGACATCAAGTGCATAATCTACATATTGC
 TCAAACCCAAAAGAGTCATCAAAGACGAAAGGAAGCATCCCAGCGCGGTTATTATCTGTATCGGTC
 CAAATGTGGCTTCTTGTGCTGAGATAACCATTAGGTTTTCTTTCAGTGAAAGGTGAATTTGCAAATA
 NAGCTGTAACAATAGGCTGCAAGGCAAGACCA

Figure S1 Results from the custom sequencing of the *DsRed*, *LeSultr4;1* and *LeGSH1* CDS regions. All CDS regions were amplified in a proof-read PCR, ligated into the pGEM-T-Easy cloning vector and sequenced with the pUC / M13 forward primer (Vector sequences are depicted in grey).

References

- Agrios, G. N. (2005). *Plant Pathology*. 5th edition, Amsterdam, Netherlands, Elsevier Academic Press.
- Altschul, S. F., Gish, W., Miller, W., Myers, E. W., and Lipman, D. J. (1990). Basic local alignment search tool. *Journal of Molecular Biology* 215, 403 - 410.
- Aoki, K., Yano, K., Suzuki, A., Kawamura, S., Sakurai, N., Suda, K., Kurabayashi, A., Suzuki, T., Tsugane, T., Watanabe, M., Ooga, K., Torii, M., Narita, T., Shin-I, T., Kohara, Y., Yamamoto, N., Takahashi, H., Watanabe, Y., Egusa, M., Kodama, M., Ichinose, Y., Kikuchi, M., Fukushima, S., Okabe, A., Arie, T., Sato, Y., Yazawa, K., Satoh, S., Omura, T., Ezura, H., and Shibata, D. (2010). Large-scale analysis of full-length cDNAs from the tomato (*Solanum lycopersicum*) cultivar MicroTom, a reference system for the *Solanaceae* genomics. *BiomedCentral Genomics*, 11, 210.
- Arie, T., Takahashi, H., Kodama, M., and Teraoka, T. (2007). Tomato as a model plant for plant-pathogen interactions. *Plant Biotechnology*, 24, 135-147.
- Bartels, A., Mock, H., and Papenbrock, J. (2007). Differential expression of *Arabidopsis* sulfurtransferases under various growth conditions. *Plant Physiology and Biochemistry* 45, 178 – 187.
- Baxter, C. J., Sabar, M., Quick, W. P., and Sweetlove, L. J. (2005). Comparison of changes in fruit gene expression in tomato introgression lines provides evidence of genome-wide transcriptional changes and reveals links to mapped QTLs and described traits. *Journal of Experimental Botany*, 56, 1591 – 1604.
- Berger, S., Papadopoulos, M., Schreiber, U., Kaiser, W. and Roitsch, T. (2004). Complex regulation of gene expression, photosynthesis and sugar levels by pathogen infection in tomato. *Physiologia Plantarum*, 122, 419 - 428.
- Berger, S., Sinha, A. K., and Roitsch, T. (2007). Plant physiology meets phytopathology: plant primary metabolism and plant-pathogen interactions. *Journal of Experimental Botany*, 58, 4019 - 4026.
- Beffa, T. (1993). Inhibitory action of elemental sulphur (S⁰) on fungal spores. *Canadian Journal of Microbiology*, 39, 731 - 735.
- Benfey, P. N. and Chua, N. H. (1990). The Cauliflower Mosaic Virus 35S Promoter: Combinatorial regulation of transcription in plants. *Science*, 250, 959 - 966.
- Bhat, R. G. and Subbarao, K. V. (1999). Host range specificity in *Verticillium dahliae*. *Phytopathology*, 89, 1218 – 1225.

- Bletsos, F., Thanassouloupoulos, C., and Roupakias, D. (2003). Effect of grafting on growth, yield, and *Verticillium* wilt of eggplant. *HortScience*, 38, 183 - 186.
- Bloem, E., Haneklaus, S., and Schnug, E. (2005). Significance of sulfur compounds in the protection of plants against pests and diseases. *Journal of Plant Nutrition*, 28, 763–784.
- Bloem, E., Haneklaus, S., and Schnug, E. (2010). Influence of fertilizer practices on S-containing metabolites in garlic (*Allium sativum* L.) under field conditions. *Journal of Agriculture and Food Chemistry*, 58, 10690 - 10696.
- Bowden, R. L., Rouse, D. I., and Sharkey, T. D. (1990). Mechanism of photosynthesis decrease by *Verticillium dahliae* in potato. *Plant Physiology*, 94, 1048 – 1055.
- Buchner, P., Takahashi, H., and Hawkesford, M. J. (2004). Plant sulphate transporters: co-ordination of uptake, intracellular and long-distance transport. *Journal of Experimental Botany*, 55, 1765 - 1773.
- Burow, M., Wittstock, U., and Gershenzon, J. (2008). Sulfur-containing secondary metabolites and their role in plant defence. *Advances in Photosynthesis and Respiration*, 27, 201 - 222.
- Cakmak, I., Hengeler, C. and Marschner, H. (1994). Changes in phloem export of sucrose in leaves in response to phosphorus, potassium and magnesium deficiency in bean plants. *Journal of Experimental Botany*, 45, 1251 - 1257.
- Chaves, M. M., Flexas, J. and Pinheiro, C. (2009). Photosynthesis under drought and salt stress: regulation mechanisms from whole plant to cell. *Annals of Botany*, 103, 551 - 560.
- Chai, Y., Zhao, L., Liao, Z., Sun, X., Zuo, K., Zhang, L., Wang, S., Tang, K. (2003). Molecular cloning of a potential *Verticillium dahliae* resistance gene *SIVe1* with multi-site polyadenylation from *Solanum lycopersicoides*. *DNA Sequence*, 14, 375 – 384.
- Chen, P., Lee, B., and Robb, J. (2004). Tolerance to a non-host isolate of *Verticillium dahliae* in tomato. *Physiological and Molecular Plant Pathology*, 64, 283 - 291.
- Clay, N. K., Adewale, M. A., Denoux, C., Jander, G., and Ausubel, F. M. (2009). Glucosinolate metabolites required for an *Arabidopsis* innate immune response. *Science*, 323, 95 – 101.
- Cooper, R. M., Resende, M. L. V., Flood, J., Rowan, M. G., Beale, M. H., and Potter, U. (1996). Detection and cellular localization of elemental sulphur in disease resistant genotypes of *Theobroma cacao*. *Nature*, 379, 159 – 162.
- Cooper, R. M. and Williams, J. (2004). Elemental sulphur as an induced antifungal substance in plant defence. *Journal of Experimental Botany*, 55, 1947 - 1953.

- Creissen, G., Firmin, J., and Fryer, M. (1999) Elevated glutathione biosynthetic capacity in the chloroplasts of transgenic tobacco paradoxically causes increased oxidative stress. *The Plant Cell*, 11, 1277 – 1291.
- Dan, Y., Yan, H., Munyikwa, T., Dong, J., Zhang, Y., and Armstrong, C. L. (2006). MicroTom - a high-throughput model transformation system for functional genomics. *Plant Cell Reports*, 25, 432 - 441.
- Davidian, J. C., and Kopriva, S. (2010). Regulation of sulfate uptake and assimilation - the same or not the same? *Molecular Plant*, 3, 314 - 325.
- Deeken, R., Ache, P., Kajahn, I., Klinkenberg, J., Bringmann, G., and Hedrich, R. (2008). Identification of *Arabidopsis thaliana* phloem RNAs provides a search criterion for phloem-based transcripts hidden in complex datasets of microarray experiments. *Plant Journal*, 55, 746 - 759.
- Diwan, N., Fluhr, R., Eshed, Y., Zamir, D. and Tanksley, S. D. (1999). Mapping of *Ve* in tomato: a gene conferring resistance to the broad-spectrum pathogen, *Verticillium dahliae* race 1. *Theoretical and Applied Genetics*, 98, 315 - 319.
- Dixon, R. A. (2001). Natural products and plant disease resistance. *Nature*, 411, 843 - 847.
- Dobinson, K. F., Lecomte, N., and Lazarovits, G. (1997). Production of an extracellular trypsin-like protease by the fungal plant pathogen *Verticillium dahliae*. *Canadian Journal of Microbiology*, 43, 227 – 233.
- Dobinson, K. F., Grant, S. J., Kang, S. (2004). Cloning and targeted disruption, via *Agrobacterium tumefaciens*-mediated transformation, of a trypsin protease gene from the vascular wilt fungus *Verticillium dahliae*. *Current Genetics*, 45, 104 – 110.
- Dreywood, R. (1946). Qualitative test for carbohydrate material. *Industrial and Engineering Chemistry, Analytical Edition*, 18, 499.
- Droux, M. (2004). S assimilation and the role of S in plant metabolism: a survey. *Photosynthesis Research*, 79, 331 - 348.
- Dubuis, P. H., Marazzi, C., Städler, E., and Mauch, F. (2005). Sulphur deficiency causes a reduction in antimicrobial potential and leads to increased disease susceptibility of oilseed rape. *Journal of Phytopathology*, 153, 27 - 36.
- Duressa, D., Rauscher, G., Koike, S. T., Mou, B., Hayes, R. J., Maruthachalam, K., Subbarao, K. V., and Klosterman, S. (2010). A Real-Time PCR assay for detection and quantification of *Verticillium dahliae* in spinach seed. *Phytopathology*, 102, 443 – 451.
- Eshed, Y. and Zamir, D. (1994) Introgressions from *Lycopersicon pennellii* can improve the soluble solids yield of tomato hybrids. *Theoretical and Applied Genetics*, 88, 891 - 897.

- Eshed, Y. and Zamir, D. (1995). An Introgression Line Population of *Lycopersicon pennellii* in the cultivated tomato enables the identification and fine mapping of yield-associated QTL. *Genetics*, 141, 1147 – 1162.
- Fahleson, J., Hu, Q., and Dixelius, C. (2004). Phylogenetic analysis of *Verticillium* species based on nuclear and mitochondrial sequences. *Archives of Microbiology*, 181, 435 - 442.
- Falk, K. L., Tokuhisa, J. G., and Gershenzon, J. (2007). The effect of sulfur nutrition on plant glucosinolate content: physiology and molecular mechanisms. *Plant Biology*, 5, 573 - 581.
- FAOSTAT (October,2012); <http://faostat.fao.org/>
- Fei, J., Chai, Y., Wang, J., Lin, J., Sun, X., Sun, C., Zuo, K., and Tang, K. (2004). cDNA cloning and characterization of the Ve homologue gene *StVe* from *Solanum torvum* Swartz. *Mitochondrial-DNA Sequence*, 15, 88 – 95.
- Fei, Z., Joung, J. G., Tang, X., Zheng, Y., Huang, M., Lee, J. M., McQuinn, R., Tieman, D. M., Alba, R., Klee, H. J., and Giovannoni, J. J. (2011). Tomato Functional Genomics Database: a comprehensive resource and analysis package for tomato functional genomics. *Nucleic Acids Research*, 39, 1156 - 1163.
- Foyer, C. H. and Noctor, G. (2011). Ascorbate and glutathione: the heart of the redox hub. *Plant Physiology*, 155, 2 - 18.
- Fradin, E. F. and Thomma, B. P. H. J. (2006). Physiology and molecular aspects of *Verticillium* wilt diseases caused by *V. dahliae* and *V. albo-atrum*. *Molecular Plant Pathology*, 7, 71 - 86.
- Fradin, E. F., Zhang, Z., Juarez Ayala, J. C., Castroverde, C. D., Nazar, R. N., Robb, J., Liu, C. M., and Thomma, B. P. H. J. (2009). Genetic dissection of *Verticillium* wilt resistance mediated by tomato *Ve1*. *Plant Physiology*, 150, 320 - 332.
- Fradin, E. F., Abd-El-Haliem, A., Masini, L., van den Berg, G. C., Joosten, M. H., and Thomma, B. P. H. J. (2010). Interfamily transfer of tomato *Ve1* mediates *Verticillium* resistance in *Arabidopsis*. *Plant Physiology*, 156, 2255 - 2265.
- Feldman-Salit, A., Wirtz, M., Hell, R., and Wade, R. C. (2009). A mechanistic model of the cysteine synthase complex. *Journal of Molecular Biology*, 386, 37 - 59.
- Finkers, R., van den Berg, P., van Berloo, R., ten Have, A., van Heusden, A. W., van Kann, J. A. and Lindhout, P. (2007). Three QTLs for *Botrytis cinerea* resistance in tomato. *Theoretical and Applied Genetics*, 114, 585 - 593.

- Fitzell, R., Evans G., and Fahy. E. C. (1980). Studies on the colonization of plant roots by *Verticillium dahliae* Klebahn with use of immunofluorescent staining. Australian Journal of Botany, 28, 357 - 368.
- Flexas, J., Bota, J., Loreto, F., Cornic, G. and Sharkey, T. D. (2004). Diffusive and metabolic limitations to photosynthesis under drought and salinity in C(3) plants. Plant Biology, 6, 269 - 279.
- Fulton, T. M. R., van der Hoeven, R., Eannetta, N. T., and Tansley, S. D. (2002). Identification, analysis, and utilization of conserved ortholog set markers for comparative genomics in higher plants. Plant Cell, 14, 1457 – 1467.
- Gadaleta, A., Giancaspro, A., Cardone, M. F., and Blanco, A. (2011). Real-time PCR for the detection of precise transgene copy number in durum wheat. Cellular and Molecular Biology Letters, 16, 652 - 668.
- Galant, A., Preuss, M. L., Cameron, J. C., and Jez, M. J. (2011). Plant glutathione biosynthesis: diversity in biochemical regulation and reaction products. Frontiers in Plant Science, 2, 1 - 7.
- Gao, N., Shen, W., Cao, Y., Su Y., and Shi W. (2009). Influence of bacterial density during preculture on *Agrobacterium*-mediated transformation of tomato. Plant Cell, Tissue and Organ Culture, 98, 321 - 330.
- Goicoechea, N. (2009). To what extent are soil amendments useful to control *Verticillium* wilt? Pest Management Science, 65, 831 - 839.
- Gomez, S. K. and Harrison, M. J. (2009). Laser microdissection and its application to analyze gene expression in arbuscular mycorrhizal symbiosis. Pest Management Science, 65, 504 - 511.
- Gong, P., Zhang, J., Li, H., Yang, C., Zhang, C., Zhang, X., Khurram, Z., Zhang, Y., Wang, T., Fei, Z., and Ye, Z. (2010). Transcriptional profiles of drought-responsive genes in modulating transcription signal transduction, and biochemical pathways in tomato. Journal of Experimental Botany, 61, 3563 - 3575.
- Guilley, H., Dudley, R. K., Jonard, G., Balázs, E., and Richards, K. E. (1982). Transcription of Cauliflower mosaic virus DNA: detection of promoter sequences, and characterization of transcripts. Cell, 30, 763 - 773.
- Harrison, S. J., Mott, E. K., Parsley, K., Aspinall, S., Gray, J. C., and Cottage, A. (2006). A rapid and robust method of identifying transformed *Arabidopsis thaliana* seedlings following floral dip transformation. Plant Methods, 2, 19.
- Heeg, C., Kruse, C., Jost, R., Gutensohn, M., Ruppert, T., Wirtz, M., and Hell, R. (2008). Analysis of the *Arabidopsis* O-acetylserine(thiol)lyase gene family demonstrates

- compartment-specific differences in the regulation of cysteine synthesis. *The Plant Cell*, 20, 168 - 185.
- Heinz, R., Lee, S. W., Saparno, A., Nazar, R. N., and Robb, J. (1998). Cyclical systemic colonization in *Verticillium*-infected tomato. *Physiological and Molecular Plant Pathology*, 52, 385 - 396.
- Hellens, R., Mullinéaux, P., and Klee, H. (2000). Technical Focus: a guide to *Agrobacterium* binary Ti vectors. *Trends in Plant Science*, 5, 446 - 451.
- Höfgen, R., and Nikiforova, V. (2008). Metabolomics integrated with transcriptomics: assessing systems response to sulfur-deficiency stress. *Physiologia Plantarum*, 132, 190 - 198.
- Höller, K., Király, L., Künstler, A., Müller, M., Gullner, G., Fattinger, M., and Zechmann, B. (2010). Enhanced glutathione metabolism is correlated with sulfur-induced resistance in Tobacco mosaic virus-infected genetically susceptible *Nicotiana tabacum* plants. *Molecular Plant-Microbe Interactions*, 23, 1448 - 1459.
- Howarth, J. R., Fourcroy, P., Davidian, J. C., Smith, F. W., and Hawkesford, M. J. (2003). Cloning of two contrasting high-affinity sulfate transporters from tomato induced by low sulfate and infection by the vascular pathogen *Verticillium dahliae*. *Planta*, 218, 58 - 64.
- Inderbitzin, P., Bostock, R. M., Davis, R. M., Usami, T., Platt, H. W., and Subbarao, K. V. (2011). Phylogenetics and taxonomy of the fungal vascular wilt pathogen *Verticillium*, with the descriptions of five new species. *PLOS One*, 6, e28341.
- Ingham, D. J., Beer, S., Money, S., and Hansen, G. (2001). Quantitative real-time PCR assay for determining transgene copy number in transformed plants. *Biotechniques*, 31, 132 - 140.
- Inoue, H., Nojima, H., and Okayama, H. (1990). High efficiency transformation of *Escherichia coli* with plasmids. *Gene*, 96, 23 - 28.
- Juszczuk, I. M., and Ostaszewska, M. (2011). Respiratory activity, energy and redox status in sulphur-deficient bean plants. *Environmental and Experimental Botany*, 74, 245 - 254.
- Joyard, J., Forest, E., Blée, E., and Douce, R. (1988). Characterization of elemental sulfur in isolated intact spinach chloroplasts. *Plant Physiology*, 88, 961 - 964.
- Kataoka, T., Watanabe-Takahashi, A., Hayashi, N., Ohnishi, M., Mimura, T., Buchner, P., Hawkesford, M. J., Yamaya, T., and Takahashi, H. (2004). Vacuolar sulfate transporters are essential determinants controlling internal distribution of sulfate in *Arabidopsis*. *The Plant Cell*, 16, 2693 - 2704.

- Kawchuk, L. M., Hachey, J., Lynch, D. R., Kulcsar, F., van Rooijen, G., Waterer, D. R., Robertson, A., Kokko, E., Byers, R., Howard, R. J., Fischer, R., and Prüfer, D. (2001). Tomato *Ve* disease resistance genes encode cell surface-like receptors. *Proceedings of the National Academy of Science U S A.*, 98, 6511 - 6515.
- Khan, M. S., Haas, F. H., Samami, A. A., Gholami, A. M., Bauer, A., Fellenberg, K., Reichelt, M., Hänsch, R., Mendel, R. R., Meyer, A. J., Wirtz, M., and Hell, R. (2010). Sulfite reductase defines a newly discovered bottleneck for assimilatory sulfate reduction and is essential for growth and development in *Arabidopsis thaliana*. *The Plant Cell*, 22, 1216 - 1231.
- Klikocka, H., Haneklaus, S., Bloem, E., and Schnug, E. (2005). Influence of S fertilization on infection of potato tubers with *Rhizoctonia solani* and *Streptomyces scabies*. *Journal of Plant Nutrition*, 28, 819 - 833.
- Klosterman, S. J., Atallah, Z. K., Vallad, G. E., and Subbarao, K. V. (2009). Diversity, pathogenicity, and management of *Verticillium* species. *Annual Review of Phytopathology*, 47, 39 - 62.
- Komori, T., Imayama, T., Kato, N., Ishida, Y., Ueki, J., and Komari, T. (2007). Current status of binary vectors and superbinary vectors. *Plant Physiology*, 145, 1155 - 1160.
- Kopriva, S., Mugford, S. G., Matthewman, C., and Koprivova, A. (2009). Plant sulfate assimilation genes: redundancy versus specialization. *Plant Cell Reports*, 28, 1769 - 1780.
- Kopriva S, Mugford SG, Baraniecka P, Lee BR, Matthewman CA, Koprivova A (2012) Control of sulfur partitioning between primary and secondary metabolism in *Arabidopsis*. *Frontiers in Plant Science*. 3:163. doi: 10.3389/fpls.2012.00163
- Krikun, J., and Bernier, C. C. (1990). Morphology of microsclerotia of *Verticillium dahliae* in roots of gramineous plants. *Canadian Journal of Plant Pathology*, 12, 439 - 441.
- Kruse, C., Jost, R., Lipschis, M., Kopp, B., Hartmann, M., and Hell, R. (2007). Sulfur-enhanced defence: effects of sulfur metabolism, nitrogen supply, and pathogen lifestyle. *Plant Biology*, 9, 608 - 619.
- Kruse, C., Haas, F. H., Jost, R., Reiser, B., Reichelt, M., Wirtz, M., Gershenzon, J., Schnug, E., and Hell, R. (2012). Improved sulfur nutrition provides the basis for enhanced production of sulfur-containing defence compounds in *Arabidopsis thaliana* upon inoculation with *Alternaria brassicicola*. *Journal of Plant Physiology*, 169, 740 - 743.
- Labate, J. A., Grandillo, S., Fulton, T., Muñoz, S., Caicedo, A. L., Peralta, I., Ji, Y., Chetelat, R. T., Scott, J. W., Jose Gonzalo, M., Francis, D., Yang, W., van der Knaap, E., Baldo, A. M., Smith-White, B., Mueller, L. A., Prince, J. P., Blanchard, N. E., Storey, D. B.,

- Stevens, M. R., Robbins, M. D., Wang, J. F., Liedl, B. E., O'Connell, M. A., Stommel, J. R., Aoki, K., Iijima, Y., Slade, A. J., Hurst, S. R., Loeffler, D., Steine, M. N., Vafeados, D., McGuire, C., Freeman, C., Amen, A., Goodstal, J., Facciotti, D., Van Eck, J., and Causse, M. (2007). Tomato. In C. Kole (Ed.), *Genome Mapping and Molecular Breeding in Plants*, Vol. 5 Vegetables, Berlin, Heidelberg, Germany, Springer-Verlag.
- Larkin, R. P., Griffin, T. S., and Honeycutt, C. W. (2010). Rotation and cover crop effects on soilborne potato diseases, tuber yield, and soil microbial communities. *Plant Disease*, 94, 1491 - 1502.
- Lazarovits, G. (2010). Managing soilborne disease of Potatoes using ecologically based approaches. *American Journal of Potato Research*, 87, 401 - 411.
- Li, J., Liu, L., Bai, Y., Finkers, R., Wang, F., Du, Y., Yang, Y., Xie, B., Visser, R. G. F, and van Heusden, A. W. (2011). Identification and mapping of quantitative resistance to late blight (*Phytophthora infestans*) in *Solanum habrochaites* LA1777. *Euphytica*, 179, 427 - 438.
- Linnaeus, C. (1753). *Species Plantarum*, Volume 1, Stockholm, Schweden, L. Salvius.
- Littell, R. C., Milliken, G. A., Stroup, W. W., and Wolfinger, R. D. (2004). SAS system for mixed models. 6th edition, Cary, North Carolina, USA, SAS Institute Inc.
- Livak, K. J., and Schmittgen, T. D. (2001). Analysis of Relative Gene Expression Data Using Real-Time Quantitative PCR and the $2^{-\Delta\Delta C_T}$ Method. *Methods*, 25, 402 – 408.
- Lee, L. Y. and Gelvin, S. B. (2008). T-DNA binary vectors and systems. *Plant Physiology*, 146, 325 - 332.
- Liedschulte, V., Wachter, A., Zhigang, A., and Rausch, T. (2010). Exploiting plants for glutathione (GSH) production: uncoupling GSH synthesis from cellular controls results in unprecedented GSH accumulation. *Journal of Plant Biotechnology*, 8, 807 – 820.
- Limpens, E., Ramos, J., Franken, C., Raz, V., Compaan, B., Franssen, H., Bisseling, T., and Geurts, R. (2004). RNA interference in *Agrobacterium rhizogenes*-transformed roots of *Arabidopsis* and *Medicago truncatula*. *Journal of Experimental Botany*, 55, 983 - 992.
- Ling, H. Q., Kriseleit, D., and Ganai, M. W. (1998). Effect of ticarcillin/potassium clavulanate on callus growth and shoot regeneration in *Agrobacterium*-mediated transformation of tomato (*Lycopersicon esculentum* Mill.). *Plant Cell Reports*, 17, 843 - 847.
- Logemann, E., Birkenbihl, R. P., Ulker, B., and Somssich, I. E. (2006). An improved method for preparing *Agrobacterium* cells that simplifies the *Arabidopsis* transformation protocol. *Plant Methods*, 2, 16.

- Lopez, J., Tremblay, N., Voogt, W., Dube, S., and Gosselin, A. (1996). Effects of varying sulphate concentrations on growth, physiology and yield of the greenhouse tomato. *Scientia Horticulturae*, 67, 207 – 217.
- Løvdaal, T. and Lillo, C. (2009). Reference gene selection for quantitative real-time PCR normalization in tomato subjected to nitrogen, cold, and light stress. *Analytical Biochemistry*, 387, 238 - 242.
- Lunde, C., Zygadlo, A., Simonsen, H. T., Nielsen, P. L., Blennow, A., and Haldrup, A. (2008). Sulfur starvation in rice: the effect on photosynthesis, carbohydrate metabolism, and oxidative stress protective pathways. *Physiologia Plantarum*, 134, 508 - 521.
- Mao, G., Wang, R., Guan, Y., Liu, Y., and Zhang, S. (2011). Sulfurtransferases 1 and 2 play essential roles in embryo and seed development in *Arabidopsis thaliana*. *Journal of Biological Chemistry*, 286, 7548 - 557.
- Matsukura, C., Aoki, K., Fukuda, N., Mizoguchi, T., Asamizu, E., Saito, T., Shibata, D., and Ezura, H. (2008). Comprehensive resources for tomato functional genomics based on the miniature model tomato micro-tom. *Current Genomics*, 9, 436 - 443.
- Miller, P. (1768). *The gardener's dictionary*, 8th edition, London, UK.
- Mittler, R., Vanderauwera, S., Gollery, M., and van Breusegem, F. (2004). Reactive oxygen gene network of plants. *Trends in Plant Science*, 9, 490 - 498.
- Monforte, A. J., and Tanksley, S. D. (2000). Development of a set of near isogenic and backcross recombinant inbred lines containing most of the *Lycopersicon hirsutum* genome in a *L. esculentum* genetic background: a tool for gene mapping and gene discovery. *Genome*, 43, 803 – 813.
- Moradi, M., Oerke, E. C., Steiner, U., Tesfaye, D., Schellander, K., and Dehne, H. W. (2010). Microbiological and SYBR green real-time PCR detection of major *Fusarium* head blight pathogens on wheat ears. *Microbiology*, 79, 655 - 663.
- Müller, L. A., Solow, T. H., Taylor, N., Skwarecki, B., Buels, R., Binns, J., Lin, C., Wright, M. H., Ahrens, R., Wang, Y., Herbst, E. V., Keyder, E. R., Menda, N., Zamir, D., and Tanksley, S. D. (2005 a). The SOL Genomics Network: a comparative resource for *Solanaceae* biology and beyond. *Plant Physiology*, 138, 1310 - 1317.
- Müller, L. A., Tanksley, S. D., Giobannoni, J. J., Van Eck, J., Stack, S., Choi, D., Kim, B. D., Chen, M., Cheng, Z., Li, C., Ling, H., Xue, Y., Scymour, G., Bishop, G., Bryan, G., Sharma, R., Khurana, J., Tyagi, A., Chattopadhyay, D., Singh, N. K., Stiekeme, W., Lindhour, P., Jesse, T., Lankhorst, R. K., Bouzayen, M., Shibata, D., Tabata, S., Granell A., Botella, M. A., Giuliano, G., Frusciante, L., Causse, M., and Zamir, D. (2005 b).

- The Tomato Sequencing Project, the first cornerstone of the International *Solanaceae* Project (SOL). *Comparative and Functional Genomics*, 6, 153 - 158.
- Nikiforova, V. J., Gakière, B., Kempa, S., Adamik, M., Willmitzer, L., Hesse, H., and Höfgen, R. (2004). Towards dissecting nutrient metabolism in plants: a systems biology case study on sulphur metabolism. *Journal of Experimental Botany*, 55, 1861 – 1870.
- Nikiforova, V. J., Kopka, J., Tolstikov, V., Fiehn, O., Hopkins, L., Hawkesford, M. J., Hesse, H., and Höfgen, R. (2005). Systems rebalancing of metabolism in response to sulfur deprivation, as revealed by metabolome analysis of *Arabidopsis* plants. *Plant Physiology*, 138, 304 – 318.
- Nogués, S., Cotxarrera, L., Alegre, L. and Trillas, M. I. (2002). Limitations to photosynthesis in tomato leaves induced by *Fusarium* wilt. *New Phytologist*, 154, 461 – 470.
- Novo, M., Gayoso, C. M., Pomar, F., Lucas, M. M., Ros Barceló, A., and Merino, F. (2007). Sulphur accumulation after *Verticillium dahliae* infection of two pepper cultivars differing in degree of resistance. *Plant Pathology*, 56, 998 – 1004.
- Noctor, G., Arisi, A. C. M., Jouanin, L., and Foyer, C. H. (1998). Manipulation of glutathione and amino acid biosynthesis in the chloroplast. *Plant Physiology*, 118, 471 – 482.
- Noctor, G., Mhamdi, A., Chaouch, S., Han, Y., Neukermans, J., Marquez-Garcia, B., Queval, G., and Foyer, C. H. (2012). Glutathione in plants: an integrated overview. *Plant Cell and Environment*, 35, 454 - 484.
- Ochiai, N., Powelson, M. L., Crowe, F. J., and Dick, R.P. (2008). Green manure effects on soil quality in relation to suppression of *Verticillium* wilt of potatoes. *Biology and Fertility of Soils*, 44, 1013 – 1023.
- Padidam, M. (2003). Chemically regulated gene expression in plants. *Current Opinion in Plant Biology*, 6, 169 - 177.
- Pantou, M. P. and Typas, M. A. (2005). Electrophoretic karyotype and gene mapping of the vascular wilt fungus *Verticillium dahliae*. *FEMS Microbiology Letters*, 254, 213 – 220.
- Papenbrock, J., Guretzki, S., and Henne, M. (2010). Latest news about the sulfurtransferase protein family of higher plants. *Amino Acids*, 41, 43 - 57.
- Pascual, I., Azcona, I., Morales, F., Aguirreolea, J., and Sánchez-Díaz, M. (2010). Photosynthetic response of pepper plants to wilt induced by *Verticillium dahliae* and soil water deficit. *Journal of Plant Physiology*, 167, 701 - 708.
- Pegg, G. F. (1984). The impact of *Verticillium* diseases in agriculture. *Phytopathologia Mediterranea*, 23, 176 - 192.
- Pegg, G. F. and Brady, B. L. (2002). *Verticillium* wilts. Wallingford, UK, CABI Publishing.

- Peralta, I. E. and Spooner, D. M. (2007). History, origin and early cultivation of tomato (*Solanaceae*). In Razdan, M. K. and Mattoo, A. K. (Eds). Genetic Improvement of Solanaceous Crops, Volume 2: Tomato. Enfield, USA, Science Publishers.
- Pierik, R., Tholen, D., Poorter, H., Visser, E. J. W. and Voeseek, L. A. C. J. (2006). The Janus face of ethylene: growth inhibition and stimulation. *Trends in Plant Science*, 11, 176 - 183.
- Pramateftaki, P. V., Antoniou, P. P., and Typas, M. A. (2000). The complete DNA sequence of the nuclear ribosomal RNA gene complex of *Verticillium dahliae*: intraspecific heterogeneity within the intergenic spacer region. *Fungal Genetics and Biology*, 29, 135 - 143.
- Pshibytko, N. L.; Zenevich, L. A., and Kabashnikova, I. F. (2006). Changes in the photosynthetic apparatus during *Fusarium* wilt of tomato. *Russian Journal of Plant Pathology*, 53, 25 - 31.
- Rausch, T., and Wachter, A. (2005). S metabolism: a versatile platform for launching defence operations. *Trends in Plant Science*, 10, 503 - 509.
- Resende, M. L. V., Flood, J., Ramsden, J. D., Rowan, M. G, Beale, M. H, and Cooper, R. M. (1996). Novel phytoalexins including elemental sulphur in the resistance of cocoa (*Theobroma cocoa* L.) to *Verticillium* wilt (*Verticillium dahliae* Kleb.). *Physiological and Molecular Plant Pathology*, 48, 347 - 359.
- Resurreccion, A. P., Makino, A., Bennett, J., and Mae, T. (2002). Effect of light intensity on the growth and photosynthesis of rice under different sulfur concentrations. *Soil Science and Plant Nutrition*, 48, 71 - 77.
- Rick, C. M. (1982). The potential of exotic germplasm for tomato improvement. In Vasil, A. K., Scowcroft, W. R. and Frey, K. J. (Eds.). *Plant Improvement and Somatic Cell Genetics.*, New York, USA, Academic Press.
- Riemenschneider, A., Nikiforova, V., Höfgen, R., De Kok, L. J., and Papenbrock, J. (2005). Impact of elevated H₂S on metabolite levels, activity of enzymes and expression of genes involved in cysteine metabolism. *Plant Physiology and Biochemistry*, 43, 473 - 483.
- Robb, J., Powell, D. A. and Street, P. F. S. (1989). Vascular coating: a barrier to colonization by the pathogen in *Verticillium* wilt of tomato. *Canadian Journal of Botany*, 67, 600 - 607.
- Robb, J., Lee, S-W., Mohan, R., and Kolattukudy, P. E. (1991). Chemical characterization of stress-induced vascular coating in tomato. *Plant Physiology*, 97, 528 - 536.

- Robb, J., Lee, B. and Nazar, R. N. (2007). Gene suppression in a tolerant tomato-vascular pathogen interaction. *Planta*, 226, 299 - 309.
- Roitsch, T. (1999). Source-sink regulation by sugars and stress. *Current Opinion in Plant Biology*, 2, 198 - 206.
- Roitsch, T., Balibrea, M. E., Hofmann, M., Proels, R., and Sinha, A. K. (2003). Extracellular invertase: key metabolic enzyme and PR protein. *Journal of Experimental Botany*, 54, 513 - 524.
- Saeed, I. A. M, McGuidwin, A. E., Rouse, D. I., and Sharkey, T. D. (1999). Limitation to photosynthesis in *Pratylenchus penetrans*- and *Verticillium dahliae*-infected potato. *Crop Science*, 39, 1340 – 1346.
- Salac, I., Haneklaus, S., Bloem, E., Booth, E., Sutherland, K., Walker, K., and Schnug, E. (2006). Influence of sulfur fertilization on sulfur metabolites, disease incidence and severity of fungal pathogens in oilseed rape in Scotland. *FAL Agricultural Research* 56, 1 – 4.
- Sarker, R. H., Islam, K., and Hoque, M. I. (2009). In vitro regeneration and *Agrobacterium*-mediated genetic transformation of Tomato (*Lycopersicon esculentum* Mill.). *Plant Tissue Culture and Biotechnology*, 19, 101 – 111.
- Schaible, L., Cannon, O. S., and Waddoups, V. (1951). Inheritance of resistance to *Verticillium* wilt in a tomato cross. *Phytopathology*, 41, 986 – 990.
- Scharte, J., Schön, H., Weis, E. (2005). Photosynthesis and carbohydrate metabolism in tobacco leaves during an incompatible interaction with *Phytophthora nicotianae*. *Plant, Cell and Environment*, 28, 1421–1435.
- Schlaeppli, K., Abou-Mansour, E., Buchala, A., and Mauch, F. (2010). Disease resistance of *Arabidopsis* to *Phytophthora brassicae* is established by the sequential action of indole glucosinolates and camalexin. *Plant Journal*, 62, 840 - 851.
- Schnug, E., Haneklaus, S., Borchers, A., and Polle, A. (1995). Relations between sulphur supply and glutathione, ascorbate and glucosinolate concentrations in *Brassica napus* varieties. *Journal of Plant Nutrition and Soil Science*, 158, 67 – 70.
- Schonhof, I., Blankenburg, D., Müller, S., and Krumbein, A. (2007). Sulfur and nitrogen supply influence growth, product appearance, and glucosinolate concentration of broccoli. *Journal of Plant Nutrition and Soil Science*, 170, 65 - 72.
- Schulze-Lefert, P. (2004). Plant immunity: the origami of receptor activation. *Current Biology*, 14, R22 - R24.

- Simko, I., Costanzo, S., Haynes, K. G., Christ, B. J., and Jones, R. W. (2004). Linkage disequilibrium mapping of a *Verticillium dahliae* resistance quantitative trait locus in tetraploid potato (*Solanum tuberosum*) through a candidate gene approach. *Theoretical and Applied Genetics*, 108, 217 – 224.
- Sinha, A. K., Hofmann, M. G., Romer, U., Kockenberger, W., Elling, L. and Roitsch, T. (2002). Metabolizable and non-metabolizable sugars activate different signal transduction pathways in tomato. *Plant Physiology*, 128, 1480 – 1489.
- Seo, Y. S., Lee, S. K., Song, M. Y., Suh, J. P., Hahn, T. R., Ronald, P., and Jeon, J. S. (2008). The HSP90-SGT1-RAR1 molecular chaperone complex: a core modulator in plant immunity. *Journal of Plant Biology*, 51, 1 – 10.
- Sparkes, I. A., Runions, J., Kearns, A., and Hawes, C. (2006). Rapid, transient expression of fluorescent fusion proteins in tobacco plants and generation of stably transformed plants. *Nature Protocols*, 1, 2019 - 2025.
- Spooner, D. M., Peralta, I. E., and Knapp, S. (2005). Comparisons of AFLPs with other markers for phylogenetic inference in wild tomatoes [*Solanum L.* section *Lycopersicon* (Mill.) Wettst.]. *Taxon*, 54, 43 – 61
- Subbarao, K. V., Hubbard, J. C., Greathead, A. S., Spencer, G. A. (1997). *Verticillium* wilt. In: Davis, R. M., Subbarao, K. V., Raid, R. N., and Kurtz, E. A. (Eds.) *Compendium of lettuce diseases*. St. Paul, USA, The American Phytopathological Society.
- Sun, H. J., Uchii, S., Watanabe, S., and Ezura, H. (2006). A highly efficient transformation protocol for Micro-Tom, a model cultivar for tomato functional genomics. *Plant and Cell Physiology*, 47, 426 - 431.
- Takahashi, H., Kopriva, S., Giordano, M., Saito, K., and Hell, R. (2011). Sulfur assimilation in photosynthetic organisms: molecular functions and regulations of transporters and assimilatory enzymes. *Annual Review of Plant Biology*, 62, 157 - 184.
- Tanksley, S. D., Ganal, M. W., Prince, J. P., de-Vicente, M. C., Bonierbale, M. W., Broun, P., Fulton, T. M., Giovannoni, J. J., Grandillo, S., Martin, G. B., Messeguer, R., Miller, J. C., Miller, L., Paterson, A. H., Pineda, O., Roder, M. S., Wing, R. A., Wu, W., and Young, N. D. (1992) High density molecular linkage maps of the tomato and potato genomes. *Genetics*, 132, 1141–1160.
- The Tomato Genome Consortium (2012). The tomato genome sequence provides insights into fleshy fruit evolution. *Nature*, 485, 635 – 641.
- Thomma, B. P. H. J., van Esse, H. P., Crous, P. W. and de Wit, P. J. G. M. (2005). *Cladosporium fulvum* (syn. *Passalora fulva*), a highly specialized plant pathogen as a

- model for functional studies on plant pathogenic *Mycosphaerellaceae*. *Molecular Plant Pathology*, 6, 379 – 393.
- Tournefort, J. P. D. (1694). *Éléments de Botanique*. Paris, France, L’Imprimerie royale
- Trail, F. (2007). Fungal cannons: explosive spore discharge in the Ascomycota. *FEMS Microbiology Letters*. 276, 12 - 8.
- Tweedy, B. G. (1981). Inorganic S as a fungicide. *Residue Reviews*, 78, 43 - 68.
- Tzfira, T. and Citovsky, V. (2006). *Agrobacterium*-mediated genetic transformation of plants: biology and biotechnology. *Plant Biotechnology*, 17, 147 – 154.
- Untergasser, A., Nijveen, H., Rao, X., Bisseling, T., Geurts, R. and Leunissen, J. A. M. (2007). Primer3Plus, an enhanced web interface to Primer3. *Nucleic Acids Research*, 35, W 71 – W 74.
- Usami, T., Itoh, M., and Amemiya Y. (2009). Asexual fungus *Verticillium dahliae* is potentially heterothallic. *Journal of General Plant Pathology*, 75, 422 - 427
- Vallad, G. E. and Subbarao, K. V. (2008). Colonization of resistant and susceptible lettuce cultivars by a greenfluorescent protein-tagged isolate of *Verticillium dahliae*. *Phytopathology*, 98, 871 – 885.
- Vanacker, H., Carver, T. L. W. and Foyer, C. H. (2000). Early H₂O₂ accumulation in mesophyll cells leads to induction of glutathione during the hyper-sensitive response in the barley-powdery mildew interaction. *Plant Physiology*, 123, 1289 - 1300.
- Vauclare, P., Kopriva, S., Fell, D., Suter, M., Sticher, L., von Ballmoos, O., Krähenbühl, U., Op den Camp, R., and Brunold, C. (2002). Flux control of sulfate assimilation in *Arabidopsis thaliana*: adenosine 5'-phosphosulfate reductase is more susceptible to negative control by thiols than ATP sulfurylase. *The Plant Journal*, 31, 729 – 740.
- Wachter, A., Wolf, S., Steininger, H., Bogs, J., and Rausch, T. (2005). Differential targeting of GSH1 and GSH2 is achieved by multiple transcription initiation: implications for the compartmentation of glutathione biosynthesis in the Brassicaceae. *The Plant Journal*, 41, 15 – 30.
- Walton, J. (2006). HC-toxin. *Phytochemistry*, 67, 1406 - 1413.
- Wang, R., Zhou, X., and Wang, X. (2003). Chemically regulated expression systems and their applications in transgenic plants. *Transgenic Research*, 12, 529 - 540.
- Wang, G., Ellendorff, U., Kemp, B., Mansfield, J. W., Forsyth, A., Mitchell, K., Bastas, K., Liu, C. M., Woods-Tör, A., Zipfel, C., de Wit, P. J. G. M., Jones, J. D. G., Tör, M., and Thomma, B. P. H. J. (2008). A genome-wide functional investigation into the roles of receptor-like proteins in *Arabidopsis*. *Plant Physiology*, 147, 503 – 517.

- Weigel, D. and Glazebrook, J. (2002). *Arabidopsis: A Laboratory Manual*. Cold Spring Harbor, New York, USA, Cold Spring Harbor Laboratory Press.
- White, T. J., Bruns, T. D., Lee, S., and Taylor, J. (1990). Amplification and direct sequencing of fungal ribosomal genes for phylogenetics. In: Innis, M. A., Gelfrand, D. H., Sninsky, J. J. and White, T. J. (Eds.), *PCR Protocols*. San Diego, USA, Academic Press.
- Wikström, N., Savolainen, V., and Chase, M. W. (2001). Evolution of the angiosperms: calibrating the family tree. *Proceedings of the Royal Society B- Biological Sciences*, 268, 2211 – 2220.
- Williams, J. S., Hall, S. A., Hawkesford, M. J., Beale, M. H., and Cooper, R. M. (2002). Elemental S and thiol accumulation in tomato and defence against a fungal vascular pathogen. *Plant Physiology*, 128, 150 – 159.
- Williams, J. S. and Cooper, R. M. (2003). Elemental sulphur is produced by diverse plant families as a component of defence against fungal and bacterial pathogens. *Physiological and Molecular Plant Pathology*, 63, 3 – 16.
- Williams, J. S. and Cooper, R. M., (2004). The oldest fungicide and newest phytoalexin – a reappraisal of the fungitoxicity of elemental sulphur. *Plant Pathology*, 53, 263 – 279.
- Xiang, C., Werner, B. L., Christensen, E. M., and Oliver, D. J. (2001). The biological functions of glutathione revisited in *Arabidopsis* transgenic plants with altered glutathione levels. *Plant Physiology*, 126, 564 – 574.
- Yang, L., Ding, J., Zhang, C., Jia, J., Wenig, H., Liu, W., and Zhang, D. (2005). Estimating the copy number of transgenes in transformed rice by real-time quantitative PCR. *Plant Cell Reports*, 23, 759 - 763.
- Yi, C. X., Zhang, J., Chan, K. M., Liu, X. K., and Hong, Y. (2008). Quantitative real-time PCR assay to detect transgene copy number in cotton (*Gossypium hirsutum*). *Analytical Biochemistry*, 375, 150 - 152.
- Zahn, M. Teuber, F., Bollig, K. and Horst, W. (2011). Quantification of *Pseudocercospora fuligena* in tomato lines carrying introgressions from *Solanum habrochaites* using a qPCR assay. *Plant Disease*, 95, 394 - 400.
- Zamir, D. (2001). Improving plant breeding with exotic genetic libraries. *Nature Reviews Genetics*, 2, 983 – 989.
- Zorn, W., Marks, G., Heß, H., and Bergmann, W. (2006). *Handbuch zur visuellen Diagnose von Ernährungsstörungen bei Kulturpflanzen*. München, Deutschland, Springer Spektrum Verlag.

References

- Zhou, L., Hu, Q., Johansson, A., and Dixelius, C. (2006). *Verticillium longisporum* and *Verticillium dahliae*: infection and disease in *Brassica napus*. *Plant Pathology*, 55, 137 – 144.
- Zuchi, S., Cesco, S., Varanini, Z., Pinton, R., and Astolfi, S. (2009). Sulphur deprivation limits Fe-deficiency responses in tomato plants. *Planta*, 230, 85 - 94.
- Zuo, J., Niu, Q. W., and Chua, N. H. (2000). An estrogen receptor-based transactivator XVE mediates highly inducible gene expression in transgenic plants. *The Plant Journal*, 24, 265 – 273.

Erklärung zur Dissertation

gemäß §6 (1) der Promotionsordnung der Naturwissenschaftlichen Fakultät der Gottfried Wilhelm Leibniz Universität Hannover für die Promotion zum Dr. rer. nat.

Hierdurch erkläre ich, dass ich meine Dissertation mit dem Titel:

Sulfur Nutrition of Tomato (*Solanum lycopersicum*) in Relation to its Resistance against Pathogens

selbständig verfasst und die benutzten Hilfsmittel und Quellen sowie gegebenenfalls die zu Hilfeleistungen herangezogenen Institutionen vollständig angegeben habe. Die Dissertation wurde nicht schon als Masterarbeit, Diplomarbeit oder andere Prüfungsarbeit verwendet.

Publikationsliste

Wissenschaftliche Veröffentlichungen

- 2013 Bollig, K., Specht, A., Myint, S. S., Zahn, M., and Horst, W. J. (2013). Sulfur supply impairs spread of *Verticillium dahliae* in tomato. *European Journal of Plant Pathology*, 135 (1), 81 – 96.
- 2011 Zahn, M., Teuber, F., Bollig, K., and Horst, W. J. (2011). Quantification of *Pseudocercospora fuligena* in tomato lines carrying introgressions from *Solanum habrochaites* using a qPCR assay. *Plant Disease*, 95, 394 - 400.
- 2009 Bollig, K., Hartwig, M., Führs, H., Zahn, M., Braun, H. P. and Horst, W. J. (2009). Transcriptomic analysis of genotypic differences in and the effect of silicon on manganese tolerance of *Vigna unguiculata* [L.] Walp.. The Proceedings of the International Plant Nutrition Colloquium XVI, Sacramento, CA, USA. (<http://escholarship.org/uc/item/8910s346?query=Bollig>)

Wissenschaftliche Vorträge

- 2012 International Workshop of the German Society of Plant Nutrition (DGP), 5. - 8. September, Bonn, Germany, Bollig, K., Specht, A., Myint, S. S., Zahn, M., and Horst, W. J.: Sulfur supply improves tomato (*Solanum lycopersicum*) pathogen resistance.
- 2012 10th conference of the European Foundation of Plant Pathology (EFPP), 1. – 5. October 2012, Wageningen, Netherlands: Bollig, K., Specht, A., Myint, S. S., Zahn, M., and Horst, W. J.: Sulfur supply improves tomato (*Solanum lycopersicum*) pathogen resistance.

Poster Präsentationen

- 2012 International Workshop of the German Society of Plant Nutrition (DGP), 5. - 8. September, Bonn, Germany: Bach, M., Bollig, K., und Horst, W. J.: Sulfur-enhanced plant defense against *Verticillium dahliae* in a tomato introgression line population.
- 2011 Gemeinsame Jahrestagung der Deutschen Gesellschaft für Pflanzenernährung (DGP) und der Gesellschaft für Pflanzenbauwissenschaften (GPW), 27. - 29. September 2011, Kiel, Germany: Bollig, K., Hogeckamp, C., Küster, H. and Horst, W. J.: Sulfur nutrition of tomato (*Solanum lycopersicum*) in relation to its resistance against pathogens.

- 2010 International Symposium of the German Society of Plant Nutrition, 30.09. - 02.10.2010, Hannover, Germany: Bollig, K., Zahn, M., und Horst, W. J.: Sulfur nutrition of tomato (*Solanum lycopersicum*) in relation to its resistance against pathogens.
- 2009 XVI International Plant Nutrition Colloquium, 26. – 30. August 2009, Sacramento, USA: Bollig, K., Hartwig, M., Führs, H., Zahn, M., Braun, H. P. and Horst, W. J.: Transcriptomic analysis of genotypic differences in and the effect of silicon on manganese tolerance of *Vigna unguiculata* [L.] Walp..
- 2009 Jahrestagung der Deutschen Gesellschaft für Pflanzenernährung (DGP), 11. - 12. Juni 2009, Osnabrück, Deutschland: Bollig, K., Hartwig, M., Führs, H., Zahn, M., Braun, H. P. and Horst, W. J.: Transcriptomic analysis of genotypic differences in and the effect of silicon on manganese tolerance of *Vigna unguiculata* [L.] Walp..
- 2007 Jahrestagung der Deutschen Gesellschaft für Pflanzenernährung (DGP), 13. - 14. September 2007, Berlin, Deutschland: Bollig, K., Hartwig, M., Führs, H., Zahn, M., Braun, H. P. and Horst, W. J.: Transcriptomic analysis of genotypic differences in and the effect of silicon on manganese tolerance of *Vigna unguiculata* [L.] Walp..

Curriculum Vitae

Persönliche Daten

Name: Katharina Klug (geb. Bollig)

Geboren: 13.10.1982, Rheinbach, Deutschland

Familienstand: verheiratet

Nationalität: deutsch

Schulische Ausbildung

21.07.2002	Allgemeine Hochschulreife, Pestalozzi Gymnasium, Herne
2001 – 2002	Pestalozzi-Gymnasium, Herne
1993 – 2001	Staatliches Wiedtal Gymnasium, Neustadt / Wied
1989 - 1993	Deutscherren Grundschule, Waldbreitbach

Universitäre Ausbildung

Seit 10 / 2008	Wissenschaftliche Mitarbeiterin am Institut für Pflanzenernährung der Leibniz Universität Hannover im Rahmen des Promotionsstudiengangs Pflanzenbiotechnologie
21.09.2008	Master of Science in Pflanzenbiotechnologie: Transcriptomic analysis of the effect of silicon on the manganese tolerance of <i>Vigna unguiculata</i> (L.) Walp..
10 / 2006 – 09 / 2008	Masterstudiengang Pflanzenbiotechnologie, Leibniz Universität Hannover
16.08.2006	Bachelor of Science in Biologie der Zellen: Charakterisierung des Ferredoxin-Gens At1g10960 in T-DNA Insertionslinien aus <i>Arabidopsis thaliana</i> (L.) Heyhn.
10 / 2003 – 09 / 2006	Bachelorstudiengang Biologie der Zellen, Universität Osnabrück
10 / 2002 – 09 / 2003	Studiengang Rechtswissenschaften, Universität Osnabrück

Danksagung

Mein ganz besonderer Dank gilt Herrn **Prof. Walter J. Horst** für die Bereitstellung des interessanten Themas und die Einführung in eine tolle Thematik im Bereich der Pflanzenernährung. Sie haben immer vollstes Vertrauen in meine Ideen und Fähigkeiten gehabt und mir sehr viel Anregung und Unterstützung in Form von Arbeitsgruppenaustausch, Tagungsteilnahmen und Vorträgen geboten. Ihre große Leidenschaft für die Wissenschaft hat mich sehr inspiriert und meine Denk- und Arbeitsweise nachhaltig geprägt.

Herrn **Prof. Helge Küster** danke ich für die Übernahme des Korreferates. Darüber hinaus möchte ich mich für die kooperative Bereitstellung und Einführung in modernste transkriptomische Technik bedanken.

Herrn **Prof. Edgar Maiss** danke ich für die Übernahme des Prüfungsvorsitzes und für so manche freundliche und hilfreiche Diskussion in molekularen Themengebieten.

Ich danke **Dr. Marc Zahn** für viele kreative Ideen und Hilfestellungen, er hat meine Arbeit maßgeblich molekular mitgestaltet und wird daher nie vergessen sein!

Ich danke **Dipl.-Ing. André Specht** für das Einbringen seines analytischen Wissens und für seine allgegenwärtige enorme Hilfsbereitschaft.

Hildegard Thölke und **Anna-Lena Koch** danke ich für eine ausgezeichnete technische Assistenz.

Bei **Claudia Hogeckamp** möchte ich mich für eine sehr nette, äußerst professionelle und produktive Zusammenarbeit im Rahmen der LMPC Technik bedanken.

Ich danke **Dr. Hendrik Führs** und **Alexander T. Fleck** für so manchen konstruktiven Gedankenaustausch.

Ein großer Dank gilt allen Studenten, die Anteil an meiner Arbeit hatten. **Inga-Mareike Bach** danke ich für ihre riesige Einsatzbereitschaft im Rahmen großer Screening-Versuche. **Theresa Robbe** und **Dominik Ehm** danke ich für ihre produktiven Beiträge im molekularen Arbeitsbereich.

Mein Dank geht auch an **Ingrid Dusy**. Sie ist die organisatorische Seele des Instituts und hat mir stets geholfen und mir so vieles erleichtert.

Ein ganz großes Dankeschön gilt meinen Eltern **Ulrike** und **Bernd Bollig**. Ihr wart und seid immer für mich da und habt mir alles ermöglicht!

Dr. Benjamin Klug, ich bin so froh, dass es dich gibt. Du vervollständigst mich!

*Es war eine sehr schöne Zeit am Institut für Pflanzenernährung
und ich danke allen sehr dafür!*